

# RECYCLING BOROSILICATE GLASS FOR A FACADE SYSTEM ASSEMBLED OF DRY- INTERLOCKING CAST GLASS COMPONENTS IMPLEMENTED IN CASA DA MÚSICA

*Eliza Scholtens*









*MSc Architecture, Urbanism and Building Sciences*

## Master thesis

*April 2019*

Student:

*Eliza Scholtens*

*4154134*

*Building Technology*

Mentors:

*Faidra Oikonomopoulou*

*Tillmann Klein*

*Telesilla Bristogianni*



# ACKNOWLEDGEMENTS

The past year has been intense, most often in a good way. I especially enjoyed working in the glass lab, making the specimens and doing the experiments. This research would not have been possible without the help and (mental) support of so many people.

Foremost, I want to thank my mentors Faidra Oikonomopoulou, Telesilla Bristogianni and Tillmann Klein. Faidra and Telesilla thank you for sharing your expertise, knowledge and giving support. But most of all I want to thank you for your enthusiasm for the subject, which inspired me a lot. Tillmann thank you for providing a different and refreshing perspective. It often kept my feet on the ground and helped me lot.

Fred Veer and Albert Bosman, I appreciate your help during the experimental part of this thesis. In addition, I would like to thank Tomasso Venturini a lot for all his help in the glass lab.

To my family Frank, Aafke, Ekko and Rixt I would like to thank you for always believing in me and supporting me, no matter what.

I want to thank my friends who have helped me a lot. It is difficult for me to express how much that meant for me. Iris, thank you so much for always being there for me and helping me out whenever I need it. Tirza, you brought clarity into my mind with your planning skills. Umit, thank you for making me laugh and always cheering me up. I have to thank the one and only Mitchel Knipscheer. You were the perfect hand model. Jarno, aka Mechani-Boy, thank you for your help with the structural calculations. Boris, a lot of thanks for your help with rendering and sharing your Photoshop skills. Thank you Juul, Anna and the rest of Villa67 for being great study-buddies, friends and awesome roommates.

My fellow BT friends it was great sharing the graduation experience with you. Especially with Charbel, sharing our interest in glass.

But above all, I especially want to express my gratitude towards Nino. I cannot thank you enough for all your support and help you provided me the past year. Your support has helped me to achieve all of this.



# ABSTRACT

Currently, tons of high-quality borosilicate glass are discarded to landfills each year, taking up space on valuable land. Within the existing soda-lime glass recycling industry it is not possible to use recycled borosilicate glass due to its higher melting temperatures and a difference in chemical composition. In fact, borosilicate glass disturbs the recycling process of soda-lime glass, resulting in more unused waste.

Borosilicate glass is a type of glass that has favourable properties for application in the built environment, such as high optical qualities and a low thermal expansion coefficient. However, due to its high melting temperature and high energy consumption it is much more expensive to produce compared to the more common soda-lime glass. Nevertheless, in general it is possible to recycle glass waste almost 1:1, therefore, it is a waste to dump such high-quality glass on landfills.

Cost and energy consumption issues related to the fabrication of borosilicate glass can be decreased by using recycled crushed glass (cullet) to the melt. Cullet reduces the required melting temperature, resulting in a lower energy consumption and a cheaper production process. However, a fully closed borosilicate glass recycling loop is not possible. The current borosilicate glass product industry has very strict quality control. Recycling glass introduces contaminations in the glass melt, which could generate flaws and cracks in the end product. This means it is not feasible to use recycled glass in these industries.

This research proposes a promising approach to tackle the borosilicate glass waste problem and the recycling issues related to contamination: using the collected borosilicate glass waste to produce cast glass components. The bulkiness of such a component allows for a higher amount of impurities without risk of failure and a decrease in quality. In addition, cast glass allows for self-supporting facade systems in many configurations due to their increased cross-section and high-compressive strength capability. To allow disassembly of such a cast glass facade system a dry-interlocking system is proposed. Such a system can 'close' the recycling loop of borosilicate glass by feeding in waste glass from traditional borosilicate products into a new cast glass recycling loop.

The challenges and opportunities regarding

recycling borosilicate glass were researched by conducting experiments. Several mixtures of borosilicate glass with different chemical compositions were cast into small specimens to assess the mixability and corresponding mechanical properties of recycled borosilicate glass.

In terms of mixability, good results were observed when the cullet is ground to powder, although there is a risk of contamination during grinding and thus degrading quality. Using fine cullet is also promising, but there is an increased risk of internal stresses. Specimens with a homogeneous chemical composition showed that it is possible to create borosilicate glass components with a lower firing temperature. In addition, these homogeneous specimens illustrated through a three-point bending test that recycled borosilicate glass has comparable mechanical properties to non-recycled borosilicate glass. This indicates that recycled borosilicate glass is suitable for application in cast glass components for use in the built environment. Due to time constraints and the preliminary nature of this research the number of specimens was relatively small.

This thesis presents a dry-interlocking cast glass component system applied in a case study. The case study concerning the existing Casa da Música is meant to illustrate the possibilities of applying high-quality glass in an aesthetically pleasing facade system and to showcase the possibilities of recycling borosilicate glass. At the end-of-life of this design the facade can be disassembled. The components can either be directly reused in another building or recycled again. The proposed solution can reduce the growing amount of glass waste.

# CONTENT

<b>0.</b>	<b>Part RESEARCH FRAMEWORK</b>	<b>11</b>
<b>0.1</b>	<b>Research framework</b>	<b>12</b>
0.1.1	Problem statement	12
0.1.2	Relevance	12
0.1.3	Objectives	14
0.1.4	Research questions	14
0.1.5	Methodology	15
<b>1.</b>	<b>Part LITERATURE STUDY</b>	<b>17</b>
<b>1.1</b>	<b>Technology of glass</b>	<b>18</b>
1.1.1	Production of glass	18
1.1.2	Glass structure	20
1.1.3	Overview of Glass Properties	22
1.1.4	Glass Types	23
1.1.5	Glass production techniques	25
1.1.6	Annealing	29
1.1.7	Cast glass in the built environment	30
1.1.8	Interlayer	34
1.1.9	Advantage of cast glass components	35
<b>1.2</b>	<b>Recycling of glass</b>	<b>36</b>
1.2.1	Energy consumption of glass production	36
1.2.2	Contamination	37
1.2.3	Closed-loop Recycling	39
1.2.4	Open-loop Recycling	39
1.2.5	Exploration of closed-loop recycling of soda-lime container glass	40
1.2.6	Current recycling Numbers	42
1.2.7	Subsectors of the glass industry	45
1.2.8	Most suitable type of glass for recycling	47
<b>1.3</b>	<b>Borosilicate glass</b>	<b>50</b>
1.3.1	A Brief history about borosilicate glass	50
1.3.3	Borosilicate glass in the built environment	50
1.3.2	Amount of produced borosilicate glass	50
1.3.4	Opportunities of recycling borosilicate glass	51
1.3.5	Field of application of borosilicate glass	52
1.3.6	Borosilicate applications	53
1.3.7	Application in a case study	54
1.3.8	Conclusions of the literature study	55

<b>2.</b>	<b>Part RESEARCH ON RECYCLABILITY OF BOROSILICATE GLASS</b>	<b>57</b>
<b>2.1</b>	<b>Recycling loop of borosilicate glass</b>	<b>58</b>
<b>2.2</b>	<b>Experiments</b>	<b>63</b>
2.2.1	Introduction to experiments	63
2.2.2	Experimental setup	63
2.2.3	Detailed description of each specimen	68
<b>2.3</b>	<b>Conclusions of experiments</b>	<b>91</b>
<b>2.4</b>	<b>Recommendations of experiments</b>	<b>93</b>
<b>3.</b>	<b>Part DESIGN RESEARCH</b>	<b>99</b>
<b>3.1</b>	<b>Case study Casa da Música</b>	<b>100</b>
3.1.1	Building description	100
3.1.2	Design concept of Casa da Música	101
<b>3.2</b>	<b>Design criteria and constraints</b>	<b>103</b>
3.2.1	Design constraints interlocking principle	103
3.2.2	Design constraints cast glass	104
<b>3.3</b>	<b>Research to existing (interlocking) cast glass structures</b>	<b>105</b>
3.3.1	Examples of produced cast glass components	105
3.3.2	Total overview of researched interlocking components	105
<b>3.4</b>	<b>Concept design criteria</b>	<b>109</b>
3.4.1	Main concept design criteria	109
3.4.2	Concept design criteria components	109
3.4.3	Design criteria interlocking element	110
3.4.4	Design criteria interlayer	111
<b>3.5</b>	<b>Design of component</b>	<b>113</b>
3.5.1	Concept design corrugated facade of Casa da Música	113
3.5.2	Concept design component + interlocking element	114
3.5.3	Structural calculations component	117
3.5.4	Final component – final interlock ellipsoid – final interlayer	123
<b>3.6</b>	<b>Application in Casa da Música</b>	<b>127</b>
3.6.1	Final design in Casa da Música	127
3.6.2	Structural calculations of dimensions of the top and bottom beam	132
3.6.3	Detailing of facade system	143
<b>3.7</b>	<b>Feasibility</b>	<b>151</b>
3.7.1	Recyclability of facade system	151



	3.7.2 Mould design	152
	3.7.3 End-of-life	154
<b>3.8</b>	<b>Conclusions final design</b>	<b>156</b>
<b>3.9</b>	<b>Recommendations final design</b>	<b>157</b>
<b>4.</b>	<b>Part CONCLUSIONS AND RECOMMENDATIONS</b>	<b>159</b>
<b>4.1</b>	<b>General conclusion</b>	<b>160</b>
<b>4.2</b>	<b>General recommendations</b>	<b>162</b>
<b>4.3</b>	<b>Reflection</b>	<b>164</b>
<b>5.</b>	<b>Part APPENDICES</b>	<b>167</b>
<b>5.1</b>	<b>References</b>	<b>168</b>
<b>5.2</b>	<b>Appendices</b>	<b>173</b>



# PART 0

RESEARCH  
FRAMEWORK



# 0.1 RESEARCH FRAMEWORK

## 0.1.1 PROBLEM STATEMENT

Currently an estimated amount of 367.000 tonne/year of borosilicate glass waste is being discarded, instead of recycled (Rodriguez Vieitez et al., 2011; Scalet et al., 2013). Next to this, current existing cast glass (facade) structures are not reusable/demountable, due to adhesive connections, e.g. as is the case for the Crystal house in Amsterdam (Oikonomopoulou, Bristogianni, Veer, & Nijssse, 2017). Both problems can be addressed through the creation of dry-interlocking cast glass components made of recycled borosilicate glass and applying them in facade structures in a reversible way.

## 0.1.2 RELEVANCE

Several factors are of importance for better understanding the relevance of the aforementioned problem. These factors will be briefly addressed in the text below: glass properties, cast glass components, types of glass, current recycling industry, characteristics of the borosilicate glass waste stream itself and reversibility of the proposed solution.

Glass is a challenging material due to its brittleness. However, its transparency and high compressive strength capabilities account for a valuable building material. Moreover, glass has in theory endless recycling possibilities, providing an endless stream of material. However, in practice an enormous amount of glass waste ends up not being recycled at all. This is caused by contaminations and impurities in the glass waste, even after purification. When these contaminations end up in the glass manufacturing process they could introduce flaws and cracks into the end product (Haldimann, Luible, & Overend, 2008).

A promising approach to tackle this problem of contamination is through creation of cast glass components. These components are solid 3D blocks of glass. Due to their increased cross-section and high compressive strength of glass, these components are self-supporting and can form 3-dimensional facades structures (Oikonomopoulou, Bristogianni, Barou, Jacobs, Frigo, & Veer, 2018). Cast glass components can

potentially tolerate a higher amount of impurities than glass produced with other production methods, such as float glass and container glass (Bristogianni, Oikonomopoulou, Justino, et al., 2018a). This is because of the 3D nature of cast glass components; a flaw is expected to be much less critical in a 3D object than in a flat 2D one. In addition, float and container glass industry have strict control demands regarding their end products; flaws are generally not allowed. Therefore, waste glass could be an attractive resource for the production of structural cast glass components.

Commercially used glass comes in several types of which the most prevalent are soda-lime glass, borosilicate glass, lead glass and aluminosilicate glass. In the context of the built environment, borosilicate glass has better properties than the more common glass type soda-lime. Section 1.1.4 describes the differences between various glass types in more detail. A high optical quality, low thermal expansion coefficient and fire safety capability make borosilicate glass highly suitable for application in buildings. However, borosilicate glass is much more expensive to produce compared to soda-lime glass, due to a much higher melting temperature (Corning Museum of Glass, 2011d).

Additionally, within the current (soda-lime) recycling industry borosilicate glass is not mixable with soda-lime glass, mainly due to the higher melting point of borosilicate glass and difference in chemical composition. If borosilicate glass ends up in the current (soda-lime) recycling process it introduces problems to the molten batch of soda-lime glass. If the contamination due to the borosilicate glass is too high, the total batch is discarded to landfills. Furthermore, an infrastructure to collect and recycle borosilicate glass does not exist yet.

Cost issues could be dealt with by using cullet (crushed or small pieces of glass) when producing borosilicate cast glass components. Introducing glass cullet into a batch in a furnace lowers the melting temperature of the glass batch, compared to using solely raw materials. This could account for a considerable reduction in the amount of CO<sub>2</sub> emitted while also providing for a significantly cheaper production process (Scalet, Garcia Muñoz, Sissa Aivi, Roudier, & Luis, 2013). In

addition, the use of glass cullet will reduce the amount of raw materials needed and reduce the glass waste production and storage necessity on landfills (Worrell & Reuter, 2014).

Soda-lime glass accounts for the most applied type of glass worldwide and thus provides the largest glass waste stream. This waste is mainly produced by the container glass industry. Currently, in Europe (EU28) an average of 74% of the container glass waste is recycled (FEVE European Container Glass Federation, 2016).

In contrast, borosilicate glass waste is mainly provided by the chemical industry, such as laboratories, and household cooking ware (Schott, 2010). However, currently there is no closed-loop recycling industry for this type of glass. This means that the waste stream is not used up to its full potential. It is either down-cycled in an open recycling loop as aggregate for e.g. highway construction, or dumped at landfills (Worrell & Reuter, 2014).

To create a closed-loop for recycling borosilicate glass a potential solution could be a dry-interlocking facade structure of cast borosilicate glass components. Such a dry-interlocking facade system offers the possibility for disassembly or reuse of the cast components. This means that high quality borosilicate glass is not lost and instead applied within the built environment. After the life time of the facade, the components can be directly recycled or applied within another building, making them a sustainable solution.

In summary, the use of borosilicate glass waste applied as dry-interlocking cast glass building components, provides for high quality building components with a comparatively cheaper production process and lower environmental impact.

However, recycled borosilicate glass needs to be considered as a new material. Therefore, research needs to be conducted to define the properties of this material in cast glass components. Furthermore, research should be done on the design of such a dry-interlocking facade structure. Finally, the behavior of such a facade system within the context of a building has to be examined. A quick note on terminology, see Figure 1 and Figure

2 for the definition of a cast glass component versus wall/facade system constructed of these components.

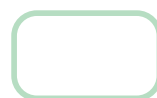


Figure 1 Component

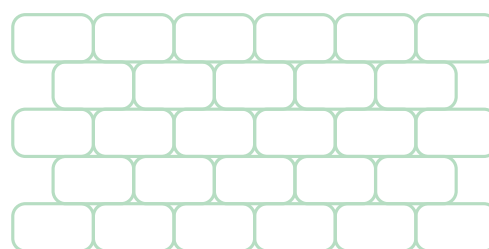


Figure 2 Wall / facade system

## 0.1.3 OBJECTIVES

### Main objectives:

1. Research on recyclability of borosilicate glass in structural cast glass building components.
2. Application of the research into a case study building such as Casa da Música in Porto, to showcase the possibilities of applying recycled borosilicate glass in a dry-interlocking cast glass component facade system.

### Sub objectives

1. Defining the recycling potential of borosilicate glass.
2. Defining the properties of recycled borosilicate glass when cast in structural glass components and validate if these components are suitable for application in facade systems.
3. Developing and improving an existing type of dry-interlocking cast glass building component to a new dry-interlocking cast glass component facade system.
4. Designing dry-interlocking cast glass component facade system for application in case study Casa da Música in Porto.

## 0.1.4 RESEARCH QUESTIONS

### Main question

***How to use recycled borosilicate glass in dry-interlocking cast glass components implemented in a reversible facade system?***

### Sub questions

1. What are the characteristics and material **properties** of glass and specifically **borosilicate** glass?
2. What is the **current** (limited) recycling process for borosilicate glass? And how to introduce a **new** recycling process for borosilicate glass?
3. What is the influence of **different** chemical compositions of borosilicate glass on the mechanical **properties** of cast glass components.
4. Is a **heterogenous** cullet **mix** suitable for cast glass components?
5. What are the **mechanical** properties of a recycled borosilicate cast glass component? And how does this compare to a non-recycled borosilicate cast glass component?
6. Which **dry-interlocking** component systems exist?
7. How can a recycled borosilicate cast glass component be **optimized** to create a **dry-interlocking** facade system?
8. How can such a dry-interlocking cast glass facade system be applied in case study building Casa da Música in Porto?



## 0.1.5 METHODOLOGY

This research is divided into two main parts; the literature study and a research to the recyclability of borosilicate glass through experiments and simultaneously a design to showcase the possibilities of applying recycled borosilicate glass in dry-interlocking cast glass component facade systems.

During the literature study, information will be gathered on glass in general: an overview on glass properties will be given, as well as an overview of different types of glass and of different glass production techniques, for the built environment of interest. Hereafter a few case studies with examples of cast glass building block will be examined. This chapter finishes with an overview of the existing building that will be used as a case study to validate the results of this research.

The second part of the literature study is about the recycling of glass. How does recycling contribute to the reduction of CO<sub>2</sub> emission during glass production? Then a chapter about the effects of contamination on glass recycling. Then, an overview of a closed- and open-loop recycling will be presented with an exploration of the closed-loop recycling of soda – lime container glass. Hereafter, current recycling numbers are investigated. Then, the subsectors of the glass industry shall be explained. After this, the most suitable type of glass for further research will be explored.

When this has been analyzed, a more in-depth research to the most suitable type of glass for this thesis, namely borosilicate glass, will follow. This is about current borosilicate glass waste numbers, the advantages of this glass type and the opportunities of recycling borosilicate glass. An overview of common applications of borosilicate glass shall be presented. An answer is given to the question where the borosilicate glass waste comes from and how can it be collected.

The second phase of this research consists of two parts; a research on the recyclability of borosilicate glass and a design to showcase the possibilities of applying recycled borosilicate glass in dry-interlocking cast glass component facade systems. The experimental part defines both the mixability of recycled borosilicate glass and the corresponding mechanical properties of this glass. Both the mixability and the mechanical properties will be defined through the physical creation of

small beam-shaped specimens of 150\*40\*40 mm. These specimens will be made in the Glass Lab at the Civil Engineering faculty of the TU Delft.

The mechanical properties of this recycled borosilicate glass that need to be determined are the flexural strength and the Young's Modulus. Both can be defined through a three-point bending test.

From the experimental part conclusions can be drawn of both the mixability and the mechanical properties of recycled borosilicate glass.

Simultaneously to the experimental part, a design of a dry-interlocking cast glass component system will be developed. First, a small literature study to dry-interlocking cast glass components systems shall be done. Secondly, a research to the case study building will be done to define design concepts. Hereafter, the dry-interlocking cast glass component system will be designed. Finally, this design will be implemented in the case study building to showcase the possibilities of designing a dry-interlocking cast glass facade system made of recycled borosilicate glass.



# **PART 1**

LITERATURE STUDY

# 1.1 TECHNOLOGY OF GLASS

*As mentioned before, glass is a versatile material, used for all sorts of applications for thousands of years. Its transparency, hardness, brittleness, high compressive strength and inertia make glass a special material. Although its brittleness can cause problems, glass is still considered a favorable material in a several sectors due to its unique properties.*

## 1.1.1 PRODUCTION OF GLASS

Glass is created out of certain raw materials, such as sand, soda and lime. These are mixed together in a furnace and heated up to temperatures around 1700-2500 °C, depending on the glass type. The material mixture melts and chemically reacts into glass (Vlakglas recycling Nederland, 2016).

This mixture of raw materials consist of three main components ; namely a former, a flux and a stabilizer (Corning Museum of Glass, 2011e; Corning Museum of Glass, 2011a). The former is the basic element of glass, therefore it takes up the largest amount in the mixture. The most common former is silicon dioxide ( $\text{SiO}_2$ ) which is found in sand. This former only becomes viscous, (and thus formable), at a very high temperature. The flux is the ingredient in glass which helps the former to turn viscous at a lower temperature. A typical flux is soda ash ( $\text{Na}_2\text{CO}_3$ ) or potash ( $\text{K}_2\text{O}$ ). The last component is the stabilizer, which ensures that the glass will not dissolve, crumble or crystalize and makes the glass water resistant and strong. A common stabilizer is calcium oxide ( $\text{CaO}$ ), which can be found in limestone. These three main components form the basic ingredients for the most common types of glass. (see Table 1).

	SODA-LIME	BOROSILICATE	LEAD GLASS	ALUMINO SILICATE	96% SILICA	FUSED SILICA
COMPOSITION (wt%)	SiO <sub>2</sub> 74 Na <sub>2</sub> O 16 CaO 5 Al <sub>2</sub> O <sub>3</sub> 1 B <sub>2</sub> O <sub>3</sub> - Other MgO 4	SiO <sub>2</sub> 81 Na <sub>2</sub> O 3.5 CaO - Al <sub>2</sub> O <sub>3</sub> 2.5 B <sub>2</sub> O <sub>3</sub> 13 Other -	SiO <sub>2</sub> 63 Na <sub>2</sub> O 3 CaO 1 Al <sub>2</sub> O <sub>3</sub> - B <sub>2</sub> O <sub>3</sub> - Other PbO 25 K <sub>2</sub> O 8	SiO <sub>2</sub> 62 Na <sub>2</sub> O 1 CaO 8 Al <sub>2</sub> O <sub>3</sub> 17 B <sub>2</sub> O <sub>3</sub> 5 Other MgO 7	SiO <sub>2</sub> 96 Na <sub>2</sub> O - CaO - Al <sub>2</sub> O <sub>3</sub> - B <sub>2</sub> O <sub>3</sub> 4 Other -	SiO <sub>2</sub> >99.5 Na <sub>2</sub> O - CaO - Al <sub>2</sub> O <sub>3</sub> - B <sub>2</sub> O <sub>3</sub> - Other -
YOUNGS MODULUS (E in kN/mm <sup>2</sup> )	73	64	59	75	67	72
THERMAL EXPAN- SION COEFFICIENT (at 20 °C in 10 <sup>-6</sup> K <sup>-1</sup> )	9	3.3	10.6	3.2	0.75	0.55
DENSITY g/cm <sup>3</sup>	2.5	2.23	3.2	2.43	2.16	2.17
STRAIN POINT °C Viscosity 10 <sup>13</sup> Pa-s	450	515	?	571	850	1000
ANNEALING POINT °C Viscosity 10 <sup>12</sup> Pa-s	550	565	411	623	950	1100
SOFTENING POINT °C Viscosity 10 <sup>10</sup> Pa-s	700	820	585	884	1550	1600
WORKING POINT °C Viscosity 10 <sup>9</sup> Pa-s	980	1260	800	?	?	?
MELTING POINT °C Viscosity 10 Pa-s	1400	>1800	?	?	?	?
TYPICAL CHARACTERISTICS	Relatively low melting temperature	Thermally shock and chemically resistant	Relatively soft High refractive index	Can be conducted with an electric film	High melting temperature Very low coefficient of expansion	High melting temperature Very low coefficient of expansion
TYPICAL APPLICATIONS	Most applied glass Container/float glass	Ovenware Laboratory ware	Table ware Glass art	Thin glass Phone/laptop screens	Most expensive glass Space vehicles	Most expensive glass Space vehicles
SOURCES All types: (Corning Museum of Glass, 2011d)	(CESEduPack, 2017d) (Schott, 2010)	(CESEduPack, 2017b) (Schott, 2010)	(CESEduPack, 2017c) (Schott, 2010)	(CESEduPack, 2017a) (Schott, 2010)	(Mittal, Kaur, & Sharma, 1992)	(Lesko, 2008)

Table 1 The six main glass families

## 1.1.2 GLASS STRUCTURE

Even though the molecules of glass are not organized in a structured lattice, it still has the mechanical rigidity of an organized crystalline structure. This is called a non-crystalline solid structure or amorphous (Callister, 2007). A schematic representation of an amorphous structure is illustrated in Figure 3 and Figure 4, where the difference can be clearly distinguished. In crystalline structures, a definite temperature forms the point the material changes phase between a solid and a liquid. With an amorphous structure, the material does not solidify the same way as materials with a crystalline structure does. (Callister, 2007). When glass is cooled down it becomes more and more viscous with decreasing temperature, but there is not an exact temperature at which the glass turns into a solid. At some point, the glass viscosity is high enough to be called a 'solid' glass and this point is called the glass transition temperature ( $T_g$ ) (Callister, 2007). Below this point the material is a 'solid' glass and above this point the glass is first a supercooled liquid and then it turns fully liquid. This process can be seen on Figure 5.

Due to the fact that glass has no exact point where the 'solid' structure turns liquid, there are some viscosity states between these phases. This phase between the glass transition temperature ( $T_g$ ), where the viscosity of the glass is high enough to be considered a solid and the melting point, where the viscosity is low enough to be considered a liquid, is divided into five stages; the strain point, annealing point, softening point, working point and the melting point (Callister, 2007).

The viscosity of glass can be plotted on a logarithmic scale versus the temperature on which these viscosity states occur (See Figure 6).

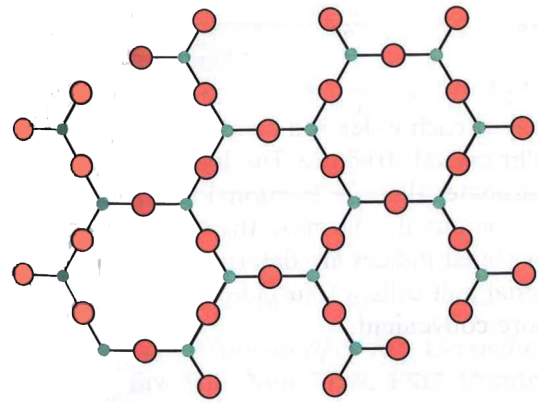


Figure 3 Crystalline structure of  $\text{SiO}_2$

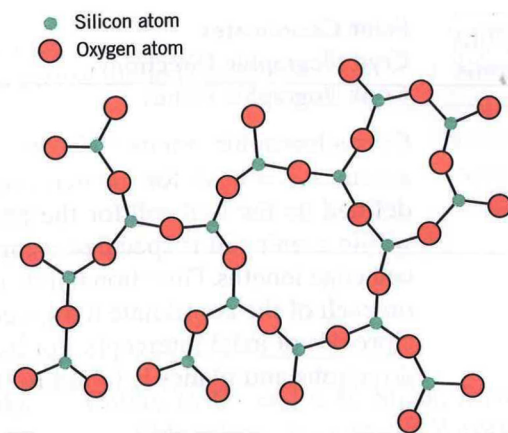


Figure 4 Non-Crystalline structure of  $\text{SiO}_2$

Source: (Callister, 2007)

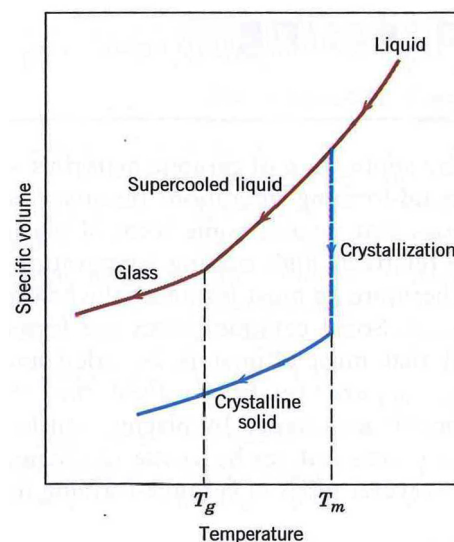


Figure 5 Glass transition phases

Source: (Callister, 2007)

Starting from the lowest temperature and therefore highest viscosity value to the highest temperature with the lowest viscosity value:

- 1) Strain point: at this point the viscosity of the glass is  $10^{13}$  Pa-s. Below the strain point, the glass will fracture when exposed to stress, instead of plastic deform. This also means that the glass transition temperature lies above the strain point.
- 2) Annealing point: this corresponds to a temperature at which the viscosity is  $10^{12}$  Pa-s. This point is the minimum temperature where atomic diffusion is fast enough that any residual stresses are relieved.
- 3) Softening point: the viscosity of the glass at this point is  $10^6$  Pa-s. This point is the maximum temperature where a glass object or piece can be edited without causing complete deformations.
- 4) Working point: the viscosity at this point is  $10^3$  Pa-s, and glass is easily deformed at this point.
- 5) Melting point: at this temperature the viscosity will be very low, namely 10 Pa-s. At this point the glass is considered a liquid.

Since the glass will be most formable between the working and the softening point, most glass-forming techniques are carried out between those two temperatures (Callister, 2007). This area between the two points is called the working range. What these temperatures exactly are, depends on the composition of the glass. As visible in Figure 6 the working range of soda-lime glass lies at a much lower temperature (700 °C) than compared to 96% silica glass (1550 °C). A lower working temperature results in less energy needed to heat up the glass, which causes significantly less CO<sub>2</sub> emitted in the air during production (Duurzaam glas, 2018).

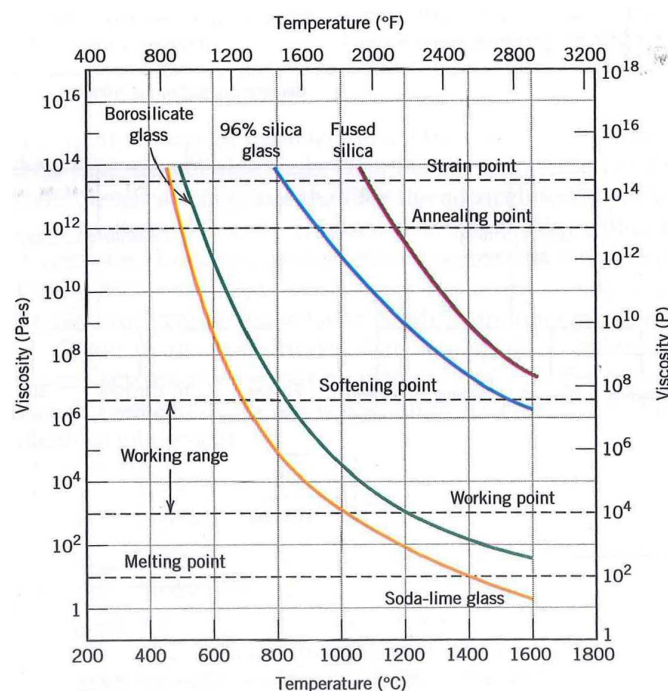


Figure 6 Viscosity states of glass

Source: (Callister, 2007)



## 1.1.3 OVERVIEW OF GLASS PROPERTIES

Glass has some unique properties. It is known for its transparency and fragility, what makes it an interesting, but challenging building material.

The fragility of the glass is caused by the brittleness of the material. Like a typical brittle material, glass will fracture without any plastic deformation (Callister, 2007; O'Regan, 2014). This means that local stress concentrations cannot be redistributed, which results in cracks in the material under high loads (Haldimann, Luible, & Overend, 2008). In Figure 7 a comparison is made with steel, a material that does yield plastically.

What is extraordinary about glass is its significantly higher compressive strength compared to its tensile strength. In theory the tensile strength of glass can reach up to 32 MPa, which is almost ten times smaller than its compressive strength. However, in practice this value is not reliable, and the actual tensile strength will be substantially lower. The reason for this lower tensile strength is due to the presence of flaws on the surface of the glass. Regularly, these flaws are not detectable to the naked eye (Haldimann, Luible, & Overend, 2008). According to Shelby, (2005) when a flaw is present on the surface or edges of a glass sheet, it will most likely develop into a crack when loaded in tension. This is because of the fact that flaws act as stress concentrators, and as explained before, the stress cannot be distributed. The more flaws occur, the lower the tensile strength capacities of the glass will be. As stated before, the compressive strength of glass is significantly higher. The reason for this is caused by the fact that surface flaws cannot develop into a cracks, when a compression load is applied. Therefore, glass compressive strength values are typically around 300 MPa (CESEduPack. 2017d).

Flaws can occur due to several reasons, such as surface contact with any material that is harder than glass, or even due to contact with other kinds of glass pieces (Shelby, 2005). These flaws inflicted during the production process, processing and handling of the glass. Also, flying debris can cause cracks. Next to this, thermal stress generated by rapid cooling of the glass can cause thermal shock, due to which cracks can occur.

Before a flaw develops into a crack, it can be removed (Shelby, 2005). This can be done by, for example, mechanical polishing or chemical etching

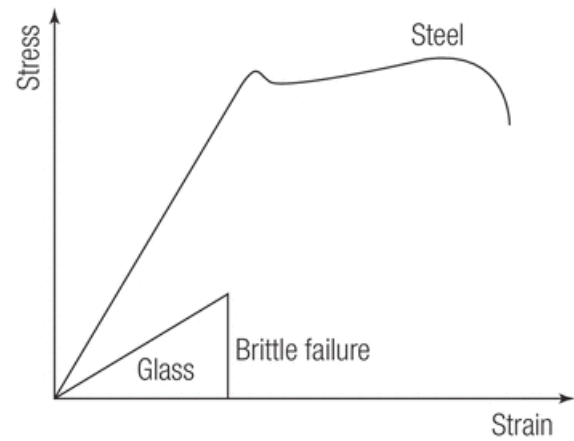


Figure 7 Stress/strain curve glass and steel

Source: (O'Regan, 2014)

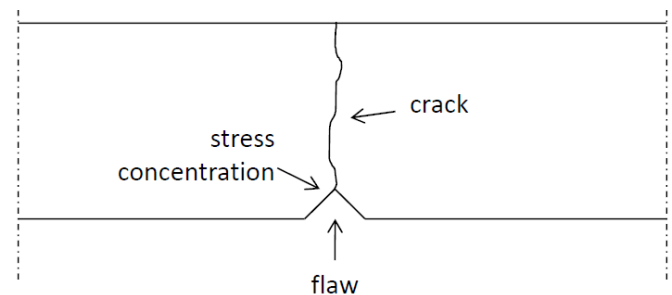


Figure 8 Development of flaw to crack

Source: (Haldimann, Luible, & Overend, 2008)

of the surface. During these processes the flaw is either removed completely or the length of the flaw is reduced below the threshold where above which the flaw can develop into a crack.

Apart from the mainly structural properties of glass, other properties in which glass excels can be distinguished:

- **Hardness:** its high hardness accounts for a good resistance against surface scratches and abrasions (Corning Museum of Glass, 2011e). This makes glass highly suitable for applications such as phone screens and windows.
- **Excellent chemical resistance:** Glass is resistant against many aggressive substances, which accounts for its various applications in the chemical and food industry. Likewise, this chemical resistance makes glass an extremely durable building material (Haldimann, Luible, & Overend, 2008).
- **Good thermal shock resistance:** Although this does account for only certain types of glass, which will be further addressed in the next chapter (Corning Museum of Glass, 2011d).
- **Optical properties:** glass reflects, bends, transmits and absorbs light very accurate (Bell

& Rand, 2006). This is convenient for all sorts of lenses, ranging from glasses to telescope lenses.

Based on the aforementioned properties, it can be concluded that the structural behavior of glass is mainly determined by the applied force and the presence of flaws.

## 1.1.4 GLASS TYPES

The values of the aforementioned properties depend on the glass composition. In this research six main glass families are explained, which can be seen in Table 1. In practice there are numerous different recipes of each type of glass (apart from fused silica and 96% silica glass), which results in different aspects and properties (Bristogianni et al., 2018a). This also means that the value of each property can differ a bit in several glass recipes, but mostly they lie within a small range, so this value can be taken as average.

The six main families are soda-lime glass, borosilicate glass, lead glass, aluminosilicate glass, 96% silica glass and fused silica glass.



### 1) Soda-lime glass:

The vast majority of produced glass is soda-lime (Scalet et al., 2013). Globally, almost 90% of all produced glass is soda-lime (Corning Museum of Glass, 2011d). This type of glass is the least expensive glass available. This glass consists of around 70% silica ( $\text{SiO}_2$ ), 15% soda ( $\text{Na}_2\text{O}$ ) and 8% lime ( $\text{CaO}$ ) (Haldimann, Luible, & Overend, 2008). Soda-lime glass does not withstand sudden temperature changes or high temperatures in general, due to its high thermal expansion coefficient of  $9 \times 10^{-6} \text{ K}^{-1}$ . It is typically applied in the food and packing industry as container glass and used for float glass in for example window panes.



### 2) Borosilicate glass:

This type of glass is mainly applied when good chemical corrosion and thermal shock resistance

are required (Schott, 2010). Borosilicate glass has a low thermal expansion coefficient of  $3,3 \times 10^{-6} \text{ K}^{-1}$ , which allows for sudden temperature changes without cracking. Borosilicate glass contains around 70-80% silica, 7-13% boric oxide ( $\text{B}_2\text{O}_3$ ), around 8% of alkali oxides such as soda or potassium oxide ( $\text{K}_2\text{O}$ ) and 2-7% alumina ( $\text{Al}_2\text{O}_3$ ) (Schott, 2010). Sometimes borosilicate glass contains alkaline-earth oxides, such as lime, but this is not essential. This type of glass is somewhat more expensive to produce, mainly because of its high melting temperature of around  $1650^\circ\text{C}$  (Scalet et al., 2013). However, due to its usefulness in chemical and thermal applications, the cost is in balance (Bristogianni et al., 2018a; Corning Museum of Glass, 2011d). Typical applications of borosilicate are laboratory ware, oven ware, light bulbs and pharmaceutical ware (Corning Museum of Glass, 2011d; Schott, 2010).



### 3) Lead glass:

Lead glass contains a high amount of lead oxide ( $\text{PbO}$ ); at least 24% and around 60% of silica (Schott, 2010). The rest of the glass consists of no special elements such as soda and potassium oxide. Although lead is a toxic material, it has often been applied due to the fact that it gives glass a high refractive index. This provides the glass a certain brilliance, which is preferred in glass artefacts and drinking glasses (Bristogianni et al., 2018a). Nowadays the use of lead in glass for the food and drink industry is not allowed, due to its toxicity (Glass alliance Europe, 2017). Still it is used by glass artists and due to its high electrical insulating properties it is used in electrical applications and thermometer tubing (Corning Museum of Glass, 2011d). Furthermore, it is applied in areas where x-ray machinery is operated: because of the high amount of lead oxide in the glass x-ray radiation cannot pass through the glass and therefore the glass protects people of the harmful radiation (Schott, 2010). Another aspect which is typical for lead glass is its relative softness and low resistance against sudden temperature changes or high temperatures in general (Corning Museum of Glass, 2011d).

### 4) Aluminosilicate glass:

This glass type is somewhat similar to borosilicate, yet it has an even better chemical resistance and it can withstand higher operating temperatures. Aluminosilicate glass consists out of around 55%



silica, 20% aluminum oxide ( $\text{Al}_2\text{O}_3$ ) and around 15% alkaline-earth such as lime or magnesium oxide ( $\text{MgO}$ ) (Schott, 2010). Due to its very high softening temperature, this type of glass is quite challenging to fabricate, which accounts for higher manufacturing costs as well. Aluminosilicate glass can be coated with an electrically conductive film and can be used as resistors in an electrical circuits (Corning Museum of Glass, 2011d). So, main fields of application of this glass are in phone and laptop displays, glass fiber, high-temperature thermometers, halogen lamps and combustion tubes (Corning Museum of Glass, 2011d). Nowadays, aluminosilicate glass is also known under product names such as Gorilla glass; which is a kind of thin glass, mainly applied in phone and laptop displays (Corning, 2017).

1600 °C. No materials are added to help the production this glass, complicating the fabrication of this glass severely. Fused silica is mainly used in space applications (Corning Museum of Glass, 2011d).

In this research the last two types of glass will not be further discussed. The 96% silica and fused silica glass are too hard and expensive to produce compared to the other four types of glass. This results into a very small application field and therefore its recyclable probabilities are very low.



#### 5) 96% silica glass:

This type of glass is produced similarly as borosilicate glass, but the process afterwards makes it a different kind of glass. After the conventional ways of making borosilicate glass, the batch is reheated up to around 1200 °C, which results in that almost all non-silicate elements are removed from the batch (Corning Museum of Glass, 2011d). Due to this, the glass can tolerate thermal shock temperatures up to 900°C, making it highly suitable for space vehicles and some special chemical glassware (Mittal, Kaur, & Sharma, 1992). Because of its extremely high production temperature this is a very expensive glass.



#### 6) *Fused silica glass:*

Fused silica is the most expensive type of glass (Lesko, 2008). It only consist of pure silica in the non-crystalline state (Corning Museum of Glass, 2011d). This type of glass is one of the most transparent glass types that exist, because of its high purity level (Mittal, Kaur, & Sharma, 1992). In addition, fused silica is the most heat resistant glass type: it can withstand temperatures up to 1200°C for a short period and temperatures up to 900°C for longer periods (Lesko, 2008). Its softening point is at a temperature of more than

## 1.1.5 GLASS PRODUCTION TECHNIQUES

Man-made glass has been known to be around for about 4000 years, but information about its invention is lacking. Most likely glass has been discovered by experimenting with heated silica-sand and an alkali. It was only available in really small pieces or chunks and mainly used as an imitation of gems and therefore considered a luxury product (Corning Museum of Glass, 2011c). Over thousands of years different glass production methods were developed and improved, which resulted into glass being the versatile material it is today.

There are numerous glass products available today, which results into several production methods to produce each kind. As visible in Figure 9 there are six main production methods for glass: drawing, blowing, pressing, floating, casting/rolling and extraction.

Since this research focusses on the applications of glass in the built environment, only floating and casting are of interest for extended research.

### 1.1.5.1 FLOAT GLASS

For nearly two millennia flat glass is used to enclose space, without compromising on the desire for openness and light (Wurm, 2007). Hence, flat glass is an important material within the field of architecture and thereby it has many applications in the built environment. Although flat glass has been around for a long time, since Modern times, glass has an unprecedented influence on the field of architecture. The demand for transparency in contemporary architecture is ever increasing, which results in constantly larger window panes and less construction.

For centuries, the production of flat glass was labor intensive and the dimensions of the glass panels were limited. As written by Weller, Unnewehr, Tasche, & Härth, (2009) the main production methods used up until the end of the nineteenth centuries were 'crown glass' and 'blown cylinder sheet glass'. Crown glass is made by a blown glass bulb, which is quickly rotated. Due to the centrifugal forces the glass forms a round sheet. The second production method makes use of a blown glass bulb, which is rolled into a cylinder. When it cools down, the ends are cut off and the cylinder is slit

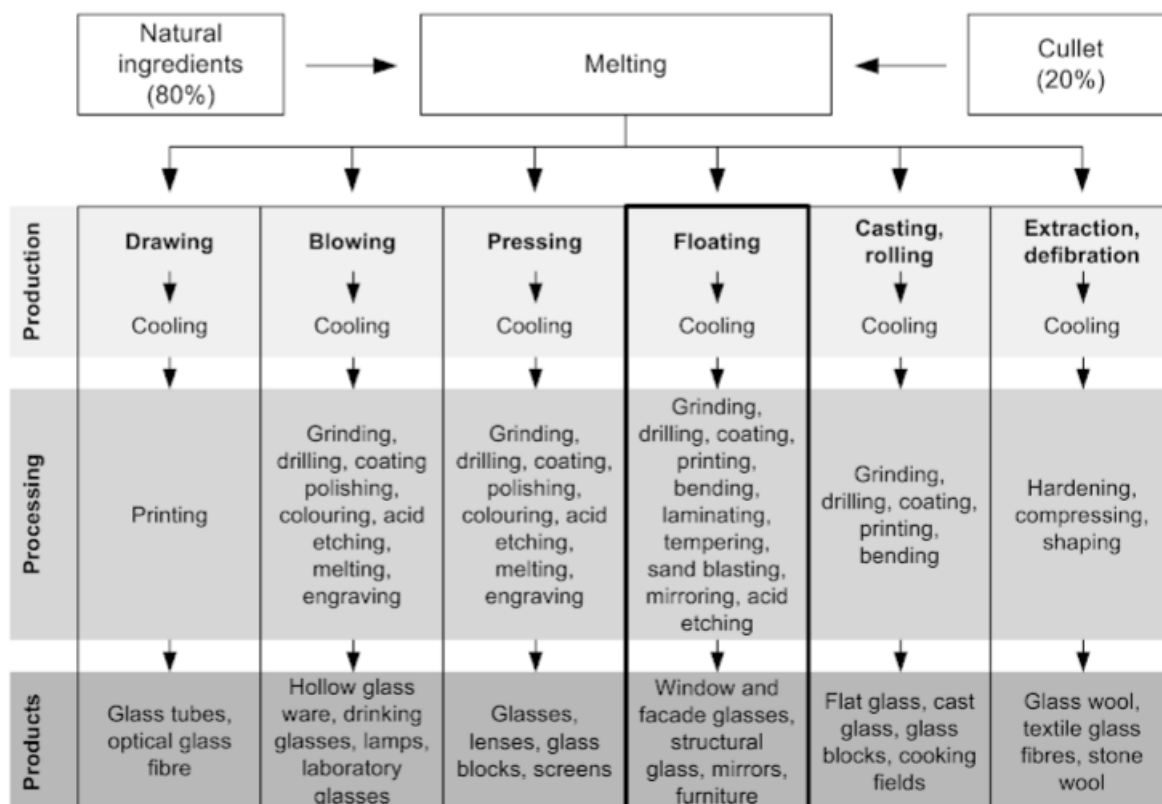


Figure 9 Glass production techniques

Source: (Haldimann, Luible, & Overend, 2008)

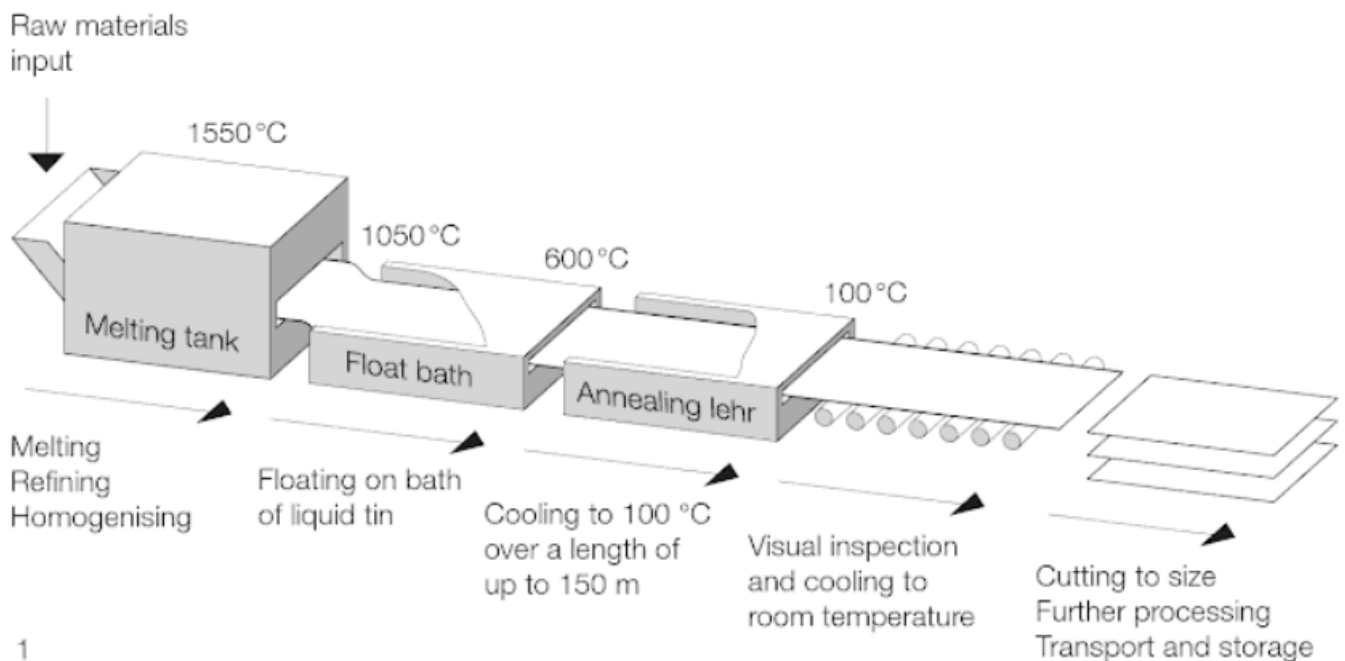


Figure 10 Float glass production

Source: (Haldimann, Luible, & Overend, 2008)

open along its length. After this the cylinder is rolled in a furnace, which creates a flat pane of glass. Both methods have several disadvantages such as high risk of contaminations and flaws and the restricted dimensions of the panels.

Therefore, at the end of the nineteenth and beginning of the twentieth century several new production methods for flat glass were invented, which marks the start of modern glass production techniques (Lauriks, Collette, Wouters, & Belis, 2012). One of these methods is a glass drawing method invented by William Clark of Pittsburgh, where molten glass is vertically drawn out of the melt into rollers. Increased dimensions of the glass sheets were possible, but on the other hand this method causes often unwanted linear distortions in the glass sheets. In addition, this production method produces glass panes with rough surfaces, thereby requiring the panes to be ground and polished to create a smooth surface (Lesko, 2008).

In 1959 this problem was solved by the Pilkington Brothers, who invented the float glass method. Up until today, this method accounts for 90% of the production of flat glass panels worldwide. The advantages of this production method lie in its low cost mass-production, high quality and large possible sizes of the glass panels (Haldimann, Luible, & Overend, 2008).

The float glass method makes use of a molten bath of tin. In a controlled environment molten glass is poured on the molten bath of tin where it will float, due to the lower density of the glass. This will form an endless ribbon of flat glass with constant

thickness. The tin bath provides for an extremely smooth surface of high quality, which does not require any additional grinding or polishing (Lesko, 2008; Weller, Unnewehr, Tasche, & Härth, 2009). The process of float glass is illustrated on Figure 10

Although the float process creates glass sheets with high accuracy, the glass sheets are highly susceptible to flaws due to its small thickness.



## 1.1.5.2 CAST GLASS

Float glass is famous for the application in buildings, whereas cast glass is relatively unknown to the built environment. It is the oldest glass forming technique, whereby glass is poured into a mould, where it will obtain its shape. The technique is used for several applications such as building blocks and art (Haldimann, Luible, & Overend, 2008). High form flexibility and solid 3D structures provide for new types of building systems made through casting glass.

### Methods

Several casting techniques exist for the production of cast glass objects. Not all techniques are relevant to discuss in the context of this thesis. Therefore, only the two main methods suitable for the production of building components will be discussed. These methods are primary and secondary casting processes. The main methods of these primary and secondary processes are *hot-pour casting* and *kiln-casting* respectively (Oikonomopoulou, Bristogianni, Barou, Veer, & Nijse, 2018c)

#### *Hot-pour casting:*

Hot pour casting is a method whereby the raw materials of glass are melted in a furnace and afterwards are poured in a pre-heated mould outside of a furnace. Here, it is left to cool down at room temperature, see Figure 12 (Rich, 1988; Oikonomopoulou, Veer, Nijse, & Baardolf, 2015; Oikonomopoulou et al., 2018c). The glass in



Figure 12 Hot pour casting method

Source: (F. Oikonomopoulou et al., 2015)

the mould cools down rapidly until it reaches its softening point, the point where the glass object does not deform under its own weight and thus does not need any additional support of a mould (Oikonomopoulou, et al., 2017). During this stage, it is necessary to cool down fast to avoid crystallization of the glass melt. When a glass is crystallized it changes its molecular structure, resulting in an opaque material (Shelby, 2005). At this softening point the glass object is placed in a different annealing oven to gradually cool down to room temperature (Oikonomopoulou et al., 2015).

#### *Kiln-casting:*

The kiln-casting method is a secondary casting process, because already created glass pieces are used and re-heated until the viscosity of the melt is low enough to be cast in the desired shape (Oikonomopoulou et al., 2018c).

In addition, the kiln-casting method differs from the hot-pour method in the way the kiln is used. One kiln is used during the total process of casting glass and the annealing phase (Oikonomopoulou et al., 2018c). Instead of melting glass before putting it into a mould outside the furnace, with kiln casting pieces of crushed glass are either directly placed into a mould in the kiln (so called “free-set”) or the crushed glass is placed into terracotta flowerpots which stand on top of the mould (see Figure 11)

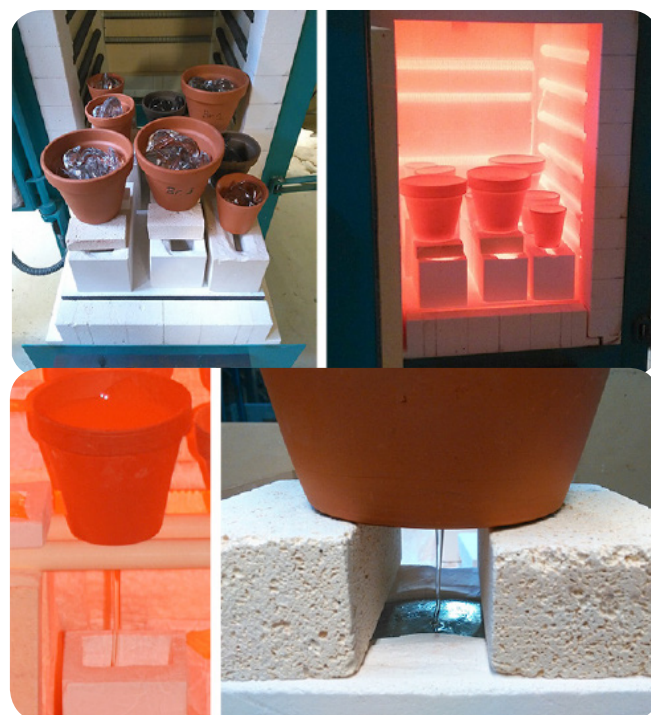


Figure 11 Kiln casting glass with terracotta pots

Source: (Bristogianni et al., 2017b)

(Bristogianni, Oikonomopoulou, De Lima, Veer, & Nijse, 2018b). When heated up the glass directly melts into the desired shape. After the glass has molten, the mould stays in the kiln during both the cooling and the gradually cooling down phase (the annealing phase; which will be discussed in section 1.1.6).

## Mould types

Several mould types are available for casting glass, as described by Oikonomopoulou et al., (2018c). Which type is preferred depends on aspects such as the production volume and the accuracy level of the end-product. The mould type affects the cost and required production time of the glass casting process. The main mould types are either disposable or permanent moulds, which can be subdivided in: disposable mould, open metal mould, metal press mould and a metal adjustable mould. These mould types are illustrated in Figure 13.

Disposable mould types are preferred when a low production volume is required, due to the significantly lower cost compared to permanent moulds. Therefore, disposable moulds are favoured for experimenting with casting glass. This disposable type of mould can be made of silica plaster or alumina-silica fibre. The silica plaster, such as Crystal Cast M248, is most suitable for firings below 1000°C. Alumina-silica fibre moulds are preferred for higher firings, making it also more expensive. For both disposable mould types, post-processing such as grinding is required to remove the translucent and rough layer where the glass was in contact with the mould. This post-processing is labour intensive and time consuming, but inevitable to create a transparent glass object. In addition, these disposable mould types have a lower level of accuracy compared to permanent moulds. Disposable mould types are commonly

used in kiln-casting.

Permanent mould types are made of steel or graphite. The steel moulds can be either adjustable, fixed or pressed, see Figure 13. The graphite moulds can be adjustable and fixed as well. These permanent moulds can be used more than once and are therefore suited to be used in high volume glass casting productions. The hot-pour method is used in combination with permanent moulds, making it a more time-efficient production process compared to kiln-casting. In addition, the level of accuracy is much higher when these permanent (non-adjustable) moulds are used for glass casting. This accounts particularly for pressed steel moulds. Adjustable moulds allow for higher form-flexibility but decrease the level of accuracy. Steel moulds used for hot-pour casting requires a coating to prevent the glass from sticking to the mould (Oikonomopoulou et al., 2015). If the steel mould is correctly pre-heated before casting, the glass object has a glossy and transparent surface, resulting in no or a minimum amount of required post-processing. However, when a complex shape is desired, a steel mould can affect the production cost negatively.

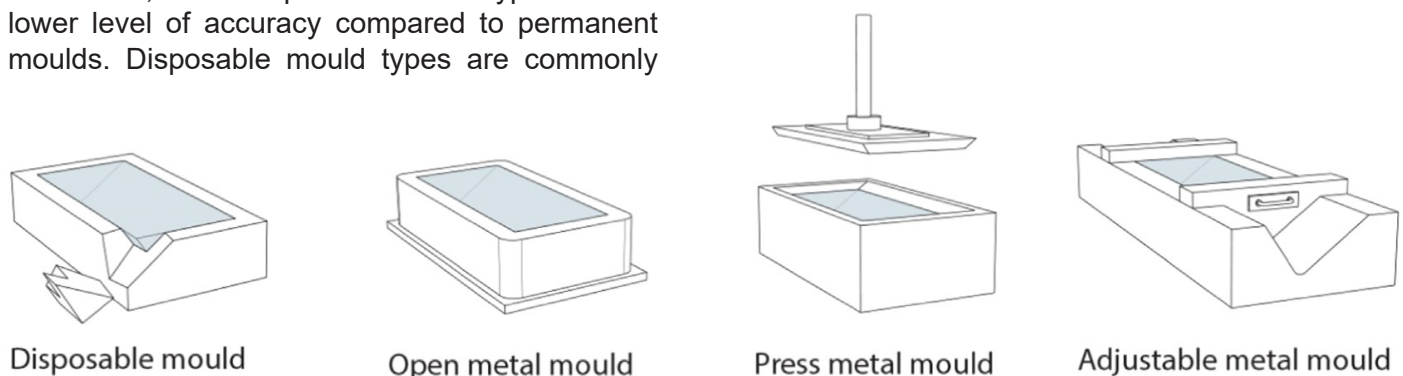


Figure 13 Most common mould types for casting glass

Source: (Oikonomopoulou et al., 2018c)

## 1.1.6 ANNEALING

An important aspect regarding the production of (cast) glass objects is the annealing phase. During this controlled process the glass is gradually cooled down between its annealing point until its strain point. This slowly cooling down of the glass is necessary to release any internal residual stresses and to avoid thermal shock (Shelby, 2005., Oikonomopoulou et al., 2015).

### Internal stresses

Internal stresses occurring in a cast glass object are mainly generated during an incorrect annealing process or introduced due to incompatible variations of the chemical composition of the glass melt (Schott, 2004). For example, when a cast object is cooled down rapidly, natural shrinkage occurs (Oikonomopoulou et al., 2017), however it is possible that its surface cools down faster than its core, creating a compression zone at the surface and a tension zone in the core (Weller, Unnewehr, Tasche, & Härth, 2009). This results into high tensile stresses in the core due to uneven shrinkage. As explained before, glass is a relatively weak material when subjected to tensile forces and therefore the risk of cracking is high. These internal stresses can be relieved when a proper annealing time is applied.

Internal stresses generated due to incompatibility of the chemical composition cannot be relieved by annealing and are therefore permanent (Schott, 2004). Variations in the glass' chemical composition can lead to local differences in thermal expansion coefficients, which result into (local) permanent internal stresses.

The applied annealing time does not solely influence the relieving of (non-permanent) internal stresses, the geometry (shape) has an important effect as well. A rounded geometry provides for homogenous shrinkage (Oikonomopoulou, et al., 2018b), which results into an internal stress-free object. In addition, sharp and pointy edges are not preferred, because they allow for inhomogeneous shrinkage. Also, as mentioned in section 1.1.3, these sharp edges are susceptible to flaws related to damaging.

Annealing time itself depends on several factors, such as the thermal expansion coefficient of the glass, shape (mainly thickness) of the cast object,

mass distribution, how much surface of the element is subjected to cooling, the kiln specifics itself (heating mechanism, size etc.) and the presence other thermal objects in the kiln (Oikonomopoulou et al., 2017).

Annealing is a very slow process. The factor that has the largest influence on the necessary time is the components mass. As Oikonomopoulou, et al., (2018b, p111) states: *"The larger the component, the exponentially longer the annealing time."* An example which perfectly illustrates this problem are the produced cast glass blocks of the Crystal House facade in Amsterdam (Oikonomopoulou, et al., 2018b). The required annealing time of a soda-lime glass block of 65 mm \* 210 mm \* 105 mm and its corresponding weight of 3.6 kg is 8 hours. When the volume of such a block is doubled to 65 mm \* 210 mm \* 210 mm and to a weight of 7.2 kg, the required annealing time increases to 36-38 hours.

The above described factors about annealing have a strong influence on the geometry of the final component, proposed in the design part of this thesis. These factors should be taken into account during the design process of such components, which will be further explained in section 3.2.2.



## 1.1.7 CAST GLASS IN THE BUILT ENVIRONMENT

Currently, cast glass component systems have not been applied a lot in the built environment. The following examples are some of the few existing ones; the *Optical House* in Japan, the *Atocha Memorial* in Madrid, the *Crystal house* in Amsterdam.

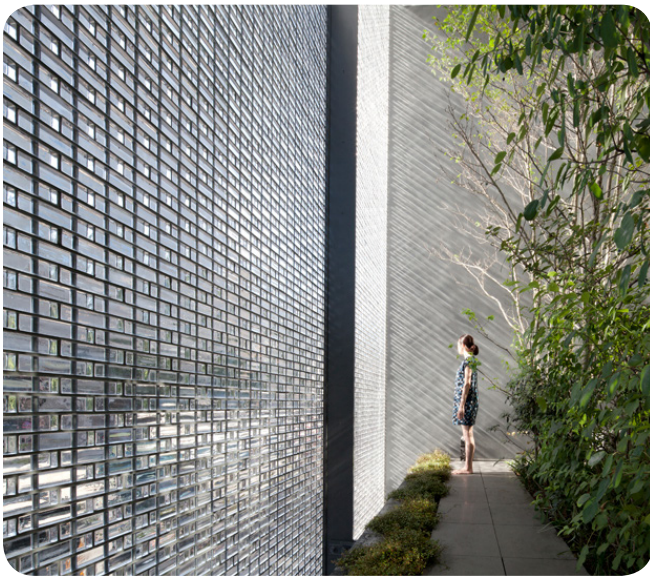


Figure 14 The Optical House in Japan

Source: © hiroshi nakamura & NAP

### The Optical House

This building is designed by Hiroshi Nakamura and located in Hiroshima, Japan. 6000 borosilicate glass blocks create a wall of high optical quality and aesthetic value. This building is an example of non-structural borosilicate cast components. Due to the 8.6 meter high façade with each component of only a thickness of 50 mm, does this façade require a substructure (Frearson, 2013). Although the components are capable of carrying their own weight, a substructure is necessary to withstand lateral forces caused by wind (Oikonomopoulou et al., 2018).

In this case, metal dowels hang from a steel beam at the top of the facade and puncture through the glass components all the way down. This threaded system does not make use of adhesives and is totally dry-assembled.



Figure 15 Component of the Optical House

Source: © hiroshi nakamura & NAP



Figure 16 Construction of the Optical House

Source: © hiroshi nakamura & NAP



Figure 17 The Atocha Memorial in Madrid  
Source: (Paech & Goppert, 2008)

### *Atocha Memorial*

A memorial in Madrid made for the victims of a terrorist attack, designed by architecture firm FAM. This 11 meter high monument is made out of roughly 15600 solid borosilicate glass blocks. Its cylindrical form, the accurate dimensions of the glass blocks and rigid adhesive connections between the glass blocks, account for a self-supporting structure without an additional metal substructure (Paech & Goppert, 2008). Due to adhesive connections, this is a permanent construction.



Figure 18 The components of the Atocha Memorial  
Source: (Paech & Goppert, 2008)



Figure 19 The components of the Atocha Memorial  
Source: (Paech & Goppert, 2008)





Figure 20 The Crystal House facade in Amsterdam  
Source: (©-Daria-Scagliola-Stijn-Brakkee)

### The Crystal house

This project is designed by architecture firm MVRDV. An all glass masonry wall was requested. The façade of 10 by 12 meter consist out of 6500 solid soda-lime glass blocks adhesively bonded together. With a thickness of 210 mm, these blocks provide a self-supporting structure. To intercept the lateral forces, buttresses of the same blocks have been build, resulting in an all glass facade (Oikonomopoulou, et al., 2017). Due to the glued connections, this facade does not allow for dis-assembly.

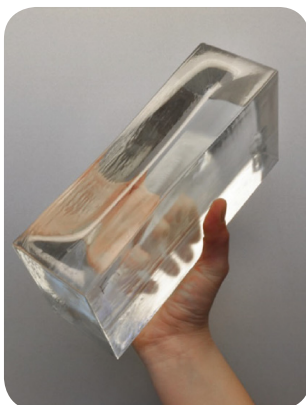


Figure 22 Component of the Crystal House facade  
Source: (Oikonomopoulou, et al., 2017)



Figure 21 Dry-interlocking cast glass components  
Source: (Oikonomopoulou et al., 2018b)

### Interlocking cast glass component systems

Although, the proposed interlocking cast glass component systems are still subject to research, potentially this could provide a good solution to create a reversible facade. A dry-assembled interlocking system provides for both exclusion of adhesive connections and metal substructures. Resulting in a reversible system and high transparency due to the absence of metal substructure (Oikonomopoulou et al., 2018a).

These interlocking cast glass component systems gain their lateral strength through the geometry of the blocks. Assuming that these blocks have accurate dimensions, self-supporting should be no issue, due to the high compressive strenght of glass. Although, dry glass to glass connections are not allowed due to possible cracking, a polymer interlayer should be used to prevent this (Oikonomopoulou et al., 2018a).

Currently, these systems are subjected to research and therefore no actual implementations in the built environment exist yet.

The main cast glass components systems described in this section are illustrated in Table 2. Here, it can be seen that both the systems with a metal substructure and dry-interlocking provide for dis-assembly. However, systems with a metal substructure decrease the overall transparency of a cast glass facade. Therefore, dry-interlocking systems are considered the best possible solution for both dis-assembly and transparency, within the scope of this thesis.

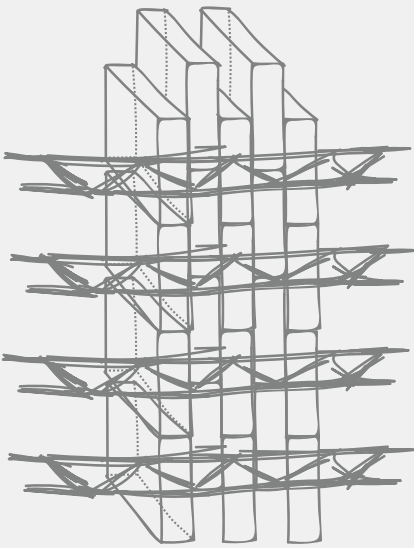
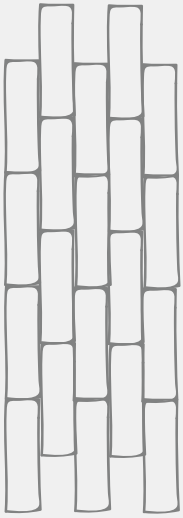
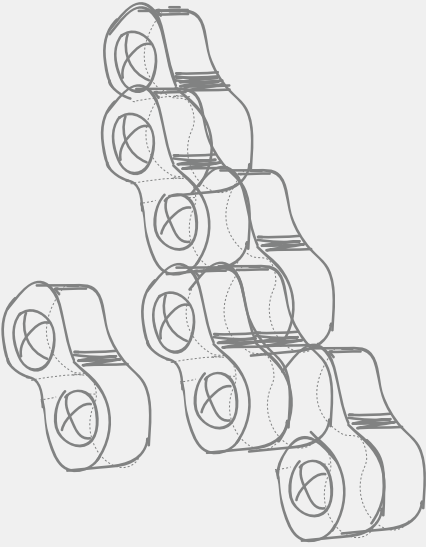
	METAL SUBSTRUCTURE	ADHESIVELY BONDED	INTERLOCKING
STRUCTURAL SYSTEM			
EXAMPLE	Crown fountain/ Optical house	Crystal House/ Atocha memorial	Ongoing research
DIS-ASSEMBLY POSSIBLE	Yes	No	Yes
EASE OF (DIS)-ASSEMBLY	Medium	Low	High
INTERLAYER NECESSARY	?	No	Yes
TRANSPARENCY	Low	High	High

Table 2 three different cast glass component systems

## 1.1.8 INTERLAYER

The chances of failure of an interlocking cast glass facade under axial load are exceedingly low, due to the high compressive strength of glass (Oikonomopoulou, et al., 2018b). In contrast, the tensile strength of glass is rather low.

As glass is a stiff material, imperfect and uneven surfaces of the cast component introduced by the production and handling of cast glass, could generate high local peak tensile stresses when in contact with other imperfections. As described in section 1.1.3, these high local peak stresses could develop into cracks. Therefore, glass to glass contact should be avoided.

To prevent such glass to glass contact an intermediate layer is necessary, see Figure 23. As seen in section 1.1.7, a layer of glue could be a solution. However, this is not a convenient solution in context of this thesis, because a glued connection is non-reversible and non-recyclable.

Hence, a dry-interlayer is proposed for accommodating an even stress distribution between the interlocking cast glass components (Oikonomopoulou, et al., 2018b). Several criteria are defined to determine the most suitable material of such a dry-interlayer applied between cast glass components. These criteria are described in section 3.4.4.

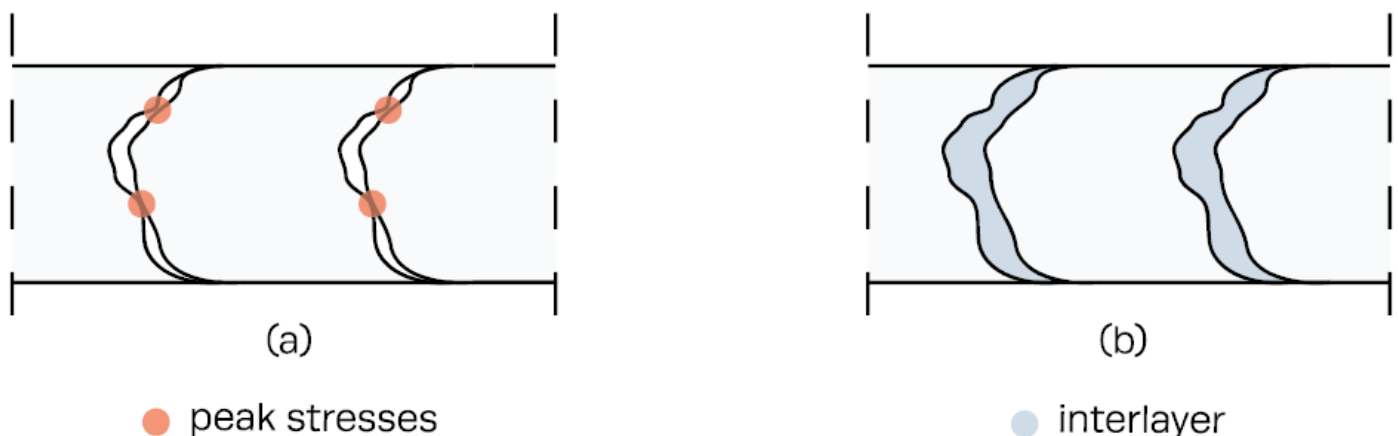


Figure 23 (a) Peak stresses between two glass components; (b) no peak stresses due to interlayer

Source: (Janssens, 2018) based on (Aurik, 2017)

## 1.1.9 ADVANTAGE OF CAST GLASS COMPONENTS

As shown in the aforementioned case studies in section 1.1.7, cast glass component systems have several interesting properties.

Due to their increased thickness, solid cast glass blocks can maintain a compressive strength of around 200MPa, which provides for carrying the deadload of a facade itself, whereby no an additionally support structure is needed (Oikonomopoulou et al., 2015).

As mentioned in the *Relevance* of this research a promising approach to tackle the problem of contamination of glass cullet is by using cast glass components. Cast glass components can potentially tolerate a higher amount of impurities than glass produced with other production methods, such as float glass and container glass, without lowering its compressive strength or optical quality (Bristogianni et al., 2018a). These cast glass components are solid 3D blocks of glass. Due to their 3D nature, a flaw is expected to be much less critical in a 3D object than in a flat 2D one. In addition, float and container glass industry have strict control demands regarding their end products; flaws are generally not allowed.

The built environment is a rather fixed industry. However, times are changing. The building industry is approaching forward towards a sustainable future. Designing structures for a lifetime and demolishing it afterwards no longer sustains. Demountable structures, which can be disassembled with excellent separation of materials are the future (Worrell & Reuter, 2014).



# 1.2 RECYCLING OF GLASS

## 1.2.1 ENERGY CONSUMPTION OF GLASS PRODUCTION

The production of glass requires high temperatures to melt the raw materials, where a large amount of energy is consumed. In the whole production process, the melting process of the raw materials accounts for the most energy consumption and the highest emission rate.

The origin lies in the carbonates in the batch being heated in a furnace. They decompose during the melting process and release CO<sub>2</sub> as waste product. Compared to other types of glass such as borosilicate and lead glass, soda-lime glass typically uses a high amount of carbonates as raw material. As a result, soda-lime glass generates a significantly higher amount of process emissions than borosilicate glass or lead glass (Schmitz, Kamiński, Maria Scalet, & Soria, 2011).

The furnace which is used during the production of the glass is fueled by fossil fuels such as natural gas or oil. Currently, natural gas is primarily utilized, followed by oil (Marcu, Roth, & Stoefs, 2014; Scalet, Garcia Muñoz, Sissa Aivi, Roudier, & Luis, 2013). Appropriate technology for furnaces to operate only on electricity is currently not available for mass production. Therefore, furnaces operating on a combination of fossil fuel and electric boosting, are for now the best performing solutions (Marcu et al., 2014). Electric boosting can be used to accelerate the melting process in a furnace and thus reduce the overall consumption of fossil fuels (Stormont, 2010).

Cullet can be used to significantly reduce the amount of energy consumption during the melting process of the glass production (Scalet et al., 2013). In this literature study, cullet is referred to as “broken glass” or “crushed glass”. This can either be purified broken glass as “furnace-ready” cullet, or contaminated broken glass as “collected” cullet, which needs to be made clear in the context of the text. This means at this point, the cullet referred to is purified broken glass suited to be re-melted.

With every 10% of cullet added to the batch of melting mass, it reduces the energy consumption of the melting process around 2.5-3.0% (Scalet et al., 2013). In addition, the cullet reduces the need for extraction of new raw materials, since cullet

can substitute those (Marcu et al., 2014). Hence, the usage of cullet results in saving energy and raw material (Scalet et al., 2013).

However, a distinction should be made concerning internal cullet versus external cullet. This is important to notice, because the quality of the cullet highly varies between both.

*Internal cullet* is composed of for example rejected glass or offcuts obtained from the production line. As a result, this cullet is of high quality since it has never been in contact with other materials. Therefore, the cullet is directly used as source for a new melting batch (Rodriguez Vieitez, Eder, Villanueva, & Saveyn, 2011; Scalet et al., 2013). So, internal cullet can be seen as furnace-ready cullet.

On the other hand, *external cullet* is composed of post-consumer glass waste or derived from external industrial sources. As a result, the composition of the cullet is not exactly specified and this limits its potential application. Next to this, due to possible contamination, the quality of the external cullet is generally lower than that of the internal cullet (Rodriguez Vieitez et al., 2011; Scalet et al., 2013). External cullet can be purified and used as furnace-ready cullet. However, if after purification the quality of the cullet is considered too low, it will not be used as a source for new glass. Further on in this research in section 1.2.4 dealing with too low quality cullet will be discussed.

## 1.2.2 CONTAMINATION

With glass recycling, challenges arise when external glass cullet is contaminated. These contaminants are materials which are undesired for the further production of glass. Contaminants exist in many forms: they can cause problems during the production and prevent the quality of the end product to meet the requirements. Contaminants can cause unaccepted inclusions, such as solid inclusions, air bubbles and knots (GROUP NSG, 2011), which results in flaws and defects in the final glass product.

According to Rodriguez Vieitez et al., (2011), the contaminants can be subdivided in two groups: non-glass material contaminants and contaminants of different kind of glass types, than the requested type for new glass manufacturing.

### The non-glass contaminants:

- Metals (cans, caps and wires)
- Ceramics, stones and porcelain (CSP)
- Glass ceramics
- Organics (food remains, plastics, textiles)
- Hazards (chemical or medical remains)

Of these contaminants, the most problematic are the ceramics, stones and porcelain (CSP) parts and glass ceramic parts. These parts have a substantial higher melting point than glass cullet. Upon melting the CSP parts and glass ceramic parts might not melt completely, depending on their size. Both can cause unaccepted inclusions in the glass.

Metals can be accounted for the second most problematic contaminant. Upon melting of the glass

Standard	Typical Limits	Typical Levels
Ferrous metals	<50 g/tonne	clear 20-40 g/tonne amber 20-35 g/tonne green 20-35 g/tonne
Non-ferrous metals	<20 g/tonne	<1 g/tonne
Ceramics and stones	<20 g/tonne	clear 20-40 g/tonne amber 20-35 g/tonne green 20-35 g/tonne
Organics	3,000 g/tonne	clear 1,000-1,500 g/tonne amber 1,000-1,800 g/tonne green 1,200-1,800 g/tonne
Moisture	shows no drainage	shows no drainage (<2%)
Particle size	<50 mm	<50 mm
Principal Colour	Typical Limits	Typical Levels
Clear	amber <2% green <2%	amber negligible green 0.5%
Amber	green <10% clear <12%	green 0-10% clear 2-8%
Green	amber <10% clear <12%	amber 0-10% clear 0-10%

Table 3 Contamination of cullet



cullet metal parts fall down towards the bottom of the furnace, where they can cause problems to the furnace. Additionally, aluminum from cans or caps reacts with the glass melt, introducing silicon metal spheres in the glass. Iron is less dangerous to the furnace or the righty of the glass, but apart from inclusions it can cause color changes in the end product as well.

### **Different composition glass contaminants**

Other types of glass than the main cullet type can affect the quality of the glass product as well. Currently, the glass recycling industry is effectively a soda-lime container glass recycling industry. Further on in section 1.2.5 will be elaborated on the current recycling industry. However, this means that for example borosilicate glass and lead glass parts are unwanted during the melting of soda-lime glass (Rodriguez Vieitez et al., 2011). Borosilicate glass has a undesirable higher melting point than soda-lime, which may cause inclusions in the glass product. Lead glass is unwanted as well, despite having a lower melting point: lead particles will end up in the glass product. Since lead is a toxic material this is a undesirable effect. Currently, the container glass industry maintains a maximum of allowed lead particles in the glass, since these containers are in contact with food (Glass alliance Europe, 2017). If more than allowed lead particles are present, the whole batch is being discarded.

A second reason for the limited recycling industry is caused by quality requirements of the various glass sectors. These sectors will be explained in section 1.2.7. Moreover, each sector has a certain acceptable contamination range (Rodriguez Vieitez et al., 2011). For example, the flat glass production is prone to contamination, therefore almost no foreign parts are allowed. In comparison, the container glass production usually allows around 20-50g of contamination per ton of glass (20-50 ppm) introduced by metals and ceramics, see Table 3 .

Therefore, the flat glass industry mainly uses internal cullet for their production, whereas the container glass production uses external cullet varying from <20 to >90% per batch, with an European average of around 50 % (Scalet et al., 2013).

Colored glass can also be accounted for quality problems of the desired end product. The container glass sector is the one that uses the most colored glass. The colors that are used are clear/flint, green, brown/amber and a color mixture. These colors are not added for any environmental reason, but are just commercially requested. There are several levels of acceptance of faulty colors in a batch, depending on the desired end product (Rodriguez Vieitez et al., 2011; Worrell & Reuter, 2014). As visible in Table 3, clear glass is way more prone to color contamination than amber and green glass. For example, if a clear lens for a telescope is requested, already a small part of brown or green glass in the cullet will affect the whole batch. In this case, the 'clear' lens will have a slightly colored tint.

## 1.2.3 CLOSED-LOOP RECYCLING

By adding glass waste as cullet back into the glass production process, a closed recycling loop is created. This is possible, because glass has the possibility to be endlessly recycled without lowering its performance (Bristogianni et al., 2018; Worrell & Reuter, 2014).

In practice, this closed-loop recycling is mainly the case for soda-lime container glass industry. As written by Worrell & Reuter, (2014), this closed-loop recycling has several environmental benefits:

- *Lower amount of required raw materials.* As aforementioned in section 1.2.1 the use of cullet provides for less raw material needed for the production of glass. Although, the raw materials used for the production of glass are not considered scarce, its acquisition of the earth's crust does use high amounts of energy. The main energy source used for mining these materials, are fossil fuels such as coal and gas, which provide for emission of greenhouse gasses.
- *Reduction of waste.* As explained in section 1.1.3, under normal conditions glass does not chemically react with other substances. This inert properties mean that glass does not decompose, is insoluble and does not leak toxic substances to the groundwater. However, glass waste utilizes space on landfills. Worldwide, this land could be exploit for a more useful function, since valuable land is scarce.
- *Reduction of energy and air pollution.* As stated in section 1.2.1, the use of cullet in the glass production process provides for a significant reduction of energy and thus a reduction of emitted greenhouse gasses.

## 1.2.4 OPEN-LOOP RECYCLING

Cullet that has been considered of too poor quality or cullet of different glass types are rejected out of the closed-loop recycling process. This cullet is either exported, recycled for alternative applications or discarded to landfills. If the cullet is applied in alternative outlets, it is called open-loop recycling (Worrell & Reuter, 2014). Currently, often borosilicate glass is subjected to open-loop recycling.

Alternative outlets for the discarded glass cullet have a broad range of variety. Ranging from the production of glass wool insulation, via glass ceramics, to aggregate for highway construction. For example, glass has proven to be highly suitable for aggregate in highway construction. The glass strength, stiffness and hardness provide for high abrasion and freezing resistance, which is important in highways (Worrell & Reuter, 2014).

Several solutions for alternative outlets exist, which depend on the type of glass waste. Research to these alternative outlets is an ongoing process and new and better solutions are available every day. These alternative outlets are out of the scope of this thesis as these outlets are considered down-cycling and not recycling of the glass waste.

## 1.2.5 EXPLORATION OF THE CLOSED-LOOP RECYCLING OF SODA-LIME CONTAINER GLASS

Figure 24 illustrates how the current recycling industry of soda-lime container glass operates (Nedvang, n.d.; Worrell & Reuter, 2014).

Household glass waste is collected at public collection points. Together with glass waste from companies it is picked up by trucks. These trucks bring the glass waste to the glass recycling plant. Here, the first step is to manually remove obvious pieces of waste such as plastics and ceramics. Then the glass pieces are crushed into small parts. The next step is to remove with a magnet all metal parts such as lids and caps. Hereafter, a sort of vacuum cleaner sucks all the smaller plastic and paper parts out of this stream. Next, a series of machines with Hyper Spectral Imaging (HIS) technology or laser technology can detect the remaining pieces of ceramics, stones and porcelain and removes them with air pressure guns (Verening Nederlandse Glasfabrikanten, 2012). The last step is again, manually remove the remaining non-glass parts, which are not detected by the machines. This process ends with a quality check to see if the cullet is suitable to use for glass production. If this is not the case, this batch of cullet is sent back into the recycling process. If afterwards the degree of contamination is still considered too high to be recycled, it will be used in the aforementioned alternative outlets, or discarded to landfills.

In the case that the quality of the cullet is approved, it is transported to the glass manufacturers where it will rest for several weeks, to remove all the remaining organic residues. These residues need a certain time to decompose. When this process is done, the cullet is suitable to use as source for the glass production. The next step in the cycle is the manufacturing of new glass products. These products will be sold and used by companies and households again, making the cycle complete.

Currently, the closed-loop recycling process is not fail proof, resulting in contaminated batches of cullet. As stated before in section 1.2.2, contaminations such as the CSP parts cause flaws or defects in the end product or disturb the recycling process.

Even though technology is available to remove these parts, in every recycling process a certain amount of CSP's is not recognized. Therefore, the machinery is not capable to remove them (Verening Nederlandse Glasfabrikanten, 2012). This accounts for glass ceramics and different types of glass as well. Because of their glass appearance, the detection machinery does not always recognize these parts (Rodriguez Vieitez et al., 2011). This means that consumers need to be made aware that solely soda-lime glass products can be recycled within the current recycling logistics and other glass types cannot be thrown in the same glass collection containers.

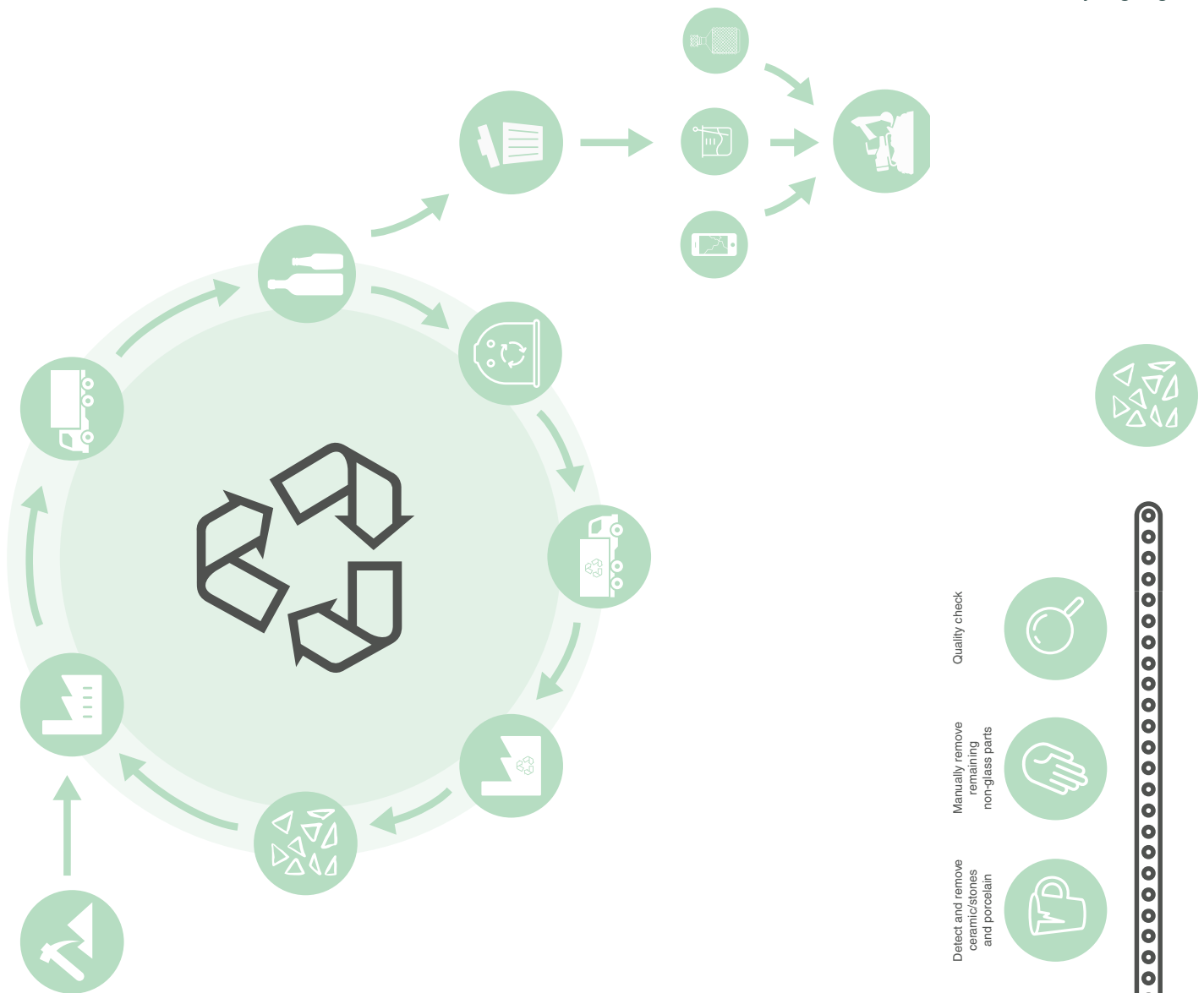


Figure 24 Cycle of recycling scheme

Source: (own drawing)



Quality check



Manually remove remaining non-glass parts



Detect and remove ceramic/stones and porcelain



Remove all plastic and paper waste



Remove all magnetic parts



Crushing the big glass parts



Manually remove big non-glass parts



Figure 25 Glass recycling in factory

Source: (own drawing)

## 1.2.6 CURRENT RECYCLING NUMBERS

### The Netherlands

In 2014, the collection rate of container glass in the Netherlands is as high as 80%, whereas the European Union (EU28) average is 74% (Verening Nederlandse Glasfabrikanten, 2012; FEVE, 2016). Out of these 80% collected container glass cullet, 68% is being used for new container glass products. (Verening Nederlandse Glasfabrikanten, 2012). On Figure 28 is visible that within the EU28 different collection rates are present and mainly Eastern Europe accounts for recycling rates below average.

Unique in Europe is the flat glass recycling company in the Netherlands; Vlakglas recycling Nederland. This company does not exclusively collect flat glass of the building sector, such as waste of building renovations, glazier, contractors, but collects flat glass waste provided by citizens as well (Vlakglas recycling Nederland, 2016). Several municipalities have collection points where people can bring their flat glass waste. Almost every flat glass piece is qualified to be recycled. The cullet from this recycled flat glass is used for 73% in the container glass industry; 19% is used in the production of glass wool and merely 4% is used in the float glass industry (Vlakglas recycling Nederland, 2016). Float glass is highly susceptible to flaws, which explains the low percentage of using external cullet for the float glass production. Most recycled external cullet contains more than the acceptable amount of contaminations for the production of float glass (GROUP NSG, 2011).

### The European glass industry

The European glass industry accounts for one of the biggest of the world, with a contribution of almost a third of the global glass market (Testa, Malandrino, Sessa, Supino, & Sica, 2017). When looked to data of the Europe Union (EU-27), an estimation can be made about the number of glass produced; waste generated; waste glass collected and glass recycled. The following data obtained through Vieitez et al., (2011) is of the EU-27 in 2007. In 2008 the economic crisis hit the world and the European glass industry has been heavily affected, due to its dependency on sectors such as building and automotive industries (Testa et al., 2017). Currently, the European glass production is increasing and is almost back to the level of 2007, see Table 6. Therefore, the more available data of 2007 will be further used.

In 2007, the total glass production in the EU was around 37.4 Mt, see Table 5. Of this 37.4 Mt produced glass, a total of 25.8 Mt glass waste was generated. This glass waste was for 14.85 Mt collected, which means 10.95 Mt glass was directly discarded to landfills.

Out of this collected glass waste of 14.85 Mt, 11.8 Mt glass has been recycled. The main part of the rest of the collected glass waste was being down-cycled to aggregate or ended up in landfills. A small part of this cullet has been exported out of the European Union. However, this amount is rather small due to high cost of transportation. Therefore, long distance import and export generally do not happen and cullet is preferably recycled locally (Rodriguez Vieitez et al., 2011).

To summarize, 14.85 Mt of glass waste was collected for recycling out of 25.8 Mt of glass waste generated, see . This accounts for a collection rate of 58% in the European Union in 2007 (Rodriguez Vieitez et al., 2011). As mentioned before, these collection rates differ a lot over the European member states. Furthermore, this is only the amount of collected glass, not the actually amount of recycled glass. Out of the total generated glass waste of 25.8 Mt is 11.8 Mt recycled, which results into a recycling rate of 46% (Rodriguez Vieitez et al., 2011). This means that not even half of the produced glass in Europe is being recycled.



Figure 26 Container glass collection rate in EU-27



Figure 27 Container glass recycling rate in EU-27



Table 4 Glass recycling numbers of the European Union (EU-27)

Source: Own drawing, based on Rodriguez Vieitez et al., 2011



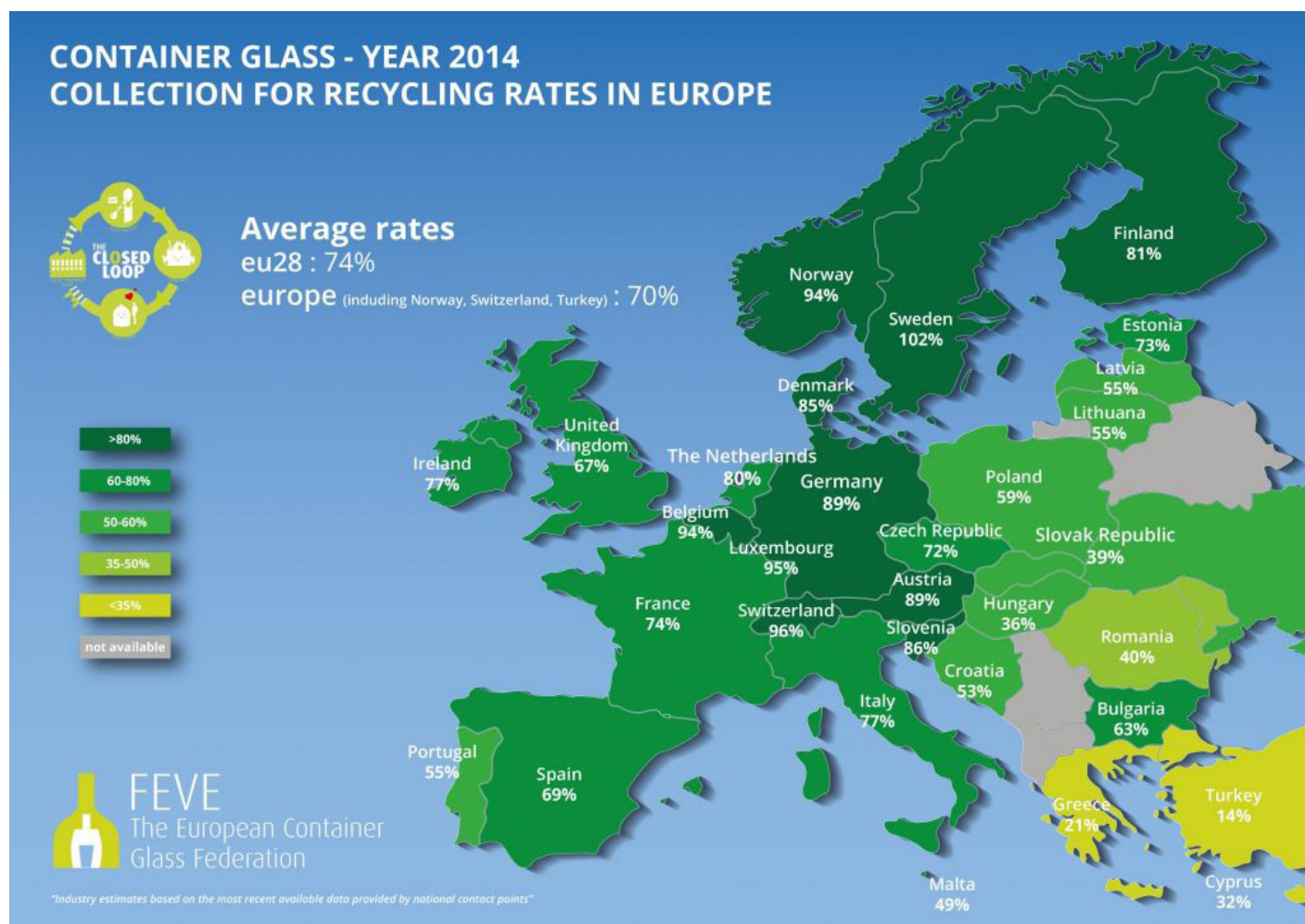


Figure 28 Container glass collection rate

Source: (FEVE, 2016)

Glass type (sector of manufacturing industry)	Production in the EU-27 in 2007 (A)	Waste glass generated in the EU-27 in 2007 (B)	Waste glass collected in the EU-27 in 2007 (C)	Waste glass recycled in the EU-27 in 2007 (D)
Container glass or packaging glass	~21 Mt	~17 Mt	~11 Mt	~8 Mt
Flat glass	~9.5 Mt	~5.1 Mt	~2.9 Mt	~2.9 Mt
Domestic glass (tableware)	~1.5 Mt	~0.8 Mt	~0.5 Mt	~0.5 Mt
Mineral wool	~3.7 Mt	~2.0 Mt	N/A	N/A
Continuous filament glass fibre	~0.7 Mt	~0.4 Mt	N/A	N/A
Special glass	~1 Mt	~0.5 Mt	~0.45 Mt	~0.40 Mt
<b>Total</b>	<b>~37.4 Mt</b>	<b>~25.8 Mt</b>	<b>~14.85 Mt</b>	<b>~11.8 Mt</b>

Table 5 EU-27 statistics on glass production, waste generated, collected and recycled

Source: Rodriguez Vieitez et al., 2011

## 1.2.7 SUBSECTORS OF THE GLASS INDUSTRY

The previous described low recycling number of the total glass production in the EU-27 is caused due to the presence of several subsectors in the glass industry. Each subsector accounts for different production and recycling rates, depending on the market.

The following six subsectors of the glass industry of the EU-27 are defined by Rodriguez Vieitez et al., (2011); Scalet et al., (2013); Schmitz et al., (2011):

1) *Container glass*: this industry is the largest subsector and fabricates mainly bottles and containers for the packaging of food and drinks. In 2007, this accounted for a production of around 21 Mt, which is 56% of the total glass production. Practically all container glass is made out of soda-lime. External cullet is used extensively.

2) *Flat glass*: sheet glass produced for applications in e.g. buildings and vehicles. In 2007, around 9.5 Mt has been produced, 25% of total glass production. Flat glass is made out of soda-lime glass. Virtually only internal cullet is used for the production.

3) *Glass fibre*: mainly applied as reinforcement of polymer composites. Glass fibre is the smallest subsector, with a production of 0.7 Mt in 2007, 2% of the total share. Primarily, aluminosilicate glass is used for the production.

4) *Domestic glass*: typical applications are tableware, cookware and glass art. Of the total production of domestic glass (1.5 Mt; 4% of total glass production), about 80% is soda-lime glass. The other 20% is manufactured of borosilicate and lead glass. Contrary to internal cullet, external cullet is not widely applied due to quality issues and specific recipes of the end products.

5) *Mineral wool*: this industry provides both glass wool and stone wool. Interesting for this research is only the glass wool. This is insulation made of mainly borosilicate glass. Of the 3.7 Mt mineral wool produced, around 1.2 Mt is glass wool.

6) *Special glass*: this subsector manufactures a wide range of different types of glass products,

such as laboratory ware, optical glass, tubing and glass ceramics. Mainly, these products are made of borosilicate and aluminosilicate glass. For the special glass sector external cullet is not widely applied due to high quality demands and specific recipes of the end products.

One note for this category is that this data is of 2007, which does not take into account the increased production of phone and laptop screens made out of aluminosilicate glass. The production of this glass for smartphones basically had just started in 2007 (Corning, 2017). Therefore, the share of the special glass subsector is expected to be higher today.

Table 5 presents per subsector, the numbers of the glass production, waste glass generated, waste glass collected and waste glass recycled.

It should be noted that for the domestic glass subsector the number of recycled waste glass is mainly generated by the recycling of internal cullet. At this point, domestic glass cannot provide a continuous flow of external cullet (Rodriguez Vieitez et al., 2011), or reliable data and statistics are lacking at this point.

For the special glass sector it is stated in Table 5 that the amount of recycled glass was 0.4 Mt. However, more recent data show an estimation of 1 Mt of recycled special glass (Rodriguez Vieitez et al., 2011).

The stated data in this section are of 2007, a verification with Table 6 indicates that the numbers used in this research still account for today.



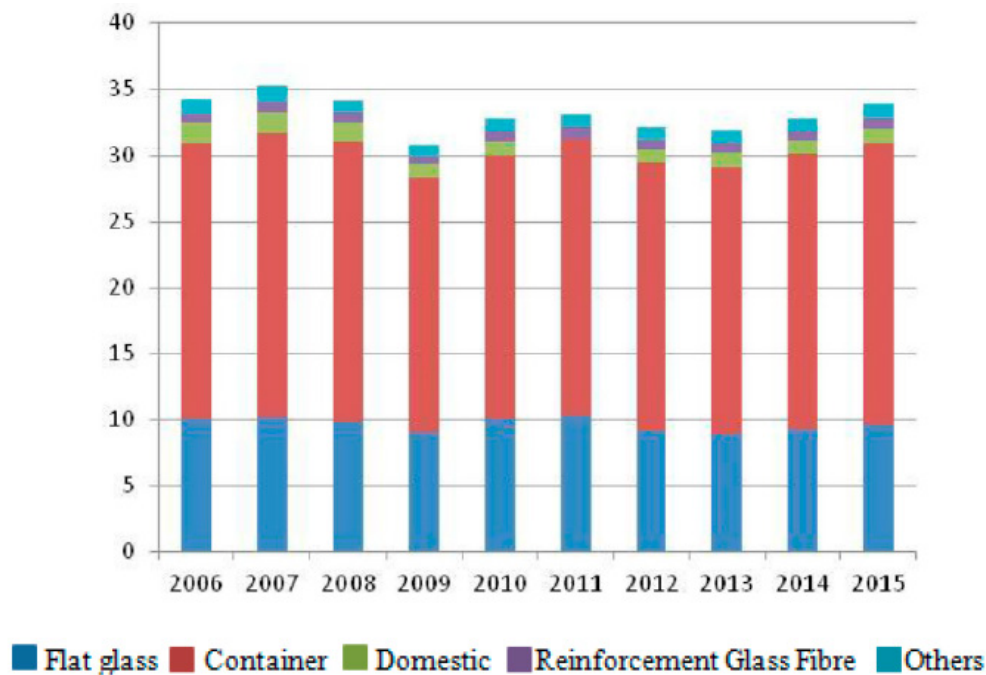


Table 6 EU-28 evolution of the glass subsectors

## Recycling of other glass types

The aforementioned subsectors all produce a certain amount of waste, however only a small share (apart from the container glass industry) is currently being recycled. Other than the container glass industry and in the Netherlands the flat glass recycling, most glass products end up on landfill disposal (Bristogianni et al., 2018; Rodriguez Vieitez et al., 2011). Other glass types cannot be recycled within the same recycling industry of the soda-lime glass container glass, due to a difference in chemical composition, higher melting temperature etc.

Other types of glass products who are currently not recycled can be anything such as household waste (cooking and tableware), laboratory waste and glass waste of electronic devices. A recycling industry for each different glass type does currently not exist. Most of these types of glass waste are considered not recyclable, owing to e.g. a small market, a difference in recipes or contamination such as adhesives and coatings. In the case of glass waste of e.g. electronic devices a complicated disassembly provides for the non-recycling of this glass (Bristogianni et al., 2018).

## 1.2.8 MOST SUITABLE TYPE OF GLASS FOR RECYCLING

To define which type of glass is the most suitable to recycle and eventually for application into structural cast glass building components, a number of criteria have been set. In Table 7 these criteria are visible for comparison.

Secondly, in Table 8 the same criteria have been set against each other, to draw conclusions which type of glass has the most potential to be recycled into structural cast glass building components.

Of these set criteria soda-lime has the best recyclability possibilities. However, this type of glass is already largely being recycled and its properties in cast glass components have been tested several times. Therefore, other types of glass are more of interest to research further.

The other three types of glass, borosilicate glass, lead glass and aluminosilicate glass all have its advantages and disadvantages for recycling into cast glass components.

Such as lead glass, which has the lowest softening point but a high thermal expansion coefficient. A low softening point is a positive aspect, but a high thermal expansion coefficient makes it less attractive for structural application. Therefore, this type of glass will not be suitable to use in this research. Also, the number of toxic lead particles in this glass will be unfavourable when doing experiments. In addition, its softness causes probably issues too. Lead glass has a lower compressive strength than the other types of glass and the question is if this amount is high enough for application in structural cast glass building components.

After excluding lead glass of the research, aluminosilicate and borosilicate glass are left. Of these two, aluminosilicate glass accounts for the most expensive type, due to its much higher softening point. In addition, when looked at the ease of recyclability this type of glass accounts for the hardest one to collect, since the glass is embedded in electronic devices. An extra step is needed to remove it and make it suitable for recycling.

At this point, borosilicate glass provides for the most interesting and suitable type of glass to be applied in structural cast glass building components. It has some high qualities such as good thermal shock resistance and transparency, which are of interest for the built environment. Additionally, borosilicate glass is expected to have the most waste collection potential, because it is widely available in for example households, laboratory's, schools and hospitals.

	SODA- LIME	BOROSILICATE	LEAD GLASS	ALUMINO SILICATE
PRICE	€	€ € €	€ €	€ € € €
SOFTENING POINT °C	700	820	585	884
COMPRESSIVE STRENGTH (MPa)	315	300	260	420
THERMAL EXPANSION COEFFICIENT at 20 °C in 10 <sup>-6</sup> K <sup>-1</sup>	9	3,3	10,6	3,2
WASTE GENERATED (Mt) (data of 2007)	~ 22,1	~ 0,5 (Total 'special' glass waste)	~ 0,3	~ 0,5 (Total 'special' glass waste)
EMBODIED ENERGY RECYCLING MJ/kg	8,24	17,5	18,3	10,9
EASE OF RECYCLABILITY	++	+	--	--

Table 7 Comparison between the four main glass types; values

	SODA- LIME	BOROSILICATE	LEAD GLASS	ALUMINO SILICATE
PRICE	++	--	+	--
SOFTENING POINT °C	+ -	-	+	--
COMPRESSIVE STRENGTH (MPa)	+	+	-	++
THERMAL EXPANSION COEFFICIENT at 20 °C in 10 <sup>-6</sup> K <sup>-1</sup>	--	++	--	++
WASTE GENERATED (Mt) (data of 2007)	++	-	--	-
EMBODIED ENERGY RECYCLING MJ/kg	++	--	--	+
EASE OF RECYCLABILITY	++	+	--	--

Table 8 Comparison between the four main glass types; rating

# 1.3 BOROSILICATE GLASS

## 1.3.1 A BRIEF HISTORY ABOUT BOROSILICATE GLASS

In 1882, glass chemist Otto Schott invented a type of glass that could endure sudden temperature changes without cracking. The solution was to add a certain amount of boron to the glass composition. Immediately, this heat resistant glass was a success. By 1915 Corning chemist W.C. Taylor developed a borosilicate glass with even higher temperature tolerances. From this borosilicate glass cookware has been developed, commercially known as Pyrex or Duran. Until today, Pyrex cooking ware is used largely (Corning Museum of Glass. 2011b).

## 1.3.3 BOROSILICATE GLASS IN THE BUILT ENVIRONMENT

Generally, borosilicate is not applied much in the building industry, mainly due to its expensive production process. However, certain aspects of borosilicate glass are of interest for built environment, proven by examples such as the *Atocha Memorial* in Madrid (Paech & Goppert, 2008) and the *Optical house* in Hiroshima (Hudson, 2013). These aspects are:

- *High optical quality:* extremely clear building components can be achieved through using borosilicate glass (Frearson, 2013; Paech & Goppert, 2008).
- *Fire resistance:* borosilicate is resistant to fire, in contrast to soda-lime glass. The explanation for this is its low thermal expansion coefficient, which accounts for resisting the stress introduced by the high temperatures of the fire (Weller, Unnewehr, Tasche, & Härth, 2009).
- *Low thermal expansion coefficient:* not only is a low thermal expansion coefficient favorable for fire resistant glazing, it also provides for a significantly lower amount of natural shrinkage upon cooling of the glass product (Oikonomopoulou et al., 2017). This results in more accuracy in the dimensions and less required post-processing of the end product. This low thermal expansion

coefficient provides for a good thermal shock resistance as well.

- *Excellent chemical corrosion resistance:* glass does not react to aggressive substances, but of more importance for a building is its good UV-radiation resistance. Unlike plastics, glass does not crumble when exposed to UV-radiation (Haldimann, Luible, & Overend, 2008).

## 1.3.2 AMOUNT OF PRODUCED BOROSILICATE GLASS

Borosilicate glass is produced for two subsectors: the domestic glass sector and the special glass sector. As mentioned in section 1.2.7 and Table 5 the share of borosilicate glass products within the domestic sector is rather small. Less than 20 percent of the domestic glass production of 1.5 Mt/year is of borosilicate glass (Scalet et al., 2013). The special glass subsector as a whole (1 Mt/year) is comparatively small to the container glass sector (21 Mt/year).

However, within the special glass subsector borosilicate glass is applied most. In the European union of 2005, an total of 434.000 ton borosilicate glass has been produced within the special glass sector (Scalet et al., 2013). In addition, this is the actually produced amount of borosilicate glass, whereas the sector has a higher capacity. In Table 9 is visible that the production of borosilicate glass tubes and bulbs is slightly over half of its possible capacity, which accounts for the other borosilicate glass products as well.

For the domestic glass sector no reliable data could be found on the exact amount of borosilicate produced. However, an estimation could be made based on the total share of the sector. A maximum of 20% is made of borosilicate glass, which accounts for 300.000 ton/year.

The total estimation of the borosilicate glass production is around 734.000 ton/year for the European Union. Compared to the total share of

Glass type	Production (tonnes)	Capacity (tonnes/yr)	Sector capacity (%)
CRT glass (panel and funnel)	230 000	280 000	21.7
Glass tubes and bulbs	384 000	692 000	53.5
Borosilicate glass (excluding tubes)	50 000	90 000	7.0
Other lighting glass (excluding quartz, tubes and bulbs)	30 000	60 000	4.6
Glass ceramics	55 000	120 000	9.3
Quartz glass	5 000	15 000	1.2
Optical glass	6 000	10 000	0.8
Other glass types	10 000	25 000	1.9
<b>Total special glass</b>	<b>770 000</b>	<b>1 292 000</b>	<b>100.0</b>

Table 9 Subsector special glass divided in production per glass type

Source: (Scalet et al., 2013)

37.4 Mt/year glass produced, this is a minor part. However, Rodriguez Vieitez et al., (2011) states in Table 5 that 0.5 Mt/year special glass waste is generated. In an estimation could be derived that half of 734.000 ton glass accounts for 367.000 ton/year of borosilicate waste generated. If this number of glass is not being recycled but discarded, an enormous of glass waste ends up at landfills.

### 1.3.4 OPPORTUNITIES OF RECYCLING BOROSILICATE GLASS

Current recycling methods for external borosilicate cullet are non-existing. It is not allowed to throw borosilicate glass in container glass collection containers, due to the higher melting point of this glass and a difference in chemical composition (Verening Nederlandse Glasfabrikanten, 2012). Such collection containers do not exist for borosilicate glass, resulting in borosilicate glass being thrown in general household waste. After collection of this household waste, it is either burned or discarded to landfills. During the burning of the household waste the borosilicate glass does not melt, resulting in residual waste for landfills. This waste utilizes valuable land and due to a world wide population growth a decrease in the amount of waste is not expected. Therefore, throwing away such a high quality glass accounts for a lost

opportunity.

In addition, the production of borosilicate glass has compared to soda-lime glass a significantly higher energy consumption and emission rate. This is illustrated by Scalet et al., (2013) in Table 10. It has to be noted that this data refers to a part of the special glass sector.

However, as mentioned before, borosilicate glass has the biggest share in the special glass sector. As illustrated in Table 10, the energy input of borosilicate glass is around 14 GJ per tonne melted glass. This is considerably higher compared to 9 GJ for the production of soda-lime glass. Additionally, the CO<sub>2</sub> output of melting borosilicate glass is about 1100 kg per tonne glass. Contrary, soda-lime glass melting accounts for less than half (about 500 kg CO<sub>2</sub>/ton melted glass) of borosilicate glass production. Currently, borosilicate glass is produced with the input of around 250 kg internal cullet per tonne melted glass, which is about 25% per tonne melted glass. The aforementioned numbers show a significantly worse production process of borosilicate glass in terms of energy consumption and environmental impact, compared to soda-lime glass.

		<b>Glass Ceramic</b>	<b>Glass tubes (borosilicate)</b>		<b>Glass lamp bulbs (soda-lime)</b>
Type of furnace		Oxy-fuel	Oxy-fuel	Cross-fired regenerative	Cross-fired regenerative
Furnace capacity		30 – 65 t/d	10 – 55 t/d	10 – 55 t/d	50 – 150 t/d
<b>Inputs</b>	Units/tonne melted glass				
Energy, gas	GJ	5.5 – 11	10 – 15	14 – 17	5 – 14
Energy, electricity	GJ	1 – 8			
Internal cullet	kg	250 – 550	200 – 400	150 – 350	100 – 500
<b>Outputs</b>					
<i>Emissions to air</i>					
CO <sub>2</sub>	kg	410 – 500	900 – 1150	950 – 1300	400 – 600

Table 10 Energy consumption of borosilicate tubes

Source: (Scalet et al., 2013)

### 1.3.5 FIELD OF APPLICATION OF BOROSILICATE GLASS

A new purpose for the enormous amount of high quality borosilicate glass waste can be generated. Dry-assembled structural cast glass building components can be the solution.

It might seem counterintuitive to advocate for using a glass type with high energy consumption. However, two points should be noted:

1) Energy consumption can be reduced drastically by increasing the amount of cullet added to the production process. Currently 15 to 35 percent cullet is added in the production of borosilicate tubes, see Scalet et al., (2013) in Table 10. In contrast, the amount of cullet added in the European container glass industry can reach up to 90 percent (Scalet et al., 2013).

2) Designing dry-assembled structures offers the possibility of circular use. Reusing the borosilicate cast glass components avoids future energy investment in their production. Simultaneously, the high-quality borosilicate waste stream ends up being used to full potential in the built environment instead of ending up on landfills.

The goal is to create a closed-loop recycling process for borosilicate glass. To find out where the external borosilicate cullet originates, the field of application of the glass should be explored. As illustrated in section 1.3.5, borosilicate glass is applied anywhere where a thermal shock resistant glazing is expected. For example: laboratory ware, kitchen ware, tubing and pharmaceutical ware.

Only the total share of yearly produced borosilicate waste is known (367.000 tonne/year). The exact amount of borosilicate glass waste per application field is unknown. It is not possible to define how much and where consumers throw away their heat-resistant glass objects. Therefore, estimations shall be made regarding to the highest share of borosilicate glass waste per field. Since the highest borosilicate glass production in Europe is corresponding to the production of tubing, light bulbs and cookware, it can be expected that the most waste will be generated in laboratories, hospitals and households.

#### How to collect and recycle borosilicate glass in the future?

The most optimal solution would be to collect the borosilicate glass waste close to the source. Add glass collection containers especially for heat resistant glazing close to laboratories, schools and hospitals. Or provide for municipal collection points where people can bring their borosilicate glass waste. This is cheaper than providing collection points everywhere, since there is currently no logistics to collect it.

## 1.3.6 BOROSILICATE APPLICATIONS



*Laboratory ware*



*Reinforcing fibers*



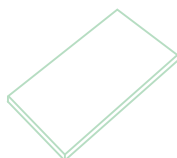
*Cooking ware*



*Flashlight lenses*



*Pipes/tubes*



*Borofloat*



*Pharmaceutical ware*



*Rapid prototyping*



*Light bulbs*



*Telescope lenses*



*Microscope applications*



*Glass art*



### 1.3.7 APPLICATION IN A CASE STUDY

The main advantages of structural borosilicate cast glass components over structural soda-lime cast glass components are its low thermal expansion coefficient and high optical quality for the built environment. Therefore, when considering a case study it is convenient to pick one where these two properties have a prominent role when applied in a building. Such a building is Casa da Música in Porto, see Figure 30. In Portugal high temperature fluctuations can occur, requiring materials that are able to withstand this. In addition, Casa da Música is a concert hall which needs light in the building, but not so much transparency is required. Furthermore, this public building has a prominent status within Porto and the field of architecture, making it highly suitable to showcase the recycling possibilities of borosilicate glass. This all suggest that Casa da Música is a perfect building to show the possibilities of a dry-interlocking cast glass component facade system made out of recycled borosilicate glass.

Designed by OMA in 2005, this building is home to the National Orchestra of Porto (Casa da Musica / OMA, 2014).

The glass facade indicated on Figure 29 has the most potential for application of a dry-assembled borosilicate cast glass component system. Designed to be a dramatic backdrop for the orchestra, this facade was designed with, at the time, innovative and transparent solutions. However, a steel substructure is necessary to withstand lateral wind forces (Casa da Musica / OMA, 2014). As indicated before, structural cast glass components can withstand those forces and no additional substructure is necessary, providing for an uninterrupted facade (Oikonomopoulou et al., 2017).

A more detailed building description can be found in section 3.1.1.

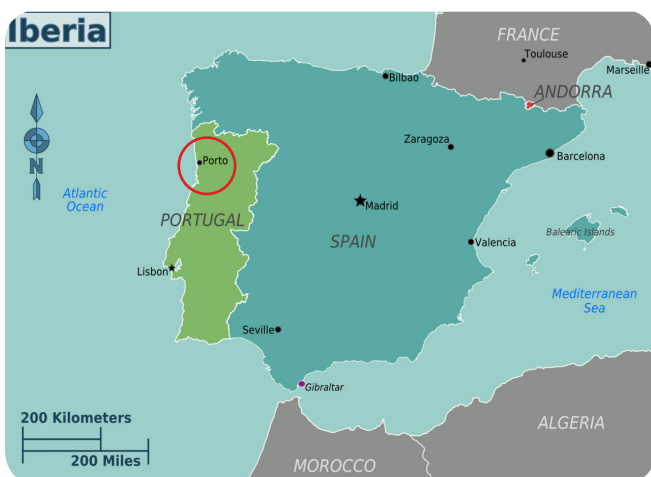


Figure 30 Location of Porto

Source: ("Wikivoyage-Iberia," n.d.)



Figure 29 Casa da Música in Porto

Source: © Philippe Ruault

## 1.3.8 CONCLUSIONS OF THE LITERATURE STUDY

Glass is valuable building material: it is transparent, has high optical quality, high compressive strength and hardness. However, due to its brittleness, a flaw can quickly become critical.

The use of glass cullet upon firing allows for energy reduction, waste reduction and raw material reduction. Lower energy consumption means costs reduction.

Even though borosilicate glass waste is a lot less compared to container glass, still a high-quality glass is thrown away and keeping up space on valuable land.

Cast glass components are interesting because they allow for high transparency, can tolerate more impurities and glass waste can be a material source.

Combining all of the above resulting in borosilicate glass applied in cast glass components, thus high-quality building components made out of waste with a cheaper production process.

Assembled in a dry structure provides for dismantling, reuse and recycling of the cast glass components. In addition, the high-quality borosilicate glass components do not lose their value at the end-of-life.

Therefore, no new materials are required when the components are reused or recycled. This allows for a reduction in production cost and energy consumption.



# **PART 2**

RESEARCH ON  
RECYCLABILITY  
OF BOROSILICATE  
GLASS

## 2.1 RECYCLING LOOP OF BOROSILICATE GLASS

As described in section 1.2.4, a current recycling industry of borosilicate glass does not exist. After the product's end of life it is discarded as waste, either ending up at landfills or downgraded to aggregate. This open-loop cycle is illustrated in Figure 33.

A solution currently not explored, resulting in the loss of a high quality glass. Therefore, this thesis proposes a closed-loop recycling for borosilicate glass, illustrated in Figure 34. Broken borosilicate glass objects such as laboratory ware and oven ware can be collected through curbside collection. In addition to existing curbside collection such as containers for brown, green and white glass, a container specific for heat resistant glass shall be placed. Consumers can throw in all their heat resistant glass waste, because it is not possible by naked eye to determine if an object is heat strengthened soda-lime or borosilicate glass.

As the borosilicate glass waste stream is much smaller than the soda-lime one, a borosilicate glass recycling industry as large as the current soda-lime recycling industry is probably not feasible. Due to the high-quality borosilicate glass these products have a longer expected life time. In addition, the market for these kinds of products is much smaller compared to soda-lime glass products. Therefore, these curbside collection containers will only be placed locally where enough borosilicate glass is expected (e.g. laboratories, universities, 'Milieustraat').

The collected mixture will be sorted and cleaned in newly build or restructured recycling plants. The result is a batch of clean external cullet, ready for the production of new borosilicate glass products. However, this clean external cullet consists of several types of borosilicate glass recipes and possible contamination. Therefore, a fully closed-loop is not feasible within the borosilicate glass industry at this point. A high-quality and specific borosilicate glass melt is required, due to high quality demands of the end products. Contamination and different glass recipes decrease the quality of the glass melt or do not allow proper mixing at all.

In the *Relevance* the possibility of allowing more contamination and impurities in a cast glass component is described. In addition, section 1.2.1 describes the reduced required melting

temperature of a borosilicate glass melt if cullet is used for melting. This results in less energy consumption during production of borosilicate glass and consequently lower production costs. Therefore, applying cast glass components in the cycle of Figure 34, resulting in a new use of recycled borosilicate glass. Figure 35 shows this improved closed-loop recycling of borosilicate glass. The production of cast glass components made of recycled clean borosilicate glass cullet will happen in new or restructured factories. The produced cast glass components can be applied within the built environment. At the end of life of the facade the components can either be reused directly within other buildings or recycled.. Direct reusing the cast glass components allows for a considerable reduction of energy consumption, as the components already exist. Recycling the borosilicate glass components reduces significantly the required energy for production of new cast components, see Figure 31. After purification of the recycled borosilicate glass clean external cullet is available for production of new cast glass components, creating a fully closed-loop.

This closed-loop proposes a mixed collection of borosilicate glass products. However, various products have a different chemical composition. This could introduce problems to the level of mixability of borosilicate glass within the glass melt. To what extent this level of mixability of borosilicate glass is allowable has been researched by experiments. A thorough description of these experiments and corresponding results is described in chapter 2.2.

It should be noted that curbside collection does require some constraints. For example, laboratory ware or hospital ware products contaminated by toxic substances are not suitable for recycling. These products need to be discarded in chemical waste disposals.

*Note: This proposed closed recycling loop assumes the biggest users/consumer groups use the laboratory ware, hospital ware and household ware. However, exact numbers of the total waste per group do not exist. It is not possible to determine exactly how much and where borosilicate glass is thrown away. Nevertheless, it is expected that these groups still provide the most potential recyclable borosilicate glass waste.*





Figure 32 Existing collection containers + new heat resistant glass collection container

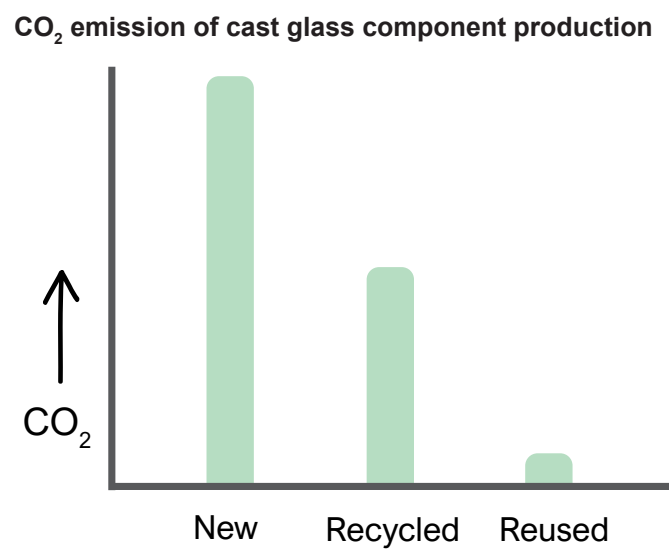


Figure 31 Schematic representation of CO<sub>2</sub> emission of cast glass component production.

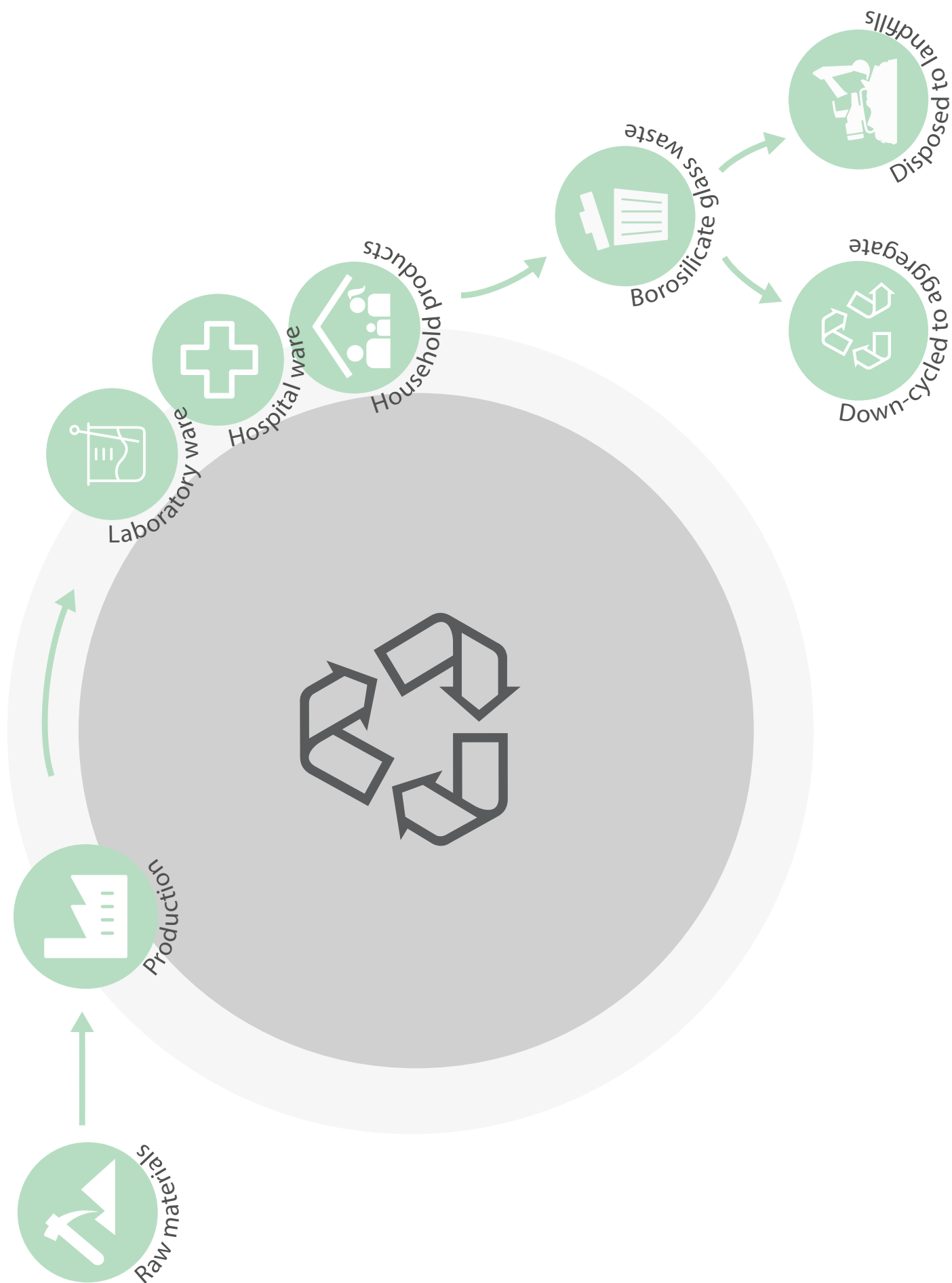


Figure 33 Current open-loop recycling of borosilicate glass

Source: Own drawing

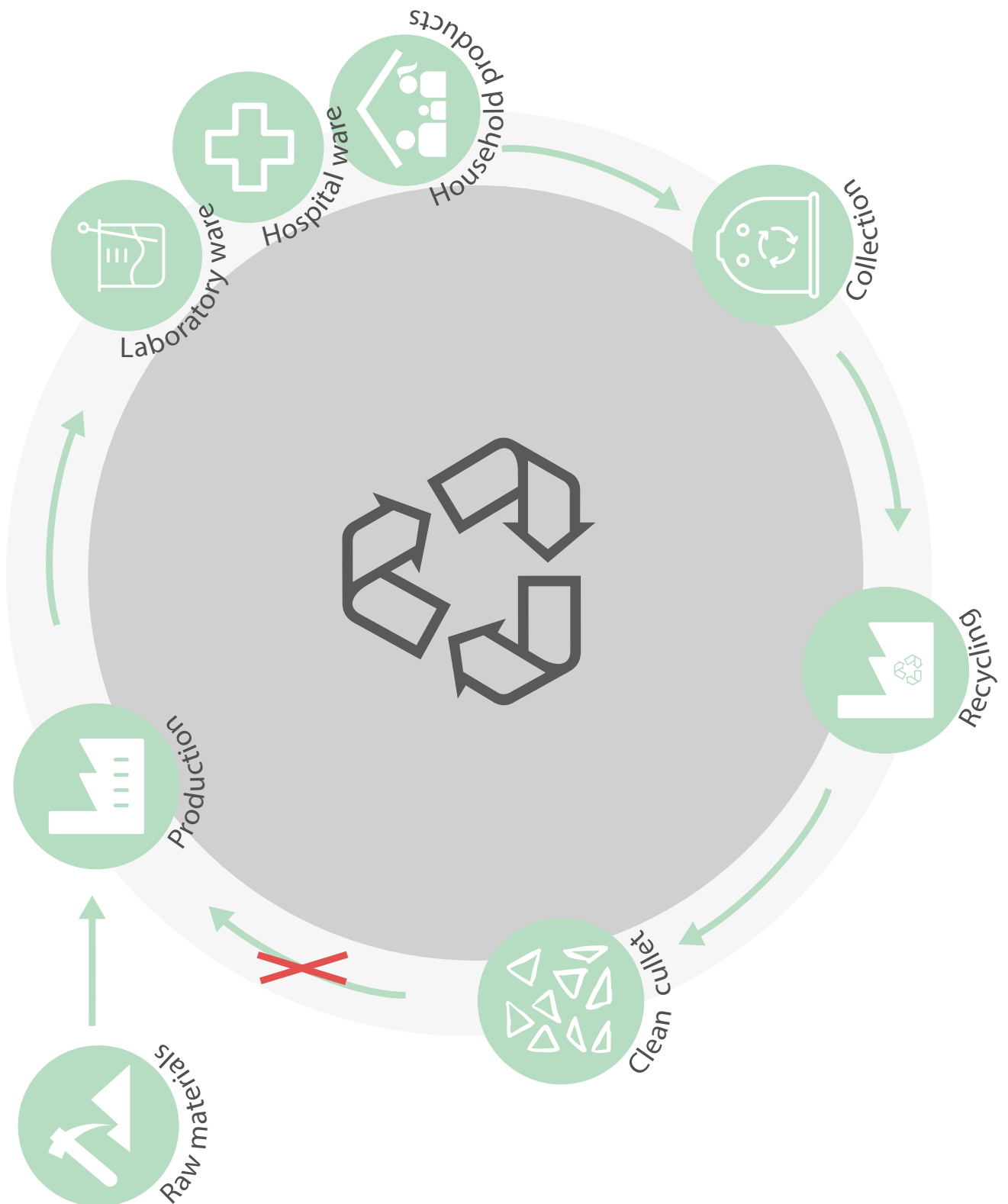


Figure 34 Proposed closed-loop recycling of borosilicate glass

Source: Own drawing

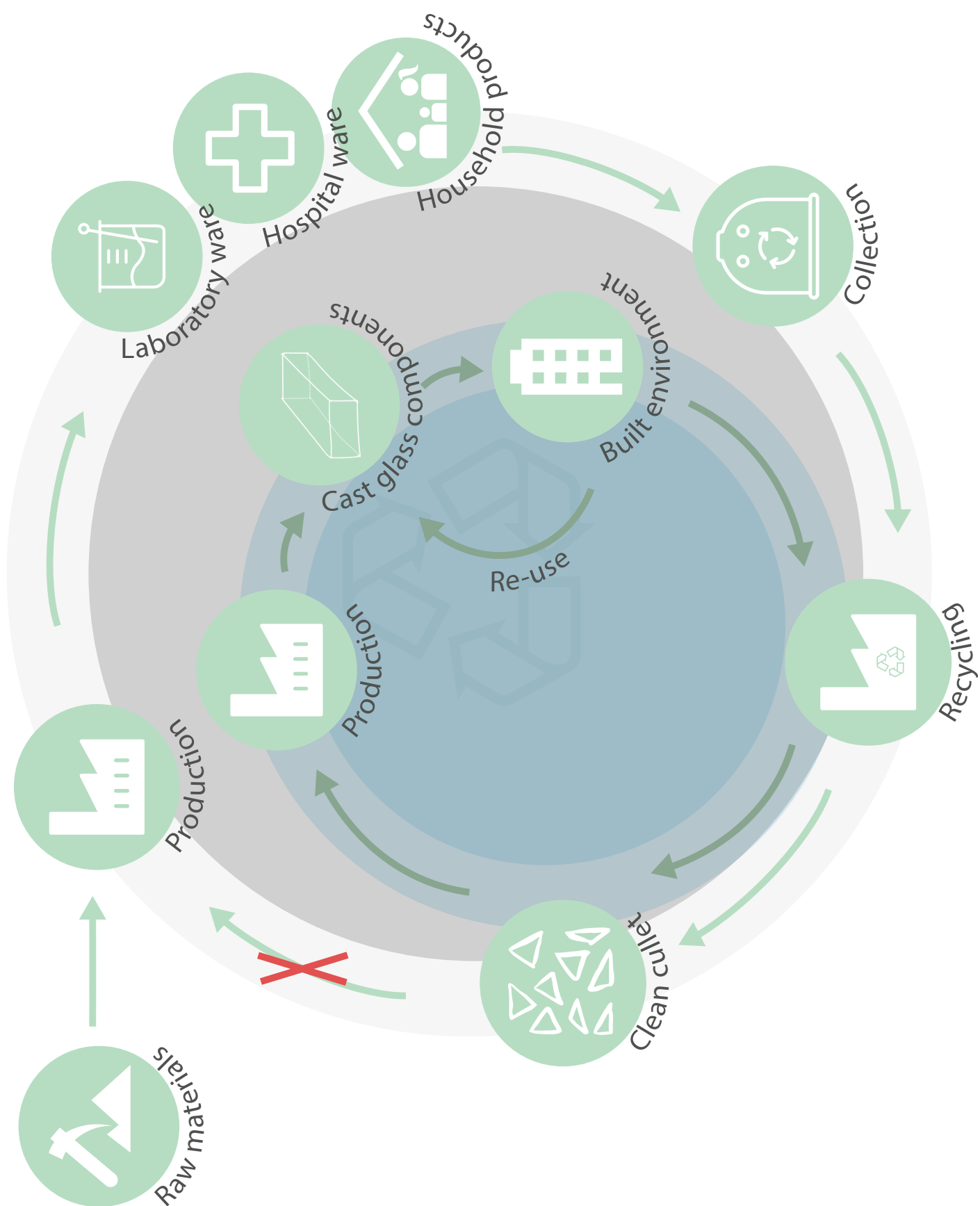


Figure 35 Proposed improved closed-loop recycling of borosilicate glass

Source: Own drawing

## 2.2 EXPERIMENTS

*This chapter is divided in four main sections. First an introduction the reasoning of these experiments, second a description about the experimental setup, then a thorough description about each specimen and final a conclusion on the both the mixability of borosilicate glass and the corresponding mechanical properties. An overview of specimen data used in the experiments is given in Table 11.*

### 2.2.1 INTRODUCTION TO EXPERIMENTS

Currently, literature is lacking on the possibility of recycling borosilicate glass in general and if the recycled glass is suitable for application in cast glass structures. Therefore, experimental research had been conducted to gain knowledge on these topics. During the experimental part of this research, several steps have been taken in order to find out if recycling borosilicate glass is indeed possible and if in practice this could be feasible.

To recycle borosilicate glass, knowledge should be obtained about the mixability of various types of borosilicate glass. Not every borosilicate glass product has the exact same chemical composition. This could reduce the possibility of proper mixing the glass and the creation of a homogenous glass end-product.

To define if recycled borosilicate glass is suitable for application in the built environment, the mechanical properties of recycled borosilicate glass should be determined. If recycled borosilicate glass has similar mechanical properties compared to regular non-recycled borosilicate glass, it is suitable to apply in buildings.

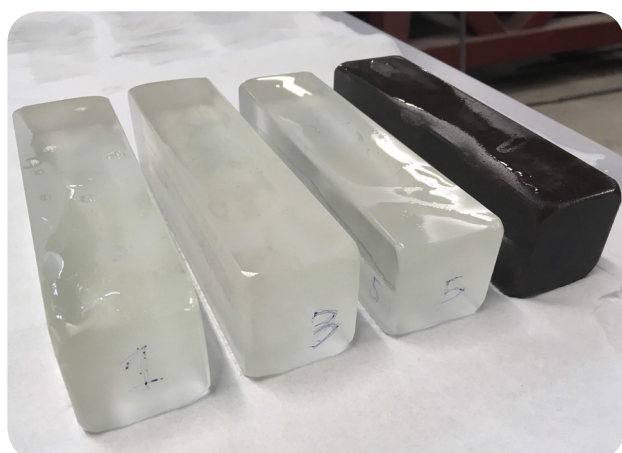


Figure 36 Created specimens of 150 \* 40\* 40 mm

### 2.2.2 EXPERIMENTAL SETUP

#### 2.2.2.1 MIXABILITY

In the Glass lab at the faculty of Civil engineering at the TU Delft, several small specimens have been made to test the mixability of borosilicate glass and to define the mechanical properties of the cast borosilicate glass. The specimens are small beams of approximately 150 \* 40 \* 40 millimetres, as visible in Figure 36. To obtain knowledge about the mixability of recycled borosilicate glass, each beam has been created out of various types and combinations of this glass. Further on in this chapter the various types and combinations of the recycled borosilicate glass applied in the beams, will be described in detail. A full description on the process of creating the beams can be found in Appendix 5.3.

#### *Firing schedule and temperature*

All specimens made for the purpose of this research have been subjected to an equal firing set-up, temperature and dwell time. The glass used for melting was placed directly into the mould, because the terracotta flowerpots, see section 1.1.5 for an explanation about this method, cannot withstand the high temperatures required for the firing of borosilicate glass. The specimens were cast at a temperature of 1120 °C. At this top temperature, the specimens were kept for a 10-hour dwell.



## 2.2.2.2 MECHANICAL PROPERTIES

To determine the mechanical properties of recycled borosilicate glass the specimens have been subjected to a three-point bending test. Only four out of six beams were suitable to use in a three-point bending test, because two of the beams had cracked during firing in the kiln. At the point of writing, the seventh specimen has not been tested yet. The four suitable beams were tested in a Zwick / Z100 testing machine (see Figure 37). Through a three-point bending test the Young's Modulus and the flexural strength of the material could be determined. See Appendix 5.9 for a table containing a summary of experiment results on mechanical properties.

### *Young's Modulus*

In practice it turned out that the Young's Modulus was not accurate to determine with the data derived from the three-point bending test. Therefore, to determine the Young's modulus an additional measurement tool was required.

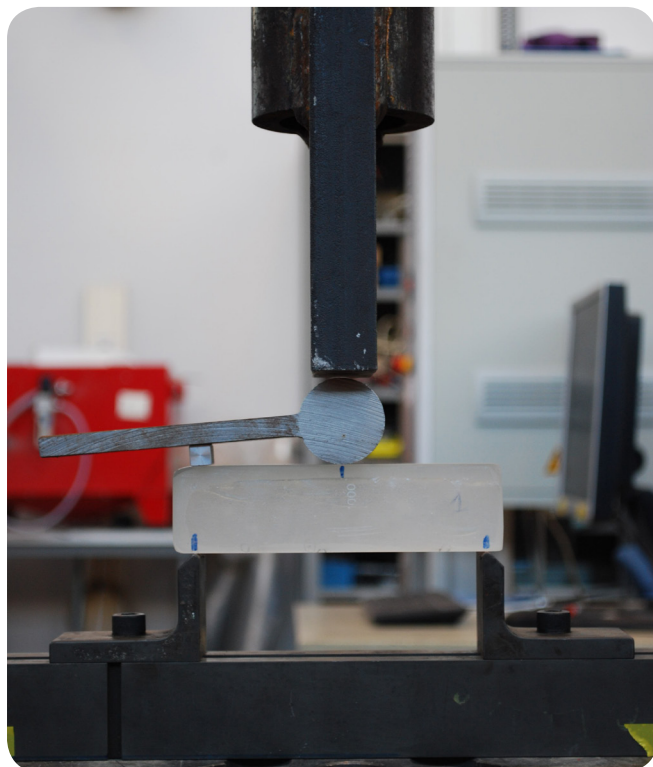


Figure 37 A Zwick / Z100 bending machine

The Young's Modulus can be calculated with equation (1):

$$v = \sqrt{\frac{E}{\rho}} \quad (1)$$

Where:

$v$  = speed of sound (m/s)

$E$  = Young's Modulus (GPa)

$\rho$  = Density (kg/m<sup>3</sup>)

To find the speed of sound in a medium, an Ultrasonic Pulse Velocity (UPV) test can be conducted. In this case, an Ultrasonic Pulse Velocity tester has been utilized to measure the speed of sound in the (broken) glass beams; visible in Figure 38. It should be noted that the first test was performed with an older UPV tester model. It was accurate enough for an indication of the Young's Modulus. A second test was done with a newer UPV tester model with a higher accuracy. Since the results were close to each other for each beam, both sets of results are presented in Table 16 as an indication of their validity. Discrepancies between the sets of results are discussed in section 2.2.3.1.

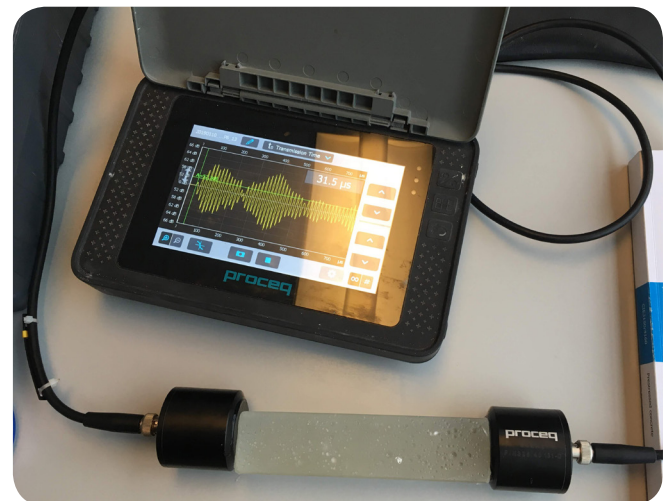


Figure 38 UPV test of specimen 7 (newer UPV model)

*Note: The accuracy of an UPV test is depending on several aspects, such as how much petroleum jelly (Vaseline) is used on the sender and receiver of the machine and on the beam itself. Vaseline is required, because the speed of sound in air, a gas, is much lower than in solids and therefore will significantly decrease the overall measured speed of sound in the glass beam. Also, cracks in the beam have a negative impact on the overall speed of sound in the glass and therefore will give a slight decrease as well. In addition, the beams were measured after breaking them in the three-point bending test, which means they were 'glued' together by using Vaseline between the fracture sides. The more irregular surfaces and places where air can pass through, the lower the speed of sound in the glass. The lower the speed of sound in the glass, the higher the Young's Modulus.*

### Flexural strength

The flexural strength of a specimen with a rectangular cross section can be calculated with equation (2):

$$\sigma_{fs} = \frac{3F_f L}{2bd^2} \quad (2)$$

Source: (Callister, 2007)

Where:

$\sigma_{fs}$  = Flexural strength (Mpa)

$F_f$  = Applied load (N) (obtained through the three-point bending test)

$L$  = Length of the specimen (mm)

$b$  = Width (mm)

$d$  = Height (mm)

For accurate comparison between the results of these experiments, it was aimed to create specimens with the same dimensions (150\*40\*40 mm). However, due to inaccurate post-processing methods, it resulted in specimens with slightly different dimensions. Therefore, for the three-point bending test and the flexural strength calculation the centre-to-centre length between the supports of the beam has been set to 136 mm (see Figure 39).

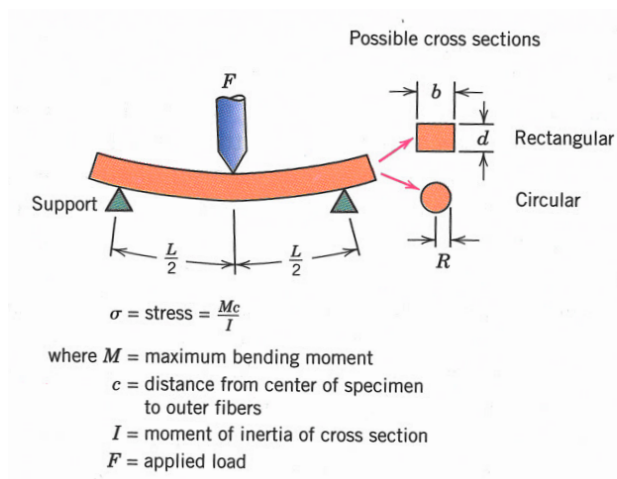


Figure 39 Flexural strength calculation rect. cross section

Source: (Callister, 2007)

Table 11 Summarizing table of created specimens used in experiments

	BEAM 1	BEAM 2	BEAM 3	BEAM 4
GLASS TYPE (All types are borosilicate)	Rods* laboratory ware*	Tube* Lab. ware* PYREX oven tray rect. PYREX oven tray round	Rods*	Rods*
COMPOSITION	Aim: 50% Rods 50% Laboratory ware	Aim: 25% Tube 25% Laboratory ware 25% Oven tray round 25% Oven tray rectangular	Aim: 100% Rods	Aim: 100% Rods
CULLET SIZE $\varnothing$	Pieces > 50 mm	Pieces > 50 mm	Pieces between 10 and 30 mm	Pieces between 10 and 30 mm
DESCRIPTION	 Clear and transparent beam. Several internal air bubble groups. A few big bubbles on top surface.	 Cracked upon annealing. Clear and transparent beam.	 Clear and transparent beam. Internal air bubble patterns follow placement of rods in the mould.	 Cracked upon annealing. Reaction with Cr Cast mould
AMOUNT OF AIR BUBBLES	Moderate	Moderate	High	Low
YOUNG'S MODULUS (GPa)	52	—	60 (Less accurate measurement tool)	—
FLEXURAL STRENGTH (MPa)	52	—	56	—
ULTIMATE FAILURE FORCE (N)	16916	—	18596	—

\* Same composition (wt%) for the rods, tube and laboratory ware (all objects by Schott)

\*\* Boron cannot be traced with the used measurement method, therefore the amount of SiO<sub>2</sub> appears too high

COMPOSITION (wt%)	Objects by Schott	Pyrex oven tray rectangular:	Pyrex oven tray round:
	SiO <sub>2</sub> 81	SiO <sub>2</sub> 91.2	SiO <sub>2</sub> 90.8
	B <sub>2</sub> O <sub>3</sub> 13	B <sub>2</sub> O <sub>3</sub> ** -	B <sub>2</sub> O <sub>3</sub> ** -
	Na <sub>2</sub> O + K <sub>2</sub> O 4.0	Na <sub>2</sub> O + K <sub>2</sub> O 5.4	Na <sub>2</sub> O + K <sub>2</sub> O 5.5
	Al <sub>2</sub> O <sub>3</sub> 2.0	Al <sub>2</sub> O <sub>3</sub> 3.1	Al <sub>2</sub> O <sub>3</sub> 3.4

BEAM 4	BEAM 5	BEAM 6	BEAM 7	CUBE
Rods*	Rods*	Tube* Lab. ware* PYREX oven tray rect. PYREX oven tray round	Tube* Lab. ware* PYREX oven tray rect. PYREX oven tray round	Tube* Lab. ware* PYREX oven tray rect. PYREX oven tray round
	<i>Aim:</i> 100% Rods	<i>Aim:</i> 25% Tube 25% Laboratory ware 25% Oven tray round 25% Oven tray rectangular	<i>Aim:</i> 25% Tube 25% Laboratory ware 25% Oven tray round 25% Oven tray rectangular	<i>Aim:</i> 25% Tube 25% Laboratory ware 25% Oven tray round 25% Oven tray rectangular
Pieces between 10 and 30 mm	Pieces between 10 and 30 mm	Powder	Pieces between 2.3 and 5 mm	Pieces between powder and 2.3 mm
	  Clear and transparent beam. Internal air bubble patterns follow placement of rods in the mould.	  Black and opaque beam. Contaminated with stone. Molecular structure changed. Extreme amount of internal air bubbles.	  Extreme amount of internal air bubbles. Placement of shards is visible as a 'waving pattern'.	  Extreme amount of internal air bubbles, although less than beam 7.
Low	High	Extreme	Extreme	Extreme
—	52	50	53	—
—	54	28	27	—
—	15555	8804	7581	—



# 2.2.3 DETAILED DESCRIPTION OF EACH SPECIMEN

In this section each beam is discussed in detail and results of the three-point bending tests are presented. A summary of the most important mixability results is shown in Table 14, most relevant results in terms of mechanical properties can be found in Table 16.

## 2.2.3.1 BEAM 1

### Description

A mixture of 50% extruded solid rods and 50% DURAN® laboratory ware, both produced by Schott, has been used to create the first specimen of this research (see Figure 41). For this specimen big shards have been used (see Figure 40).

### Composition of both Schott borosilicate glass objects

SiO <sub>2</sub> :	81 wt%
B <sub>2</sub> O <sub>3</sub> :	13 wt%
Na <sub>2</sub> O + K <sub>2</sub> O:	4 wt%
Al <sub>2</sub> O <sub>3</sub> :	2 wt%

(SCHOTT DURAN®, n.d.)

The exact number of applied weights of each type of borosilicate glass can be found in Table 14 in section 2.3.

### Dimensions after post-processing

Appendix 5.3 illustrates the dimensions of the beam after post-processing.

### Beam description

At first examination the created beam looks relatively homogenous and highly transparent. The beam contains some air bubble entrapment inside, but not a high amount. On the top surface several big air bubbles are present. The biggest air bubble on the top surface has a diameter of 6,65 millimetre. Most air bubbles on the top surface have a diameter between 1 and 2 mm. Generally, the internal air bubbles have a diameter smaller than 1 mm. However, there are some bubbles present with a diameter of more than 1 mm. Most internal air bubbles are clustered together into small groups.

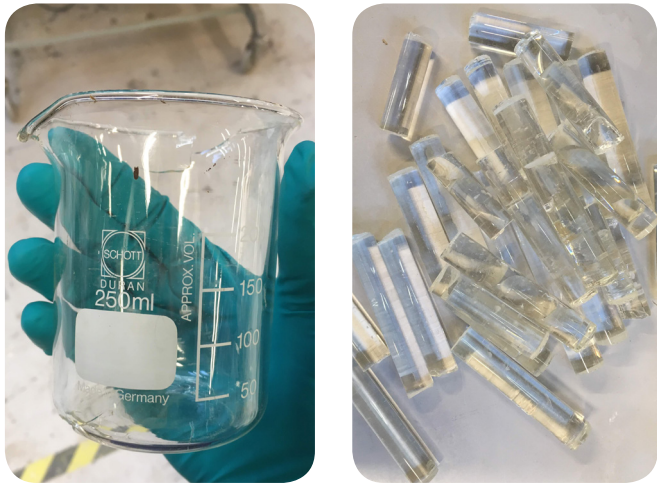


Figure 41 Schott laboratory ware and Schott rods



Figure 40 Big shards in mould for casting beam 1

An interesting fact is that certain letters, originally present on the laboratory glass, are embedded on one side of the beam (see Figure 42 and Appendix 5.10).

The internal air bubbles are physical entrapment of atmospheric gases, formed during the initial phase of melting in the kiln (Shelby, 2005). The gases present in the interstices between the glass cullet could be trapped when the cullet starts to soften and forms a liquid of high viscosity surrounding these interstices. The smaller the cullet diameter within the melt, or an applied cullet batch of widely variable cullet size, the more present interstices, resulting in more potential air bubble entrapment. This is particularly clear in specimen 6 and 7, which will be described in more detail in section 2.2.3.4



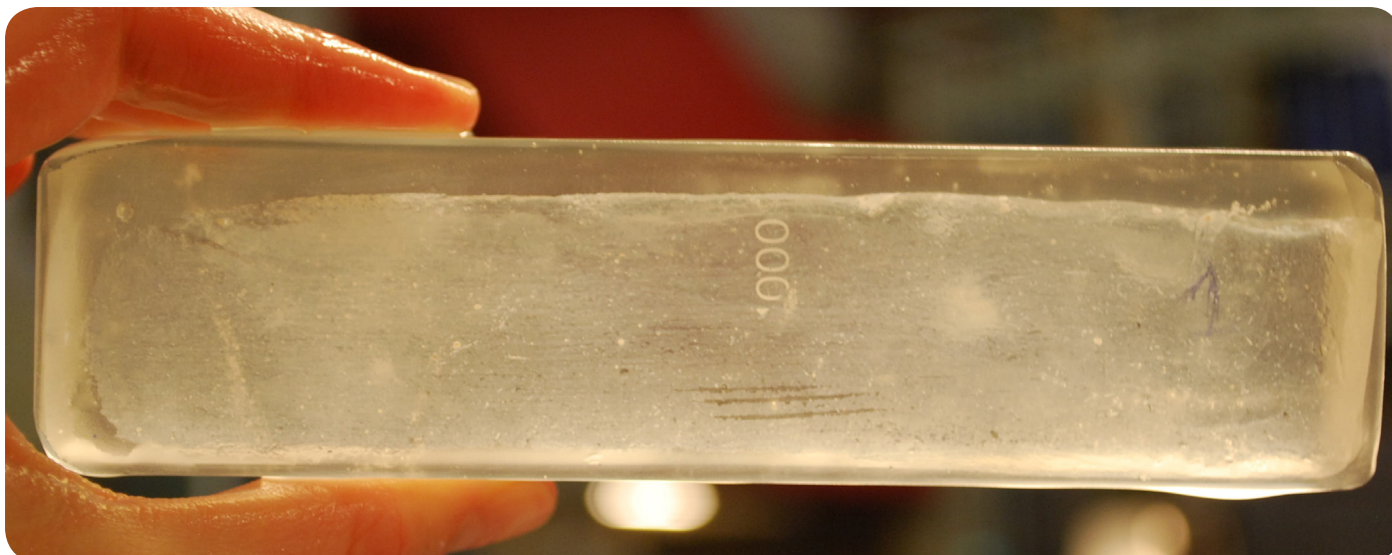


Figure 42 Specimen 1, with embedded letters

and 2.2.3.5 respectively.

The presence of internal air bubbles in the specimen after firing can be attributed to the high viscosity used upon firing. For borosilicate glass the applied temperature of 1120 °C corresponds to a viscosity between  $10^3$ - $10^4$  Pa-s (Callister, 2007). Shelby (2005) states that normally, internal air bubbles will be removed during firing due the Buoyancy effect. This effect means that the lower density of an air bubble, compared to its surrounding liquid, results in automatically rising of the air bubble to the surface of the melt where it will burst. However, when the viscosity of the melt is high, air bubbles will rise too slow and therefore cannot reach the surface before the melt solidifies. This results in internal air bubble entrapment.

In glass technology, internal air bubbles appearing as very small spheres, a diameter less than 0.4 mm, are generally referred to as 'seeds' (Shelby, 2005). Often these seeds are present in clusters within the glass specimen.

Most likely, the present embedding of the letters is caused by the flowability of the glass during firing. Under the applied firing conditions the viscosity of the glass is high and shards do not melt completely into a fluid. The shards remain too viscous to properly mix and therefore only fuse together. This means that the original shard with the letters, probably did not melt completely but remained at its position in the mould and only fused with its neighbouring shards. In addition, this effect of merely fusing together of the shards could be the reason of the internal air bubble entrapment. This effect is particularly clear for specimen 3 and 5, where the air bubble patterns follow the placement of the rods inside the mould before firing. For a more detailed explanation about specimen 3 and 5

see section 2.2.3.3.

### *Stress analysis and flaw description*

As mentioned in section 1.1.6, for glass casting two main reasons exist for the generation of internal stresses; insufficient annealing precaution and variations within the chemical composition of the glass melt. These internal stresses can be visualized with a source of white polarized light and a crossed circular polarized filter. Glass with internal stresses shows birefringent behaviour (McKenzie, H.W., & Hand, R.J., as cited in Bristogianni, et al., (2017b)). As light passes through a birefringent material it is circularly polarized. By placing a polarization filter in front of a glass specimen, back lighted by a source of polarized white light (such as a computer screen), internal stresses can be visualized. Areas with internal stress will be visible as isochromatic fringes (bands of light with the same colour) (McKenzie and Hand 2011, as cited in Oikonomopoulou, et al., 2017). Non-birefringent areas of the glass, alias isoclinic areas, exhibit no internal stress and appear dark (Schott, 2004). When a specimen shows white, greyish or light blue colours it is an indication of low internal stress. If colours are visible, it shows that the amount of internal stress is higher (Oikonomopoulou et al., 2017).

This applied method is solely a qualitative analysis to determine if there is any residual internal stress present. The method is inadequate for assessing internal stress levels quantitatively, i.e. assigning a certain stress value to a specific colour. See Shribak (2015) for a detailed discussion on the interpretation of the colours.

Figure 43 and Appendix 5.10 present the pictures of beam 1 created with the aforementioned method

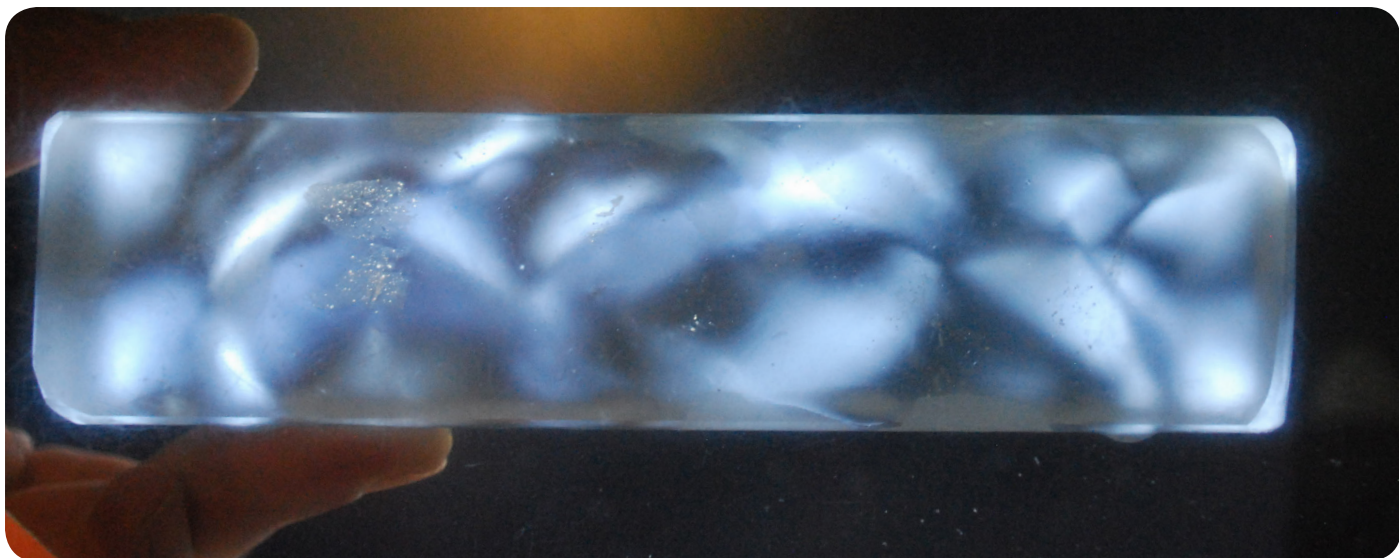


Figure 43 Specimen 1, bottom view stress analysis

of using a polarized light and filter. Mainly blue, grey and white colours are visible. As written before, those colours do not represent levels of high internal stress. However, is not totally clear what exactly these colours do represent. There is an indication that these colours do not only represent low internal stresses. It is possible that the present internal air bubbles refract the light different as well, resulting in colour changes. In addition, the internal air bubbles itself could introduce internal stress to their adjacent areas. This could explain why the colours correspond largely to the internal air bubble patterns. This phenomenon is particularly clear in specimen 3 and 5, discussed in detail in section 2.2.3.3. Most likely, the white blue colours occurring at the corners are due to internal stress related to natural shrinkage upon cooling

the beam. The same effect is visible in Figure 44 for the Crystal Houses bricks made by Poesia (Oikonomopoulou et al., 2017).

Although the appearing colours represent an indication of weaker areas within the glass beam, those areas are most likely not crack initiators. Most of these lighter coloured areas are corresponding to the internal air bubble pattern. As air has a lower density than the borosilicate glass, and since a crack will always follow the path of less resistance, the crack shall propagate through the internal air bubble pattern.

Therefore, internal air bubbles are considered as flaws, especially with increasing diameter of the bubble (Shelby, 2005).

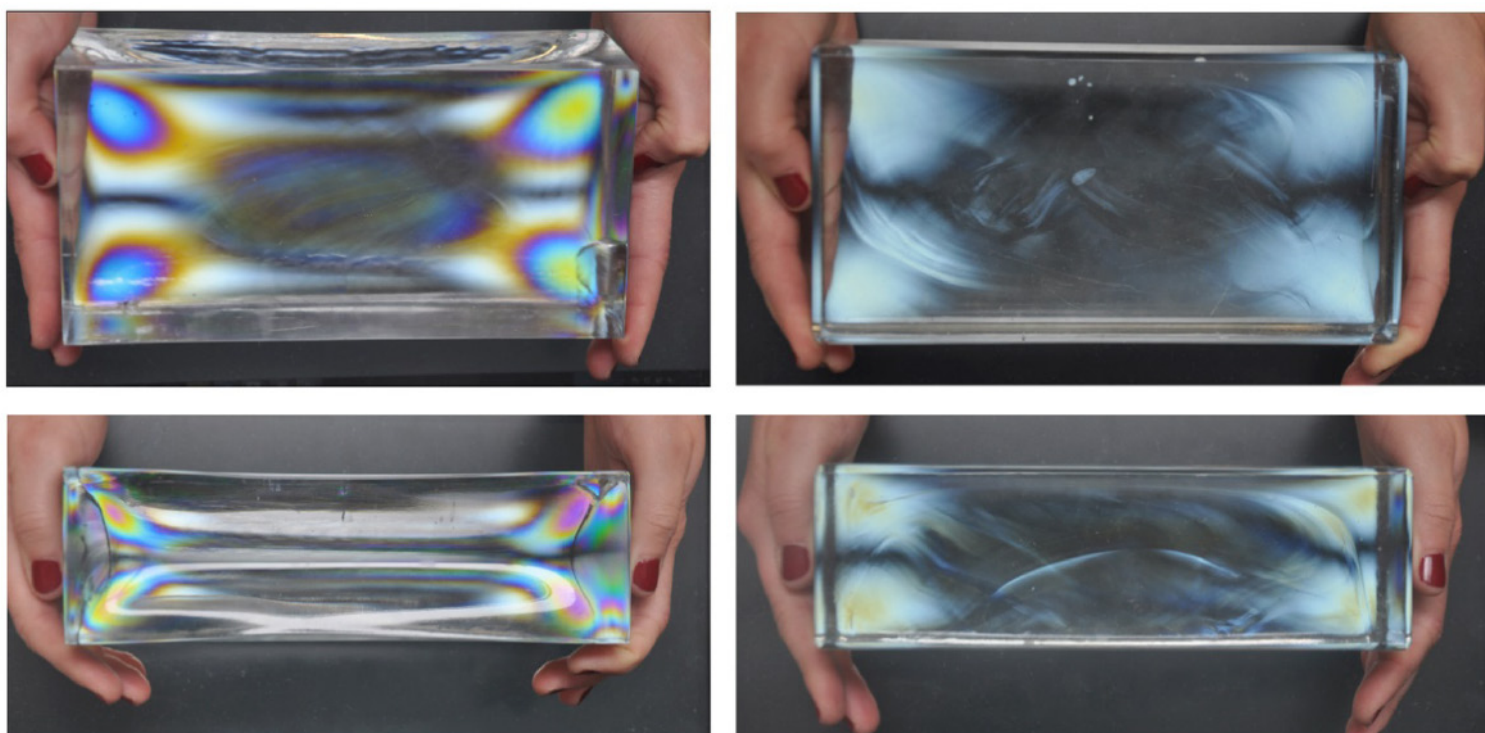


Figure 44 Stress analysis of the Crystal House bricks



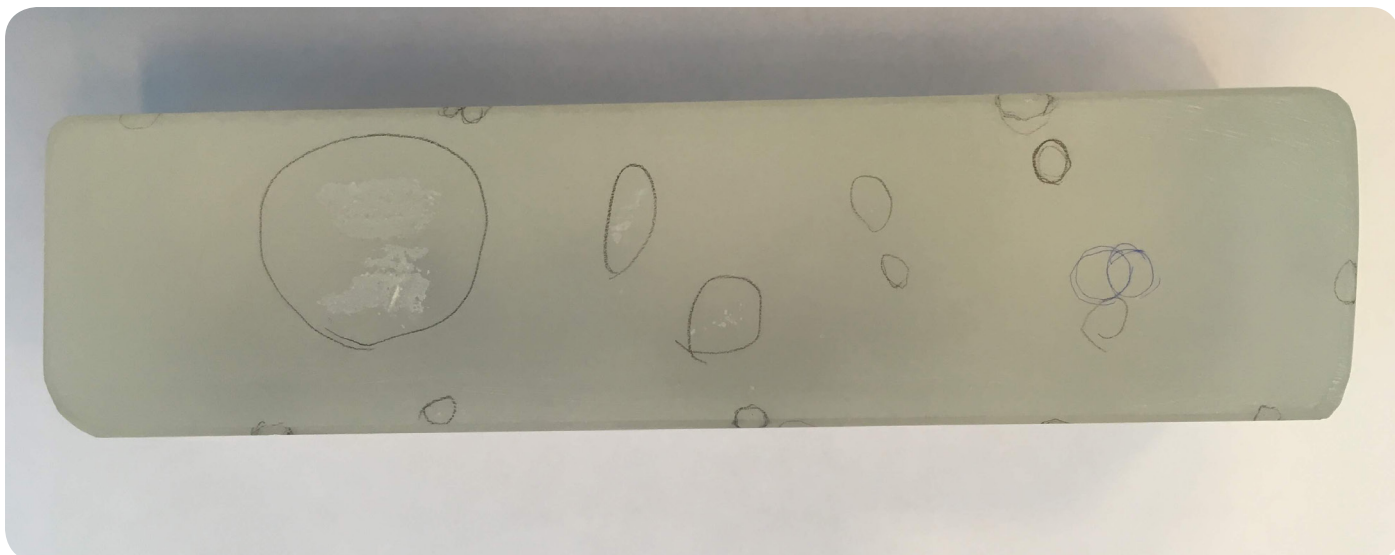


Figure 45 Specimen 1, bottom view present flaws

*Note: Although it was assumed that the two types of borosilicate glass are both a product of Schott DURAN, it could be that the rods either have a slightly different chemical composition compared with the laboratory ware, or it could be that the rods are not a product of Schott DURAN, resulting in a different chemical composition as well. Either way, this could introduce internal stresses, due to not completely mixing, but fusing of the different shards. However, as stated before, this improper mixing could also be a result of the high viscosity related to the applied temperature of 1120 °C. If the latter is the case, then it is possible that the colours represent either stress due to improper fusing of the shards, or the colours do not indicate merely stress, but are also a representation of the present internal air bubbles.*

### Flaws

Figure 45 highlights several flaws or abrasion zones present on the bottom side of the beam. These flaws could be the result of the applied casting method. During the three-point bending test, the top surface of the beam will act in compression, whereas the bottom surface will act in tension. As mentioned in section 1.1.3, a flaw present on the glass surface acts as a stress concentrator when a tensile force is applied. This results in high risk of cracking, starting at those specific flaws. Therefore, the presence of such flaws could decrease the potential flexural strength of the beam.

### Fracture analysis

After breaking the beam in the three-point bending test, a fracture analysis of the crack surface can be done. Examining a crack provides information

about the stress level upon breaking, where the crack initiated and the source of cracking (Callister, 2007). This is valuable information to investigate if the specimens cracked for example due to present (internal) flaws or high internal stress levels.

As a crack interacts with the microstructure of the glass, it shows typical features on the fracture surface (Callister, 2007). This is illustrated in Figure 46.

The flat and smooth mirror region around the origin of the crack represents the surface that developed during the initial acceleration stage during crack propagation. This mirror region is practically visible when the tensile stress was high upon cracking (Ono & Allaire, 2004). Information about the amount of stress during the crack nucleation stage can be defined by measuring the radius of the mirror region. When the acceleration rate is high during crack propagation, the earlier the crack reaches its terminal velocity, forming a smaller mirror radius. When the fracture stress increases, the acceleration rate increases as well, resulting in decreasing of the mirror region (Callister, 2007). As the crack propagation velocity approaches the terminal velocity, the crack changes propagation direction. Right before it begins to branch it will form a rough hazy surface, called a mist. Clearly visible branches are called hackle marks. These indicate the crack propagation direction. A high amount of branching hints at higher stresses. Wallner lines are another fracture feature. These are arc-shaped features perpendicular to the crack propagation direction. They can indicate either surface or internal flaw present before failure, or the point where the crack reaches terminal velocity (Ono & Allaire, 2004).

Figure 47 shows the fracture surface of specimen 1. A clear mirror region can be identified, as well as a mist and hackle region. A lot of branching is

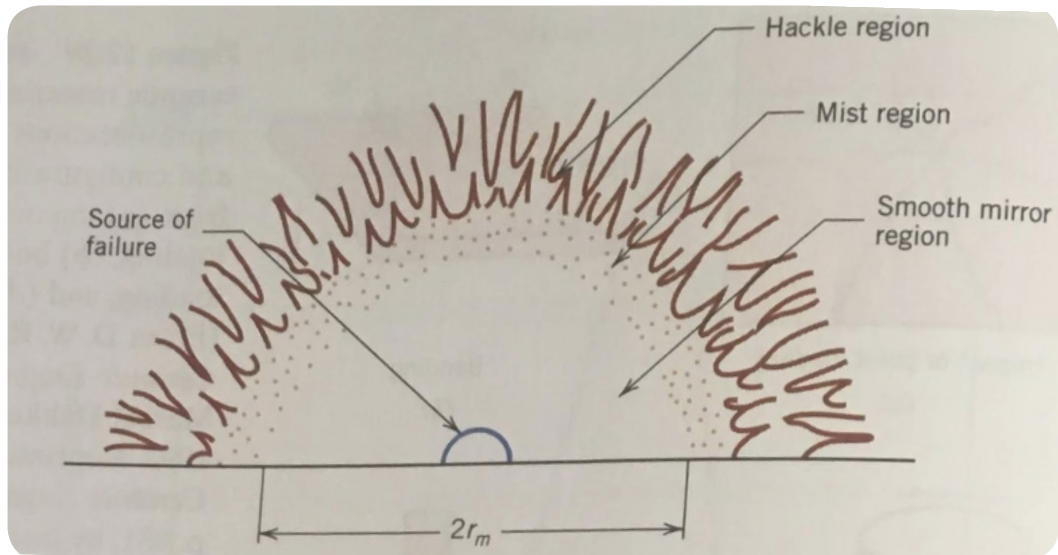


Figure 46 Typical features of a fracture surface

(Callister, 2007)

visible in the hackle region, indicating high stress. The location of the origin (at the edge on the bottom surface of the beam) means that failure happened by tension at a surface flaw, instead of at an internal flaw. This surface flaw was not marked beforehand. Most likely the flaw was too small to spot with the naked eye. When comparing the fracture location with the internal stress pictures, it also seems that the fracture occurred at a location without any or very low internal stresses. Failure occurred at an applied force of 16.9 kN.

## Mechanical properties

### Young's modulus

As described in section 2.2.2.2, the Young's Modulus ( $E$ ) can be calculated with equation (1):

The initial measured speed of sound ( $v$ ) in beam 1 is: 30  $\mu\text{s}$  (micro seconds).

(measured with older model of the UPV tester)

The length of the beam is 0.155 m

The density of borosilicate glass is 2230  $\text{kg/m}^3$

This results in:

$$E = 59 \text{ GPa}$$

The second measurement of the speed of sound ( $v$ ) in beam 1, done with the newer model of a UPV tester, resulted in: 32.1  $\mu\text{s}$ .

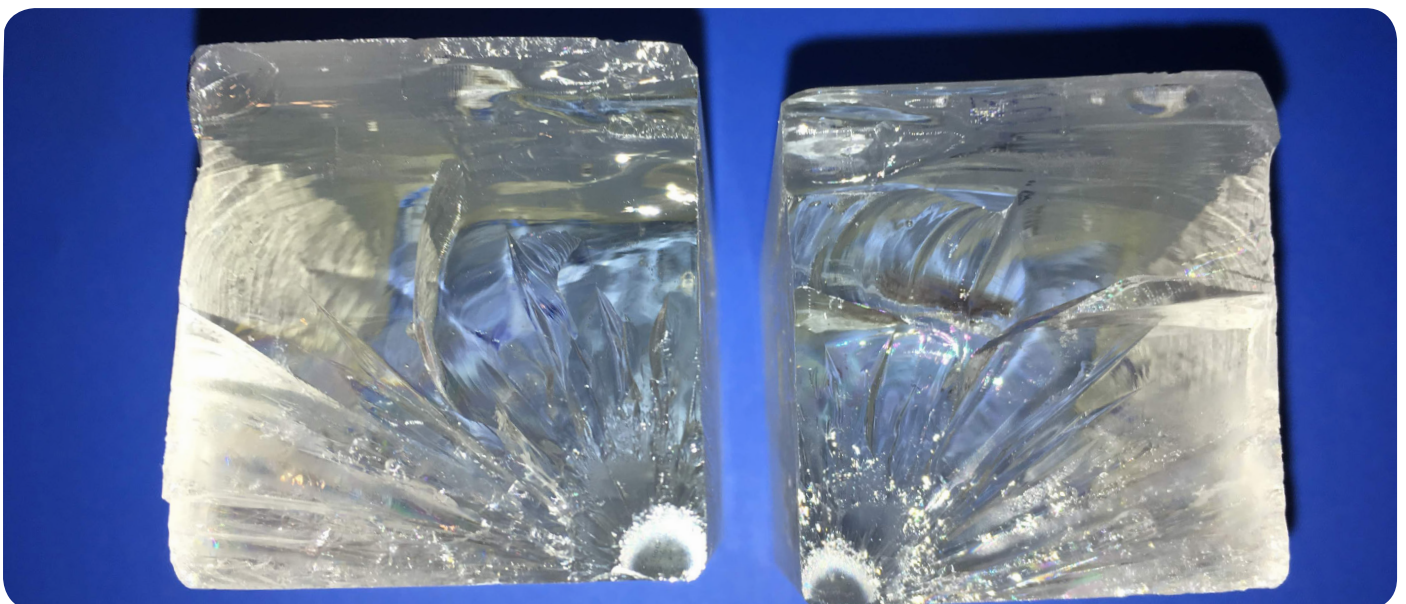


Figure 47 Specimen 1, fracture surface

Calculated with equation (1) this resulted in a Young's Modulus of 52 GPa.

For comparison, non-recycled borosilicate glass has a Young's Modulus of 64 GPa.

The above described results seem to indicate that this specific recycled borosilicate glass mixture (rods and laboratory glass) has a somewhat lower Young's modulus than non-recycled borosilicate glass. However, this cannot be stated with certainty, due to several possible reasons. One reason could be the applied inaccurate measurement methods, see section 2.2.2.2 for a detailed explanation. Another reason could be the presence of internal air bubbles. As described in section 2.2.2.2, the air inside the bubbles possibly lowers the measured speed of sound. Most likely, this explains why the second measurement with the newer, more accurate UPV tester, results into an even lower Young's Modulus.

Even though the results of the UPV test are somewhat lower compared to non-recycled borosilicate glass, the aforementioned reasoning suggests the deviation is relatively small. Therefore, this test suggests that borosilicate glass retains a similar Young's Modulus after recycling.

### *Flexural strength*

As described in section 2.2.2.2, the flexural strength of the beam can be calculated with equation (2):

Where for beam 1:

$\sigma_{fs}$  = Flexural strength (Mpa)

$F_f$  = 16916,11 (N)

$L$  = 136 (mm)

$b$  = 38,95 (mm)

$d$  = 41,3 (mm)

This resulted in a flexural strength of 52 MPa.

For comparison, the flexural strength of non-recycled borosilicate glass (Pyrex) made in an industrialized production process is 69 MPa (Callister, 2007).

There are several possibilities why the flexural strength of the beam is somewhat lower compared to non-recycled borosilicate glass. The applied inaccurate casting method of the beams could

introduce flaws to the specimen, resulting in cracking before the maximum amount of tensile stress of borosilicate glass is reached. In addition, the specimen has not been polished very fine, compared to an industrialized production process, resulting in small flaws as well. It is expected that when a highly accurate production process is applied for recycled borosilicate glass components that the flexural strength will be closer to the standard value.

Another possible reason could be that the two Schott products have a slight difference in chemical composition, allowing for less optimal mixing of the glass cullet.



## 2.2.3.2 BEAM 2

### Description

A mixture of four different types of borosilicate glass has been used to create the second specimen. The same laboratory ware as used in beam 1 has been combined with a borosilicate rod, also produced by Schott and two different PYREX oven trays, produced by Corning. Thus, this beam consists of 25% borosilicate rod and 25% DURAN® laboratory ware, combined with 25% PYREX oven tray (square) and 25 % PYREX oven tray (round). For this specimen big shards of glass have been used. Figure 48 shows the glass products that have been used during this experiment and Figure 49 shows the big shards in the Crystal Cast M248 mould.

### Composition of both Schott borosilicate glass objects

SiO <sub>2</sub> :	81 wt%
B <sub>2</sub> O <sub>3</sub> :	13 wt%
Na <sub>2</sub> O + K <sub>2</sub> O:	4 wt%
Al <sub>2</sub> O <sub>3</sub> :	2 wt%

### Composition of both PYREX borosilicate glass objects:

The composition of both PYREX oven trays is listed in Table 12 and Table 13. This data is obtained through analysis with a Panalytical Axios Max WD-XRF spectrometer. The element boron could not be traced with this method, therefore the SiO<sub>2</sub> component appears too high. However, when comparing these values with the ones of the

borosilicate objects by Schott, the composition of the PYREX oven trays is largely similar.

### Rectangular tray

Compound Name	Conc. (wt%)	Absolute Error (wt%)
1 SiO <sub>2</sub>	91.186	0.3
2 Na <sub>2</sub> O	4.828	0.06
3 Al <sub>2</sub> O <sub>3</sub>	3.091	0.05
4 K <sub>2</sub> O	0.631	0.03
5 Cl	0.078	0.009
6 Fe <sub>2</sub> O <sub>3</sub>	0.045	0.009
7 CaO	0.039	0.01
8 ZrO <sub>2</sub>	0.034	0.006
9 SO <sub>3</sub>	0.032	0.006
10 TiO <sub>2</sub>	0.026	0.008
11 P <sub>2</sub> O <sub>5</sub>	0.01	0.003

Table 12 Rectangular oven tray composition

### Round oven tray

Compound Name	Conc. (wt%)	Absolute Error (wt%)
1 SiO <sub>2</sub>	90.799	0.3
2 Na <sub>2</sub> O	4.882	0.06
3 Al <sub>2</sub> O <sub>3</sub>	3.391	0.05
4 K <sub>2</sub> O	0.591	0.03
5 Cl	0.181	0.01
6 CaO	0.063	0.01
7 Fe <sub>2</sub> O <sub>3</sub>	0.043	0.009
8 ZrO <sub>2</sub>	0.027	0.005
9 SO <sub>3</sub>	0.024	0.005

Table 13 Round oven tray composition



Figure 48 Four different borosilicate glass objects for melting



In Friedrich & Dimmock, (2014) the following composition of PYREX glass objects has been found:

SiO <sub>2</sub> :	80.6 wt%
B <sub>2</sub> O <sub>3</sub> :	13 wt%
Na <sub>2</sub> O + K <sub>2</sub> O:	4 wt%
Al <sub>2</sub> O <sub>3</sub> :	2.3 wt%

Again, largely similar to the tested PYREX oven trays and to the borosilicate glass objects by Schott.

These PYREX oventrays have a slight different thermal expansion coefficient compared to the Schott objects as well.  $3.25 \cdot 10^{-6} \text{ K}^{-1}$  and  $3.3 \cdot 10^{-6} \text{ K}^{-1}$  respectively

### Beam description

A highly transparent glass beam, with a relatively moderate amount of air bubble entrapment. It contained severe cracks in several parts of the beam. Therefore, this beam was not suitable to use in further mechanical testing.

### Stress analysis

Possible reason why this beam cracked during the annealing phase, could be that the shards were too big to melt into a homogenous mixture under these firing conditions. Based on previous experiments smaller shard sizes could be a solution for proper mixing of different borosilicate glass types. Experiments with such smaller shard sizes, but the



Figure 49 Four different types of borosilicate objects in the mould

with the same glass composition as this specimen 2, have been conducted and analysed in section 2.2.3.4, section 2.2.3.5 and section 2.2.3.6. Another possible reason could be that the different borosilicate glass types have a slight difference in thermal expansion coefficient, resulting in internal stresses and potential cracking.

### Fracture analysis

As this beam showed severe internal cracks, it was not suitable for using in a three-point bending test. In addition, the Young's modulus of this beam has not been determined.

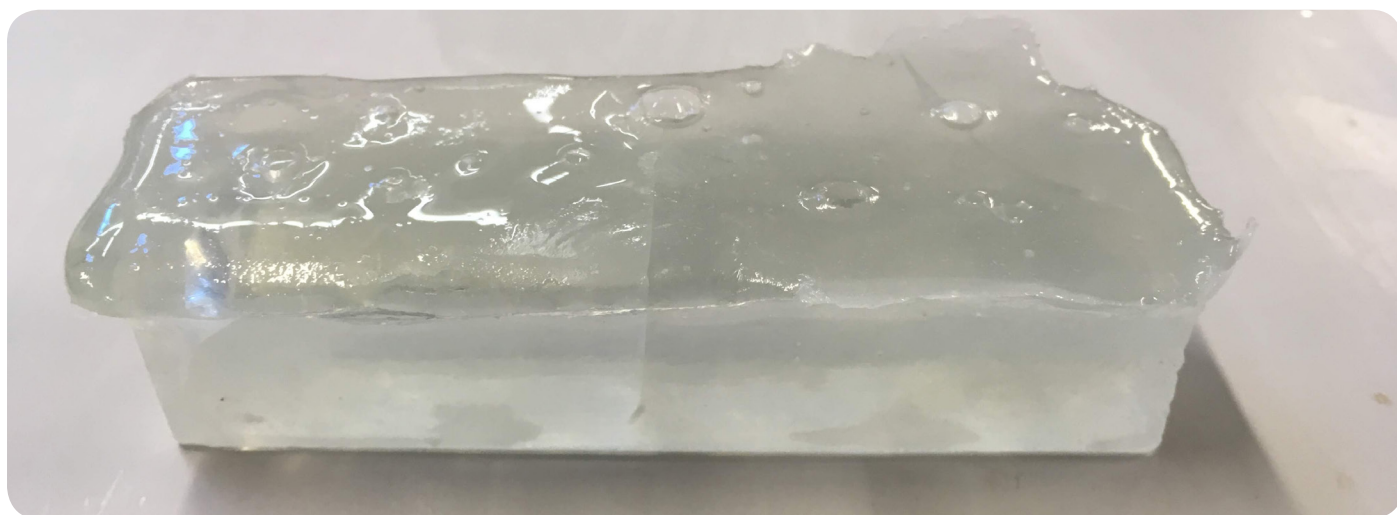


Figure 50 Beam 2, with internal cracking

### 2.2.3.3 BEAM 3, 4 & 5

#### *Description*

Specimen 3, 4 and 5 were created of solely borosilicate rods by Schott. Based on specimen 1 and 2 a smaller shard size was preferred, therefore pieces with a diameter of roughly one to three centimetres were placed in the Crystal Cast mould (see Figure 51).

#### *Composition*

The chemical composition of the rods is described in section 2.2.3.1.

#### *Firing*

Beam 4 had internally cracked and partly crystallized during firing. A possible explanation is that, without any clear reason, the glass reacted with the Crystal Cast mould and due to a difference in thermal expansion coefficient, it cracked internally. Due to the internal cracking the beam was not suitable to use in further mechanical testing.

### **Beam 3**

#### *Beam description*

A transparent beam with a relatively high amount of air bubble entrapment inside. A few bigger bubbles are present on the top surface. Most internal bubbles have approximately a diameter of less than 1 millimetre. In Figure 53 internal diagonal air bubble patterns are clearly visible. It seems that these patterns are introduced by the positioning of the rods in the mould, see Figure 54. As under the applied firing conditions, the rods solely fused to each other. This fusing under high viscosity could have trapped the air bubbles within the liquid. As illustrated on Figure 55, above the vertical standing rods, other rods were placed. This could also have prevented the air bubbles from escaping. As the air bubble entrapment present in the beam is related to the high viscosity of the glass melt upon firing, a longer annealing time or a slightly higher firing temperature could help to relieve the internal air bubbles.



Figure 51 Borosilicate rods in the mould

#### *Dimensions after post-processing*

Appendix 5.5 illustrates the dimensions of the beam after post-processing.

#### *Stress analysis*

Figure 52 presents the pictures of beam 3 created with a polarized light and filter. As with beam 1, the colours are mainly blue, grey and white, indicated either low levels of internal stresses or the presence of internal air bubbles (which could also introduce low levels of stress). The latter seems the most likely, because the colours corresponded largely with the internal diagonal air bubble patterns. As described before, these air bubble patterns or potential internal stresses are most likely not crack starters but could be weaker points in the beam.



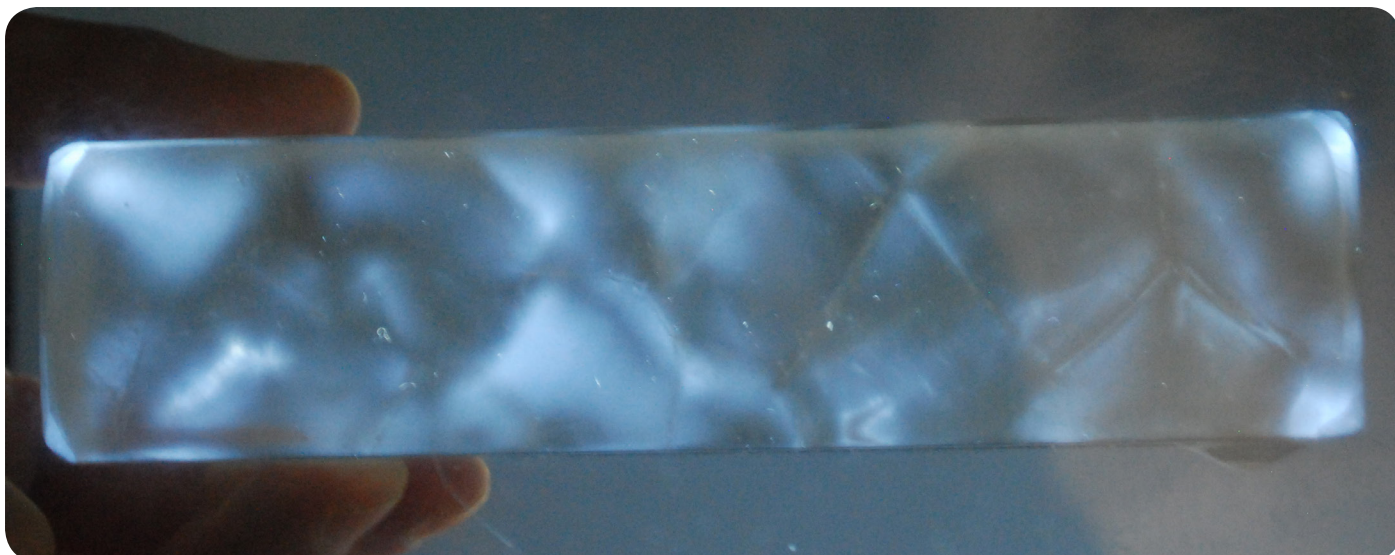


Figure 52 Specimen 3 bottom view stress analysis

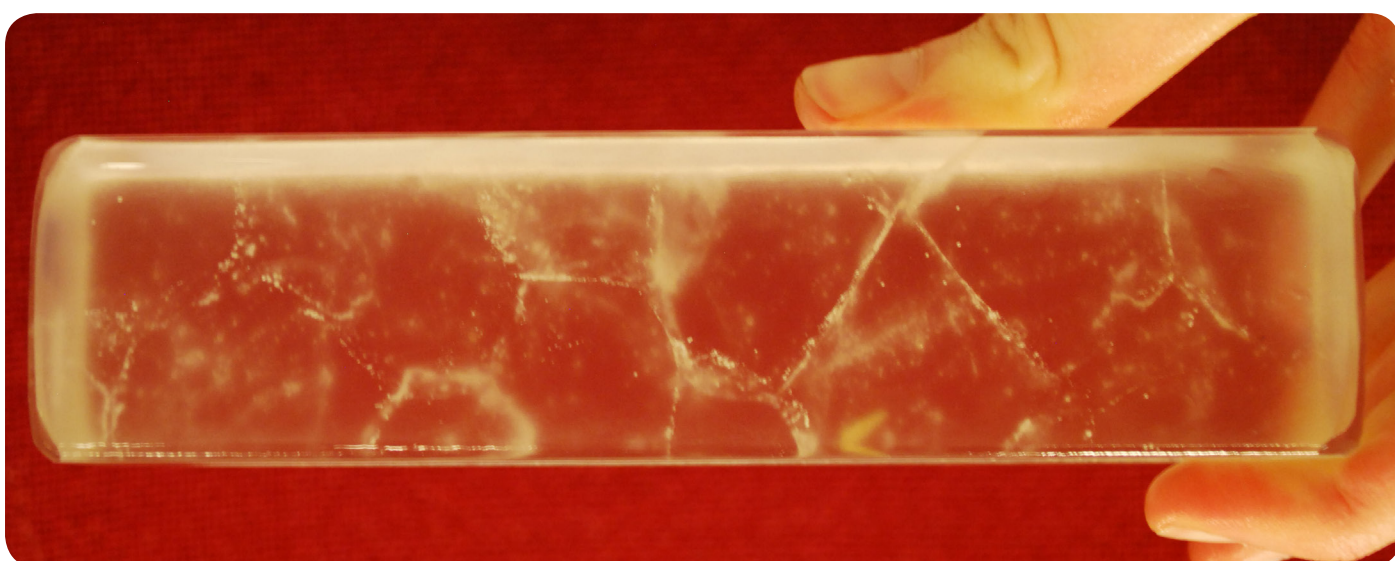


Figure 53 Specimen 3, bottom view air bubble entrapment



Figure 54 Specimen 3, placement of the rods in the mould, corresponding to air bubble patterns, top view

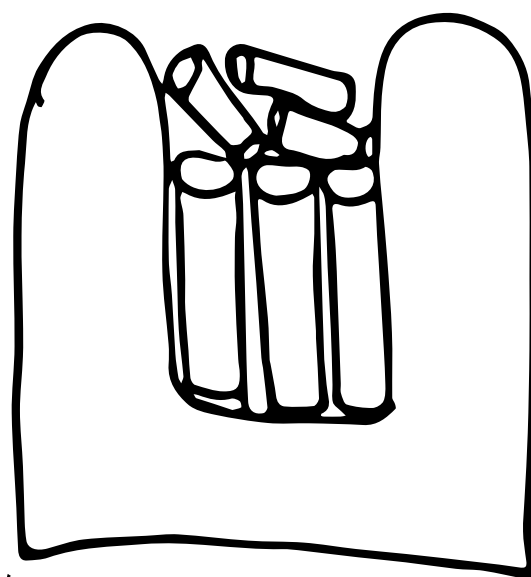


Figure 55 Specimen 3, placement of the rods in the mould, side view

### *Fracture analysis*

The fracture surface of specimen 3 shows comparable features to specimen 1. Beam 3 is visible in Figure 56. Here, again the fracture surface indicates high stresses upon failure. The origin of the crack is on the bottom side of the beam, right under the applied force, as well. For beam 3 no particular flaw has been visible with the naked-eye at the crack origin before failure. In addition, only low internal stresses had been examined at the fracture location, meaning that the fracture did not occur due to internal stress. Failure occurred at an applied force of 18.6 kN

A microscopic picture of the fracture surface of specimen 3 is visible in Figure 57. This picture clearly shows the mirror, mist and hackle region.

### *Mechanical properties*

As described in section 2.2.2.2, the flexural strength of the beam can be calculated with equation (2):

Where for beam 3:

$\sigma_{fs}$  = Flexural strength (Mpa)

$F_f$  = 18596,02 (N)

$L$  = 136 (mm)

$b$  = 37.75 (mm)

$d$  = 42.2 (mm)

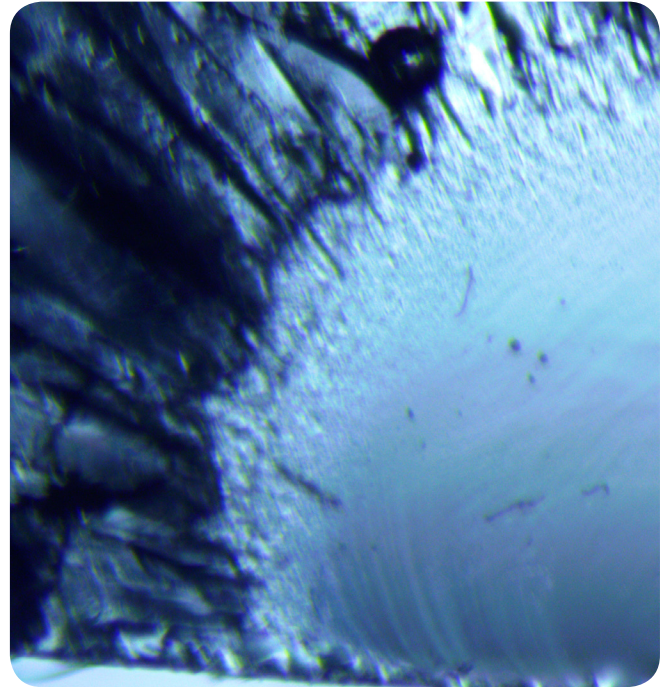


Figure 57 Specimen 3 microscopic picture of fracture surface

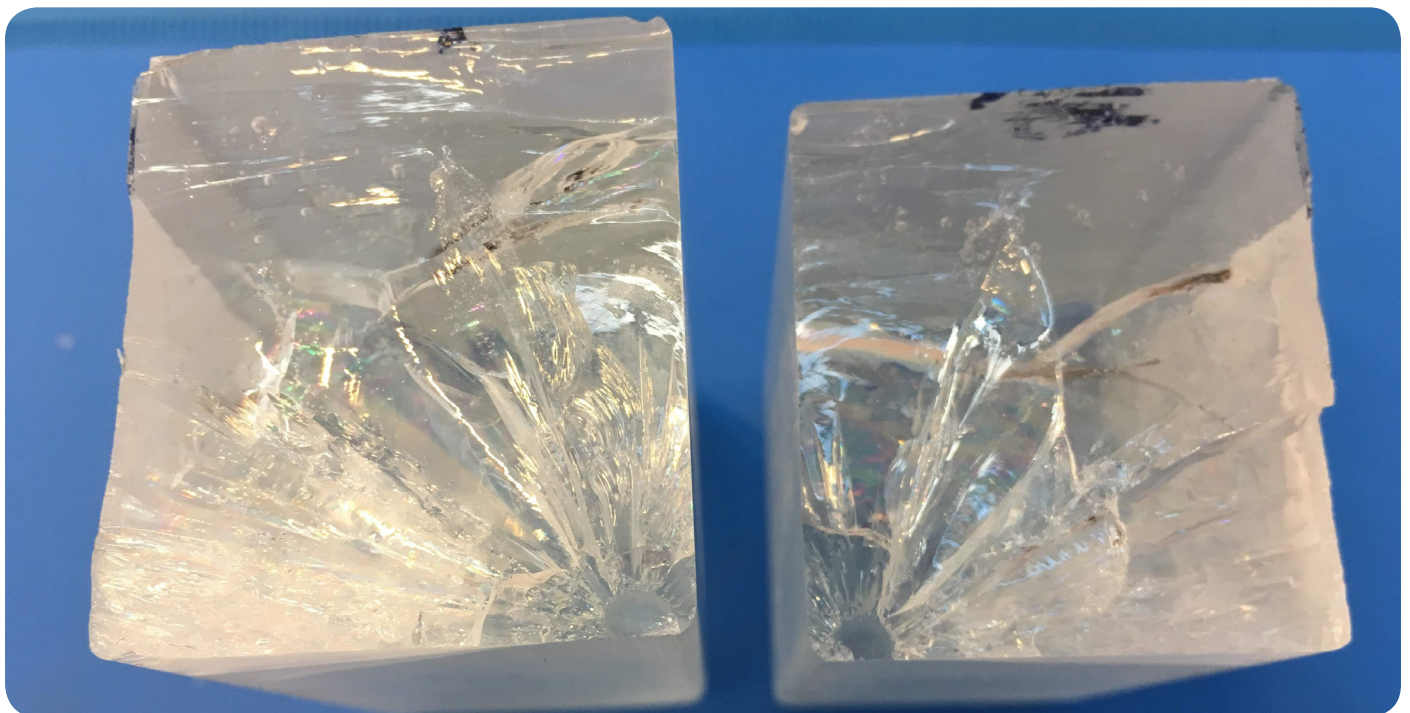


Figure 56 Specimen 3, fracture surface



This resulted in a flexural strength of 56 MPa. For comparison, the flexural strength of non-recycled borosilicate glass (Pyrex) is 69 MPa (Callister, 2007).

#### *Young's modulus*

As described in section 2.2.2.2, the Young's Modulus ( $E$ ) can be calculated with equation (1).

The initial measured speed of sound ( $v$ ) in beam 3 is: 30  $\mu$ s (micro seconds).

(measured with the older model of the UPV tester)

The length of the beam is 0.156 m

The density of borosilicate glass is 2230 kg/m<sup>3</sup>

This resulted in a Young's Modulus of 60 GPa.

The second measurement of the speed of sound ( $v$ ) in beam 3, done with the newer model of a UPV

tester, could be done with only a half part of the beam. At the time of measuring, the other half was not in my possession. This resulted in a deviant value for the Young's Modulus and therefore will not be taken into account.

## **Beam 5**

#### *Beam description*

Specimen 5 shows several similarities compared to specimen 3. About the same amount of air bubble are present inside the beam. Again, most internal air bubbles have a diameter of less than 1 millimetre. The few air bubbles present on the top surface have a slightly bigger diameter than 1 millimetre. As with specimen 3, the placement of the rods in the mould of specimen 5 had the same effect on the internal air bubble patterns, were diagonal lines are clearly detectable.

#### *Dimensions after post-processing*

Appendix 5.6 illustrates the dimensions of the beam after post-processing.

#### *Stress analysis*

Figure 58 presents the pictures of beam 5 created with a polarized light and filter, showing similar patterns to beam 3. As with beam 1 and 3 the colours are mainly blue, grey and white, indicated either low levels of internal stresses or the presence of internal air bubbles (which could also introduce low levels of stress). The latter seems the most likely, because the colours corresponded largely with the internal diagonal air bubble patterns.

As described before, these air bubble patterns or potential internal stresses are most likely not crack starters but could be weaker points in the beam.

In Figure 61 a strain microscope picture is visible, showing a quantification of the amount of stress. This picture indicates that the amount of stress present is rather low. Yellow to red colours indicate higher levels of stress. The maximum occurring stress is 61nm. On this scale, this is quite low.

#### *Fracture analysis*

The fracture surface of specimen 5 shows comparable features to specimen 1 and 3. The fracture surface of beam 5 is visible in Figure 60. Here, again the fracture surface indicates high stresses upon failure. The origin of the crack is on the bottom side of the beam, right under the applied force, but slightly inwards compared to beam 1 and 3. For beam 5 no particular flaw has been visible with the naked-eye at the crack origin before failure. In addition, only low internal stresses had been examined at the fracture location, meaning that the fracture did not occur due to internal stress. Failure occurred at an applied force of 15.6 kN

#### *Mechanical properties*

##### *Young's modulus*

As described in section 2.2.2.2, the Young's Modulus ( $E$ ) can be calculated with equation (1).

The initial measured speed of sound ( $v$ ) in beam 5 is: 31  $\mu$ s (micro seconds).

(measured with the older model of the UPV tester)

The length of the beam is 0.155 m

The density of borosilicate glass is 2230 kg/m<sup>3</sup>

This resulted in a Young's Modulus of 55 GPa.

The second measurement of the speed of sound



Figure 58 Specimen 5 stress analysis



Figure 59 Specimen 5 air bubble entrapment

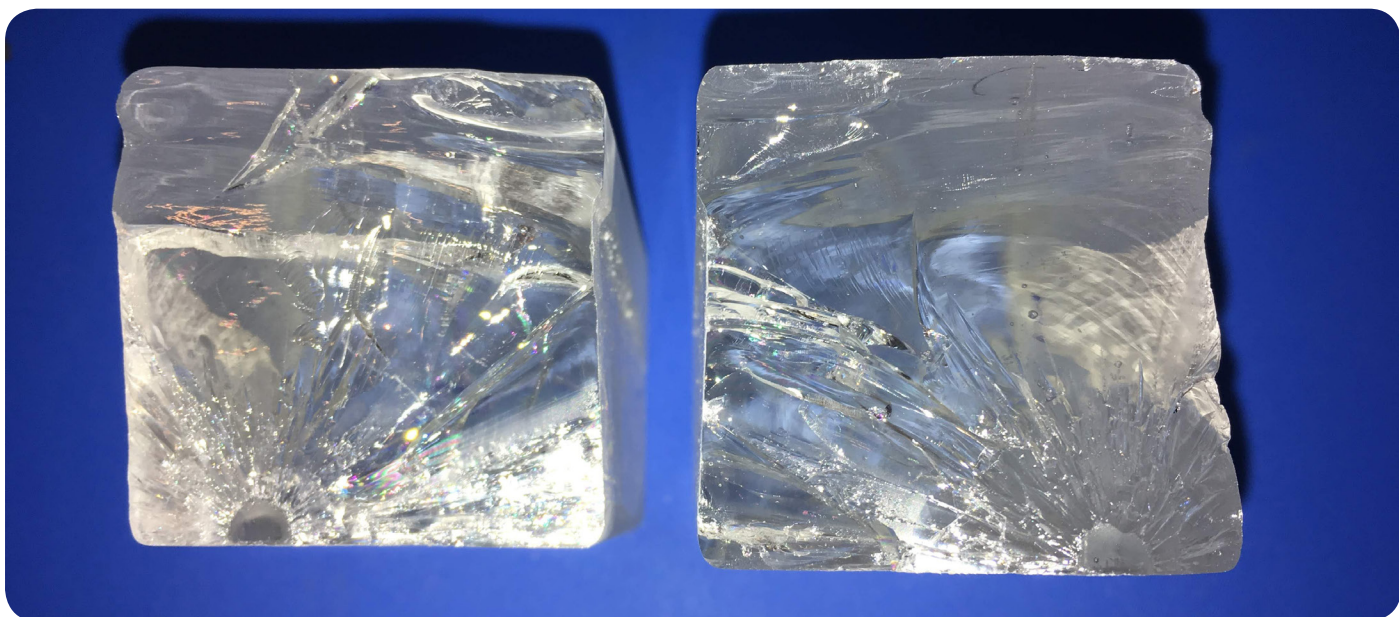


Figure 60 Specimen 5 fracture surface



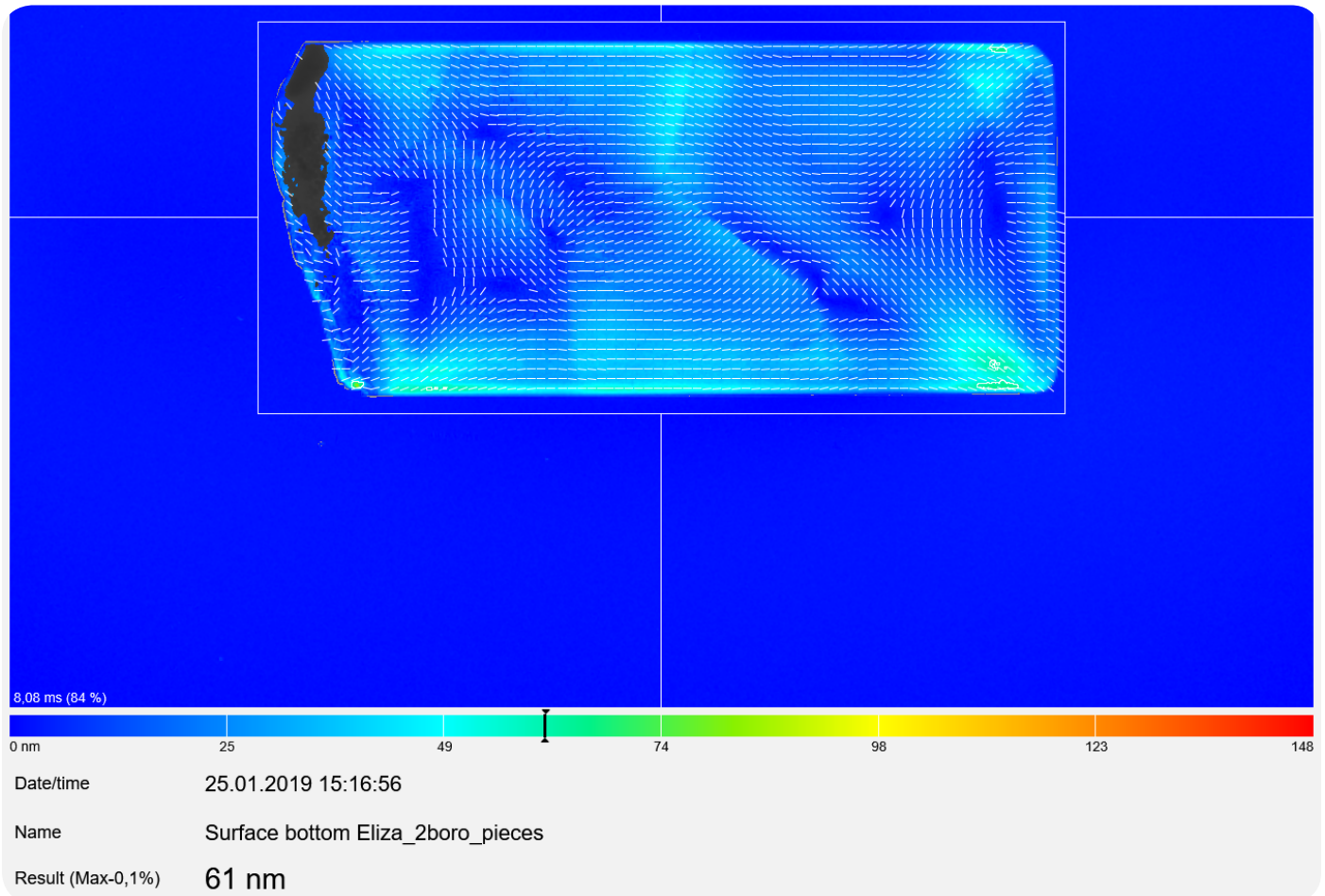


Figure 61 Specimen 5 stress analysis strain microscope. Yellow to red colours indicate higher levels of stress. The maximum occurring stress is 61nm. On this scale, this is quite low.

(v) in beam 5, done with the newer model of a UPV tester, resulted in: 32.1  $\mu$ s.  
 Calculated with equation (1) this resulted in a Young's Modulus of 52 GPa.

### Flexural strength

As described in section 2.2.2.2, the flexural strength of the beam can be calculated with equation (2):

Where for beam 5:

$\sigma_{fs}$  = Flexural strength (Mpa)

$F_f$  = 15554,54 N)

$L$  = 136 (mm)

$b$  = 38.85 (mm)

$d$  = 38.8 (mm)

This resulted in a flexural strength of 54 MPa.

For comparison, the flexural strength of non-recycled borosilicate glass (PYREX) is 69 MPa (Callister, 2007).

## 2.2.3.4 BEAM 6

### *Description*

The same four types of borosilicate glass products as applied in beam 2, have been grinded to powder to define if this does provide for better mixing of borosilicate glass with different chemical compositions.

### *Composition*

The powder of this beam is a mixtue of the same four different kind of glass objects as used in specimen 2. Again, aimed was for 25% laboratory ware, 25% rod, 25% PYREX round oven tray and 25% PYREX rectangular oven tray. The exact chemical composition can be found in section 2.2.3.2 of beam 2.

### *Beam description*

After firing, beam 6 turned out to be totally opaque and black. The applied glass cullet has been grinded to powder before firing and it seems that the used machines were contaminated with stones. Therefore, it indicates that fine stone powder has contaminated the glass mixture. The stone changed the molecular structure of the beam, however remarkable it did not crack. Another significant phenomenon is the enormous amount of internal air bubbles. As described in section 2.2.3.1, this is probable introduced trough the usage of powder. Adding a refining agent to the glass melt during firing could solve this problem. A refining agent introduces extra gasses to the melt, creating big bubbles. These large bubbles manage to absorb smaller bubbles and release them at the surface of the glass melt (Shelby, 2005).

Figure 64 illustrates the enormous amount of internal air bubbles magnified under a microscope.

### *Dimensions after post-processing*

Appendix 5.7 illustrates the dimensions of the beam after post-processing.

### *Stress analysis*

As this beam is opaque, an optical stress analysis could not be conducted.



Figure 62 Borosilicate powder in the mould





Figure 63 Specimen 6 opaque beam

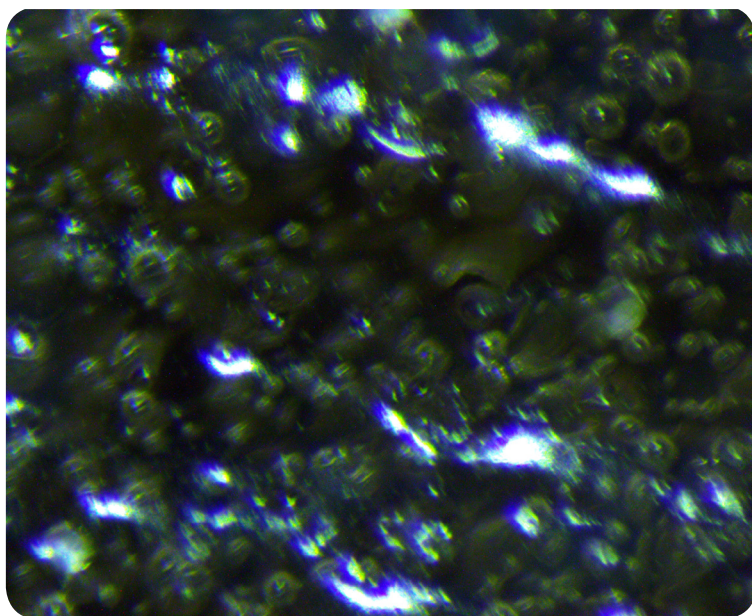


Figure 64 Specimen 6 extreme amount of air bubble entrapment under microscope

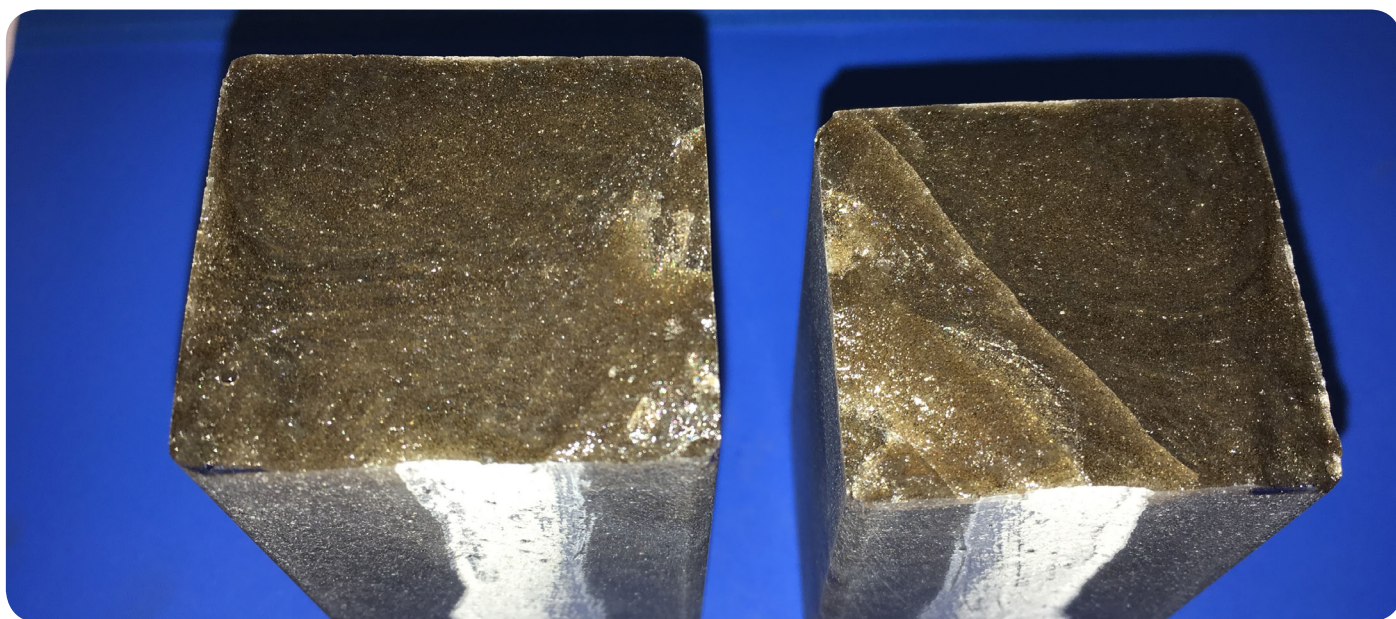


Figure 65 Specimen 6 fracture surface

### *Fracture analysis*

The fracture surface of specimen 6 showed significant difference compared to specimen 1, 3 and 5. A much more smooth fracture surface can be observed in Figure 65. The failure of this specimen occurred at 8.8 kN, resulting in significantly lower tensile stress upon cracking. The lower the stresses, the cleaner the fracture surface (Ono & Allaire, 2004). The origin of the crack could not be observed as clearly as in the other three specimens. For example, a mirror region could not be identified.

### *Mechanical properties*

#### *Flexural strength*

As described in section 2.2.2.2, the flexural strength of the beam can be calculated with equation (2):

Where for beam 6:

$\sigma_{fs}$  = Flexural strength (Mpa)

$F_f$  = 8804,21 (N)

$L$  = 136 (mm)

$b$  = 38.08 (mm)

$d$  = 41.0 (mm)

This resulted in a flexural strength of 28 MPa.

This flexural strength is almost half compared to the other specimens. Most likely, the stony contamination is reason for this. The stone affected the molecular structure of the beam and created weaker internal bonds between the molecules. As the total molecular structure has changed, this beam should not be compared with specimen 1, 3 and 5 in terms of mechanical properties.

#### *Young's Modulus*

As described in section 2.2.2.2, the Young's Modulus (E) can be calculated with equation (1).

The initial measured speed of sound ( $v$ ) in beam 6 is: 29  $\mu$ s.

(measured with the older model of the UPV tester)

The length of the beam is 0.153 m

The density of borosilicate glass is 2230 kg/m<sup>3</sup>

This resulted in a Young's Modulus of 62 GPa.

The second measurement of the speed of sound ( $v$ ) in beam 6, done with the newer model of a UPV tester, resulted in: 32.4  $\mu$ s.

Calculated with equation (1) this resulted in a Young's Modulus of 50 GPa.

This beam has an extreme amount of internal air bubbles, which most likely decreases the measured speed of sound and thus increases the calculated Young's Modulus. This is particularly clear in the speed of sound measurement done with the older UPV tester.



## 2.2.3.5 BEAM 7

### *Description*

The same four kinds of borosilicate glass products have been applied to examine if fine cullet does provide for better mixability of the different kinds of borosilicate glass and to reduce the risk of contamination. The applied cullet has a diameter between  $>2.3$  and  $<5$  mm and has been well mixed before putting it in the mould.

### *Composition*

The cullet of this beam is a mixture of the same four different kind of glass objects as used in specimen 2. Again, aimed was for 25% laboratory ware, 25% rod, 25% PYREX round oven tray and 25% PYREX rectangular oven tray. The exact chemical composition can be found in section 2.2.3.2 of beam 2.

### *Beam description*

After firing this beam shows several remarkable aspects. A clear waving pattern is visible in Figure 69. In addition, this beam contains an extreme amount of internal air bubbles as well. Also, several crystalized bodies are present within the glass beam. These inclusions could be a form of contamination, but this has not been identified yet.

### *Dimensions after post-processing*

Appendix 5.8 illustrates the dimensions of the beam after post-processing.

### *Stress analysis*

The stress analysis pictures of beam 7 are presented in Figure 68 and Appendix 5.14. Not only the light grey and blue colours are present, but more intense yellow, orange and even purple are present as well. Most likely, these colours do represent high levels of internal stresses. It is possible that these stresses are introduced due to a difference in thermal expansion coefficient. Figure 72 shows a close-up view of the internal stresses corresponding to the cullet size. Figure 70 presents a strain microscope picture, showing a quantification of the amount of stress. It indicates that there is a higher level of stress compared to



Figure 66 Borosilicate cullet of  $>2.3$  mm  $< 5$  mm



Figure 67 Borosilicate fine cullet in the mould

specimen 5, but the amount is not extremely high.

### *Fracture analysis*

This specimen failed at an ultimate force of 7.6 kN, which is lower than specimen 6. Most likely, this is the result of the large amount of internal stresses, creating weaker bonds between the molecules. The fracture surface of beam 7 is visible in Figure 71. Here, a wavy and bumpy surface can be seen, corresponding roughly to the small cullet size. Most likely, the beam failed due to the present internal stresses. However, Figure 73 illustrates that at the starting point of the crack several flaws were present. Those are marked by the circles. This could mean that the beam failed at a lower ultimate force due to the internal stresses, the present flaws or both (because flaws and internal stresses influence each other). At this point, it is not possible to define the exact course of failure.

### *Mechanical properties*

#### *Flexural strength*

As described in section 2.2.2.2, the flexural strength of the beam can be calculated with equation (2):

Where for beam 7:

$\sigma_{fs}$  = Flexural strength (Mpa)

$F_f$  = 7580,66 (N)

$L$  = 136 (mm)

$b$  = 35.5 (mm)

$d$  = 40.5 (mm)

This resulted in a flexural strength of 27 MPa.

As with specimen 6, this flexural strength is almost half compared to the other specimens. As described in the *Fracture analysis of beam 7*, this is probably caused due to the internal stresses, creating weaker areas. Another reason could be the present flaws on the tensile zone of the beam.

#### *Young's Modulus*

As described in section 2.2.2.2, the Young's Modulus (E) can be calculated with equation (1).

When the older model of the UPV tester has been used to measure the speed of sound of the beams, this beam was not created yet. Therefore, the speed of sound of this beam has only been measured with the newer model of the UPV tester.

The measured speed of sound in beam 7 is: 31,5  $\mu$ s.

The length of the beam is 0.154 m

The density of borosilicate glass is 2230 kg/m<sup>3</sup>

This resulted in a Young's Modulus of 53 GPa.

This beam has an extreme amount of internal air bubbles, which most likely affects the measured speed of sound and thus the calculated Young's Modulus.



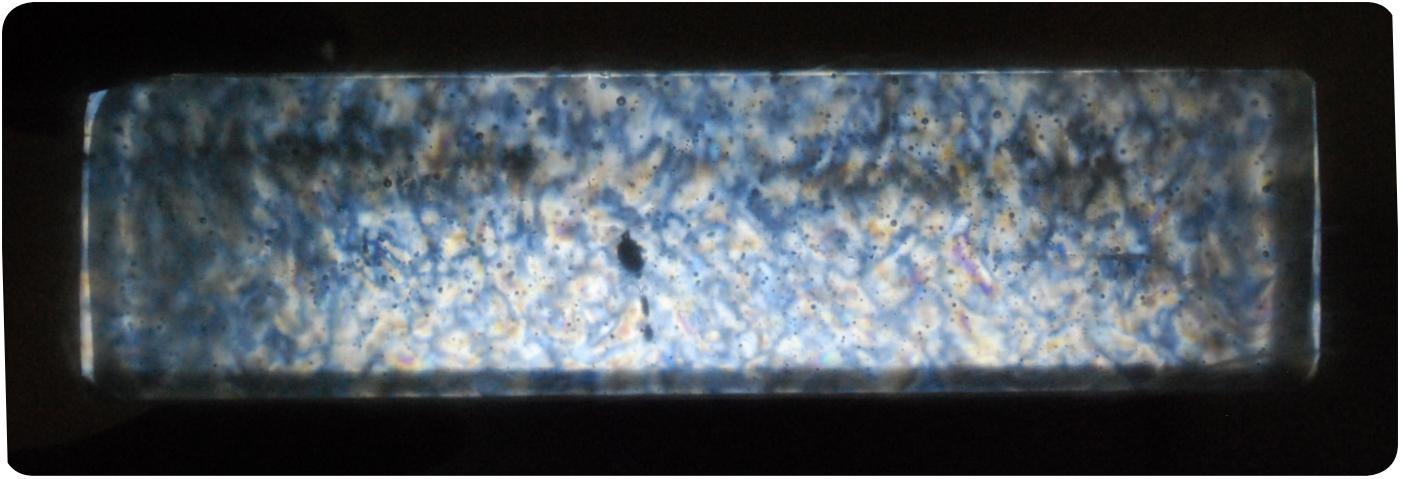


Figure 68 Specimen 7 stress analysis

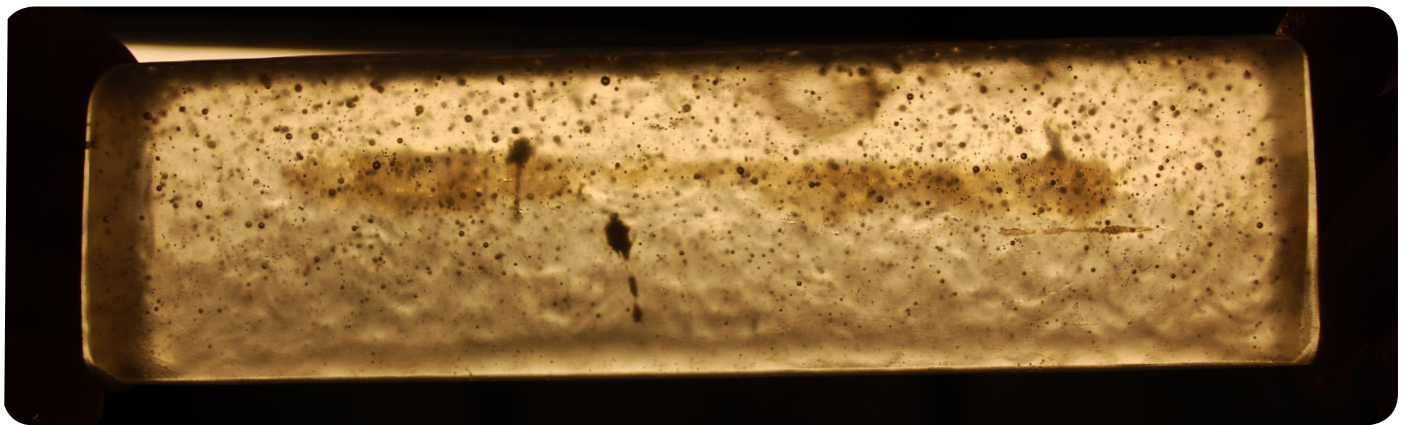


Figure 69 Specimen 7 air bubble entrapment and visible waving pattern

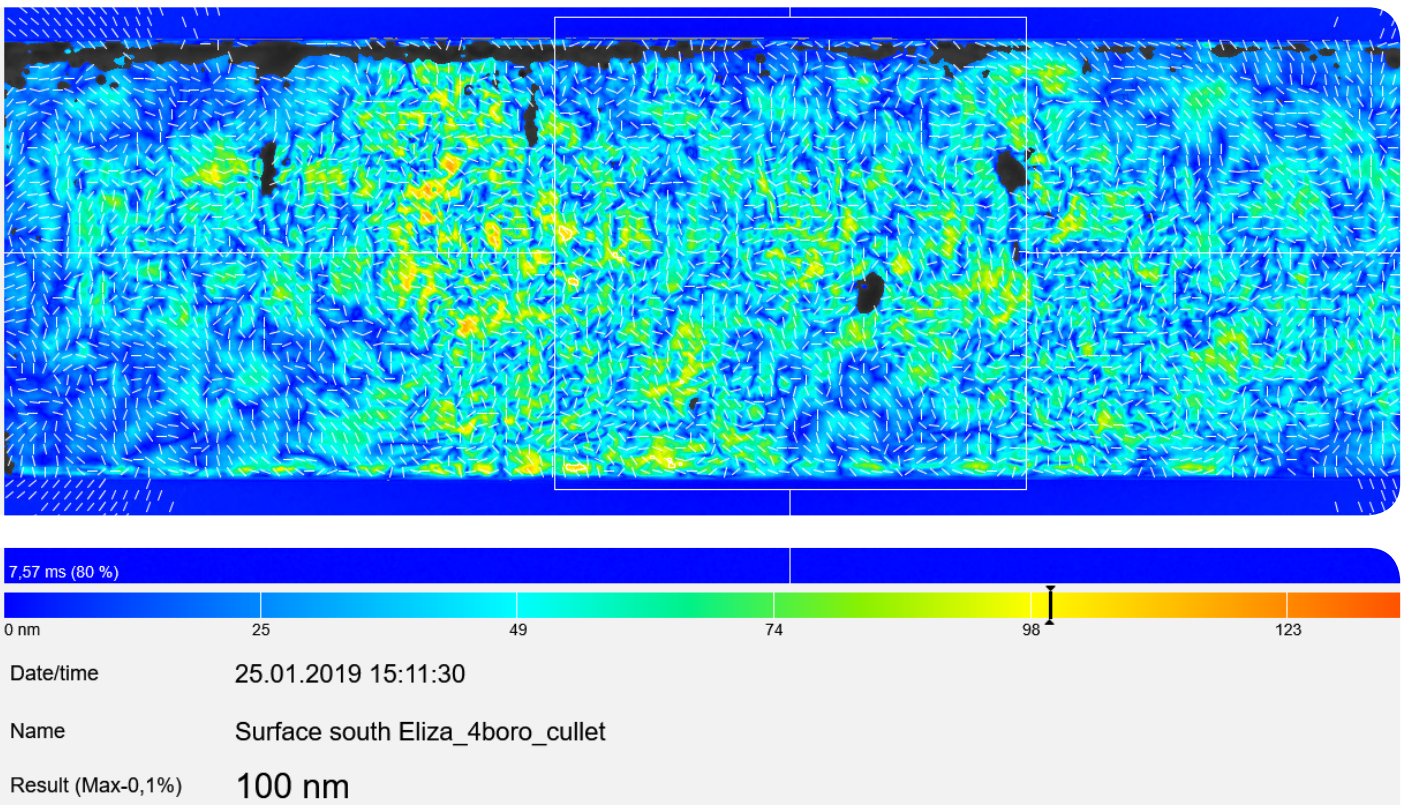


Figure 70 Specimen 7 stress analysis strain microscope



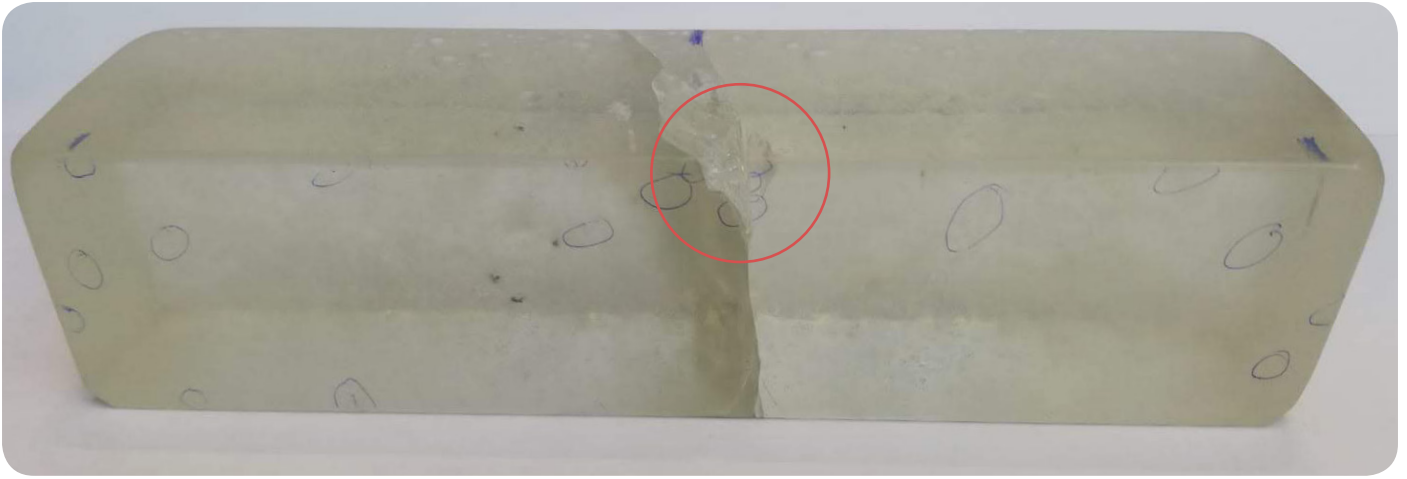


Figure 73 Specimen 7 marked flaws at tensile surface. Circle indicating the starting point of the crack.

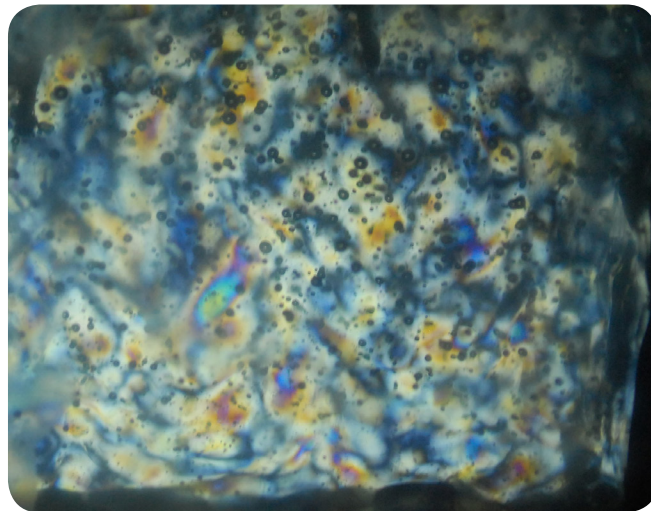


Figure 72 Specimen 7 detailed view of internal stresses; cullet size clearly visible

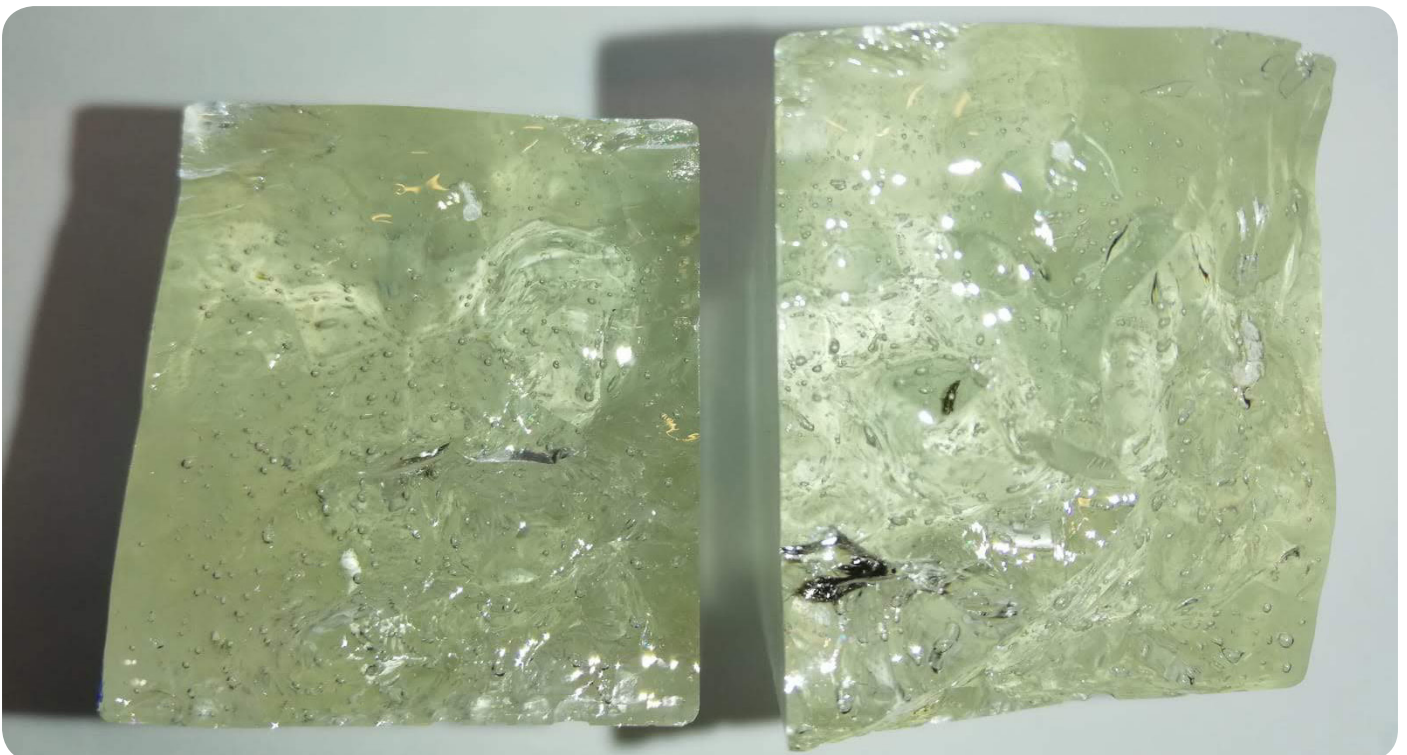


Figure 71 Specimen 7 fracture surface

### 2.2.3.6 CUBE

#### *Description*

For the cube the same four kinds of borosilicate glass products as for beam 2, 6 and 7 have been applied to examine if fine cullet does provide for better mixability of the different kinds of borosilicate glass and to reduce the risk of contamination. In addition to beam 7, this cube has been fired at a higher temperature (1200°C) to examine if this will reduce the internal stresses and amount of air bubbles. The applied cullet has a diameter between >powder and >2.3 mm and has been well mixed before putting it in the mould. The cube has been made to solely test the mixability of this glass mixture upon a higher firing temperature.

#### *Composition*

The cullet of this cube is a mixtue of the same four different kind of glass objects as used in specimen 2. Again, aimed was for 25% laboratory ware, 25% rod, 25% PYREX round oven tray and 25% PYREX rectangular oven tray. The exact chemical composition can be found in section 2.2.3.2 of beam 2.

#### *Beam description*

The cube shows several similarities to beam 7. Here, an extreme amount of internal air bubbles is present as well, although slightly less. Apart from this no extraordinary elements were seen.

#### *Dimensions after post-processing*

The cube measures approximately 50\*50\*50 mm.



Figure 74 Borosilicate cullet of >powder and <2.3 mm



Figure 75 Borosilicate fine cullet (<2.3mm) in the mould

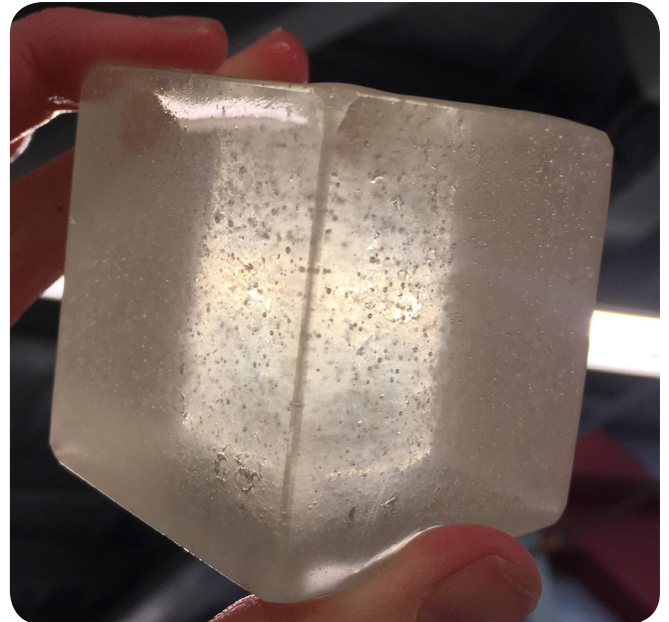


### *Stress analysis*

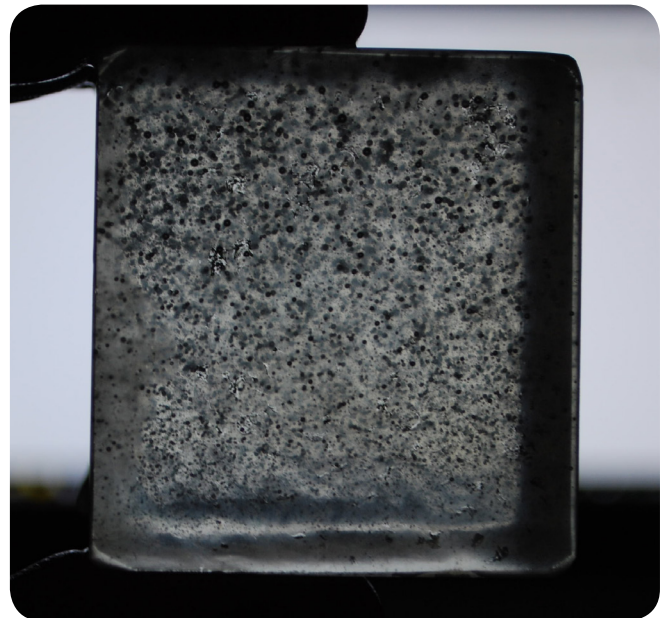
Figure 78 and Appendix 5.15 show the internal stresses present in the cube. As with beam 7, the different cullet pieces are visible, indicating a difference in thermal expansion coefficient. Despite this, the colours are less intense and are mainly light blue, grey and white, indicating lower stresses. The yellow/orange colour present at the corners are most likely related to natural shrinkage upon cooling of the cube.

### *Mechanical properties*

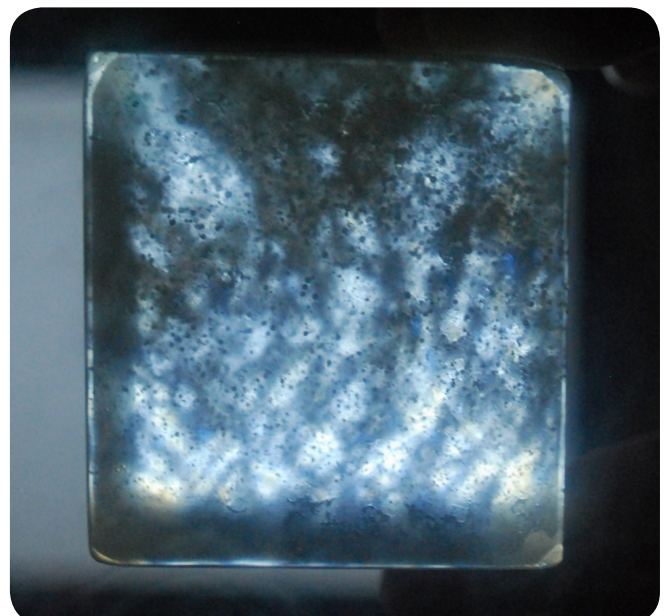
The mechanical properties of this cube have not been defined, as this shape is not comparable to the beams. Therefore, no flexural strength and Young's Modulus have been determined.



*Figure 76 Cube made of fine cullet*



*Figure 77 Extreme amount of internal air bubbles*



*Figure 78 Cube internal stress analysis (side view)*

## 2.3 CONCLUSIONS OF EXPERIMENTS

### 2.3.3.1 CONCLUSIONS ON MIXABILITY

Combining different borosilicate glass products with various chemical compositions demonstrated several potentials and challenges. A summary about the mixability of borosilicate glass can be found in Table 14 and Table 15.

Mixing pieces of presumably the same chemical composition suggest that through applying recycled cullet, lower firing temperatures for a borosilicate glass melt are possible.

Mixing four different types of borosilicate glass through powder showed its potential in beam 6. Even though this specimen is contaminated by stone, it did not crack. However, powder introduces two main challenges: an extreme amount of internal air bubbles and risk of contamination. The extreme amount of internal air bubbles can be relieved by either raising the temperature of the glass melt or adding a refining agent. In an industrialized process, stirring the glass melt would be an option as well. Raising the temperature of the glass melt is not favourable, because it increases the energy consumption of the glass production. The risk of contamination such as stone is expected to be less during an industrialized process.

Mixing four different types of borosilicate glass through fine cullet showed its potential in beam 7. Although, this specimen exhibited a higher amount of internal stresses, it did not crack. These internal stresses correspond to the applied cullet size, indicating that these stresses probably are related to a difference in chemical composition. If so, such stresses cannot be relieved through a longer annealing time and are considered permanent. If these stresses are not introduced due to a difference in composition, then a longer annealing time or a slightly higher firing temperature could reduce the internal stresses. The cube illustrated the potential of applying a slightly higher firing temperature for relieving the internal stresses and decreasing the amount of internal air bubbles. Although internal stresses corresponding to the cullet size are still present in the cube, the stress analysis suggests a decrease compared to beam 7. In addition, the cube contained slightly less internal air bubbles.

Thus, at this point, sorting recycled glass well

is required to provide for a homogenous glass composition, suitable for melting borosilicate glass at low temperatures. Melting an unsorted batch of borosilicate glass requires either powder or fine cullet to allow for proper mixing and thus creating a homogenous end-product.

Important to notice is the rather small sample size of these experiments. To draw more scientific conclusions more research with larger sample sizes should be conducted.

### 2.3.3.2 CONCLUSIONS ON MECHANICAL PROPERTIES

The three-point bending test of specimen 1, 3, and 5 showed a flexural strength of recycled borosilicate glass of similar values compared to non-recycled borosilicate glass as found in (Callister, 2007). The flexural strength of the specimens is presented in Table 16.

The fact that the three comparable beams (1, 3 and 5) failed at approximately the same applied force is a strong indication that all three beams failed because stress levels in the beams approached the ultimate tensile strength of borosilicate glass and not because of the presence of significant internal flaws or surface flaws. The fact that all three beams have a flexural strength close to that of non-recycled borosilicate glass implies that recycling of borosilicate glass has little effect on the mechanical properties of the glass.

The contaminated specimen 6 has a flexural strength of half the value compared to specimen 1, 3 and 5. As the stone contamination changed the molecular structure of the beam it failed at a lower ultimate force during the three-point bending test. Probably, the stone interrupts the molecular network of the borosilicate glass, introducing weaker bonds between the glass molecules. However, as the molecule structure of specimen 6 is significantly different, this specimen should not be compared in terms of mechanical properties.

Beam 7 has a flexural strength of almost half the value compared to specimen 1, 3 and 5, as well. In this case this is probably introduced due to

the higher amount of internal stresses, creating weaker bonds between the glass molecules. Also, several flaws were present on the tensile surface of the beam, creating a higher risk for cracking. Therefore, the exact course of failure could not be defined.

The applied casting method and post-processing could affect the surface of the beams, resulting in small flaws (not always visible with the naked eye). If the specimens were cast in an industrialized process, it is expected that they can withstand higher forces and thus shall the flexural strength be similar to non-recycled borosilicate glass.

As described in section 2.2.2.2, the Young's modulus of the specimens has been measured twice. Both sets of results are presented in Table 16. Both are included to indicate that the amount of internal air bubbles influences the Young's Modulus measurement. Therefore, the second measurement done with the improved UPV tester showed lower results than the first measurement. However, both sets of results are comparable to the standard value of non-recycled borosilicate glass.

This section suggests that based on these test results recycled borosilicate glass has similar mechanical properties to non-recycled borosilicate glass.

	SAME CHEMICAL COMPOSITION	DIFFERENT CHEMICAL COMPOSITION
BIG PIECES	✓	✗
FINE CULLET	✓	~
POWDER	✓	✓

Table 14 Summarizing table mixability of recycling borosilicate glass



## 2.4 RECOMMENDATIONS OF EXPERIMENTS

These experiments on the recyclability of borosilicate glass are one of the first, resulting in several recommendations for further research.

As stated before, more research should be conducted on the mixability and corresponding mechanical properties of recycled borosilicate glass, as this thesis only investigates a small sample size.

Attention should be paid to the use of PYREX cooking ware. There are some indications that this cooking ware is made of tempered soda-lime glass today, instead of borosilicate glass. However, this accounts probably only for the United States (Lewis, n.d.).

As stated in section 2.3.3.1 the amount of air bubbles could possibly be reduced by adding a refining agent to the melt, by raising the firing temperature (though less desirable due to higher energy consumption) or by stirring the melt.

To reduce internal stresses in the specimens, either a longer annealing time or a slightly higher firing temperature could be beneficial.

The mixability and mechanical properties of using fine cullet combined with using glass of different chemical compositions are inconclusive as shown in Table 14. Higher amounts of internal stresses were observed in beam 7 and the cube but they did not crack. Fine cullet of heterogeneous composition is most desirable because collected glass will be mixed and fine cullet has lower risk of contamination compared to powder. More experiments on specimens similar to beam 7 and the cube are advised.

Table 15 Summarizing table mixability of recycling borosilicate glass

	BEAM 1	BEAM 2	BEAM 3	BEAM 4
GLASS TYPE (All types are borosilicate)	Rods* laboratory ware*	Tube* Lab. ware* PYREX oven tray rect. PYREX oven tray round	Rods*	Rods*
AMOUNT OF EACH GLASS TYPE <small>per beam; around a total of 616 grams necessary</small>	<i>Aim:</i> 50% Rods 50% Laboratory ware = 308 gr each  <i>Used:</i> Rods: 349 gr Laboratory ware: 267 gr	<i>Aim:</i> 25% Tube 25% Laboratory ware 25% Oven tray round 25% Oven tray rectangular = 154.19 gr each  <i>Used:</i> Tube: 155.6 gr Laboratory ware: 154.2 gr Oven tray round: 154.1 gr Oven tray rect.: 155.8	<i>Aim:</i> 100% Rods = 616 gr  <i>Used:</i> Rods: 640.2 gr	<i>Aim:</i> 100% Rods = 616 gr  <i>Used:</i> Rods: 640.1 gr
CULLET SIZE $\varnothing$	Pieces > 50 mm	Pieces > 50 mm	Pieces between 10 and 30 mm	Pieces between 10 and 30 mm
DWELL TIME AT TOP TEMPERATURE (1120 °C)	10 hours	10 hours	10 hours	10 hours
DESCRIPTION	 Clear and transparent beam. Several internal air bubble groups. A few big bubbles on top surface.	 Cracked upon annealing. Clear and transparent beam.	 Clear and transparent beam. Internal air bubble patterns follow placement of rods in the mould.	 Cracked upon annealing. Reaction with Cast mould.
AMOUNT OF AIR BUBBLES	Moderate	Moderate	High	Low
INTERNAL STRESSES <small>Estimated with a polarization filter</small>	 Most internal stresses correspond with internal air bubble patterns.	_____	 Most internal stresses correspond with internal air bubble patterns.	_____

\* Same composition (wt%) for the rods, tube and laboratory ware (all objects by Schott)

\*\* Boron cannot be traced with the used measurement method, therefore the amount of SiO<sub>2</sub> appears too high

COMPOSITION (wt%)	Objects by Schott	Pyrex oven tray rectangular:	Pyrex oven tray round:
SiO <sub>2</sub>	81	91.2	90.8
B <sub>2</sub> O <sub>3</sub>	13	-	-
Na <sub>2</sub> O + K <sub>2</sub> O	4.0	5.4	5.5
Al <sub>2</sub> O <sub>3</sub>	2.0	3.1	3.4

4	BEAM 5	BEAM 6	BEAM 7	CUBE
*	Rods*	Tube* Lab. ware* PYREX oven tray rect. PYREX oven tray round	Tube* Lab. ware* PYREX oven tray rect. PYREX oven tray round	Tube* Lab. ware* PYREX oven tray rect. PYREX oven tray round
	<p><i>Aim:</i> 100% Rods = 616 gr</p> <p><i>Used:</i> Rods: 640.7 gr</p>	<p><i>Aim:</i> 25% Tube 25% Laboratory ware 25% Oven tray round 25% Oven tray rectangular = 154.19 gr each</p> <p><i>Used:</i> Tube: 159.6 gr Laboratory ware: 140.7 gr Oven tray round: 159.0 gr Oven tray rect.: 159.6 gr</p>	<p><i>Aim:</i> 25% Tube 25% Laboratory ware 25% Oven tray round 25% Oven tray rectangular = 154.19 gr each</p> <p><i>Used:</i> Tube: 155.2 gr Laboratory ware: 155.2 gr Oven tray round: 155.5 gr Oven tray rect.: 155.7 gr</p>	<p><i>Aim:</i> (300 gr glass for cube) 25% Tube 25% Laboratory ware 25% Oven tray round 25% Oven tray rectangular = 75 gr each</p> <p><i>Used:</i> Tube: 76.82 gr Laboratory ware: 75.70 gr Oven tray round: 75.11 gr Oven tray rect.: 82.50 gr</p>
between 10 mm	Pieces between 10 and 30 mm	Powder	Pieces between 2.3 and 5 mm	Pieces between powder and 2.3 mm
hrs	10 hours	10 hours	10 hours	10 hours at 1200 °C
				
upon ng. n Crystal ould	Clear and transparent beam. Internal air bubble patterns follow placement of rods in the mould.	Black and opaque beam. Contaminated with stone. Molecular structure changed. Extreme amount of internal air bubbles.	Extreme amount of internal air bubbles. Placement of shards is visible as a 'waving pattern'.	Extreme amount of internal air bubbles, although less than beam 7.
	High	Extreme	Extreme	Extreme
—	 Most internal stresses correspond with internal air bubble patterns.	Not possible to see internal stresses.	 Very high internal stresses. Waving pattern clearly visible.	 Internal stresses corresponding to cullet size

	BEAM 1	BEAM 2*	BEAM 3	BEAM 4*
YOUNG'S MODULUS Measurement 1 (GPa)	59	—	60	—
YOUNG'S MODULUS Measurement 2 (GPa)	52	—	Not available	—
FLEXURAL STRENGTH (MPa)	52	—	56	—
AMOUNT OF AIR BUBBLES	Moderate	—	High	—
GLASS TYPE (Borosilicate)	Rods & lab beaker	Rods Lab beaker Oven tray rect. Oven tray round	Rods	Rods

Beam 2 and beam 4 cracked upon firing. Mechanical properties could not be defined.

Table 16 Summarizing table mechanical properties of recycling borosilicate glass



BEAM 5	BEAM 6	BEAM 7	STANDARD NON-RECYCLED BOROSILICATE GLASS
5 5	6 2	—	6 4
5 2	5 0	5 3	6 4
5 4	2 8	2 7	6 9
High	Extreme	Extreme	—
Rods	Rods Lab beaker Oven tray rect. Oven tray round	Rods Lab beaker Oven tray rect. Oven tray round	—

Continuation of previous table



# **PART** 3

DESIGN RESEARCH

# 3.1 CASE STUDY CASA DA MÚSICA

*A case study has been chosen for application of the proposed facade system to showcase both the possibilities of recyclability of borosilicate glass and of dry-interlocking cast glass components. As described in section 1.3.7, Casa da Música has been selected as the case study building for this thesis.*

## 3.1.1 BUILDING DESCRIPTION

### General information

- Location: Porto, Portugal
- Architect: OMA
- Building year: 2005
- Area: 22000 m<sup>2</sup>

by Casa da Musica / OMA, (2014)

An innovative concert hall, housing the National Orchestra of Porto, has been designed by OMA in 2005. The building is designed as a faceted 'box' of white concrete. At either end of the several music halls giant corrugated glass facades are located. The largest corrugated glass facade measures 25 \* 15 m. The middle one is 22 \* 12 m and the smallest one is 14 \* 9 m. For a concert hall it is uncommon to have such large glass facades in the music halls, but this makes this building special. A lot of daylight can reach each auditoria through the corrugated facades, creating interesting reflections.



Figure 79 Casa da Música in Porto

Source: © Philippe Ruault



### 3.1.2 DESIGN CONCEPT OF CASA DA MÚSICA

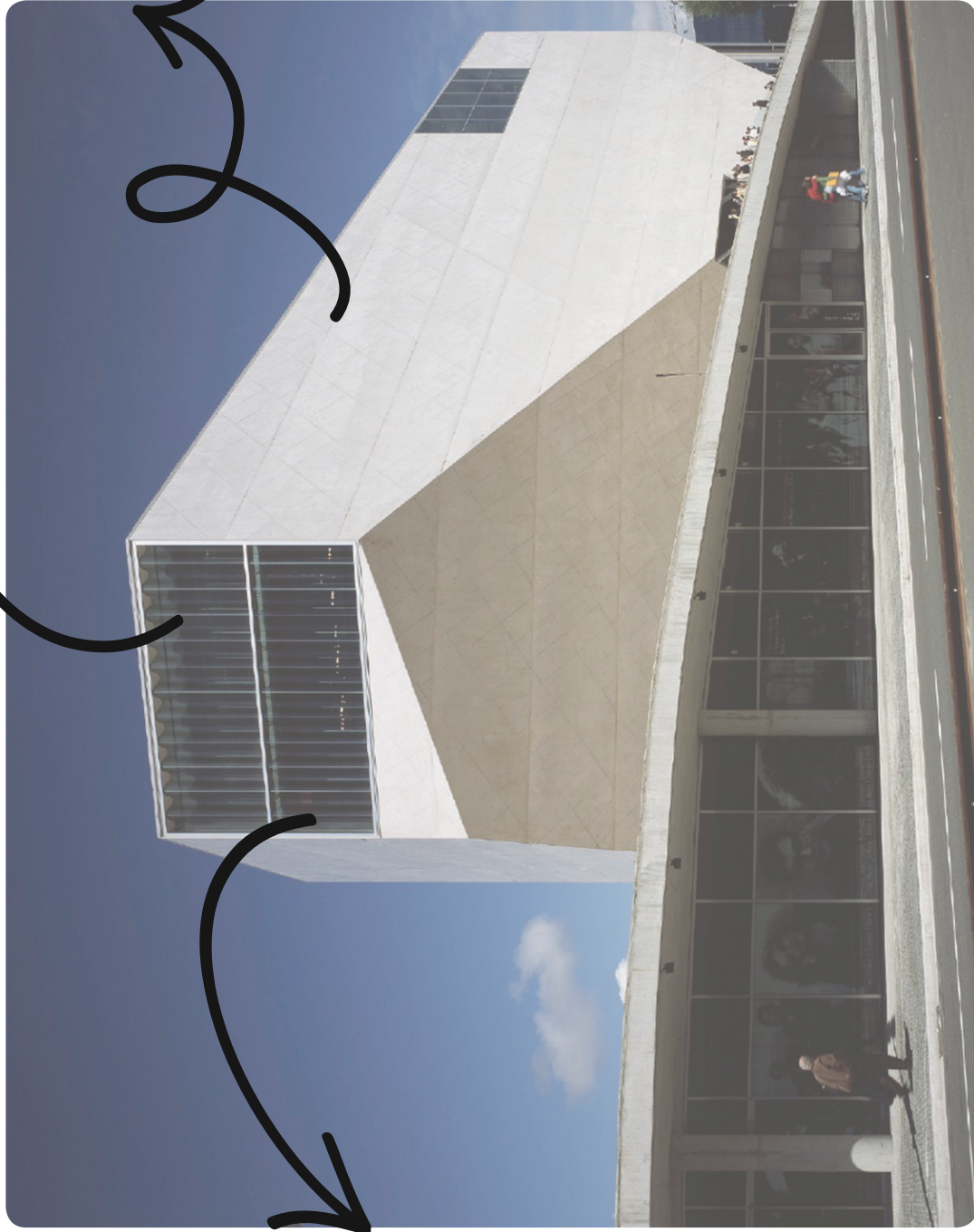
With this design of Casa da Música, the architects wanted to reshape the 'standard' "shoe-box" concert hall and create something more interesting. Another design aspect was to create a relationship between the inside of the building and the public square outside. An important design aspect was to create an appealing contrast between the corrugated, shining and brilliant glass facade and the flat, smooth, white surface of the concrete. For these corrugated facades as much glass as possible, with as less steel as possible was aimed for. The architect wanted preferable no steel construction around the glass facade; so no 'steel-spaghetti' close to the facade (Nijssse, 2009).

The main design concepts of Casa da Música are illustrated in Figure 81.



Figure 80 Close-up of Casa da Música  
Photo by Tirza Izelaar

CORRUGATED,  
SHINING AND  
BRILLIANT GLASS  
FACADE



FLAT, WHITE AND  
SMOOTH CONCRETE  
FACADE

GLASS FACADE  
WITH AS LESS  
STEEL AS  
POSSIBLE

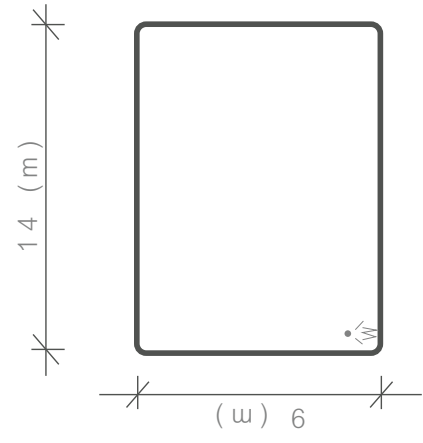


Figure 81 Main design concept of Casa da Música

## 3.2 DESIGN CRITERIA AND CONSTRAINTS

Several types of dry-interlocking systems exist, such as topologically interlocking, protrusions and depressions and tongue and groove. Well-known examples in architecture are Roman arches and Japanese wood joints. However, these principles not are suitable to directly translate to cast glass. The nature of glass (e.g. its brittleness) does not allow for the same treatment as conventional building materials like wood and stone. Therefore, new design criteria are defined based on the characteristics of glass as a construction material. Section 3.2.1 and section 3.2.2 describe these new defined criteria for both the interlocking principle and constraints regarding to casting glass.

### 3.2.1 DESIGN CONSTRAINTS INTERLOCKING PRINCIPLE

The following criteria are based on previous research described by (Oikonomopoulou, et al., 2018b):

- *Movement constraint*

To create a facade structure that behaves in a monolithic way and provides enough structural integrity to transfer lateral forces, the interlock system has to constrain movement in the x- and y-directions. In the z-direction of the facade, the movement is constraint due to the deadload of the cast glass components itself.

- *Shear abilities*

The interlocking keys or connectors should represent a smooth and convex shape to allow for an even shear force distribution. Conventional interlocking keys or connectors should be avoided

due to the stiff and brittle behaviour of glass. Generally, these conventional interlockings are very small or thin compared to the total component, which could generate stress concentrations and thus possible risk of failure.

Therefore, a general rule has been defined to avoid too thin interlocking keys. Figure 82 illustrates that generally the thickness of the component should be divided by three equal parts, to maintain an equal force distribution.

- *Ease of assembly*

To reduce construction time and cost, the components should be able to self-align. This means that during construction the components will fit easy on top of each other, reducing risk of construction mistakes and damaging the component.

- *Component dimensions*

Jacobs (2017) defined that lower components with lower interlocking keys have a higher risk of bending when subjected to shear force, see Figure 83. In addition, such components have a higher uplifting risk. However, in the proposed facade system uplifting is counteracted due to the compressive deadload of the facade itself.

In contrast, higher components are more resistant to bending, but have an increased risk of shear key failure, see Figure 83. The interlocking elements transfer the shear loads between components. If the components are too high, shear load on the relatively small interlocking elements can become too high resulting in the elements chipping off.

The desirable failure mode of the proposed facade would be shear key failure. The total cast component is still intact and can provide structural integrity.

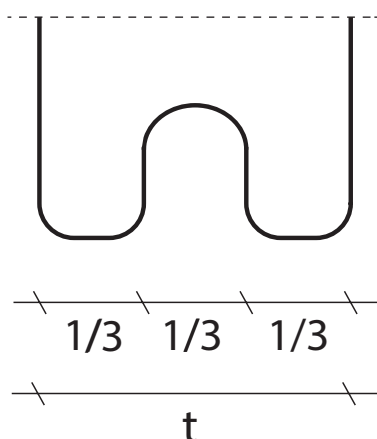


Figure 82 Ratio between thickness component ( $t$ ) and interlocking holes



## 3.2.2 DESIGN CONSTRAINTS CAST GLASS

### Expectations for height variations

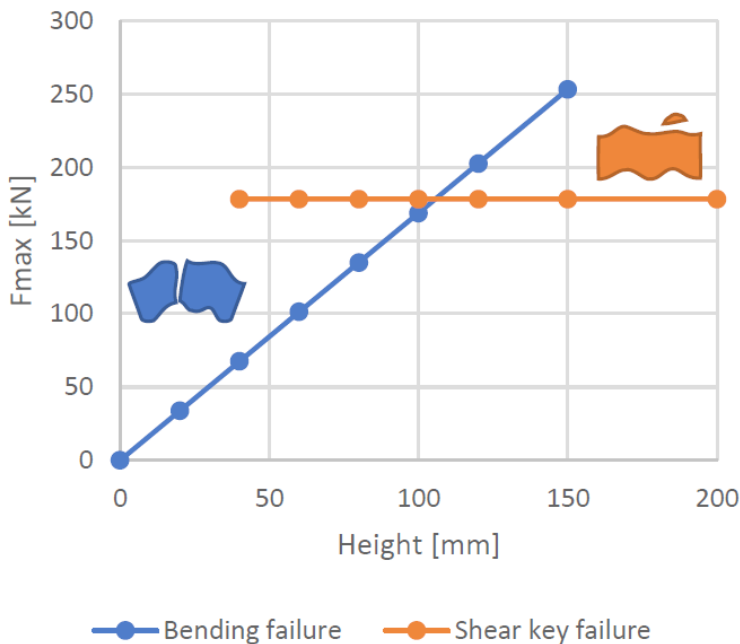


Figure 83 Bending versus shear key failure mechanisms related to component height

Source: Jacobs (2017)

- *Maximum weight*

In section 1.1.6 the important, but time-consuming process of annealing of casting glass is described. The components mass is the critical factor in influencing the required annealing time.

In addition, this thesis proposes a dry-interlocking facade system, so that it can be dismantled and recycled at its end of life. Hence, ease of (dis-) assembly of such a facade system is essential.

Therefore, the maximum weight of one cast glass component has been set to 10- 12 kg.

- *Homogenous mass distribution and rounded geometry*

As described in section 1.1.6, annealing of a cast glass component is essential to relieve any residual internal stresses. Section 1.1.6 also indicates that this is convenient in rounded geometry, due to a homogenous mass distribution. For example, a sphere or ellipsoid shape are most suitable for annealing, though not for construction purposes. Any sharp, thin or pointy shapes should be avoided, to decrease the risk for residual internal stresses.

- *Maximum number of different component types*

The more different types of components are applied in interlocking structures, the ease of (dis-)assembly decreases and manufacturing cost increase. To enhance ease of assembly an interlocking structure constructed of only one type of component would be most favourable. In addition, for one component only one type of mould is required, which allows for a more standardized, thus cheaper, production process. However, as one type of component is unlikely for most facade constructions, two or three different types of components are acceptable as well.



# 3.3 RESEARCH TO EXISTING (INTERLOCKING) CAST GLASS STRUCTURES

*As described in section 1.1.7, not much cast component systems are applied in the built environment. This chapter describes the few produced cast glass components. The second part of this chapter provides an overview of dry-interlocking cast glass components. These interlocking components have not been applied within the built environment yet, but are still subjected to research or some components are developed within the context of graduation projects.*

## 3.3.1 EXAMPLES OF PRODUCED CAST GLASS COMPONENTS

Table 17 illustrates the few examples of produced of cast glass components, corresponding to the buildings described in section 1.1.7. Most of these components are largely similar to general brick shapes. These produced components are based on the design constraints, related to casting glass, as described in section 3.2.2. This table shows that due to the much lower thermal expansion coefficient of borosilicate glass ( $3.3 \cdot 10^{-6} \text{ K}^{-1}$ ), compared to soda-lime glass ( $9 \cdot 10^{-6} \text{ K}^{-1}$ ), the annealing time of a similar component in weight drastically decreases. This is clearly illustrated in the component of the Atocha Memorial; 20 hours of annealing for a component of 8.4 kg versus the Crystal House component of 38 hours of annealing for a component of 7.2 kg.

## 3.3.2 TOTAL OVERVIEW OF RESEARCHED INTERLOCKING COMPONENTS

Table 18 shows the several existing studies to interlocking cast glass components. From these options one type of component will be chosen in chapter 3.4 for the further design.

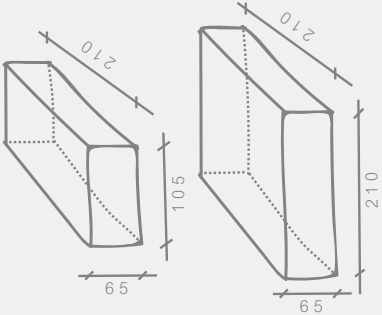
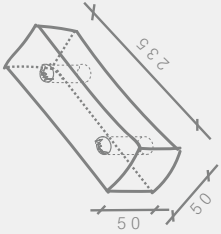
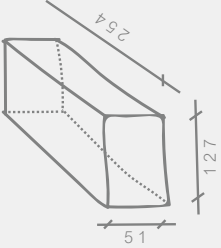
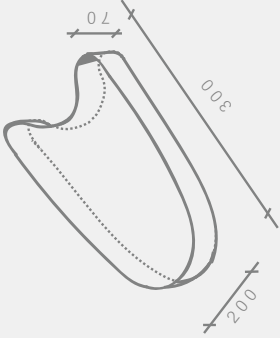
CRYSTAL HOUSE	OPTICAL HOUSE	CROWN FOUNTAIN	ATOCHA MEMORIAL
SHAPE & DIMENSIONS (mm) 			
BLOCK WEIGHT (Kg)	2.2	4.5	8.4
ANNEALING TIME (h)	Unknown	Unknown	20
TYPE OF GLASS	Borosilicate	Soda-lime	Borosilicate

Table 17 Comparison between the four produced cast glass components

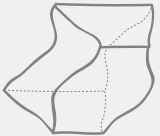

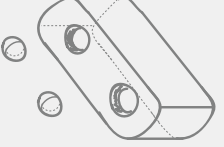
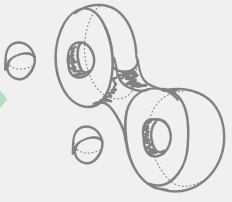

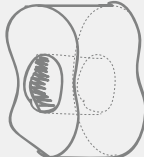
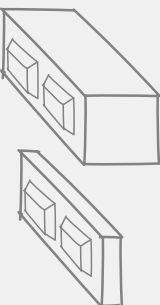

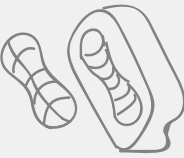
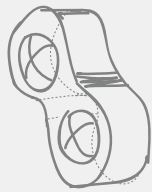
	OIKONOMOPOULOU & BRISTOGIANNI 1	JANSSENS	DE VRIES 1	DE VRIES 2	JACOBS
SHAPE					
SUITABLE IN EXTERNAL WALL CONFIGURATION	Yes	No	Yes	No	Yes
SHEAR FORCE CAPACITY	High	High	Sufficient/ high	Sufficient/ high	High
HOMOGENEOUS COOLING IN CASTING	Effective	Effective	Risk of internal residual stresses	Effective	Effective
REDUNDANCY	Yes	No	Yes	Yes	Yes
EASE OF (DIS)-ASSEMBLY	High	Low	Medium	Medium	High

Table 18 Comparison between the existing studies to interlocking cast glass components.

AKERBOOM	BAROU	SOMBROEK/ AURIK	OIKONOMOPOULOU & BRISTOGIANNI 2	OIKONOMOPOULOU & BRISTOGIANNI 3
				
No	Yes	No	Maybe	Maybe
Sufficient	Sufficient	-	Moderate	Moderate/ high
Effective	Risk of internal residual stresses	Risk of internal residual stresses	Risk of internal residual stresses	Effective
No	Yes	No	Yes	Yes
High	High	Low	Medium	High

Continuation of previous table



## 3.4 CONCEPT DESIGN CRITERIA

*This chapter describes the design concept criteria for the dry-interlocking cast glass facade system on overall facade/building level, component level, interlocking level and on interlayer level.*

### 3.4.1 MAIN CONCEPT DESIGN CRITERIA

Create a contrast between the white smooth concrete and the glass façade. Reintroducing the waving pattern, but with bigger waves. Bigger waves contribute to less obstruction of the view and give an interesting distortion.

The structural integrity of the facade is provided by the wave-like shape made of dry-interlocking cast glass components under compression of the façade's own weight.

As less steel sub-construction as possible. Intergrade the steel within the facade or preferably inside the glass components.

The appealing contrast between the flat, white concrete and the glass facade will be not solely created through the bigger waving shape. It will be enhanced by applying recycled borosilicate glass for the interlocking components, as well. This high optical quality glass shall give the facade a beautiful brilliance.

In addition, the glass facade shall show the possibilities of building environmentally friendly by applying recycled material in an aesthetically pleasing facade system.

The smallest glass facade of Casa da Música, corresponding to Hall 2, has been selected for application of the proposed design for this thesis. This facade measures a 14-meter width and 9-meter height.

### 3.4.2 CONCEPT DESIGN CRITERIA COMPONENTS

The main set criterium of the components is its dry-interlocking principle. In addition, these components shall be a showcase of the recyclability and optical quality of borosilicate glass.

Since the focus of this research is mainly on the recyclability, applicability in the built environment and corresponding material properties of borosilicate glass, the shape of the component is based on an existing concept by de Vries (2018). This concept is illustrated in Figure 84. Here a type of dry-interlocking system using loose shear keys is proposed. This system is preferred over fixed shear keys, because there is more freedom of movement. This means that there is less risk of chipping the shear keys off, when the facade is subjected to high shear forces.

Components should be as slender as possible, to maintain a high level of transparency. In addition, the components should be as large as possible within the set limits described in section 3.2.1 and 3.2.2. As large as possible means less horizontal and vertical lines visible in the final facade.



Figure 84 Starting concept of component, designed by de Vries (2018)

### 3.4.3 DESIGN CRITERIA INTERLOCKING ELEMENT

In this section the preferred dry-interlocking system using loose shear keys has been explained. Based on de Vries (2018) argumentation a sphere would be the best shape to apply as interlocking key. A sphere is a very strong shape, because anywhere pressure is applied the stress will be the same. The stress will be distributed symmetrically and evenly along the entire surface of the sphere.

As these shear keys will lie loose in the cast glass components, they can solely transfer shear forces, such as the wind load, down to the components, see Figure 86 The compression forces introduced by the facade's own weight, will be transferred down through the flat surfaces into the components itself, see Figure 85.

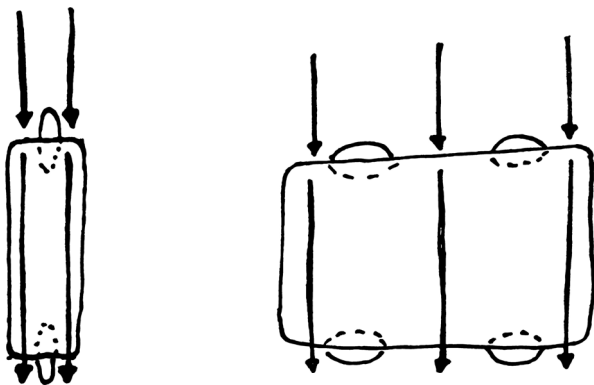


Figure 85 Compression forces transfered down through the flat surface of the component

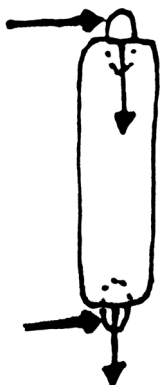


Figure 86 Shear forces transferred through interlocking keys to the component

The total proposed facade system should be a showcase of recyclability of building materials. Therefore, the interlocking key should be made of recycled material.

Other criteria related to the material of the interlocking key are:

- The tension strength should be at least similar to borosilicate glass of 28 Mpa.
- Fracture toughness at least similar to borosilicate glass ( $0.6 \text{ Mpa} \cdot \text{m}^{0.5}$ )
- Maximum service temperature of 50 °C
- Durability against UV-radiation

Based on the above stated criteria, many solutions are possible according to CESEduPack. However, most of these possibilities are either some metal or glass. Metal is an opaque material, which will make the interlocking keys highly visible. The aim of this design is to create a transparent as possible facade system, therefore metals will be excluded. Based on recyclability and hardness, the glass types that are most promising for the interlocking sphere are borosilicate and alumino silicate. Of these two glass types, alumino silicate has a higher tensile strength of 39 MPa and a higher hardness. Therefore, the interlocking sphere shall be made of alumino silicate glass.

### 3.4.4 DESIGN CRITERIA INTERLAYER

As described in section 1.1.8, glass to glass contact introduces high peak stresses. This means that the cast glass components should be protected with an interlayer. Section 1.1.8 describes the importance of applying a (dry)-interlayer when creating a cast glass component interlocking system.

A suitable material should be chosen based on certain criteria, as such an interlayer is applied between the interlocking cast glass components, and decreases the overall structural integrity of the facade system (Oikonomopoulou, et al., 2018b).

These criteria are based on (Oikonomopoulou, et al., 2018b) and (Aurik, Snijder, Noteboom, Nijse, & Louter, 2018). :

- A minimum compressive strength of higher than that of the maximum dead load of one 'sub-column' of the facade; > 2MPa. (See section 3.5.3.2 and appendix Appendix 5.18 for more detailed information on the deadload)
- Good resistance to static long-term compressive load and creep.
- Shore hardness of 60A-80A. The shore hardness of a material expresses the ratio between compressive resistance and piercing resistance (Leeuwen, n.d.). For example, harder polyurethanes have less compressibility and are stiffer. Both resulting in insufficient stress distribution and a lower tolerance to accommodate imperfections between the cast glass components. See Figure 88 for examples of polyurethanes with different shore hardness's.
- Transparent
- Durability against UV-lighting
- Maximum service temperature of 50 °C
- A minimal thickness of 3-4 mm. Based on experiments done by (Aurik et al., 2018). Below a 3 mm thickness there is a non-uniform contact area between the interlayer and the glass, see Figure 87. This results in an uneven distribution of forces, which introduces peak stresses.
- The material should be able to be formed in the desired shape.
- Recyclable

Based on the aforementioned criteria, the most suitable currently available material for such an interlayer is Neoprene. However, this is a black and opaque material. Therefore, the second-best option would be transparent Polyurethane 70 Shore A to apply as interlayer between the cast glass interlocking components. In addition, because the interlocking keys are made of alumino silicate glass an interlayer is necessary between the keys and the cast glass components as well. Thermoforming the Polyurethane around the interlocking keys creates a tight-fitting layer providing good stress distribution and overall structural integrity.

Between the glass components and the steel end-connections of the facade a neoprene interlayer shall be applied.

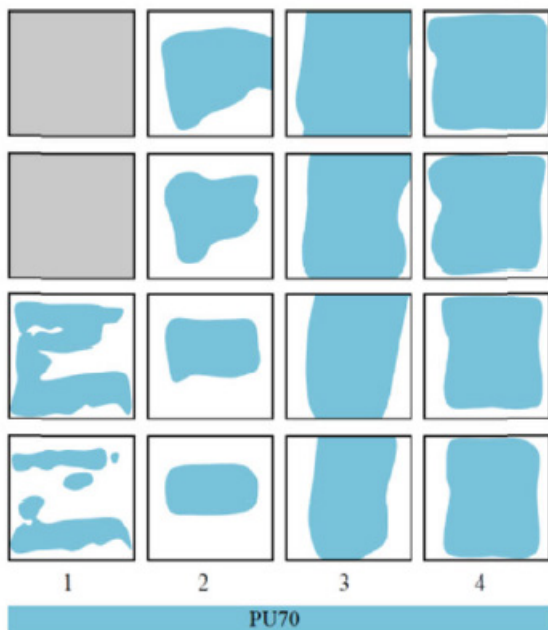


Figure 87 Experiment results of PU70 showing contact area corresponding to thickness of interlayer

Source: (Aurik et al., 2018).

## SHORE HARDNESS SCALES

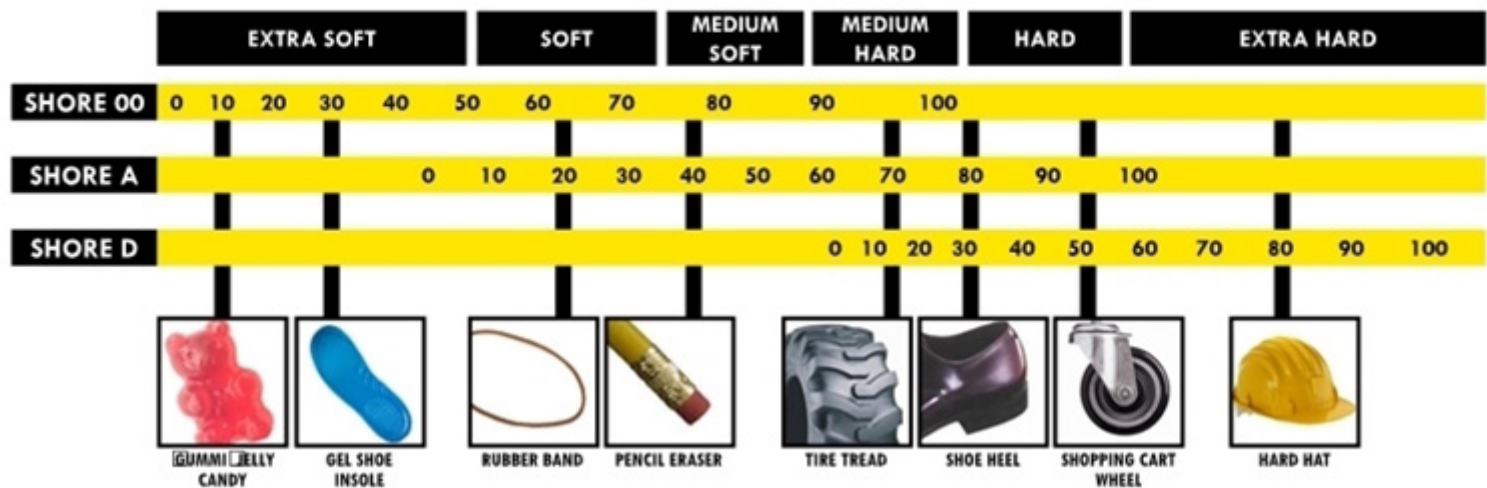


Figure 88 Shore hardness scale

Source: (Leeuwen, n.d.)

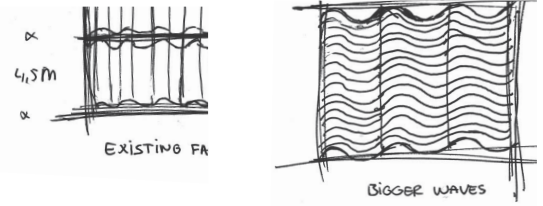


## 3.5 DESIGN OF COMPONENT

### 3.5.1 CONCEPT DESIGN CORRUGATED FACADE OF CASA DA MÚSICA

As described in section 3.1.2, the main concept criterium of the proposed facade system is to recreate the appealing contrast between the flat, smooth and white concrete facade and the corrugated, shining glass facade. The existing glass facade is constructed out of a small waving pattern supported by a steel sub-construction.

The proposed facade system constructed of the interlocking cast glass components has several advantages compared to the existing one. Due to the high compressive strength of glass and the increased thickness are the interlocking cast glass components capable of carrying themselves and the deadload of the components above. An additional steel support structure is not necessary. This self-supporting aspect allows for increasing of the wave-like pattern. When bigger waves are applied, less view is obstructed, while maintaining the appealing contrast between the concrete and the glass facade.



To determine the perfect shape for the glass facade, several potential wave-like shapes have been modelled. Some of these models can be found in Appendix 5.21. These initial studies to the most desirable corrugating pattern were rejected due to several reasons. For example, some waves were too symmetrical, introducing two weird-looking bumps in the middle of the facade. Others were too small, resulting in too much resemblance with the existing facade. Further, the initial amplitude of the waves was rather narrow.

Considering all of the above, the final waving shape represents two and one quarter sinus waves, so that it is not symmetrical in exactly the middle of the facade, see Figure 89. Furthermore, the final wave has a higher amplitude, resulting in a deeper waving pattern. This final corrugated shape enhances the contrast of Casa da Música between the flat, smooth concrete facade and the glass perfectly.

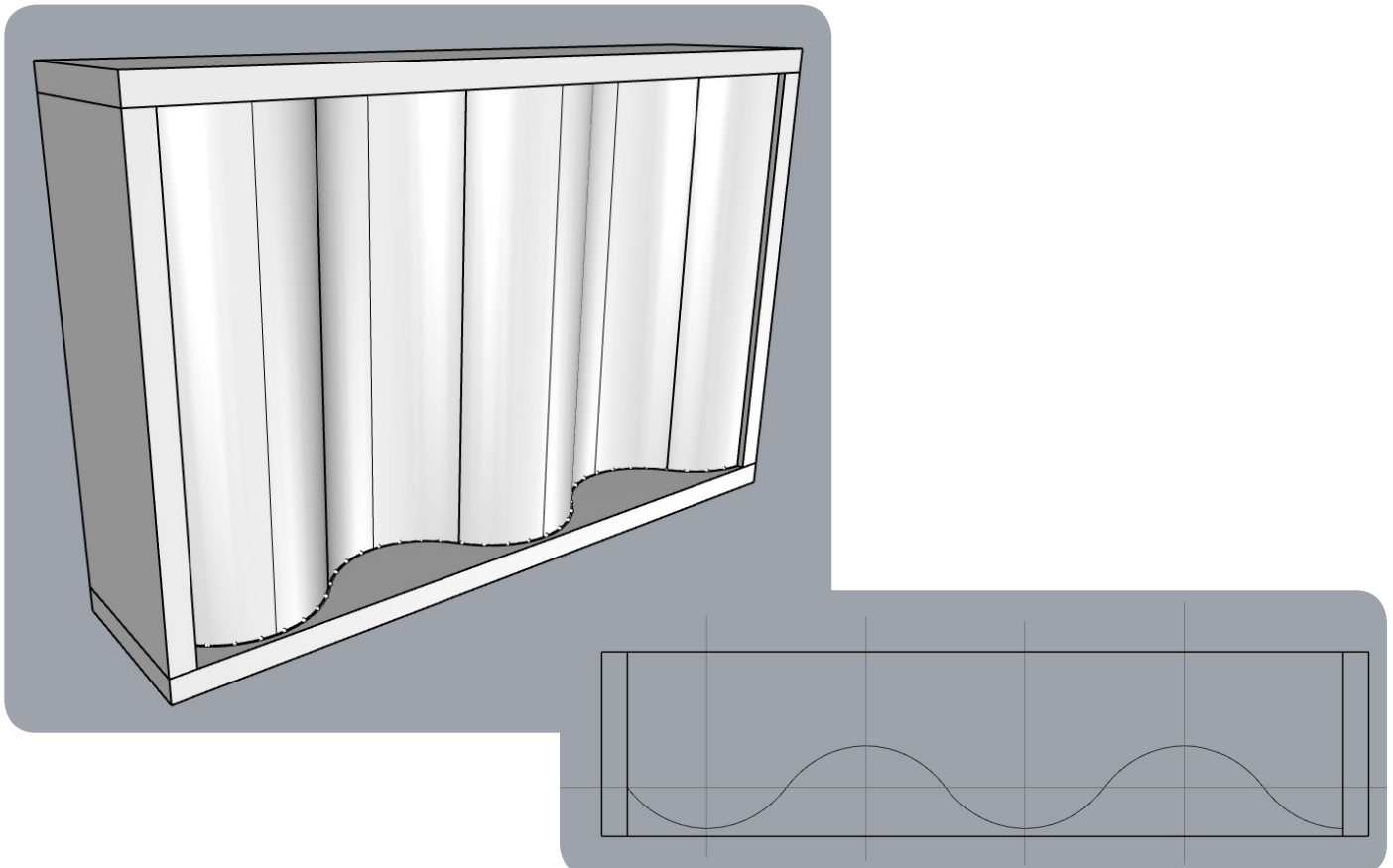


Figure 89 Proposed concept of waving shape

### 3.5.2 CONCEPT DESIGN COMPONENT + INTERLOCKING ELEMENT

In the context of this thesis, no extensive shape optimization study has been performed. However, the concept from (de Vries, 2018) has been adapted and designed for application in Casa da Música. Figure 90 illustrates this initial concept of the component, based on the concept of (de Vries, 2018). This concept consists of a rectangular block shaped cast glass component with spherical interlocking and a dry interlayer applied between the components. Although this interlocking system can perfectly transfer the compression forces down the facade and transfer lateral forces introduced by the wind load down through the shear keys, extra pre-tension steel cables should provide extra structural integrity and safety (Dyskin, Pasternak, & Estrin, 2012). These cables will reach through channels in some components to guarantee as less visible steel as possible, see Figure 91.

To fit more to the design concept and criteria of Casa da Música, a curved component following the curvature of the facade (see section 3.5.1) has been opted to design further. To define the potential dimensions of such a curved component, relating to the set maximum weight (10-12 kg), several sketches have been made. These are visible in Figure 92.

An initial simple buckling check for a monolithic glass facade of 14 \* 9 meters resulted in a minimal required thickness of 2.7 centimetres. This will be described in more detail in section 3.5.3.1. However, 2.7 centimetres seemed rather thin for a cast glass component to apply an interlocking element onto, therefore a thickness of the component between 6 – 8 cm would be more reasonable.

To maintain the design concept of a as large and thin possible component, within the set constraints described in section 3.2.2, a component of 6\*45\*17 cm has been proposed. This is illustrated in Figure 95.

This concept component illustrated that the proposed interlocking sphere corresponding to the thickness of the component, as described in section 3.2.1, would be too small to guaranty a proper interlocking mechanism and risk uplifting of the components.

To increase the diameter of the interlocking sphere and applying the 1/3-1/3-1/3-rule, the thickness

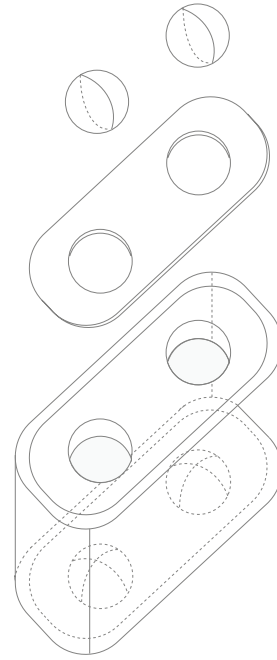


Figure 90 Initial concept of component based on (de Vries, 2018)

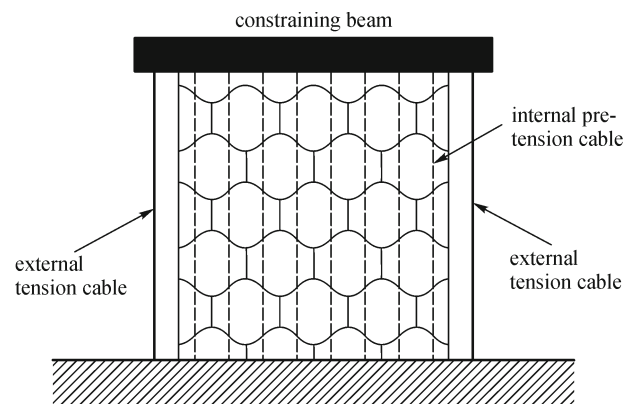


Figure 91 Pre-tensioned cable principle by (Dyskin, Pasternak, & Estrin, 2012)

of the component should increase drastically as well. As this is undesirable, an ellipsoid is opted as a new interlocking key, to maintain a smaller thickness of the component, see Figure 94. In addition, an ellipsoid provides for a larger interlocking surface, reducing the risk of uplifting and increasing the shear strength of the facade. Furthermore, related to the annealing process of the glass (i.e. homogenous shrinkage) an ellipsoid is the perfect annealing shape.

The interlocking ellipsoid should not be too thin or too small, in that case it would represent more of a rectangular interlocking or rod-like shape, which both are unfavourable in terms of annealing and stress distribution.

Structural calculations to define the exact dimensions of the interlocking ellipsoid and corresponding thickness of the component, are described in section 3.5.3.

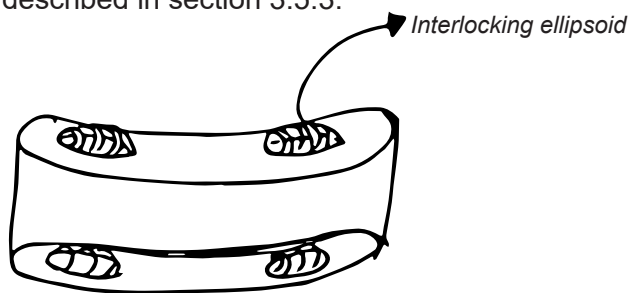


Figure 94 Interlocking ellipsoid

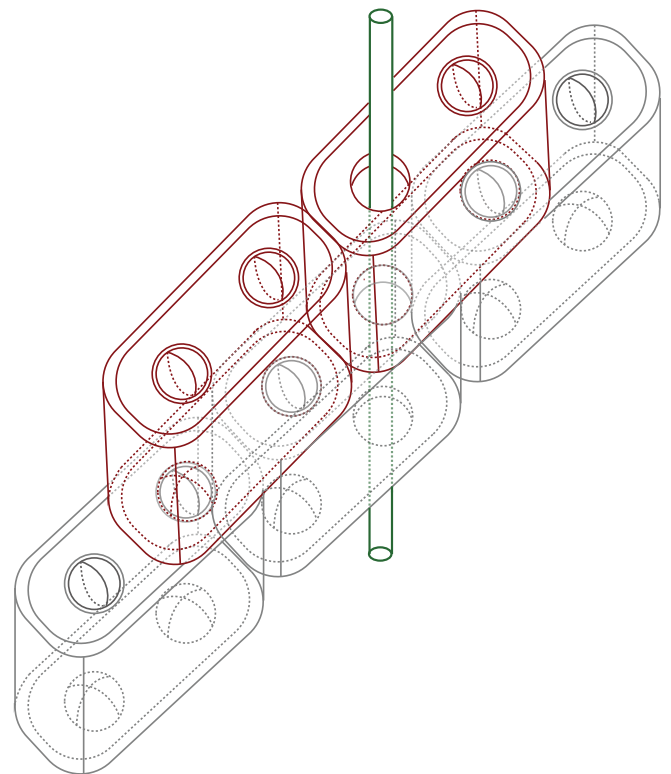


Figure 93 Initial sketches of interlocking system

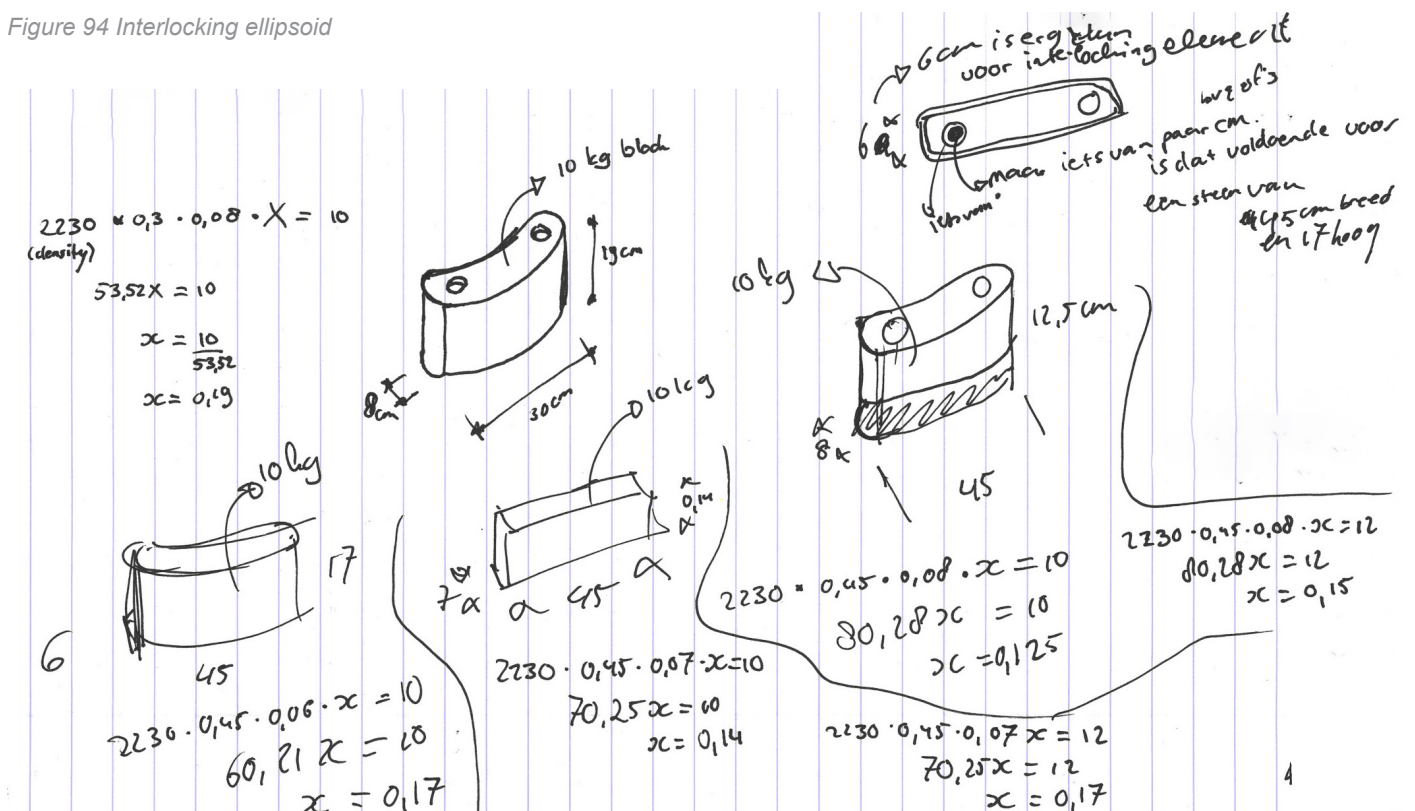


Figure 92 Initial component dimensions sketches

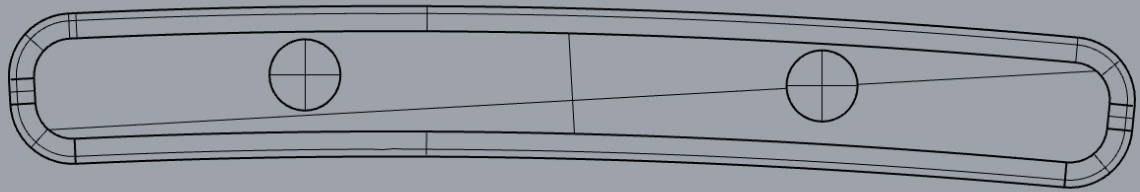


Figure 95 Initial component of 6 \* 45 \* 17 cm

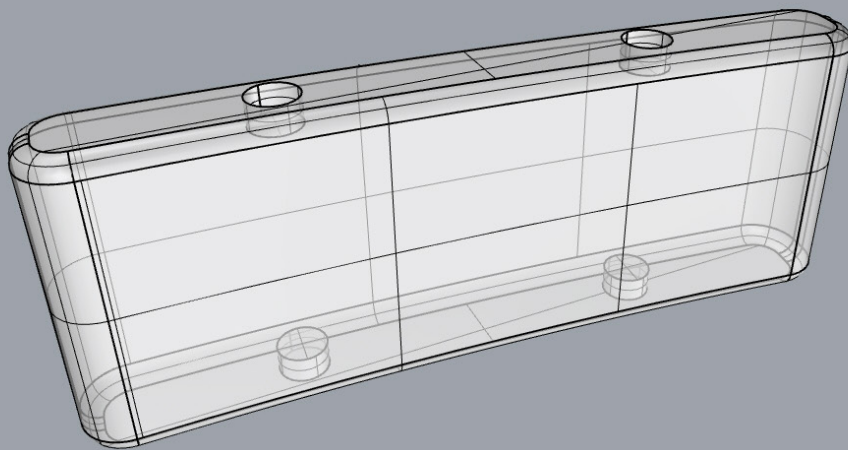


Figure 96 Initial component of 6 \* 45 \* 17 cm and very small interlocking holes

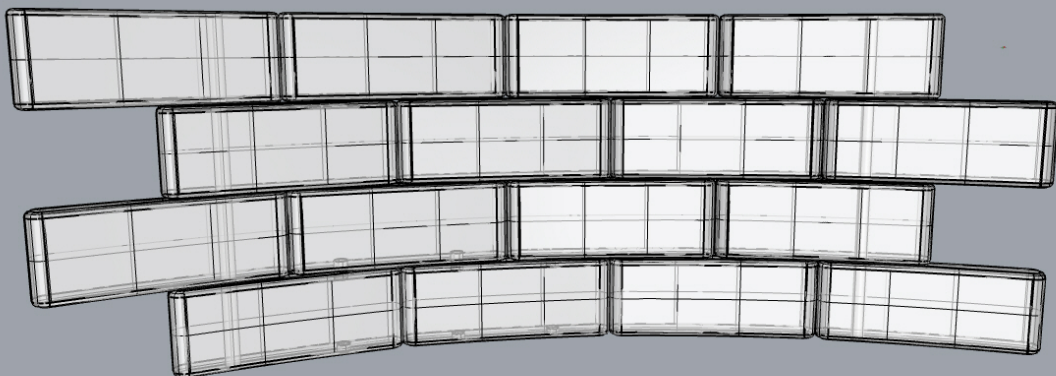


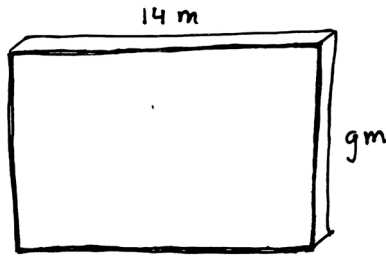
Figure 97 Initial component system and very small interlocking holes

### 3.5.3 STRUCTURAL CALCULATIONS COMPONENT

#### 3.5.3.1 MONOLITHIC PLATE BUCKLING CHECK

To determine the minimal thickness of a borosilicate glass facade of 14 m by 9 m, a simple buckling calculation can be done.

For the initial hand calculation, a monolithic plate of 14\*9 m is assumed for simplification of this calculation. Done with Bryans' Equation (Barou, 2016), this resulted in a minimal thickness of 2.7 cm. The total calculation can be found in Appendix 5.16.



To verify this, a more extensive calculation has been done to determine the minimal thickness of the borosilicate glass facade.

For this calculation Eulers equation for buckling has been applied (The Engineering Toolbox, 2012). With equation (3) the critical load of the wall can be determined. Eulers buckling equation:

$$F_{cr} = \frac{c\pi^2 EI}{L^2} \quad (3)$$

Where:

$F_{cr}$  = Critical load (N)

$c$  = Factor depending on end connections

$E$  = Modulus of elasticity (N/m<sup>2</sup>)

$I$  = Second moment of area (m<sup>4</sup>)

$L^2$  = Height of the wall (m)

In this case,  $c = 4$  since the end connections of the 'column' are clamped.

Since the thickness of the wall is unknown at this point, the second moment of area ( $I$ ) cannot be determined yet. However, for a simple rectangular cross-section the second moment of area can be calculated with the following equation:

$$I_x = \frac{bt^3}{12} \quad (4)$$

Where:

$b$  = Width of the wall

$t$  = Thickness of the wall

Therefore, combining equation (4) and (3) results in equation (5)

$$F_{cr} = \frac{4\pi^2 Ebt^3}{12L^2} \quad (5)$$

$F_{cr}$  in this equation represents the force at which buckling occurs. In practice the design should be such that the allowable load never approaches the critical load. Therefore, a safety factor of 4 will be used. Reasoning for this high factor is that the proposed interlocking glass facade has never been tested and applied at this scale before.  $F_{cr}$  with safety factor can be calculated with equation (6)

$$F_{cr} = \frac{\left( \frac{4\pi^2 Ebt^3}{12L^2} \right)}{4} \quad (6)$$

The facade should be able to carry its own dead load. The dead load is maximum at the bottom of the facade and decreases going upward. However, the dead load is assumed to be constant throughout the facade having maximum the value everywhere. The (overestimated) dead load of such a facade can be calculated with equation (7):

$$F_{dl} = m * g = v * \rho * g = b * h * t * \rho * g \quad (7)$$



Where:

$F_{dl}$  = Dead load of the façade (N)

$m$  = mass of the façade (kg)

$g$  = Gravity constant ( $m/s^2$ )

$v$  = Volume of the facade (kg)

$\rho$  = Density of borosilicate glass ( $kg/m^3$ )

The minimal thickness of the facade, subjected to its own weight, can now be determined by plotting the critical load of the façade ( $F_{cr}$ ) and the dead load of the façade ( $F_{dl}$ ), (equation (6) and equation (7) respectively, against the thickness.

The result is visible in Graph 1. The intersection point between  $F_{cr}$  and  $F_{dl}$  lies below 2 cm, which means the minimal thickness of the facade, based on the previous described calculation, is even lower then the initial buckling calculation (2.7 cm).

### 3.5.3.2 SUB-COLUMN BUCKLING CHECK

However, the previous calculation is based on one monolithic glass plate of 14\*9 m, which in reality will not be the case. The proposed façade consists of interlocking glass components, where each component overlaps the next by half. Each 'column' of interlocking components can be expressed as

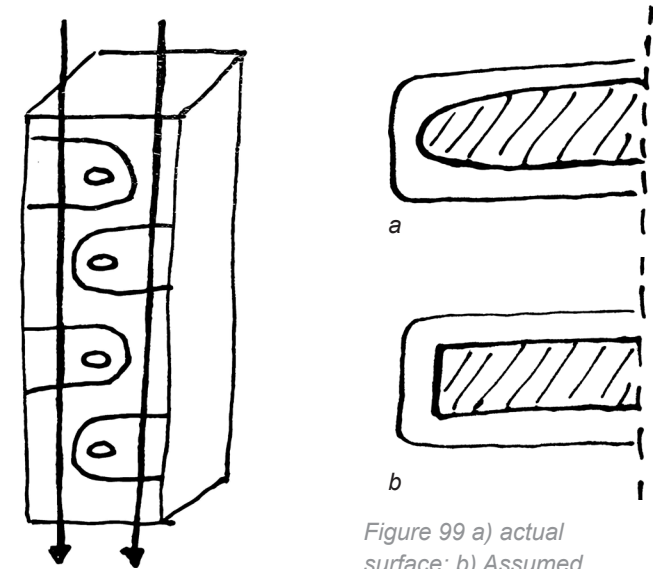


Figure 98 Sub-column principle

Figure 99 a) actual surface; b) Assumed rectangular surface

one 'sub-column' of the total wall. This principle is illustrated on Figure 98. This expression as sub-column is necessary to determine the thickness of one component more precisely. For simplification, one component will be assumed as a rectangular surface, without interlocking elements, see Figure 99

The aforementioned calculation can be applied for one sub-column with corresponding sub-column dimensions. The result of the sub-column calculation is visible in Figure 101. The intersection point between  $F_{cr,sub}$  and  $F_{dead,sub}$  corresponds to the same thickness as seen for the total wall. However, logically, the total force one sub-column can withstand is lower compared to force the total

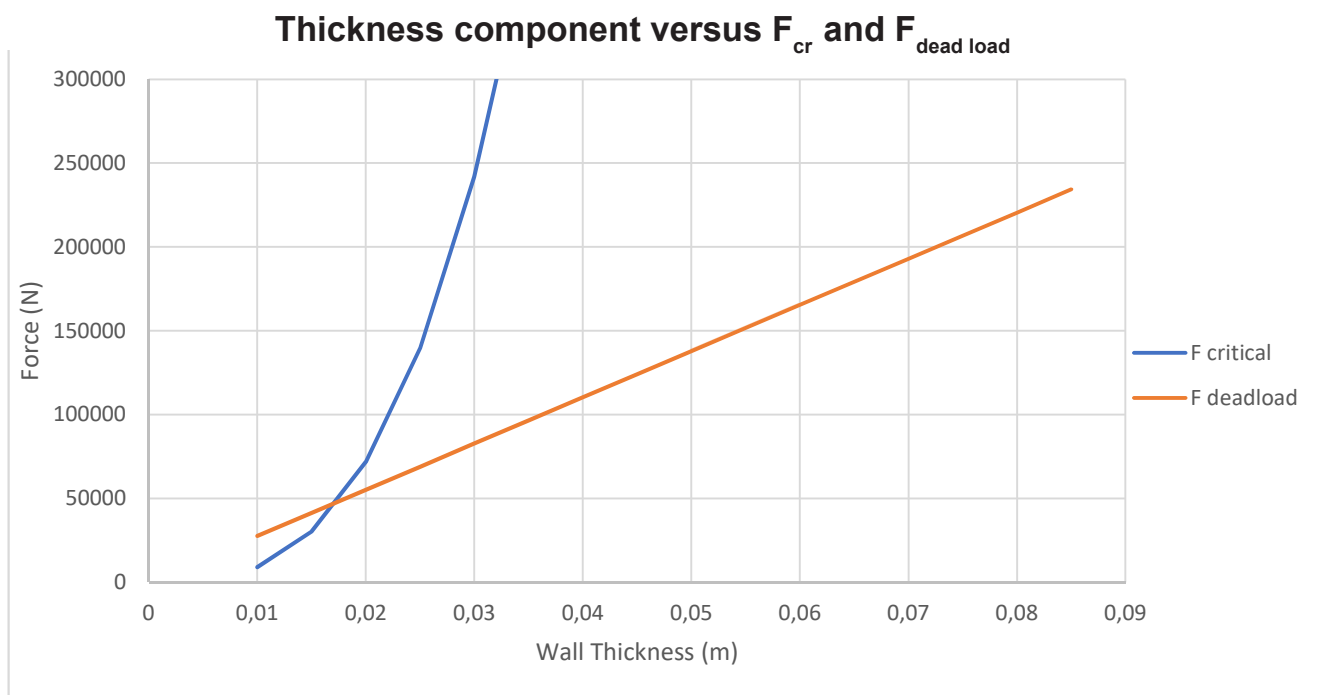


Figure 100 Thickness component versus  $F_{cr}$  and  $F_{dead load}$

wall can withstand.

This can be explained mathematically. When comparing buckling out of the wall plane of the entire facade with that of a subcolumn, the only aspect in equation (6) and equation (7) that changes is the width. In the former the width is that of the wall and in the latter the width is half of a component.  $F_{\text{dead load}}$  and  $F_{\text{cr}}$  are both linear in width (b) resulting in the same thickness found.

*Note: as explained in section 1.1.8, an interlayer is necessary between each component. For simplification, the interlayer has not been taken into account for the  $F_{\text{dead load}}$  calculation. The weight of the interlayer can be neglected when considering the overall weight of the façade. However, it should be noted that those interlayers negatively affect the overall stiffness of such a dry-interlocking facade.*

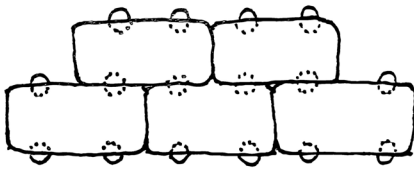


Figure 102 Interlocking principle

### 3.5.3.3 SUB-COLUMN BUCKLING CHECK WITH HOLE FOR INTERLOCKING ELEMENT

To examine if the necessary minimal thickness of the component to counter buckling changes when interlocking holes are applied, the previous calculations were iterated with these holes taken into account. The surface of the interlocking hole needs to be subtracted of the total force-distributing surface of a component. As written in section 3.4.3, the interlocking elements do not distribute the compression forces of the facade, but only transfer the shear forces (wind load).

Section 3.5.2 describes that for the proposed component design an elliptical interlocking element shall be applied.

Therefore, to determine  $F_{\text{critical, sub column, with interlocking ellipse}}$  the second moment of area of the ellipse needs to be determined first.

The second moment of area of an ellipse ( $I_{\text{ellipse}}$ ), calculated around the x-axis is as follows:

$$I_x = \frac{\pi}{4} ab^3 \quad (8)$$

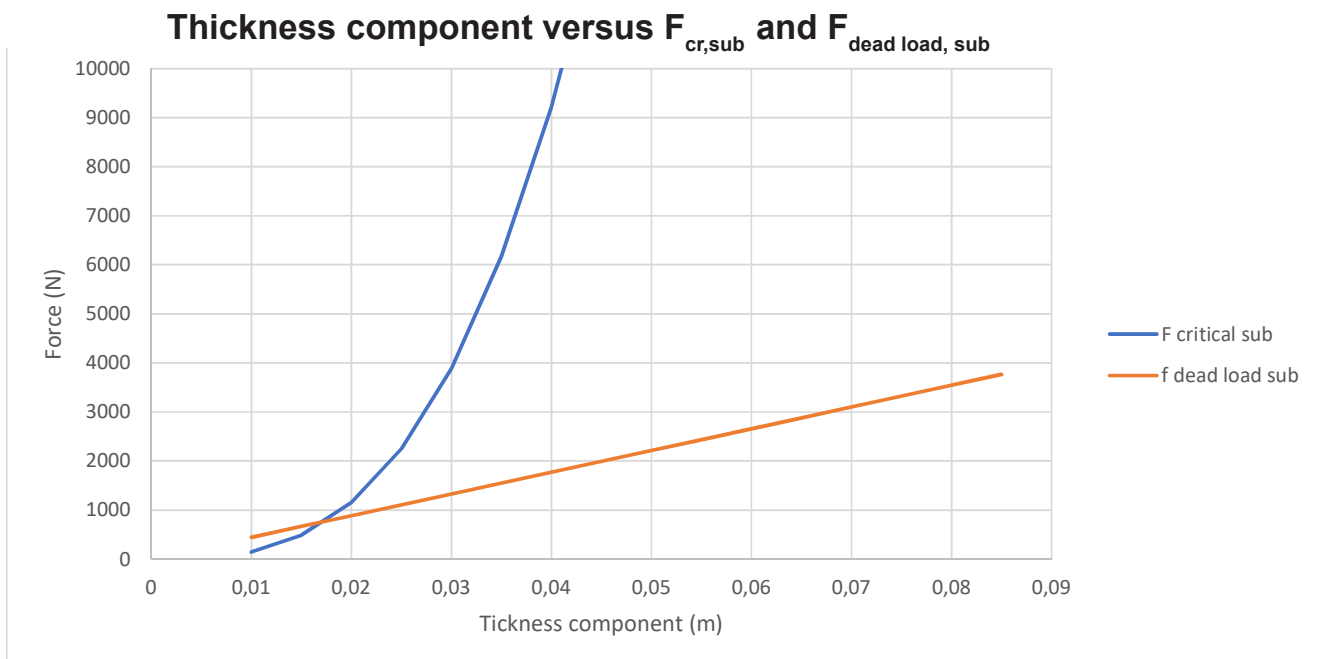


Figure 101 Thickness component versus  $F_{\text{cr, sub}}$  and  $F_{\text{dead load, sub}}$

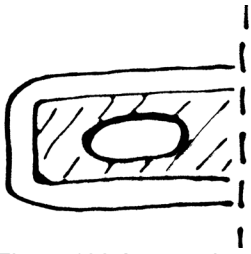


Figure 106 Assumed rectangular surface with interlocking ellipse

Where for an ellipse  $a$  represents the semi-major axis and  $b$  the semi-minor axis, see Figure 105. Section 3.2.1 describes that for an equal force distribution and optimal resistance to the shear force, the ratio between the edges of the total component and the interlocking element should be equal, see Figure 82;  $(1/3-1/3-1/3)$ . Since the thickness of the glass component is divided in three sections, this means that the width of the ellipse ( $2b$ ) represents  $1/3t$ . Conveniently, the semi-minor axis of the ellipse can be expressed in terms of the thickness of the component,  $b(t) = 1/6t$ .

Another convenience arises when realizing that the semi-major axis and semi-minor axis can be expressed in terms of each other. Namely, that  $a$  as well can be expressed in terms of the component thickness.

To express  $a$  as a function of  $t$  an explanation of the mathematical expression of an ellipse is necessary. In mathematics, a conic section can be determined by eccentricity ( $e$ ) (Weisstein, n.d.). This eccentricity is a number which determines how much a conic section differs from a circle ( $e = 0$ ) ("Introductory Astronomy: Ellipses", n.d.). Figure 104 illustrates that  $e = 0.7$  represents an 'optimal' elliptical shape, suitable for the thickness of an

interlocking element for a cast glass component with a relatively small thickness. For this reason and for simplicity, the eccentricity of the ellipse has been set to  $e = 0.7$ .

$$e = \sqrt{1 - \frac{b^2}{a^2}} \quad (9)$$

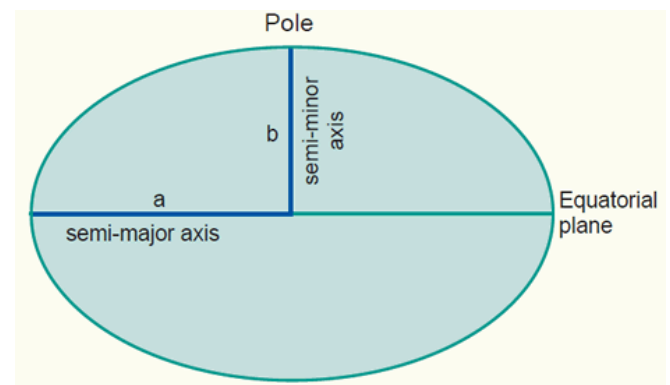


Figure 105 Ellipse  
Source: (Weisstein, n.d.)

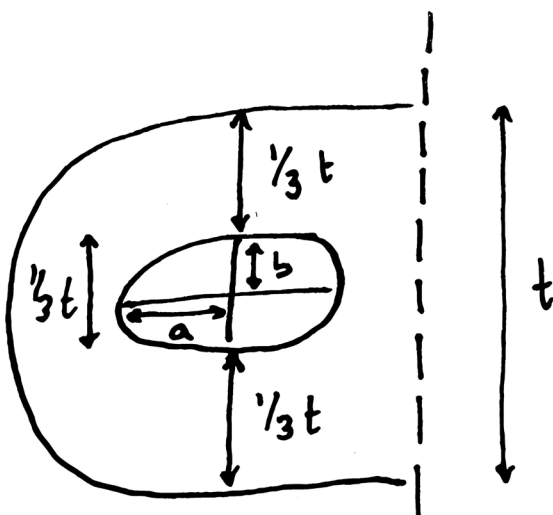


Figure 103 Distances of interlocking ellipse related to thickness of component

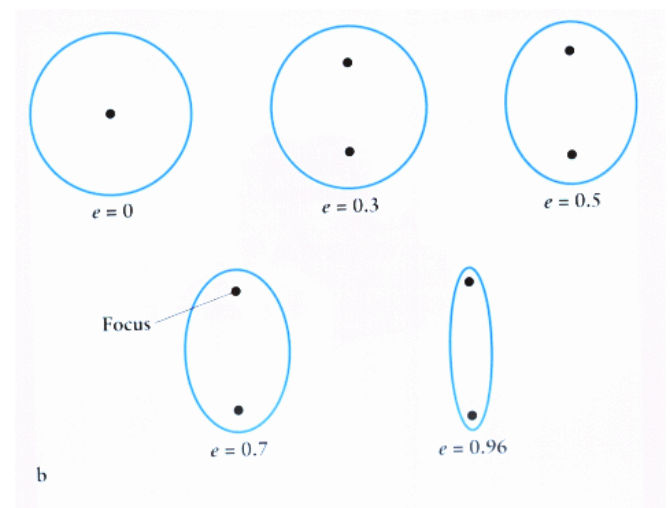


Figure 104 Eccentricity of ellipse  
Source: ("Introductory Astronomy: Ellipses", n.d.)

The equation for the eccentricity of an ellipse is as follows:

Where:

$e$  = eccentricity

$b$  = semi-minor axis

$a$  = semi-major axis

$$a = \sqrt{\frac{b^2}{1 - e^2}} = \sqrt{\frac{(\frac{1}{6}t)^2}{1 - e^2}} \quad (10)$$

Since all these terms are known, it is possible to express  $a$  as a function of the thickness ( $t$ ):

As both  $a$  and  $b$ , the dimensions of the ellipse, are expressed as a function of the thickness ( $t$ ), it is easy to find  $F_{\text{critical, sub-column}}$ , with interlocking as of function of  $t$ , by simply subtracting  $I_{\text{rect}} - I_{\text{ellipse}}$  in equation (3).

As illustrated in graph Figure 107, the minimal thickness of the component remains almost the same as for  $F_{\text{critical, sub-column}}$ , without the interlocking part. This means that the interlocking holes essentially have a negligible influence on the thickness of the component necessary against

buckling (valid from a certain minimal thickness).

Based on the calculations described in this section and simultaneously designing potential components, a final component of  $0.15 \times 0.45 \times 0.08$  m has been defined. This thickness corresponds to a reasonable thickness of the interlocking keys. In contrast, a 0.06 m thick component corresponds to a small thickness of the interlocking key, where the key started to resemble too much of a rectangular interlock. Therefore, a thickness of 0.08 is under these conditions and design constrains the best possible solution.

### Thickness component versus $F_{\text{cr,sub}}$ with interlocking holes and $F_{\text{dead load, sub}}$

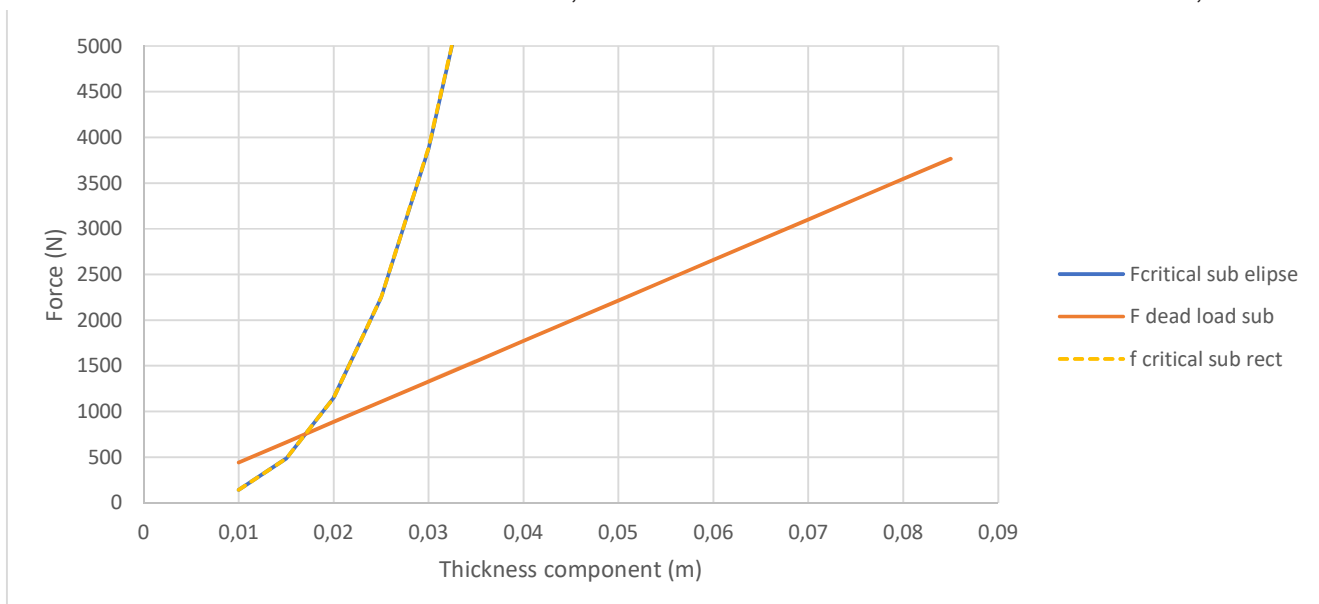


Figure 107 Thickness component versus  $F_{\text{cr,sub}}$  with interlocking holes and  $F_{\text{dead load, sub}}$

### 3.5.3.4 INTERLOCK ELEMENT SHEAR STRESS CALCULATION UNDER WIND LOAD

*This part describes the calculation of the shear stress occurring in the interlocking ellipsoid, introduced to the façade by the wind load. The maximum occurring shear stress in the interlocking ellipsoid needs to be found and subsequently checked to verify if it is lower than the maximum allowable shear stress of glass.*

It is assumed the wind load ( $F_{\text{wind}}$ ) on the total façade of Casa da Música is 1 kN/m<sup>2</sup>. This number is based on 0.56 kN/m<sup>2</sup> of (Dlubal Software GmbH, n.d.), however for safety reasons (accounting for extreme cases) it is assumed to be 1 kN/m<sup>2</sup>.

Since the chosen dimensions of the final component are 0.15\*0.45\*0.08 m, this results in a surface of 0.15 \* 0.45 = 0.0675 m<sup>2</sup> per component subjected to the wind load.

The total wind load active on one component is then:

$$0.0675 * 1 = 0.0675 \text{ kN}$$

$$F_{\text{wind}} = 67.5 \text{ N}$$

Dividing this by 4 results in the wind load per interlocking ellipsoid:

$$67.5/4 = 16.88 \text{ N}$$

To determine the shear stress active in the interlocking ellipsoid the following equation will be used:

$$\tau = \frac{V}{A} \quad (11)$$

Where

$\tau$  = Shear stress (MPa)

$V$  = Shear force (N)

$A$  = Surface (m<sup>2</sup>)

For simplification, the chosen interlocking ellipsoid will be assumed as a rectangular cross-section, as illustrated in Figure 108.

$$A = 0.0266 * 0.074 = 0.00198 \text{ m}^2$$

This results in  $\tau = 16.88 / (0.00198)$

$$\tau = 8575.49 \text{ Pa}$$

$$\tau = 0.0086 \text{ MPa}$$

Hence, the maximum shear stress occurring in one interlocking ellipsoid is 0.0086 MPa. To compare, for alumino silicate glass the maximum acceptable stress lies below its tensile strength of circa 39 MPa (CESEduPack, 2017a). Therefore, the maximum shear stress caused by the wind load, occurring in one interlocking ellipsoid (0.0086 MPa) is much lower than the maximum acceptable tensile stress for alumino silicate (39 MPa). This means, the wind load will not affect the interlocking element of the façade to an extent that it could break an interlocking element.

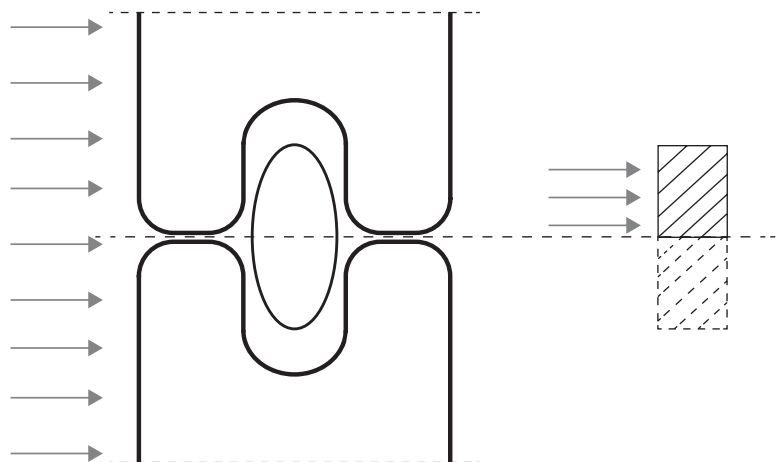


Figure 108 Wind load active on interlock.  
Interlock assumed as rectangular cross-section



### 3.5.4 FINAL COMPONENT – FINAL INTERLOCK ELLIPSOID – FINAL INTERLAYER

As described in section 3.5.3.3, the final component is 150\*450\*80 mm. This final component, the corresponding interlayer between the components and interlocking keys with interlayer are illustrated in Figure 109, Figure 110 and Figure 111.

The top view of the component, with a pre-tensioned cable is illustrated in Figure 112.

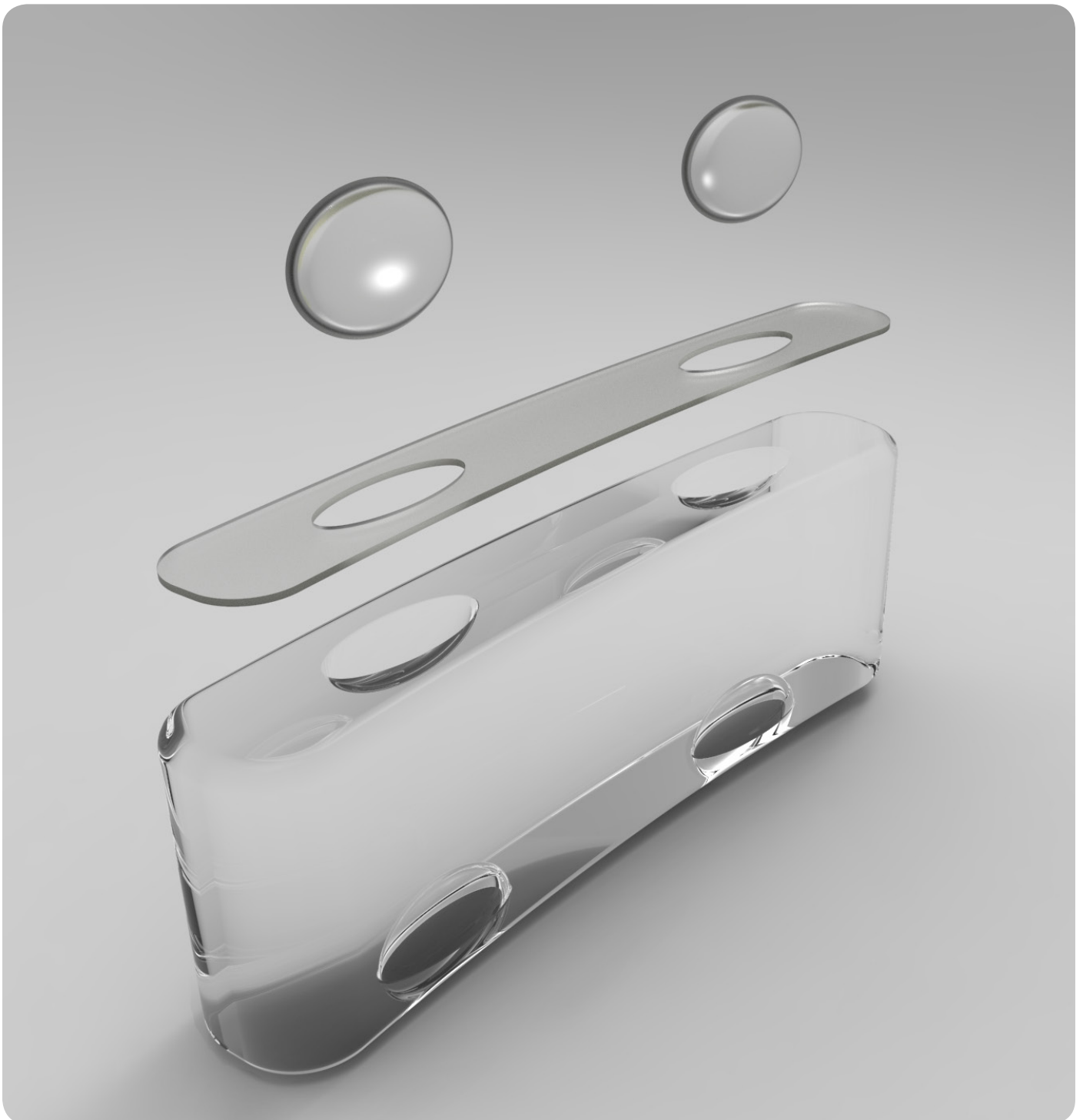


Figure 109 Exploded view of final component

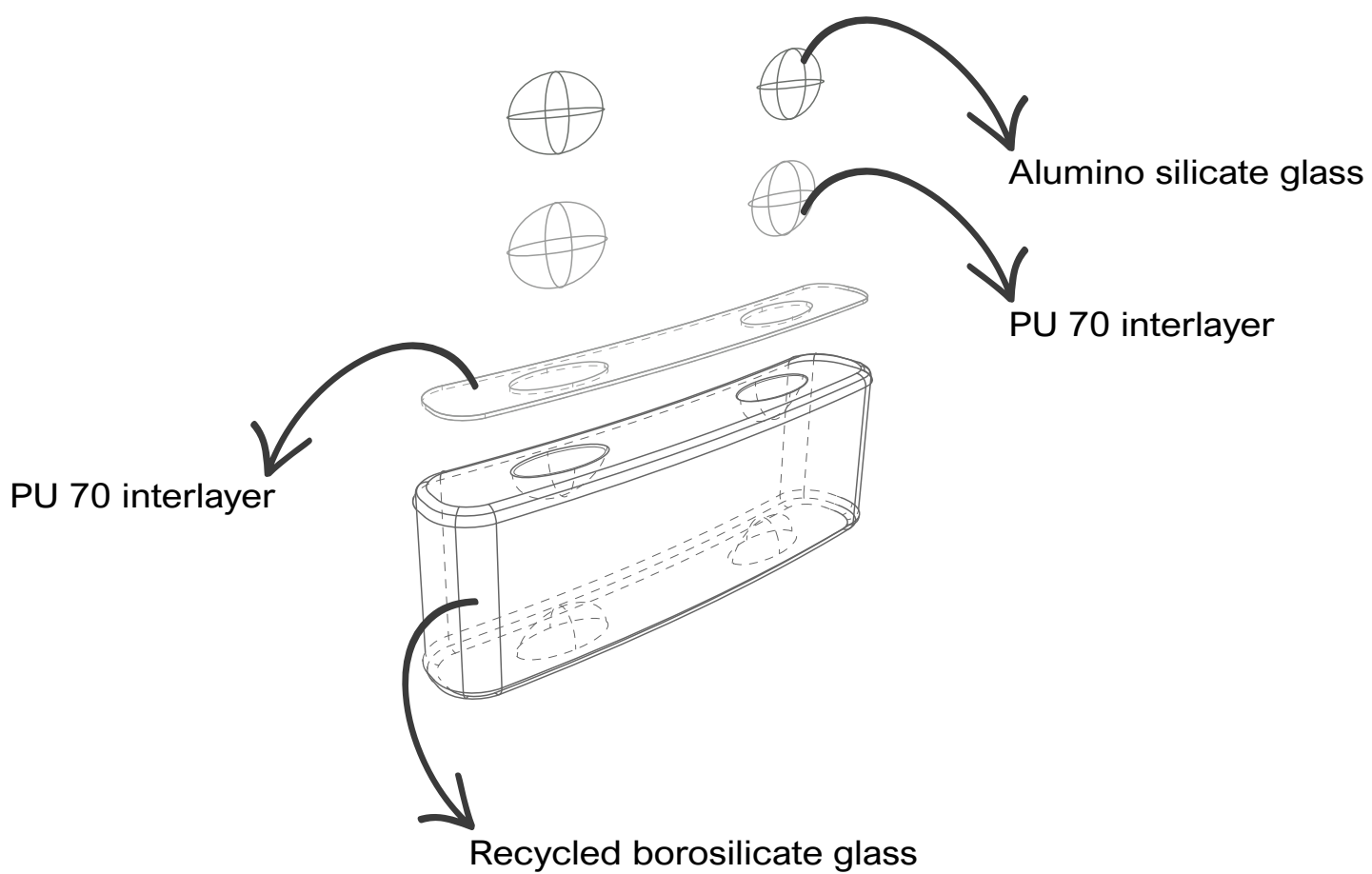


Figure 110 Materialization of final component

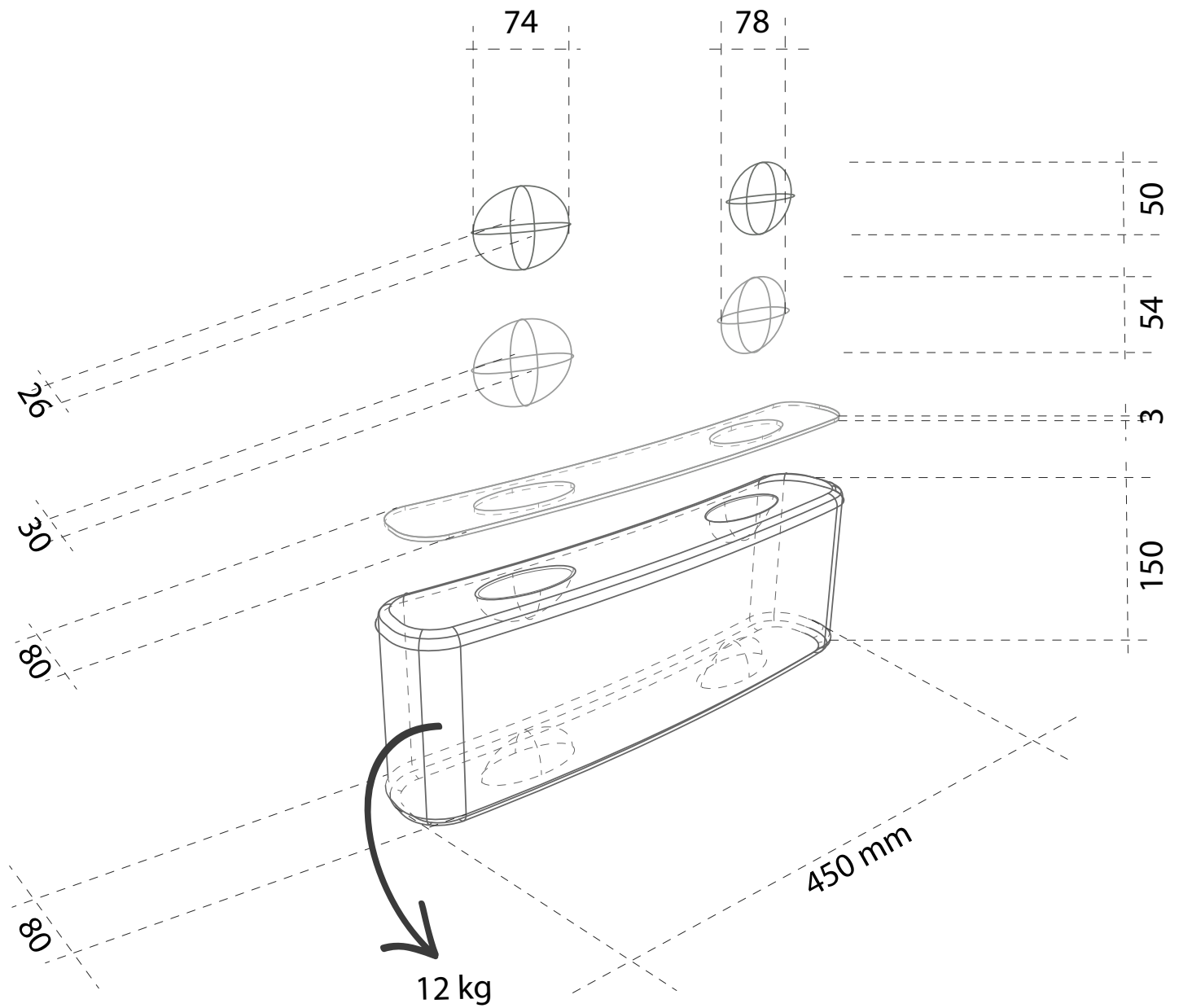


Figure 111 Dimensions of final component

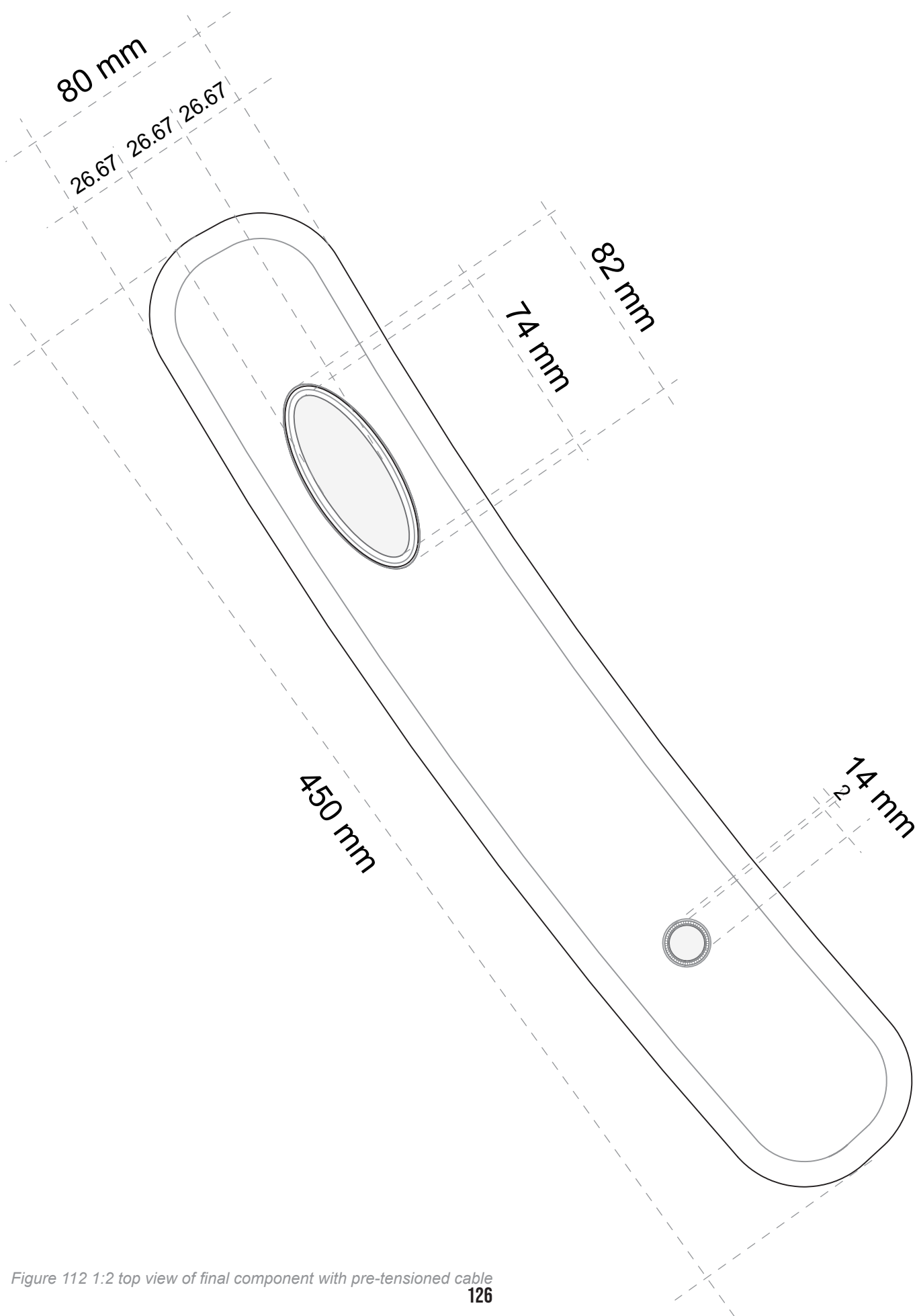


Figure 112 1:2 top view of final component with pre-tensioned cable

## 3.6 APPLICATION IN CASA DA MÚSICA

### 3.6.1 FINAL DESIGN IN CASA DA MÚSICA

The proposed interlocking cast glass components will construct the new corrugating facade of Casa da Música. This is illustrated in Figure 112.

The plan view of the facade is shown in Figure 117. The components follow exactly the  $2^{1/4}$  sinus curve. The pre-tension steel cables are positioned every four components.

The specific designed interlocking system is illustrated in Figure 111.

As visible, the interlayer (yellow) lies between every component (green). Around the interlocking alumino silicate glass key (pink) is a thermoformed interlayer as well. The neoprene interlayer, applied between the steel plate and the glass components, is visible in black. A pre-tensioned steel cable is

illustrated in grey, with a white protective socket around it.

The total system is supported by a steel plate with interlocking bumps. This steel plate is only to fixate the component system. The total force of the facade and the pre-tensioned steel cables are transferred down to a beam. A top-beam fixates the component system similar to the bottom of the facade. This top-beam also holds the top part of the pre-tensioned cables. The steel beams transfer the forces of the facade down to the concrete construction of Casa da Música.

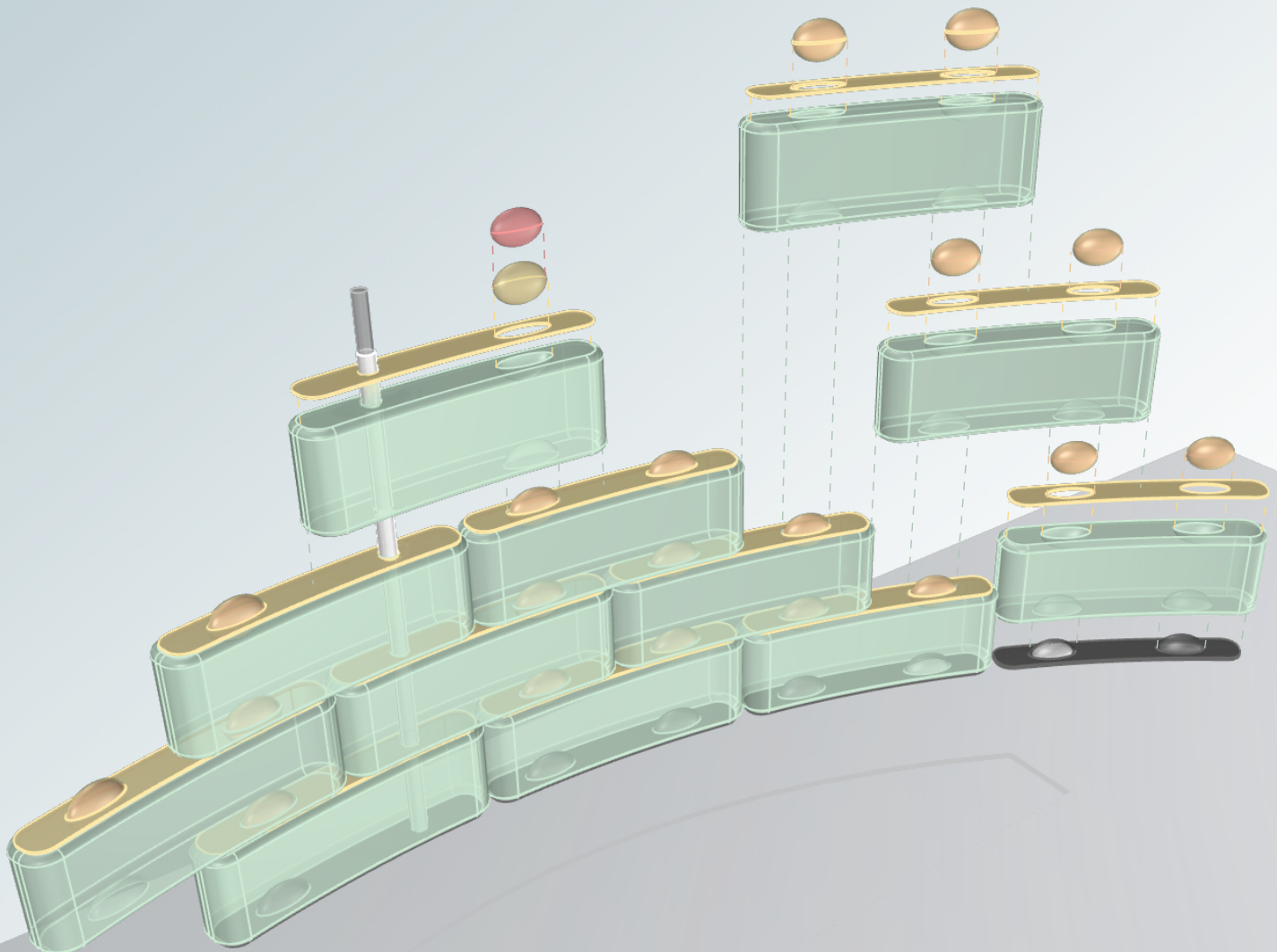
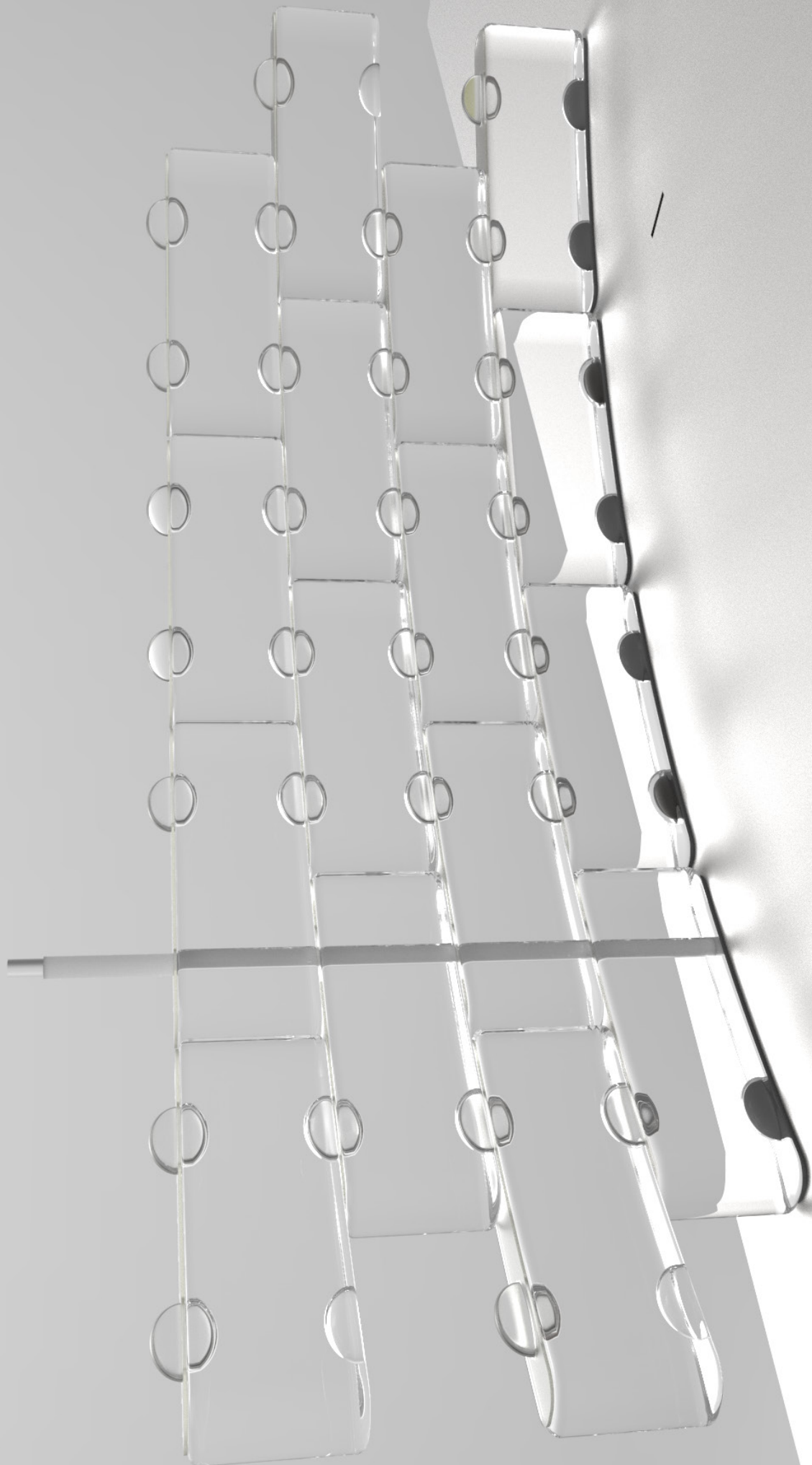


Figure 113 Exploded view of proposed dry-interlocking facade system





*Figure 114 Render of a part of the dry-interlocking cast glass component system*





*Figure 115 Proposed interlocking facade in Casa da Musica*





Figure 116 Proposed interlocking facade in Casa da Musica



3.6.2 STRUCTURAL  
CALCULATIONS OF  
DIMENSIONS OF THE TOP  
AND BOTTOM BEAM

To define the exact dimensions of the beams required to withstand the forces of the proposed facade system, several calculations have been made.

Two iterations have been performed for this set of calculations based on different starting assumptions. These iterations are: 1) single, straight beam (top and bottom), wind load is 1 kN/m<sup>2</sup>; 2) three beams (at top and bottom of facade), middle, normative beam carries 5 cables, wind load is 1 kN/m<sup>2</sup>.

These iterations are detailed in this section. Eventually, iteration 2 was used for detailing of the facade.

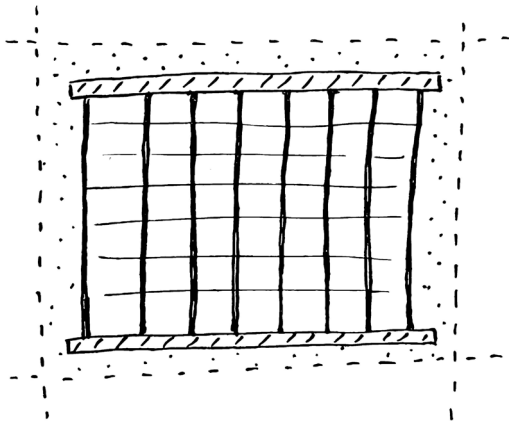


Figure 118 Static scheme of the proposed facade, a top and bottom beam, supported by the existing concrete facade. Pre-tensioned cables span between the beams

Figure 118 illustrates the static scheme of the facade. As visible, the glass component facade is supported by a steel top and bottom beam. The lateral forces (wind load) acting on the facade are being absorbed by nine vertical pre-tensioned cables, hanging every 1.8 meter. (Later in this section is a description about the reason for this 1.8m) These cables hang from the top beam and are fastened at the bottom beam. In addition, the cables go through channels inside the interlocking glass components. It should be noted that for simplification the calculation will be done for straight beams, and the curvature of the actual beams has not been taken into account, see Figure 119.

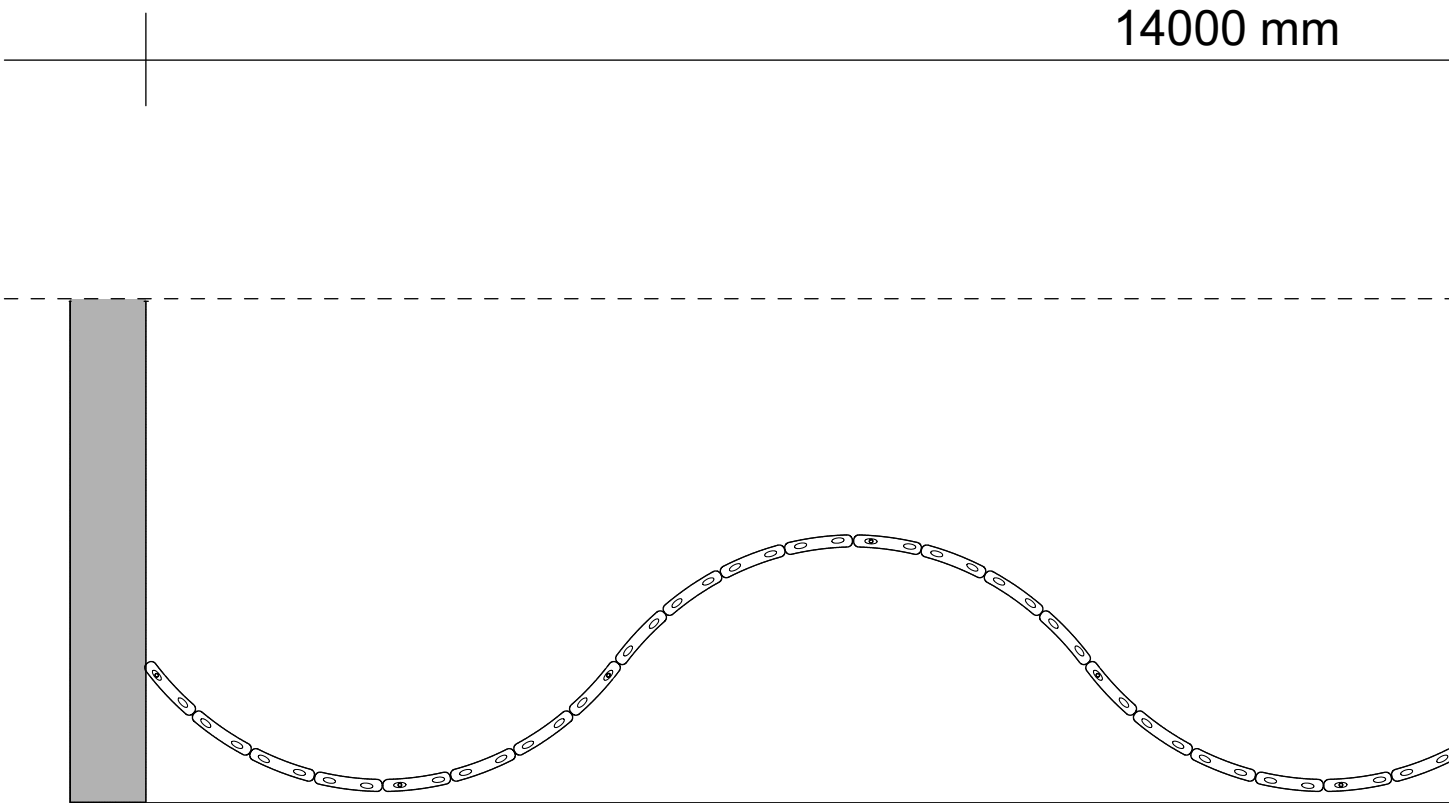


Figure 117 Proposed interlocking facade plan view 1:50





Figure 119 Curved beam

In order to determine the dimensions of the top and bottom beam, several steps have to be taken.

To determine the force acting on the top beam, the force in each pre-tensioned cable should be calculated first. The tension force necessary to withstand the wind load, given a maximum allowable deflection, can be calculated with the following equation based on (Module 3 : Cables, n.d.):

$$H = \frac{qL^2}{8y_m} \quad (12)$$

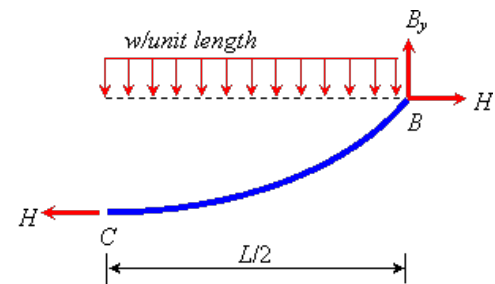
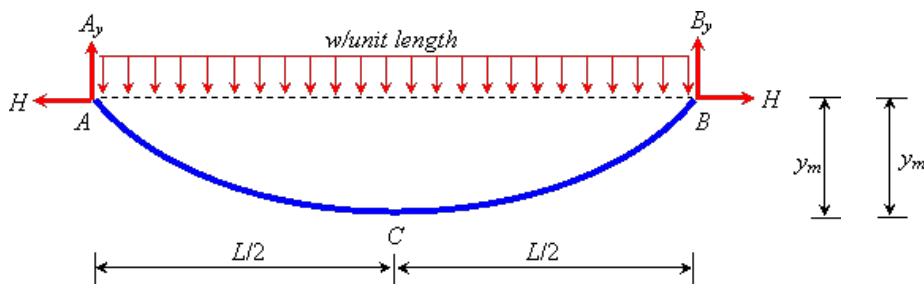
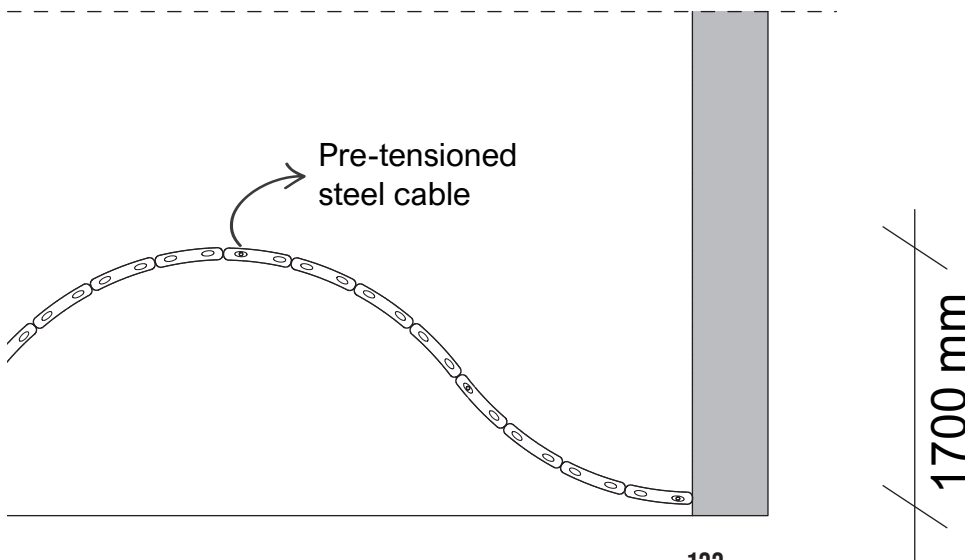


Figure 120 Free body diagram of a cable under uniform distributed load

Source: (Module 3 : Cables, n.d.).



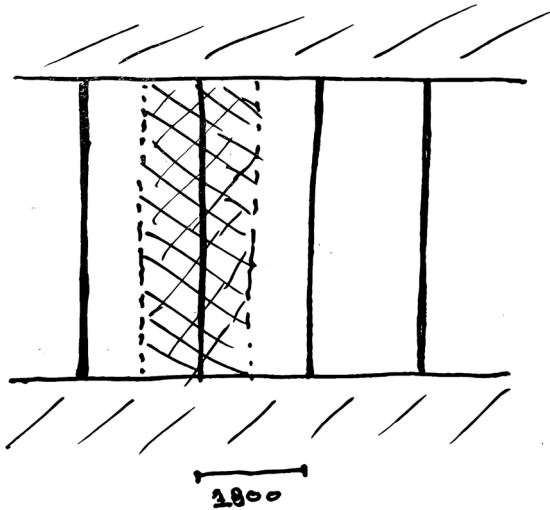


Figure 121 Distance between pre-tensioned cables

As written before, the wind load active on the façade is 1.0 kN/m<sup>2</sup>. In Figure 121 is visible that the distance between two cables is 1,8 m. This distance is based on the dimensions of one component (width of 0.45 m) times four components, which results in  $0.45 * 4 = 1.8$  m distance between the cables. Therefore, every fourth component is fixed by a pre-tensioned cable.

It is assumed that one cable absorbs the wind load on a surface consisting of the facade height times a half of the distance to the adjacent cable (see Figure 121). The wind load active on one cable is:

$$q = 1.0 * 1.8 = 1.8 \text{ kN/m}$$

$$q = 1800 \text{ N/m}$$

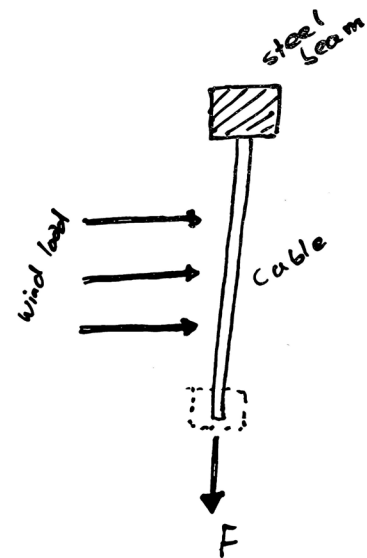


Figure 125 Scheme of wind load active on the pre-tensioned cables

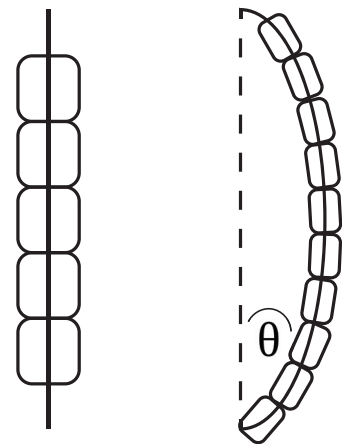


Figure 123 Maximum angle of rotation at bottom of the cable

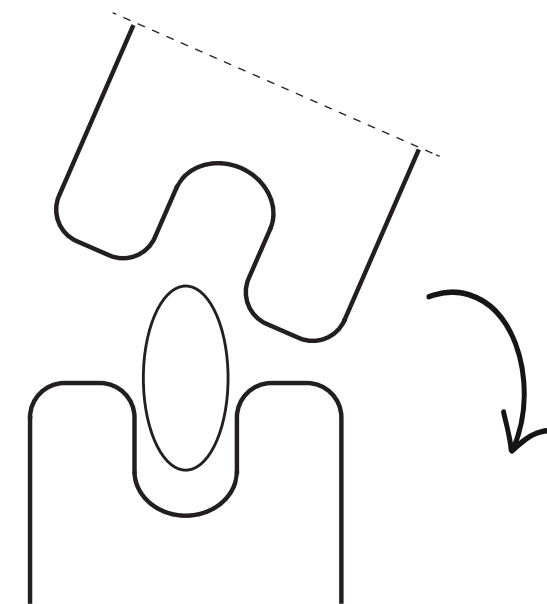


Figure 122 Too far rotation of component, resulting in component falling out of the facade

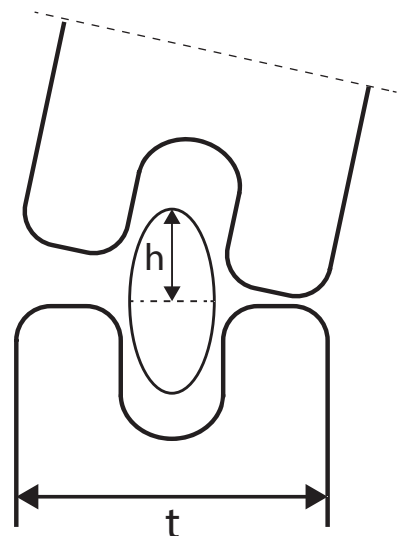


Figure 124 The interlocking ellipse never pops out when under this angle of rotation

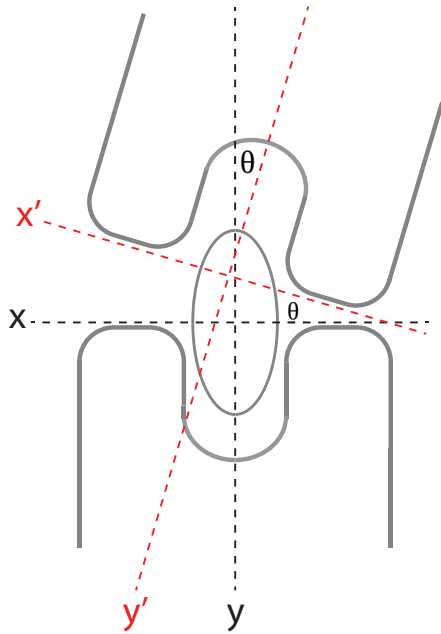


Figure 126 Representation of angle of rotation

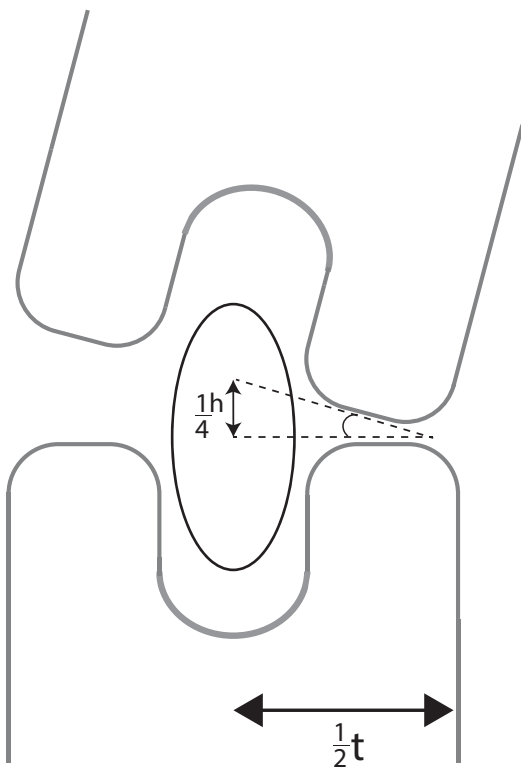


Figure 127 Representation of angle of rotation

The deflection ( $y_m$ ) of the cable that is allowable for this facade is based on the maximum allowable angle of rotation between two glass components. If two components rotate too far relative to each other, the interlocking ellipse cannot function anymore and the top component could fall out of the façade, see Figure 122.

It is assumed that the components perfectly follow the shape of the cable, when subjected to the wind load. In reality, the components have some mass counteracting the deflection and rotation caused by the wind load. The maximum angle of rotation is at the bottom of the cable, which is illustrated in Figure 123. The maximum allowed angle of rotation is defined in such a way that the interlocking ellipsoid between two components never pops out, when under this angle, see Figure 124. If the vertical axis of the top component is rotated by  $\theta$ , its horizontal axis is also rotated by  $\theta$ , exposing the interlocking ellipsoid, see Figure 126.

To prevent the ellipsoid from popping out, half of its exposed height ( $h$  in Figure 127), must be covered by the top component at all times. This means that equation (13) holds

(13)

$$\tan \theta = \frac{\frac{1}{2} h_{exp \cdot ellip.}}{\frac{1}{2} t} = \frac{\frac{1}{4} h_{total \cdot ellip.}}{\frac{1}{2} t}$$

Where:

$\tan \theta$  = Maximum rotation

$h_{exp \cdot ellip.}$  = Height of exposed ellipsoid

$t$  = Thickness of total component

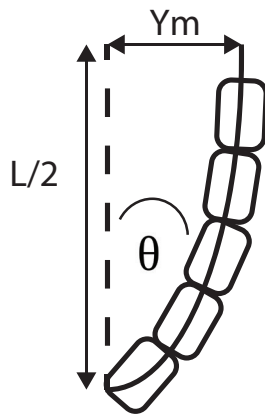


Figure 128 Relation between maximum deflection and maximum rotation

Figure 128 shows how the maximum rotation is related to the maximum deflection ( $y_m$ ). See equation (14) where equation (13) is used to express ( $y_m$ ).

$$y_m = \tan \theta * \frac{L}{2} = \frac{\frac{1}{4} h_{total \cdot ellip.}}{\frac{1}{2} t} * \frac{L}{2} \quad (14)$$

When  $y_m$  is defined, the tension force (H) acting on one cable can be calculated. This results into a tensile force of 13 kN per cable. As the tensile force per cable is known, the total forces acting on the top beam can be modelled as point forces. This is illustrated in Figure 129. For simplification it is assumed that the rightmost and leftmost loads act directly above the supports, however in reality this is not the case. The cables are hanging slightly inwards at both ends. This accounts for the middle point load as well; the chosen interval of the cables (each 1.8 m) ensures that in reality there is no point load exactly in the middle (see Figure 137).

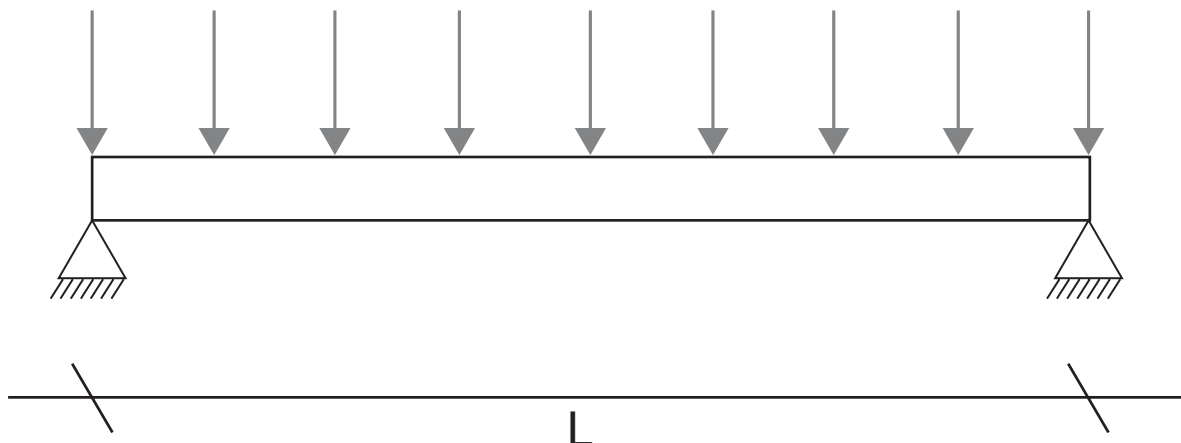


Figure 129 Relation between maximum deflection and maximum rotation

### 3.6.2.1 BEAM DEFLECTION ANALYSIS

The required flexural rigidity (EI) of the top beam to withstand the forces of the pre-tensioned cables, can be found considering the allowable deflection of the beam. For simply supported beams with intermediate loads, the deflection of the beam can be calculated with the following equation:

$$\delta = \frac{Fbx}{6LEI} (L^2 - b^2 - x^2) \quad (15)$$

For ( $0 \leq x \leq a$ ) and  $a \geq b$

Where:

$\delta$  = Maximum deflection (mm)

F = Point load (N)

x = Point of deflection (in this case the midpoint of the beam)

L = Length of the beam (mm)

E = Modulus of elasticity (N/mm<sup>2</sup>)

I = Second moment of area (mm<sup>4</sup>)

See Figure 130 for the principle of this calculation (Beam Deflection Tables, n.d.).



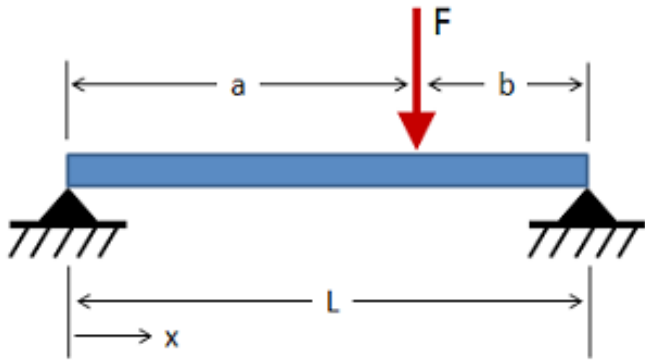


Figure 130 Principle of beam deflection calculation

Source: (Beam Deflection Tables, n.d.).

As Figure 131 illustrates, this beam can be seen as a symmetrical one. Therefore, load F2, F3 and F4 will be doubled in this calculation. Since load F1 acts exactly in the middle of the beam, it will not be doubled. Load F5 acts directly above the support of the beam and shall therefore be excluded from this calculation.

Assuming construction steel means  $E = 210000$  MPa. In this situation, the second moment of area of the beam is the value that is required to determine the minimal dimensions of the beam.

Therefore, the maximum deflection of the beam will be set to a certain value. This maximum deflection is chosen based on the façade system; as the beam hangs slightly above the glass interlocking components, there is not much space to deflect. If the beam deflects too much, there will be a high risk of breaking the glass components or pushing them out of the façade system. A maximum deflection of 20 mm is assumed to be acceptable.

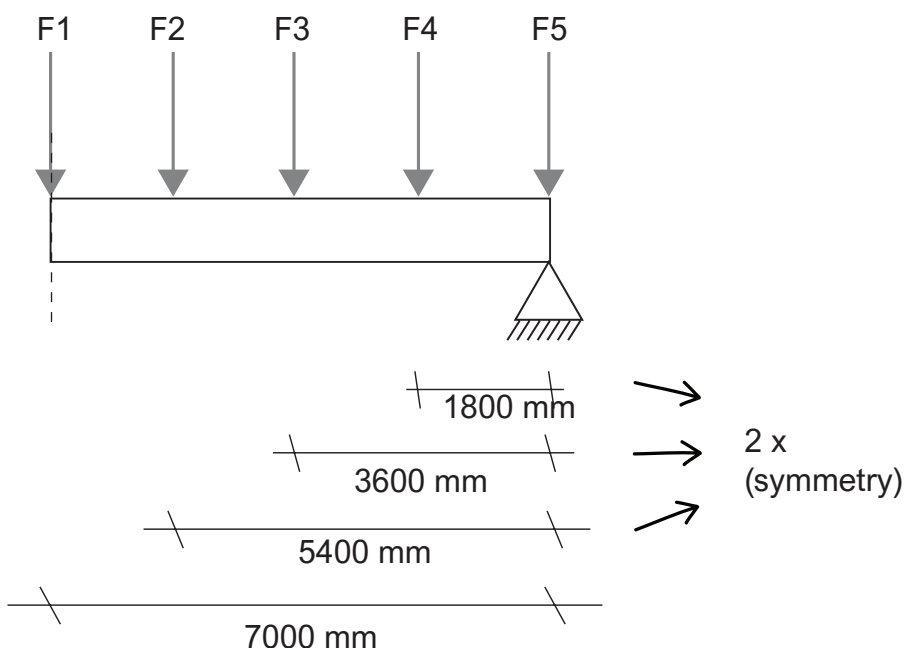


Figure 131 Symmetrical principle of beam

Solving equation (15) in Microsoft Excel, results in the required second moment of area ( $I$ ):

$$I_{\text{required}} = 8.88 \cdot 10^8 \text{ mm}^4$$

This value for a second moment of area ( $I$ ) is high, though still not uncommon. For example, commercial steel IPE-profiles go up to  $9.2 \cdot 10^8 \text{ mm}^4$  (Bouwen met Staal & van Eldik, 2006).

However, an Iw-profile is not favourable for the proposed façade. The pre-tensioned cables hanging from this profile, need to be fixed at the bottom side of the profile, as visible in Figure 132. Due to the eccentric tension forces of the cables, the I-profile is subjected to torsion.

In addition, the cables need to be fixed and tensioned when positioned in the façade. To make this possible, profiles such as rectangular tubes are not possible.

Therefore, a U-profile is proposed as the best solution for this situation.

However, the required second moment of area ( $I_{\text{required}}$ ) is a lot higher than commercialised U-profiles. Hence, a custom-made U-profile will be proposed.

The basis for the custom-made U-profile will be the largest commercially available one; UPE 400. For details and exact dimensions, see Appendix 5.17.

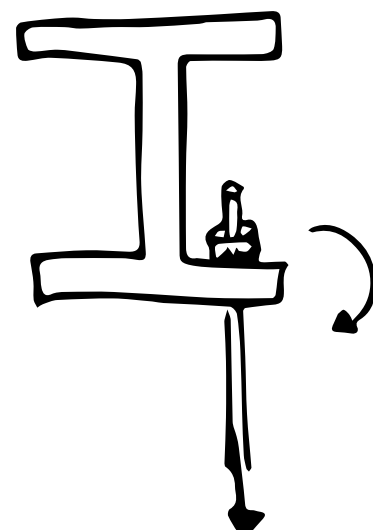


Figure 132 Eccentric loading of an I-profile

Some conditions should be noted first:

- the beam cannot be too high --> There is not enough space above the case study façade in Casa da Música to place a very high beam.
- a certain minimal width of the beam is required --> there needs to be enough space to fixate the pre-tensioned cables.

*Note: for simplification, eccentricity in this beam will not be taken into account, because it is not normative for dimensioning the U-profile.*

The maximum commercially available U-profile (UPE 400) has a height of 400 mm (h) and a width of 115 mm (b + t<sub>w</sub>), see Figure 133. This UPE 400 has an I<sub>x</sub> of 2.1\*10<sup>8</sup> mm<sup>4</sup>; more than 4 times lower than required. To create a beam that is suitable to use in the proposed design, it is necessary to increase the second moment of area to more than I<sub>required</sub> = 8.88 \* 10<sup>8</sup> mm<sup>4</sup>. Through enlarging the dimensions of the standard U-profile, the second moment of area will increase. This is most of all effective by increasing the flanges.

First, the height of the required beam will be set to 600 mm; higher than the standard profile, but not extremely high. Second, the width of the required beam will be set to 150 mm; enough space is left

to fixate the cables.

To calculate the required second moment of area, the following equation has been applied:

$$I_{required} = \frac{1}{12} * t_w * h^3 + 2 * \left( \frac{1}{12} * b * t_f^3 + b * t_f * \left( \frac{1}{2}h - \frac{1}{2}t_f \right)^2 \right) \quad (16)$$

Where:

t<sub>w</sub> = width of the web  
h = height of the profile  
t<sub>f</sub> = height of the flange  
b = width of the profile - t<sub>w</sub>

To increase the flanges, several possible solutions have been calculated in Microsoft Excel.

This resulted in an increase of t<sub>f</sub> from 18 mm (UPE 400) to 26 mm (custom-made profile).

To prevent local buckling of the profile web (t<sub>w</sub>), this needs to be increased as well. This t<sub>w</sub> factor does not contribute to an enormous increase of the second moment of area. By calculation in Excel, t<sub>w</sub> has been increased from 13.5 mm to 18 mm.

The increased dimensions result in an increased second moment of area:

$$I_{proposed} = 8.90 * 10^8 \text{ mm}^4$$

Although, the I<sub>proposed</sub> is not much higher than I<sub>required</sub>, several safety factors have already been applied, such as the set deflection of 20 mm. As explained before, the maximum deflection has been set to 20 mm due to practical reasons. However, a deflection of 20 mm on a span of 14 meter is considered very low. Therefore, a beam that has been designed to not deflect more than allowed, is considered safe.

In addition, considering safety factors, the radius



Figure 134 Radius of a UPE beam

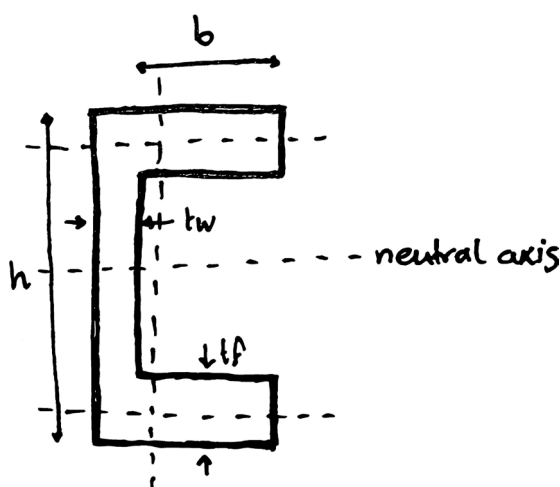


Figure 133 Dimensions of a UPE beam

between the flange and the web of a beam (see Figure 134), has not been taken into account for simplified calculation. However, in reality material present at those specific places, accounts for a higher second moment of area; thus, a higher strength of the total beam.

## Second iteration

The proposed solution suffers from two practical problems. Firstly, a single beam carrying all 9 cables (spread out over the wave-like façade shape) would have to be 1.7 m wide to attach all cables or would have to follow the wave-like shape (i.e. a curved beam). Both solutions would be difficult in practice or impossible even. Secondly, a maximum deflection under maximum wind load of 1.4 m is very high. To put in contrast, the facade of the Market Hall in Rotterdam has a maximum deflection of 0.7 m under extreme circumstances (octatube, n.d.).

A second iteration was performed with two major differences: a lower allowed maximum deflection and three beams to carry the 9 cables. The same assumption as in the last iteration concerning the components has been used: the components do not aid in counteracting the wind load deflection, only the cables carry this load.

In this case only 12.5% of the total interlocking ellipsoid height is allowed to be exposed under the maximum wind load. This results in a maximum rotation angle (on the bottom of the cable) of approximately 9 degrees and a maximum deflection (in the middle of the cable) of 0.7 m. The tensile force in a cable in this situation is 26 kN, which is doubled compared to the previous situation (13kN).

The second issue concerning the attachment



Figure 135 Instead of 1 curved beam, three straight beams are proposed

of the cables is solved using three beams, see Figure 135. In this case, the middle beam carries 5 cables. The top and bottom beam carry 2 and 3 beams respectively. Therefore, the middle beam is normative for the dimensioning of the other beams. This means that the top and bottom beam are oversized, however due to practical reasons it is less complicated when detailing the façade.

In reality, the points loads (the cables) on the middle beam are fastened asymmetrical, see Figure 136. To make simplified calculations the point loads are shifted in the 'beam deflection analysis' to get a symmetrical loading of the beam. This resulted in a second moment of area for the proposed middle beam of:

$$I_{\text{required,new}} = 9.99 \cdot 10^8 \text{ mm}^4$$

The value for  $I_{\text{required,new}}$  is higher than the initial calculated ( $8.88 \cdot 10^8 \text{ mm}^4$ ). This can be explained by the lower allowable deflection of one cable, which results into a higher required tension force per cable. Five of these tension forces act on only the middle beam (4 for simplified calculation). This means that the total force acting on the middle beam with 4 point loads, is higher than the total force acting on one beam with 9 point loads (7 for calculation) in the first situation.

For this new situation with three beams of equal dimensions, a new proposed  $I_{\text{proposed}}$  per beam is defined at  $1.00 \cdot 10^9 \text{ mm}^4$ . This corresponds to a beam with dimensions as illustrated on Figure 139.

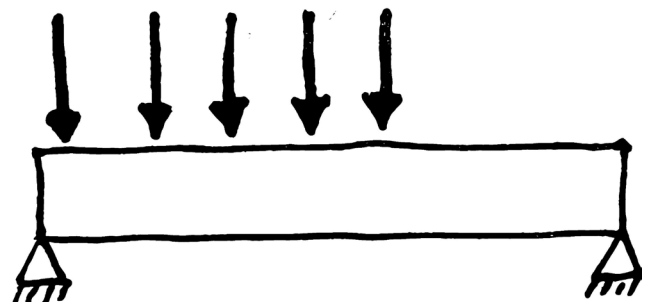


Figure 136 Asymmetrical loading

## Recommendation

As aforementioned calculations are simplified, a more thorough (i.e. numerical) analysis is required to properly evaluate the beam design. In addition, the total forces acting on the facade are quite high. If the current structural situation in Casa da Música is able to transfer and withstand such high forces, it needs more thorough analysis as well.

The assumed wind load of 1 kN/m<sup>2</sup> is probably too high. As the wind load has an enormous effect on the design of the cables and the top/bottom beam, an analysis of peak wind load on the exact location should be conducted to prevent extreme overdesigning.

To increase the strength of the beam, steel webs can be introduced at certain intervals as illustrated in Figure 138. In this way the required height of the beam could be lowered compared to the current design.

*Note: the aforementioned design proposes 9 pre-tensioned cables. However, this number is based on a set distance of a cable every 4 \* components of 0.45 m = 1.8 m, which only makes sense for a straight facade. As in the proposed design the façade is curved, following a sine-wave shape making two full waves and one quarter wave, it should contain 10 cables. Figure 117 illustrates where the 10 cables are positioned.*

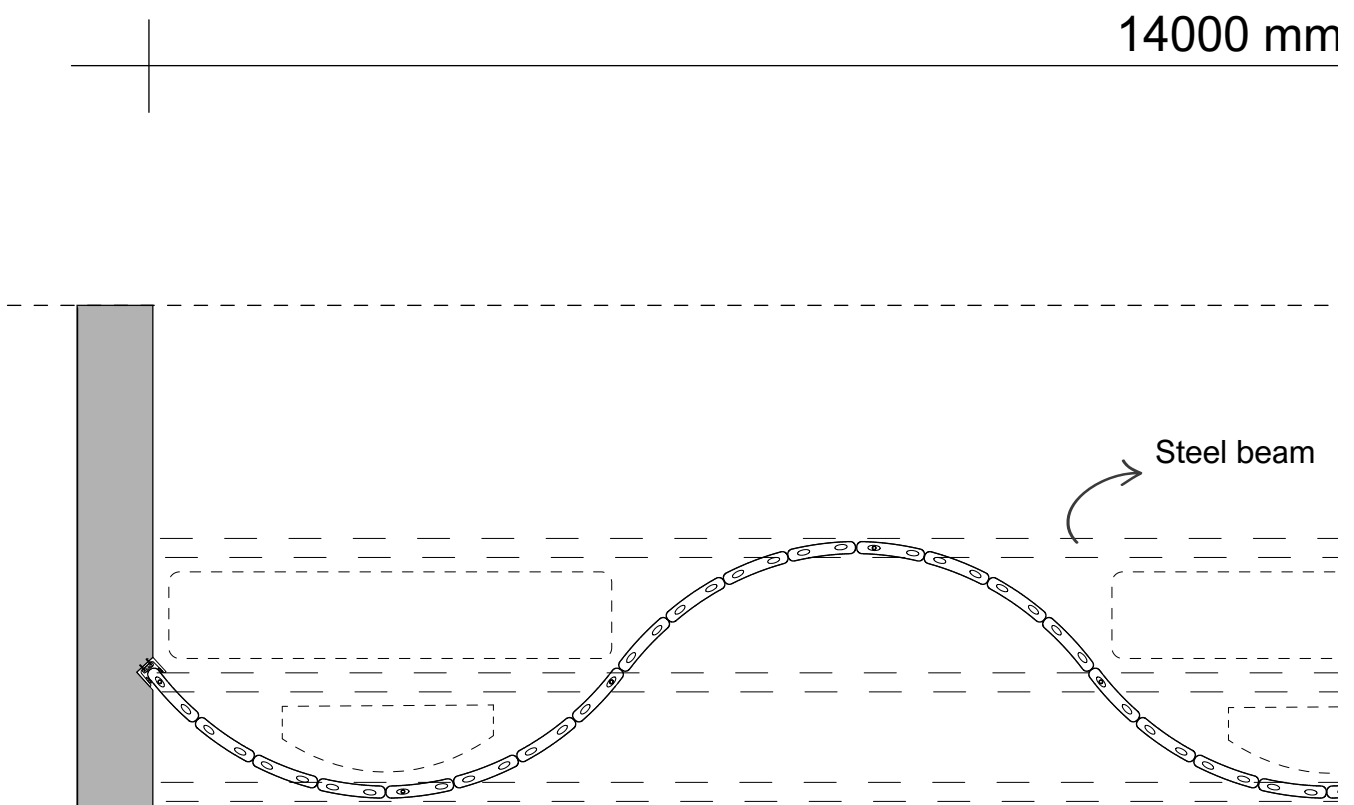


Figure 137 1:50 floor plan with the three beams and holes for maintenance

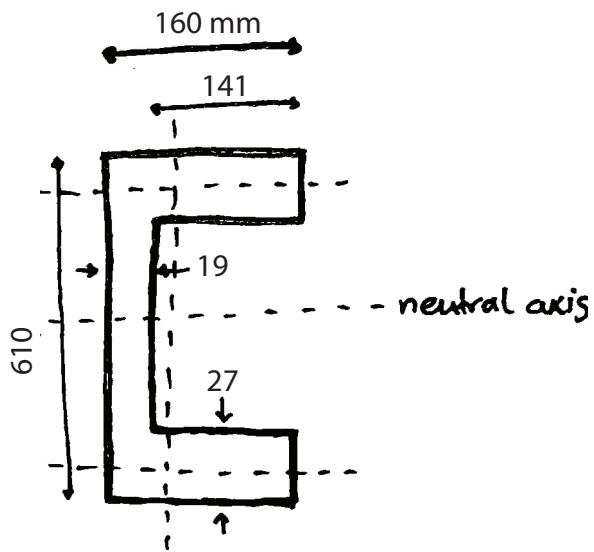


Figure 139 Dimensions of the proposed UPE beam

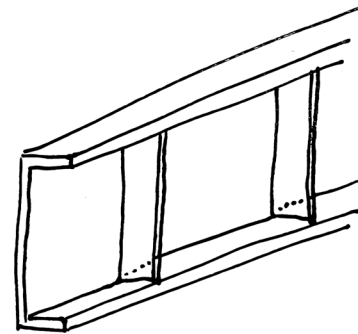
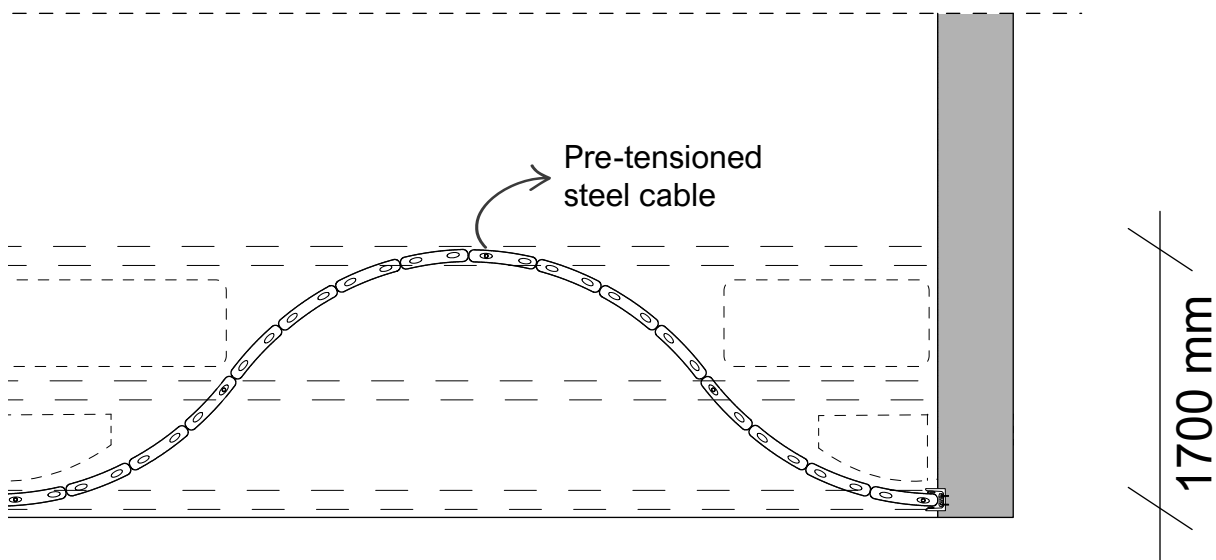
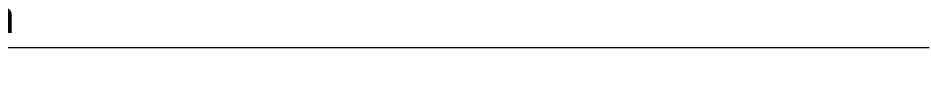


Figure 138 Creating a stronger beam





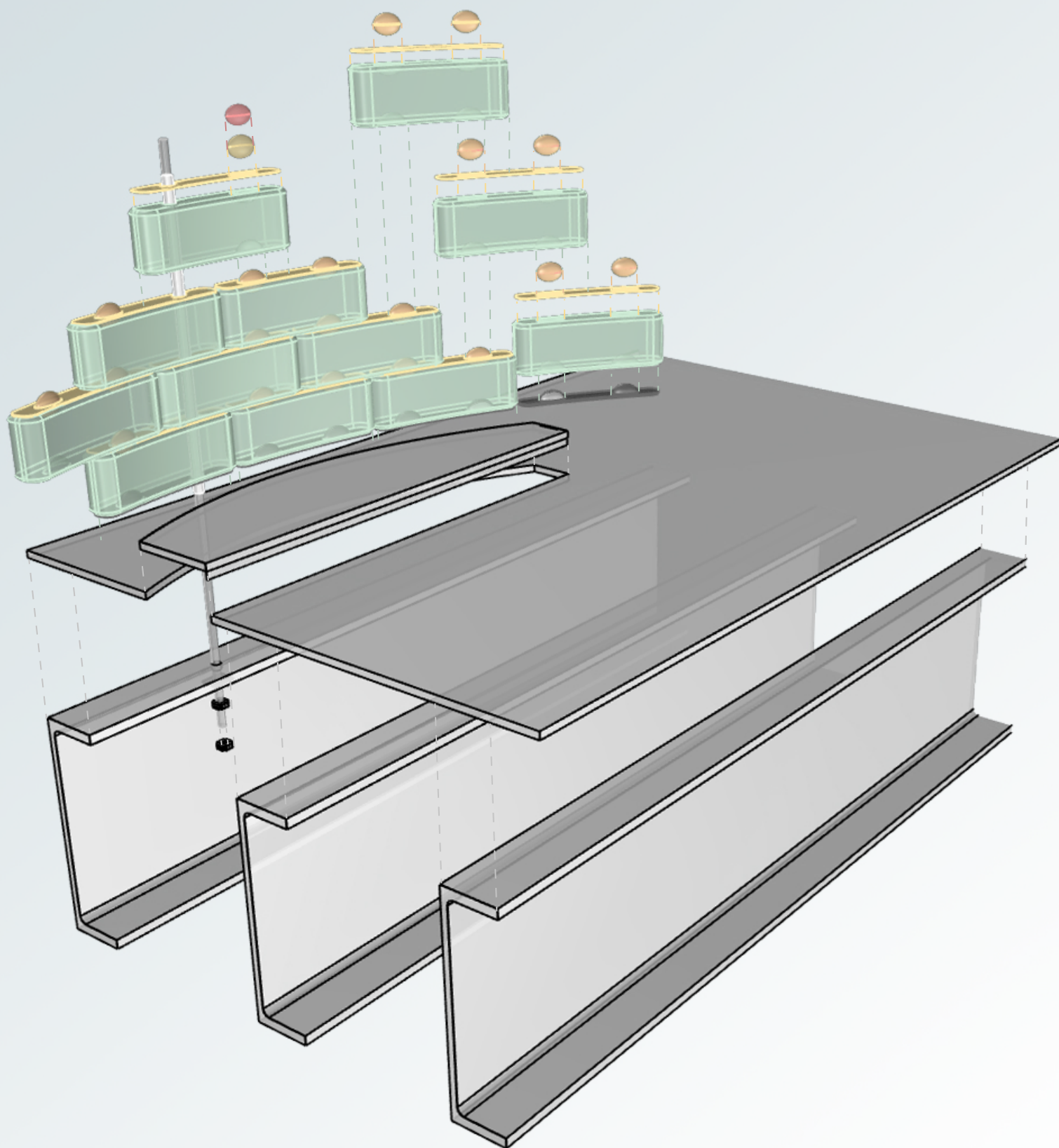


Figure 140 Exploded view total facade system

### 3.6.3 DETAILING OF FACADE SYSTEM

Figure 140 illustrates an exploded view of a part of the facade system. Here, it is visible that the facade system is supported by the three beams. The pre-tensioned cables are tensioned below the top flench of the UPE- profiles. The cable, with a protective plastic socket around it, runs through a channel in the steel plate and upwards through channels of the cast glass components. When maintenance is required on the pre-tensioned cable, this can be done by opening the hole in the steel plate.

A 1:20 vertical detail of the proposed facade system is illustrated in Figure 142. The three top and three bottom beams are most noticeable. As described in section 3.6.2, these beams are the consequence of the tensile force introduced by the ten pre-tension steel cables subjected to extreme wind loads. These cables are tensioned between the bottom beam and the top beam.

As visible on the 1:20 horizontal detail in Figure 142, the steel beams transfer the forces of the facade to the existing concrete structure of Casa da Música. On top of the bottom beams a steel plate with interlocking bumps is positioned, to fixate the component system in the building. The top part of the total construction is basically mirrored compared the bottom part (see Figure 141). Also illustrated on the horizontal 1:20 are the pre-tensioned steel cables, positioned every four components.

The total interlocking facade with pre-tensioned cables is dimensioned based on calculations of shear force introduced by the wind load. However, the shear force by impact would probably be higher. Nevertheless, the probability of such impact is rather low, i.e. a protection bar in front of the facade would be enough.

A 1:5 vertical detail is illustrated in Figure 145. It shows in more detail the construction of the facade system and the sealing between the elements. The facade system is water tightened by applying transparent silicon between the glass components. In addition, a concrete plate is bolted to the outer most steel beam, to finish the facade.

The 1:5 horizontal detail, illustrated in Figure 144 shows the top view of the facade system and the end-connection to the left part of Casa da Música. The bottom beams, supporting the

facade system transfer the forces down to main concrete construction of the existing facade, this is illustrated on the left part on this detail. The steel beams are bolted to the existing concrete wall of Casa da Musica. Here, it is also visible that half components are required at both ends of the facade system, every other level of components, see Figure 143.

The cast glass component system is positioned between a steel U-profile, bolted to the concrete facade. This U-profile ensures that the facade is fixed against the concrete, although the connection is not clamped. Between the U-profile and the glass a layer of neoprene is added to prevent glass to steel contact.

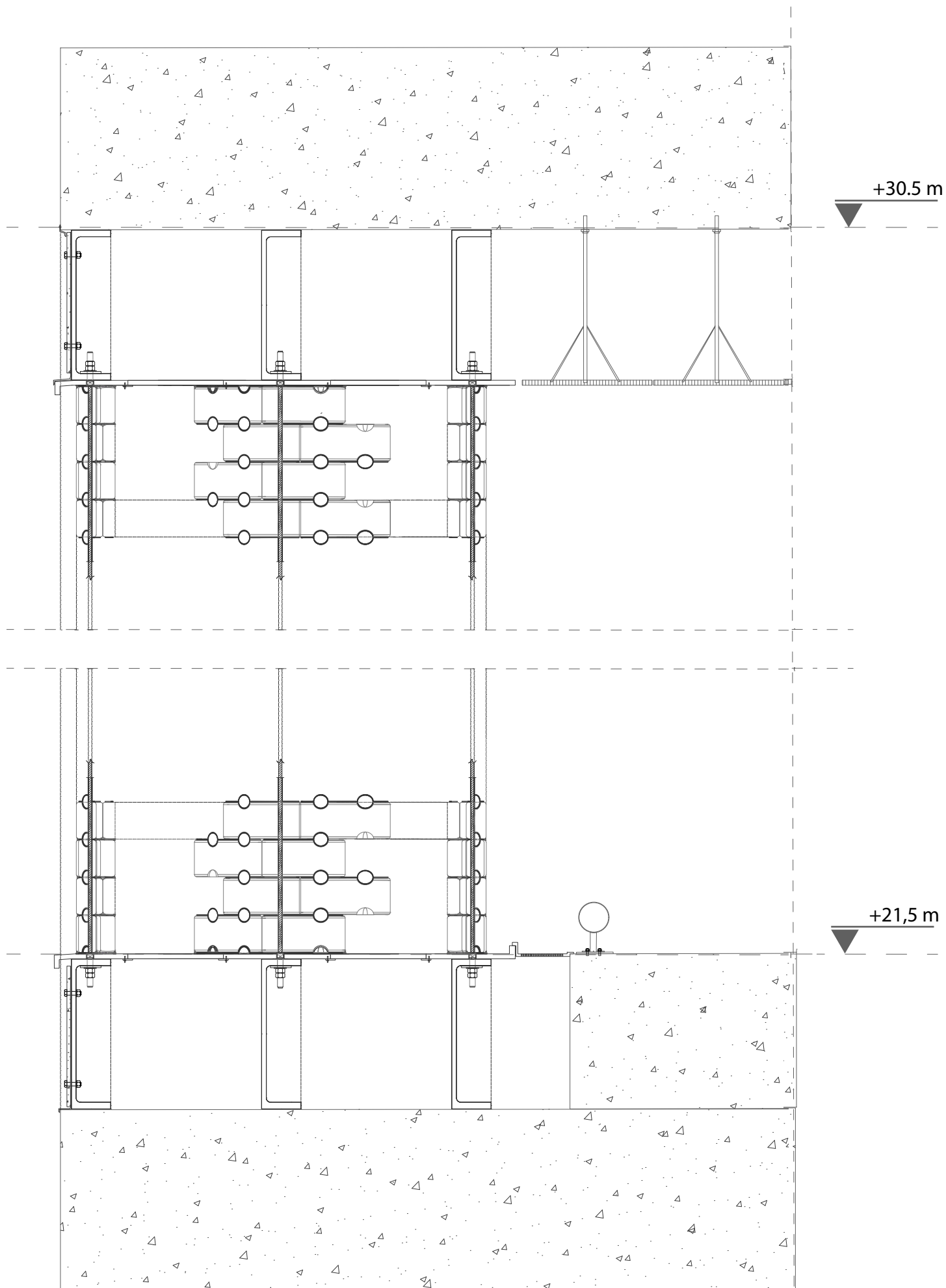


Figure 141 1:20 vertical detailing of facade system

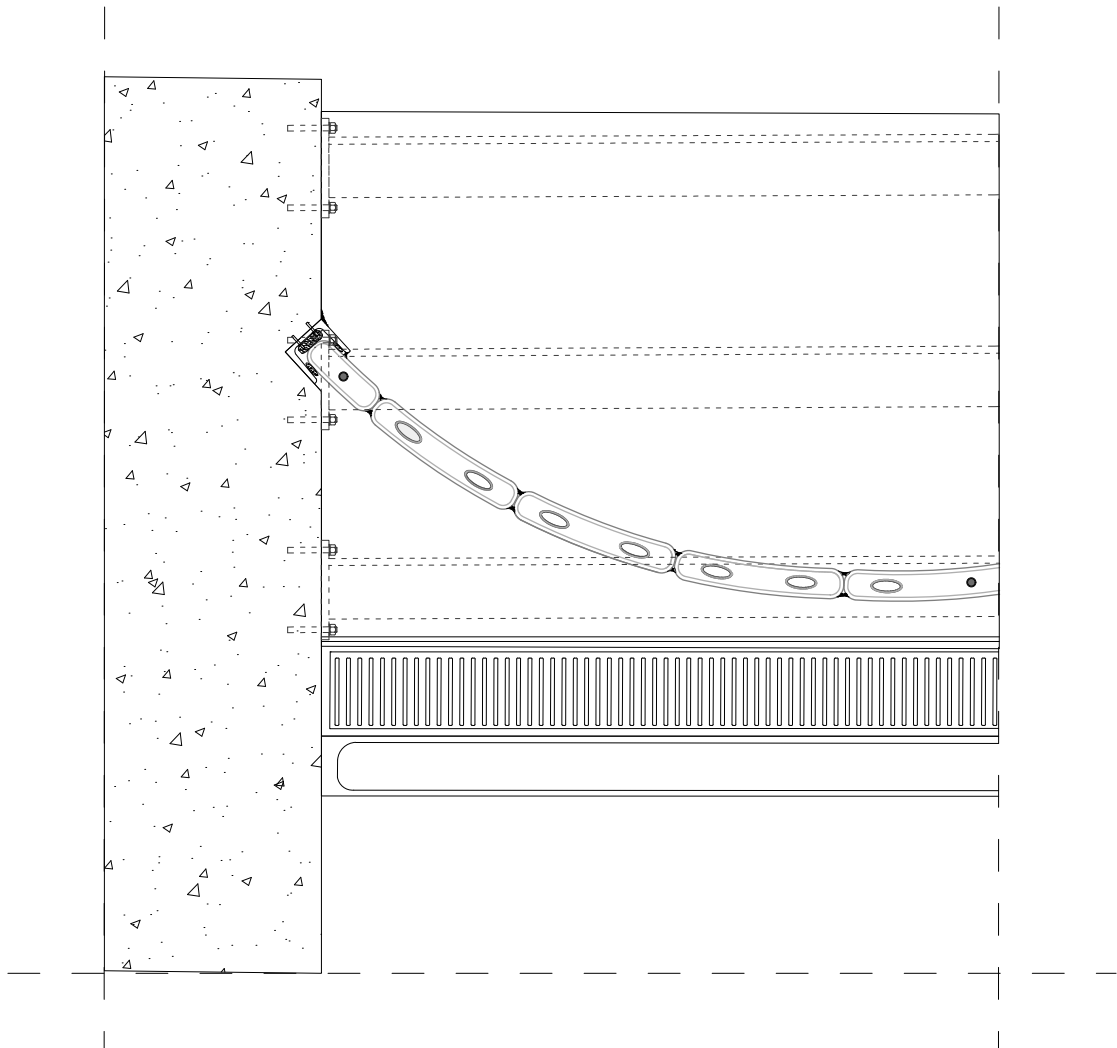
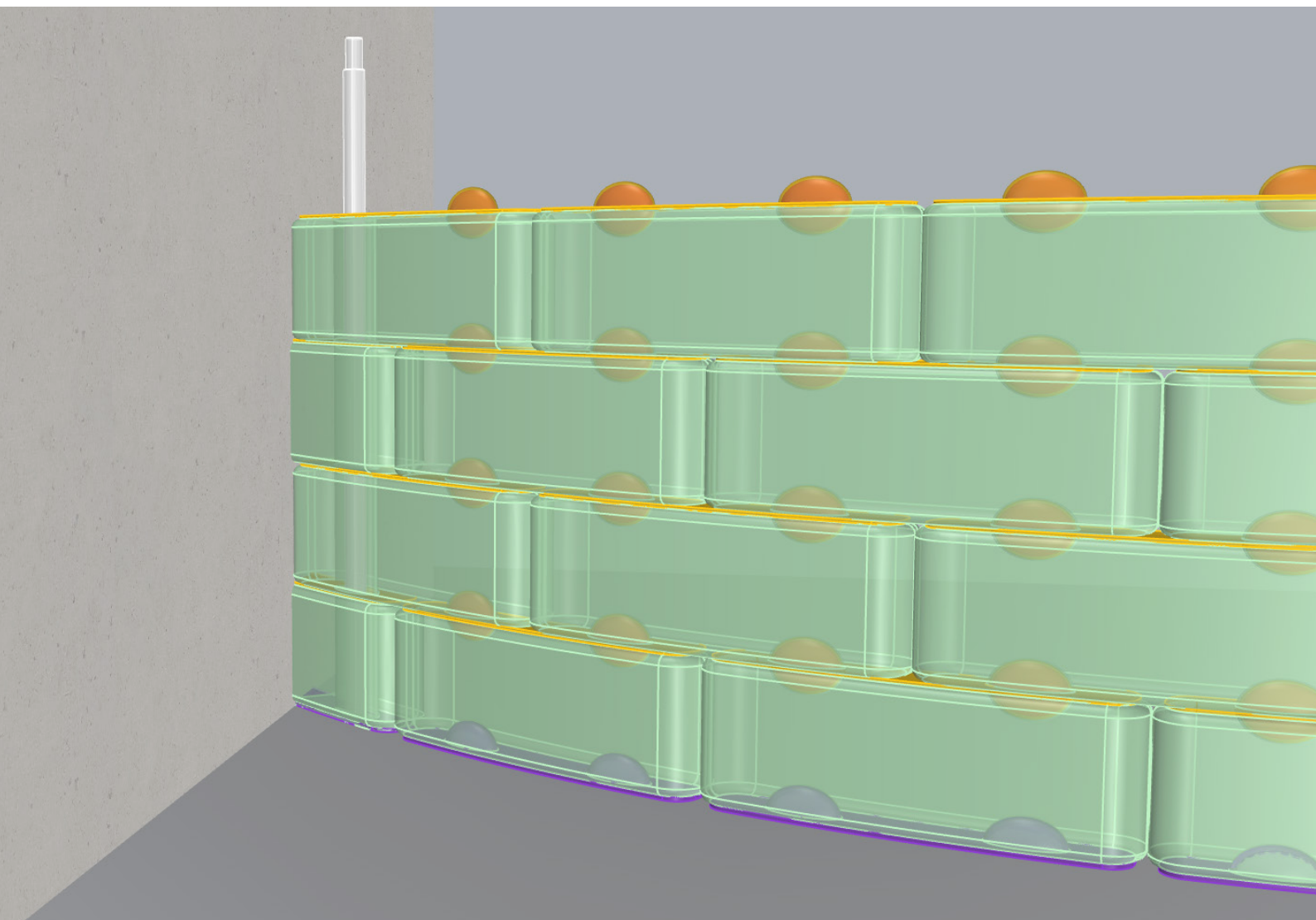


Figure 142 1:20 horizontal detailing of facade system



*Figure 143 Close-up of the facade system with half components adjacent to the concrete wall*



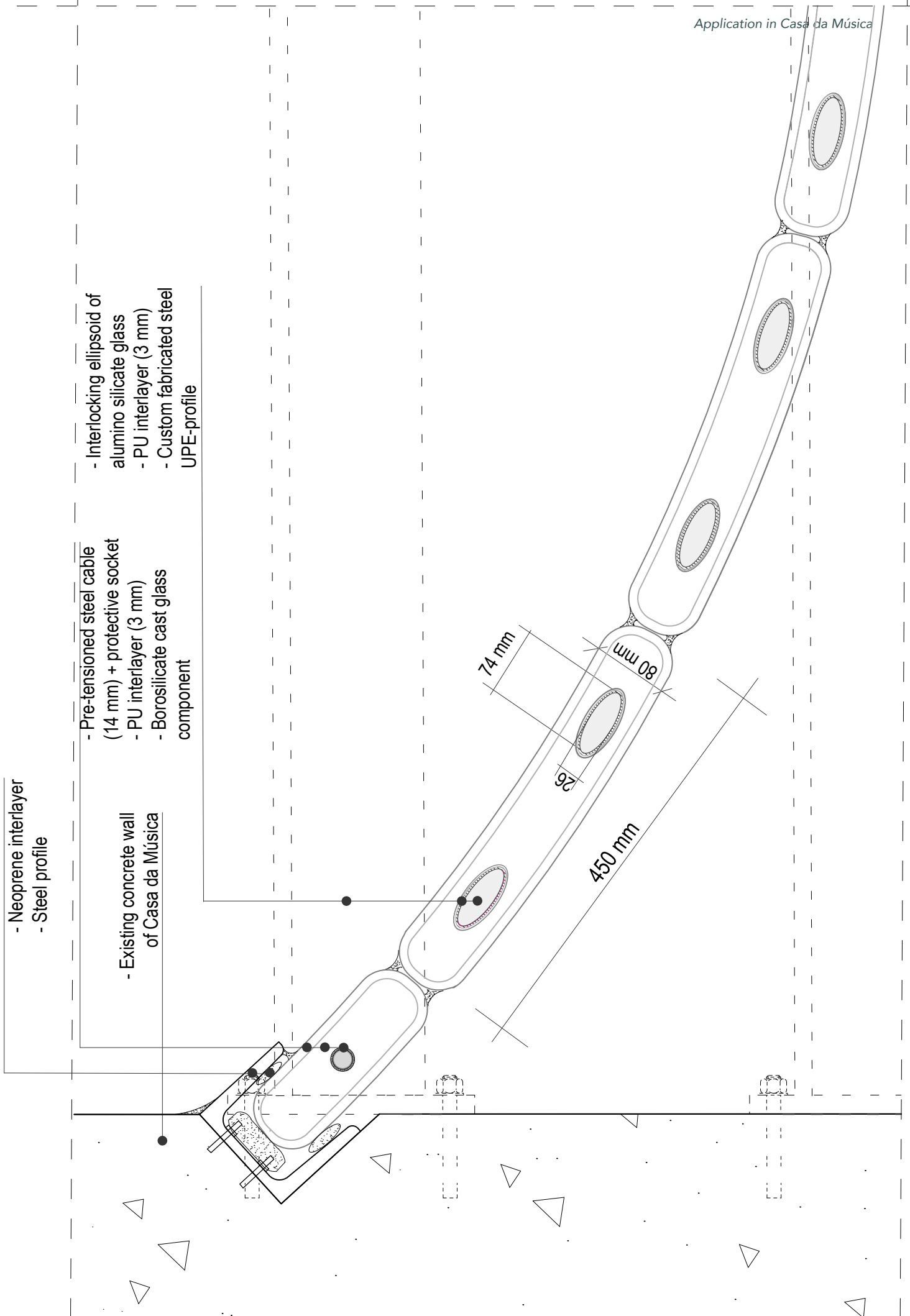


Figure 144 1:5 horizontal detail of the facade system

Figure 145 1:5 vertical detail of the facade sytem

- Pre-tensioned steel cable (14 mm)
- Protective plastic layer ( 2mm)
- Interlocking ellipsoid of aluminosilicate glass
- PU interlayer (3 mm)
- Borosilicate cast glass component

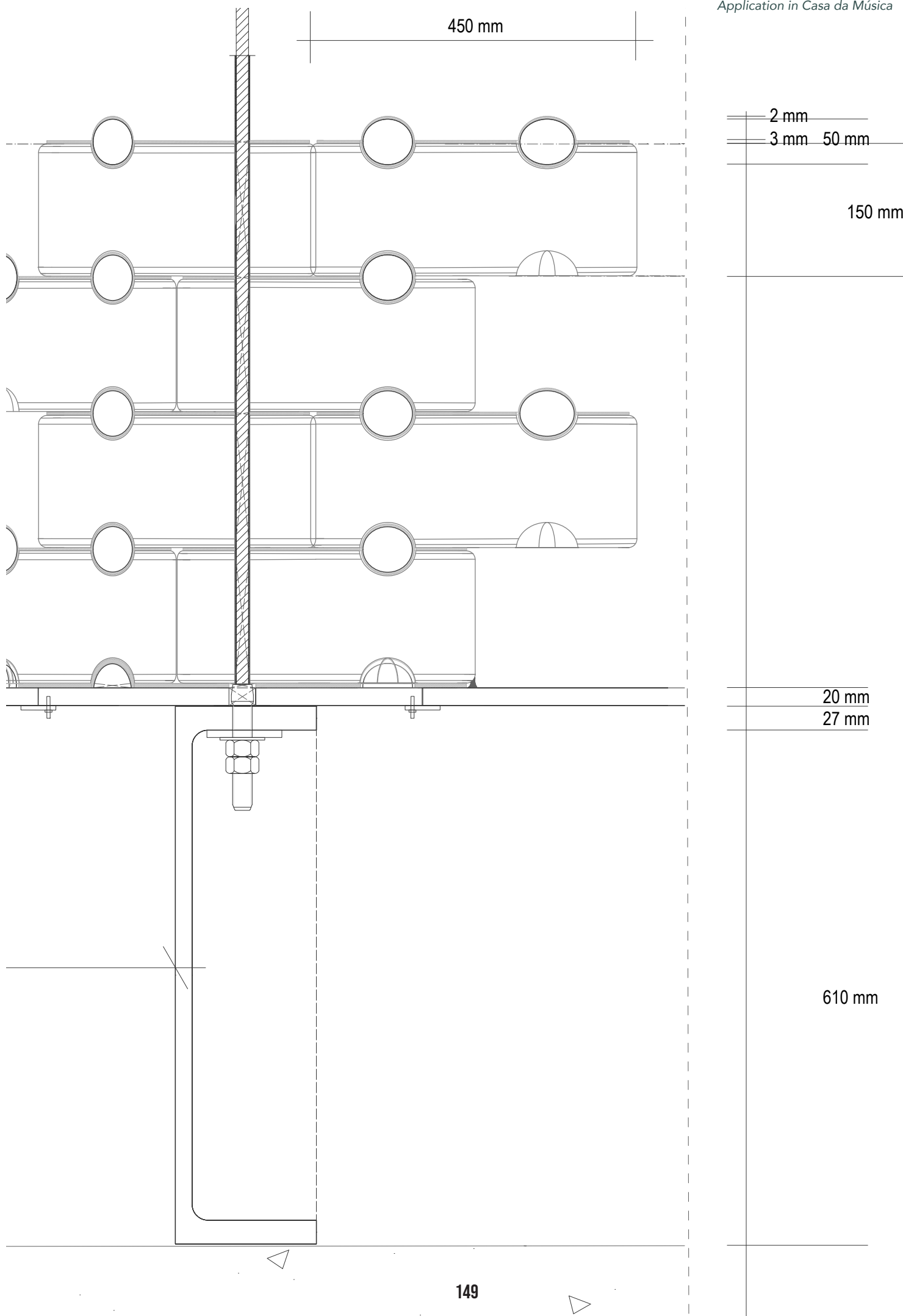
- PU interlayer (3 mm)
- Transparent silicon

- Steel plate with interlocking elements
- Neoprene interlayer (5 mm)
- Transparent silicon

- Custom made steel beam
- Concrete facade element

- Existing concrete structure of Casa da Música

630 mm





*Figure 146 Render of proposed facade system as seen from hall 2 in Casa da Música*

## 3.7 FEASIBILITY

*This chapter describes the feasibility of the design concerning several aspects: the recyclability of the elements of the facade system, the mould design of the components and the end-of-life of the proposed facade system.*

### 3.7.1 RECYCLABILITY OF FACADE SYSTEM

An important part of this thesis is the recyclability of the applied materials. As been thoroughly described in chapter 2.2, applying recycled borosilicate glass in cast glass components is suitable. As glass can be recycled endlessly, these components could be recycled at their end of life.

According to CesEduPack the Polyurethane 70 of the applied interlayer could be recycled after its lifetime. However, it is not totally clear if the interlayer could also be fabricated of recycled polyurethane.

Currently, the alumino silicate glass applied in the interlocking keys is not possible to recycle. However, the potential of recycling alumino silicate glass has been tested by (Bristogianni, Oikonomopoulou, De Lima, et al., 2018) and showed promising results.

The recycling industry of construction steel that is used in the steel plate and the beams does exist for years. Therefore, creating these elements out of recycled steel should be no problem.



### 3.7.2 MOULD DESIGN

In section 1.1.5.2 different existing types of mould have been discussed. For the production of the designed component a press steel mould is proposed. This type of mould allows for a cast component with high precision. In addition, those steel press moulds require solely a minimum amount of post-processing or none at all, which reduces the production costs. A steel press mould is in this case also preferred to create the interlocking holes and filleted corners. If an open steel mould would be used, the interlocking would be much less accurate, thus creating issues when stacking the components.

The proposed mould for this component consists of three parts; a bottom plate with interlocking holes and filleted corners, a middle part and a top press part, with interlocking holes and filleted corners as well. Where the mould parts touch each other, a seam could occur. It is important to prevent any seams on the curial parts of the glass component. Meaning, seam present on the glass component could introduce weaker spots. This could lead to failure of the component due to the risk of flaws, if such a seam is present on the tensile zone of the beam. Therefore, the mould parts are designed such that the seams are only present on the sides of the component and not on the top or bottom part. The three different parts are illustrated in Figure 147. A different mould is designed for the components with channels inside. These channels are required for the pre-tensioned cables of the facade system. Figure 148 illustrates this type of mould. The only thing that is different compared

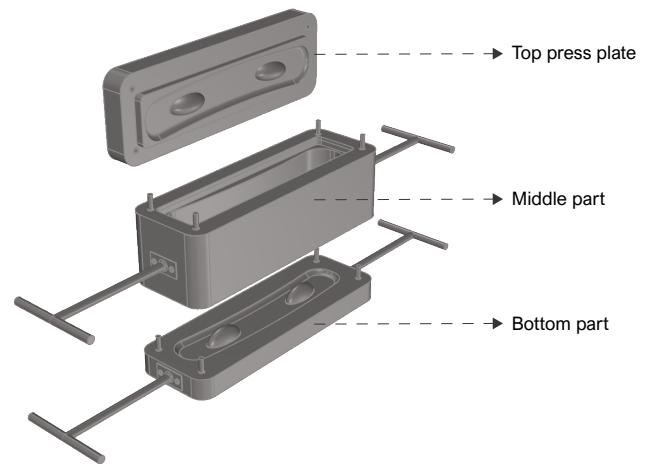


Figure 147 Mould design of standard component

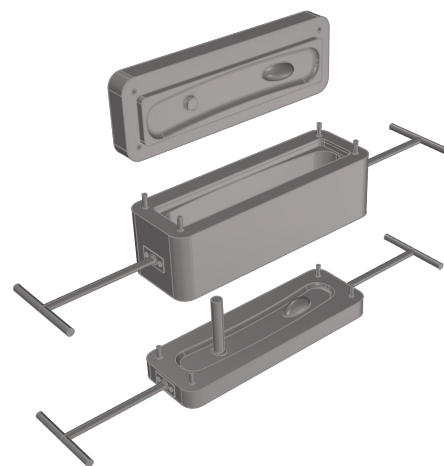
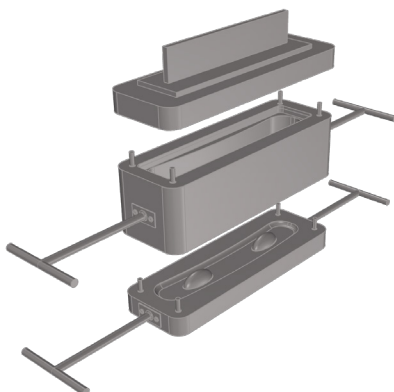


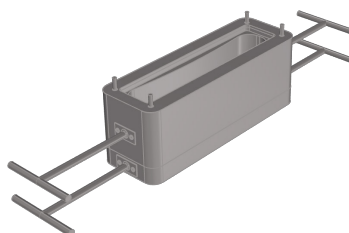
Figure 148 Mould design of component with channels

to the original component mould, is the steel rod which creates the channel.

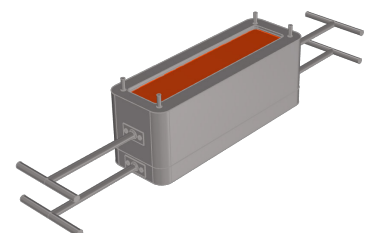
The process of casting the component is illustrated in the steps below and on page page 153.



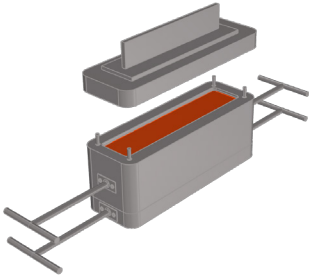
Steel press mould set-up; a bottom plate, middle part and a top press plate



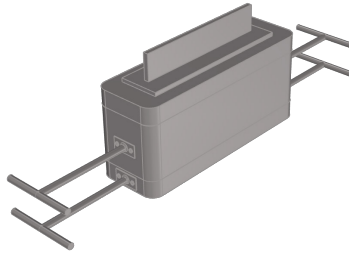
Step 1: Bottom part and middle part are preheated and assembled together



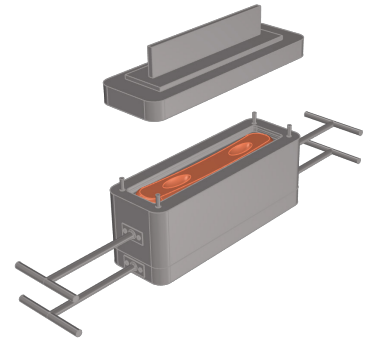
Step 2: Molten glass is poured into the mould



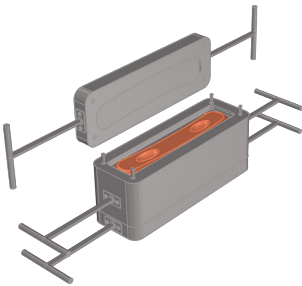
*Step 3: The top part of the mould is pressed onto the molten glass*



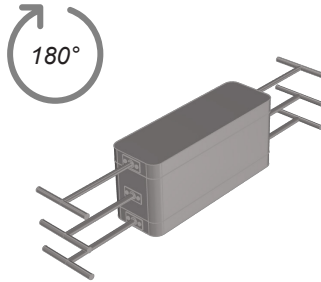
*Step 4: The glass component is shaping inside the mould*



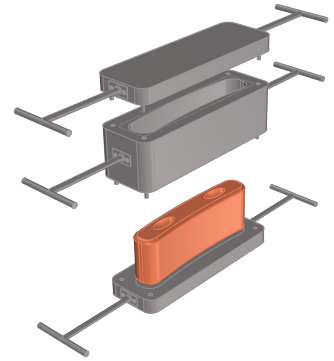
*Step 5: After the fast cooling down phase, the press part is removed.*



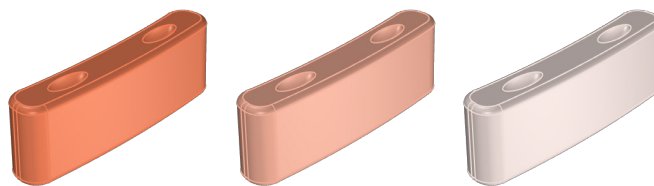
*Step 6: A flat plate is introduced to make it possible to slide the component in the annealing oven.*



*Step 7: The mould is rotated 180 degrees.*



*Step 8: The bottom and middle part of the mould are removed. The component is placed inside the annealing oven.*



*Step 9: In the annealing oven the component slowly cools down in a controlled environment to release any internal stresses.*

### 3.7.3 END-OF-LIFE

Chapter 2.1 introduces the possibility of reusing or recycling the borosilicate cast glass components. This is illustrated in Figure 35 on page 62. The inner loop in this Figure 35 represents the closed-loop of reusing and recycling the dry-interlocking cast glass components.

This section provides a more detailed description about this closed-loop and more specific on the end-of-life of such a dry-interlocking cast glass component facade system. Figure 149 illustrates the more detailed closed-loop of reusing and recycling the components.

Here, it is visible that there are two options after dis-assembling the facade system. Either the components are directly reused in another building, or the components are recycled. Application in another building does not necessarily mean the exact same component configuration is required.

If the components are not applied in another building, they will be recycled. This waste stream is kept separate from the curbside collected borosilicate glass and therefore pure and contaminant-free borosilicate glass cullet can be provided. This high-quality cullet can be used to cast new glass components. Of course, the recycled cullet from the collection containers will be used as well, but the additional recycling and cleaning step is not required when the components are recycled without mixing it with curbside collected borosilicate glass. After casting the recycled borosilicate glass in the desired component shape, they can be transferred to a new building site and assembled. A closed-loop for the production and application of recycled borosilicate cast glass components is created.

The end of life of such a dry-interlocking cast glass component facade system can be due to several reasons. Components could be damaged and require replacement. For example, such damage can be introduced due to heavy impact of a stone or metal object. The damaged components can be recycled and replaced by new components. If the facade is too heavily damaged to repair, or the client wishes a new facade, the dry-interlocking cast glass component facade can be dismantled and recycled.

The in this thesis proposed dry-interlocking cast glass components can be seen as a possibility of applying recycled borosilicate glass in the built environment. However, this exact shape of the component will not be a standardized commercial product. As mentioned in chapter 2.1, the creation of a borosilicate recycling as large as the current soda-lime glass recycling industry is expected to be not feasible. The total amount of borosilicate glass waste is much lower compared to soda-lime glass. However, it is expected that the proposed heat-resistant glass collection containers should provide enough borosilicate glass waste to create a small market for the production of cast glass components.

Production of cast glass components in such a small market is expected to have high cost, although less than existing production methods. Therefore, public buildings are considered most suitable, because funding of these buildings could cover the cost of such a facade system.

In addition, public buildings could provide a prominent role in showcasing the recycled cast glass components and thus creating awareness for the glass waste problem.

Examples of public buildings which have most potential for application of such a dry-interlocking cast recycled borosilicate glass facade could be museums, concert halls, public transport halls etc.

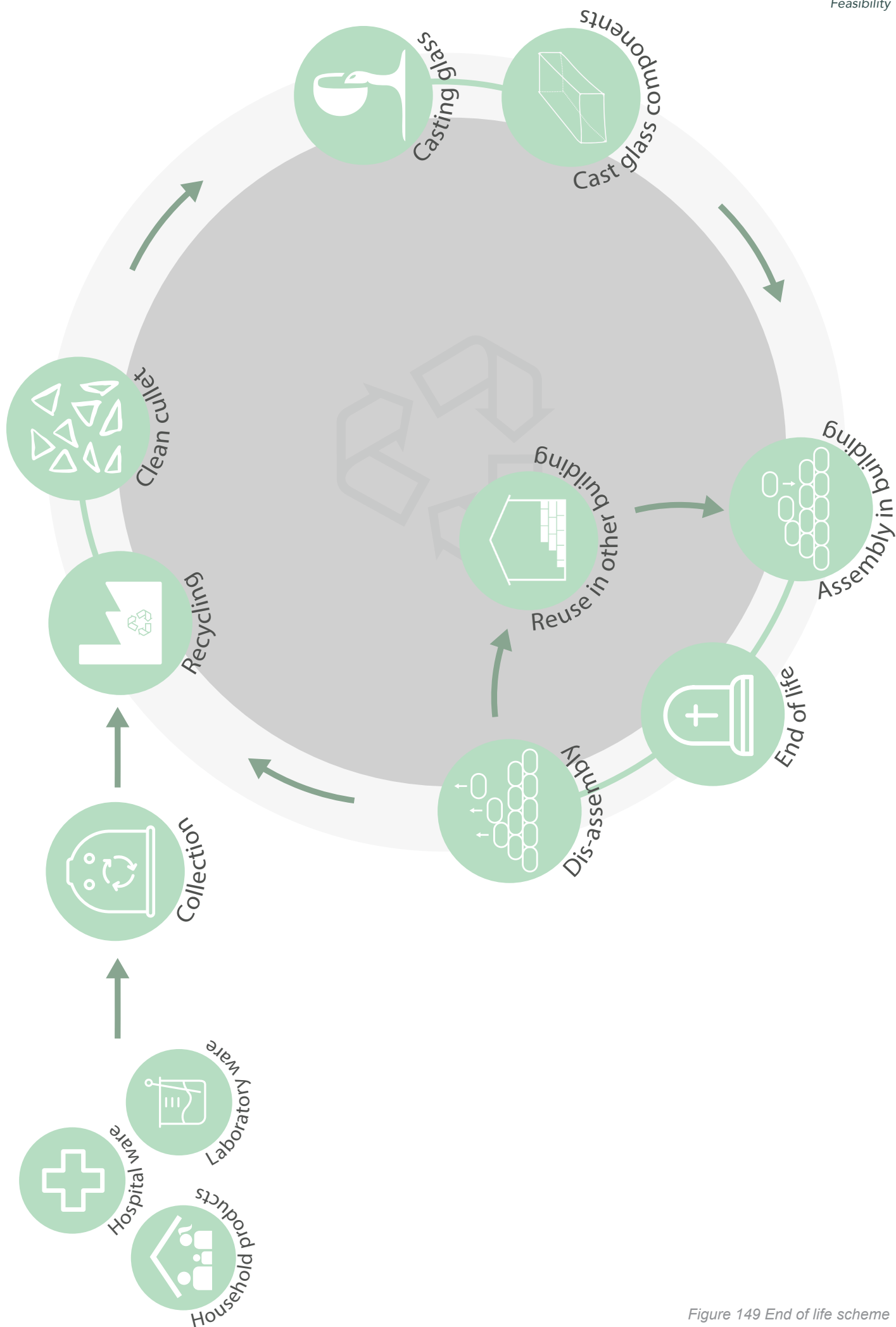


Figure 149 End of life scheme

## 3.8 CONCLUSIONS FINAL DESIGN

A facade system constructed of dry-interlocking components made of recycled borosilicate glass has been developed to showcase the possibilities of recycling borosilicate glass and cast glass component facade systems.

A dry-interlocking system has been chosen to allow for dis-assembly and thus recycling or reusing of the cast glass components.

The facade system has been applied in case study Casa da Música to develop an actual facade system and showcase the possibilities of cast glass interlocking components within the built environment. Based on the design concept of this building, the interesting contrast between the flat, white smooth concrete facade and the corrugated glass facade system has been recreated and improved. Therefore, the interlocking system follows a bigger wave-like shape; a 2.25 sinus curvature. Due to this curve, the components itself have a slight curvature as well.

For this facade an existing type of cast glass component has been developed further and improved. The result is a slightly curved component of 45\*15\*8 cm of 12 kg.

An loose interlocking ellipsoid has been designed specific for this component. The interlocking key is made of recycled alumino silicate glass; a strong material perfect for transferring high shear forces. Dry-interlocking with loose shear keys is preferred over fixed shear keys due to freedom of movement. Loose shear keys have less risk of chipping of when subjected to high shear forces.

The cast glass component and the interlocking key form together a total dry-interlocking facade system with structural integrity due to the corrugated shape of the facade. However, pre-tension steel cables are necessary to transfer extreme lateral forces. Between the cast glass components a transparent dry-interlayer of Polyurethane 70 Shore A with 3 mm thickness is required to prevent glass to glass contact and allow for an even force distribution. This accounts for the alumino silicate glass interlocking keys as well. A PU70 interlayer is thermoformed around the interlocking keys.

The ten required pre-tensioned steel cables are fixed between three bottom and three top beams. In addition, these beams support the interlocking cast glass facade structure. If necessary, these cables could be reached through holes in the steel plate where the facade structure is resting on.

The actual application in Casa da Música showed some issues related to the construction. Most likely Casa da Música would not be the best suitable building to apply this facade system onto. The proposed facade system is rather heavy. In addition, the six beams supporting the facade are also quite heavy. The concrete of the existing facade would presumably not be suitable to withstand such high amount of extra load, because the building is not designed to do so. In addition, these proposed beams require quite some extra mounting space, which looks like such space is not present in the building.

In conclusion, the interlocking cast glass system itself shows its potential, but application in this case study Casa da Música would not be recommended.



## 3.9 RECOMMENDATIONS FINAL DESIGN

When applying a facade system as proposed in this thesis it should be considered beforehand if the building is suitable in terms of construction. Such a facade system requires either a specific designed construction to support such a heavy facade or application on ground level would be more suitable.

The proposed interlocking system does not carry any load other than its own dead load. However, it would be interesting to research the structural capacities of such a cast glass system.

At this point, such a dry-interlocking cast glass facade system has not been applied in the built environment yet. Therefore, creating an actual facade with accurate watertightness and construction in an existing building require more research.

A possible future design of such a dry-interlocking cast glass system should be evaluated through numerical analysis and small-scale tests.

Concerning the interlocking keys made of aluminosilicate glass, recyclability of this material seems promising but further evaluation is required.

The choice for PU-70 for the interlayer was based on previous research. However, new interlayer (mostly polyurethane) materials are being developed currently. A future design should keep track of such developments. In addition, the recyclability of these materials requires more research.



# **PART 4**

CONCLUSIONS AND  
RECOMMENDATIONS

## 4.1 GENERAL CONCLUSION

This thesis contributes to creating awareness of the existing glass waste problem. Currently, a specific type of glass, borosilicate glass, is not recycled. Although the total share of borosilicate glass waste is rather small compared to soda-lime glass waste, it is relevant to reduce the total amount of glass waste. Most of this high-quality borosilicate glass takes up space at landfills or is down-cycled to aggregate. Borosilicate glass can also end up in recycling batches of soda-lime glass. When this happens, it can negatively affect the recycling process or even render the batch unusable. A closed-loop of recycling borosilicate glass could keep borosilicate glass away from landfills and soda-lime recycling batches, reducing these problems.

However, recycling introduces impurities and contaminations in the glass melt. Due to strict quality control demands of the current borosilicate glass product industry a fully closed-loop is not possible. The loop could be closed by finding a purpose for the recycled borosilicate glass with less strict quality demands. This effectively creates an internal cycle within the recycling loop of borosilicate glass. In the proposed internal cycle the recycled borosilicate glass is applied in a dry-interlocking cast glass component facade system. Cast glass components can tolerate more impurities due to their bulkiness. At end-of-life the facade system can be disassembled. The components can remain in the cast glass recycling loop by either being reused directly or by recycling them once more.

At present, borosilicate glass is not applied frequently in the built environment. Production from raw materials is very expensive and has a large carbon footprint due to high melting temperatures. Costs and emissions can be reduced significantly using recycled borosilicate glass cullet which lowers melting temperatures during production. This opens up the possibility to use this high-quality material for relatively lower costs and environmental impact.

The opportunities and challenges of recycling borosilicate glass have been researched with several experiments. In these experiments the mixability of different chemical compositions has been tested by mixing various borosilicate glass products. Subsequently, corresponding

mechanical properties have been assessed. Homogeneous chemical compositions showed lower possible firing temperatures of borosilicate glass. Mixing cullet consisting of different chemical compositions but grinding the cullet to powder also showed good results. Fine cullet could also work but introduced a higher amount of internal stresses. The mechanical properties of specimens from cullet with a homogeneous chemical composition were comparable to the mechanical properties of non-recycled borosilicate glass. This indicated that recycled borosilicate glass would be suitable to create cast glass components for application in the built environment.

Using cast glass to tackle the borosilicate glass waste is a versatile solution. The cast glass components can be applied in a variety of configurations and contexts. In this thesis one such context has been adopted for further research on actual implementation in the built environment. Through a case study of the Casa da Música in Porto it has been shown that it is possible to exploit the high-quality properties of borosilicate glass in an aesthetically pleasing facade system. This case study also serves as a showcase of expanding the recyclability of glass in general by presenting an unconventional application for recycled glass. A similar solution could be used for alumino silicate glass or other types of glass.

The cast glass components are not intended as a commercial product. Creating a borosilicate glass recycling industry as large as the current soda-lime recycling industry is probably not feasible. The amount of manufactured borosilicate glass products is much lower than the amount of soda-lime glass products. In addition, due to the high-quality of borosilicate glass these products have a longer expected life time, resulting in less waste. This borosilicate glass waste can be collected in new (heat-resistant glass) collection containers but will only be placed locally where high quantities of borosilicate glass waste is expected (e.g. laboratories, universities). These collection containers should provide enough borosilicate glass waste to create a small market for the production of cast glass components.

The proposed solution can reduce the growing amount of borosilicate glass waste and the

amount of unusable soda-lime recycling batches in the near future. Application in public buildings seems appropriate for two reasons. Firstly, funding for public building enables production of the components (collection and creation of moulds) without a mature collection system and mass production infrastructure in place. Secondly, through application in public building a prominent showcase is created for the glass waste problem.



## 4.2 GENERAL RECOMMENDATIONS

In this chapter higher level recommendation on the overall research are presented. For more detailed recommendations on possible future experiments or a similar facade system design the reader is referred to chapter 2.4 and 3.9, respectively.

In the literature study an inquiry was done on the amounts of borosilicate waste currently generated. The results were indicative of sufficient amounts of waste for a small recycling market but they were not conclusive. This aspect was not the focus of this thesis and exact data does not exist at present. A proper feasibility study on recycling borosilicate for cast glass components requires further research on exact amounts of borosilicate waste. Such a research could track waste amounts at the largest consumer groups: laboratories and hospitals. Collecting this data is more difficult for household waste because of the large spread of the waste. Another important aspect for feasibility is assessing the demand on the market for such a product. Furthermore, an evaluation on costs of logistics for collection is required as well.

The number of specimens in the experiments in this study was relatively small. The sample size was sufficient to indicate that recycled borosilicate glass has potential for use in the built environment and for a preliminary comparison of specimens. However, for a thorough evaluation of effects of cullet size and chemical composition on mixability and mechanical properties the experiments should be reproduced with more specimens.

Several issues were identified in the case study, as detailed in chapter 3.9. If such a facade would be applied in a future project these aspects should be taken into consideration from the first steps of the design.



## 4.3 REFLECTION

### Graduation process

*How is your graduation topic positioned in the studio?*

The main goal of the Building Technology graduation studio is to create a sustainable design within the built environment. The tracks that contribute to this are Façade design, Structural design, Climate design and Design informatics. As the goal of my research is to create a façade system made of recycled borosilicate glass applied into interlocking cast glass components, the tracks Structural design and Façade design suit the most.

*How did the research approach work out (and why or why not)? And did it lead to the results you aimed for? (SWOT of the method)*

*If applicable: what is the relationship between the methodical line of approach of the graduation studio (related research program of the department) and your chosen method*

*How are research and design related?*

The main research approach of my thesis has been that of 'Design through research'. My thesis consists of two parts: a research to the recyclability of borosilicate glass and an application of this glass in a façade system. First, for both a literature study has been done. Secondly, an experimental research to the recyclability of borosilicate glass has been conducted. Thirdly, a design has been proposed to apply the recycled borosilicate glass into an interlocking cast glass façade system. To a certain point, this design was based on literature and previous studies. Then research through design has been done to finalize the design part.

The experimental research done to the recyclability of borosilicate glass showed some promising and interesting results, however this is based on merely a few created specimens. In addition, this research is one of the first that has been done on this topic, which creates a lot of possibilities for other researchers. For scientific relevance more research should be conducted to the recycling of borosilicate glass for building applications.

The design of the façade system has been based on literature and previous studies. The design has been created to show the possibilities of recycling high quality glass such as borosilicate.

The experimental research was very time consuming, however I enjoyed it a lot. The creation of the glass specimens was very labour intensive, which required some good planning skills. When encountering problems, asking the advice or help of several experts helped a lot.

*Did you encounter moral/ethical issues or dilemmas during the process? How did you deal with these?*

Recycling borosilicate glass reduces the environmental impact of the existing and growing pile of glass waste and reduces the melting temperature during the production of the glass. However, the production of glass still needs very high melting temperatures, where a lot of CO<sub>2</sub> gasses are emitted. Although this amount is much less compared to normal borosilicate glass production, it still is a lot. Nonetheless, recycling this high-quality glass is still better than throwing it away.

### Societal impact

*To what extent are the results applicable in practice?*

This research is one of the first of its kind concerning the application of recycled borosilicate glass in the built environment. The results show that recycled borosilicate glass is comparable to normal borosilicate glass. This means that recycled borosilicate glass is applicable in the built environment. However, extensive research to go from experiments to an actual product needs to be conducted.

Previous studies show the possibilities of an interlocking cast glass façade. This study contributes to this and adds the possibility of an actual façade system. However, this has not been structural analysed thoroughly. Further research needs to be done on this topic as well. In addition, the design proposes a façade system which has never been built before. In terms of for example water tightness and feasibility extended research is necessary as well.

*To what extent has the projected innovation been achieved?*

*Does the project contribute to sustainable development?*

*What is the impact of your project on sustainability (people, planet, profit/prosperity)?*

This research contributes to innovation and sustainable development in several ways. Research to the recycling of borosilicate glass has never been done before to this extent. Currently, this high-quality glass ends up at landfills, while in general glass can be recycled almost 1:1. Through recycling borosilicate glass the environmental impact of the glass production and the glass waste can be reduced.

In addition, this thesis adds to the previous research in development of the interlocking cast glass system. Not only is it possible to apply such a system into a façade, but it can also be applied in for example internal walls.

*What is the socio-cultural and ethical impact?*

None

*What is the relation between the project and the wider social context?*

This project is a showcase of recyclability. To show that it is possible to create a (glass) façade out of recycled material. In addition, it shows that it is possible to create an aesthetically pleasing façade out of solely recycled glass. Making people aware that recycling/reusing is the future.

*How does the project affects architecture / the built environment?*

This thesis contributes to research of new building materials created through recycling old materials. To show to architects and designers that building environmentally friendly and aesthetically pleasing is possible. In addition, such a design as proposed in this thesis gives a higher aesthetical value to buildings.





**PART**

**5**

BIBLIOGRAPHY  
AND APPENDICES

# 5.1 REFERENCES

- Aurik, M. (2017). *Structural Aspects of an arched Glass Masonry Bridge*. TU Delft: Civil Engineering and Geosciences.
- Aurik, M., Snijder, A., Noteboom, C., Nijse, R., & Louter, C. (2018). Experimental analysis on the glass-interlayer system in glass masonry arches. *Glass Structures & Engineering*, 3(2), 335–353. <https://doi.org/10.1007/s40940-018-0068-7>
- Bell, V. B., & Rand, P. (2006). *Materials for architectural design*. London: Laurence King Publishing.
- Beam Deflection Tables. (n.d.). Retrieved February 19, 2019, from Mechanicalc: <https://mechanicalc.com/reference/beam-deflection-tables>
- Bouwen met Staal, & van Eldik, C. H. (2006). *Wegwijzer constructiestaal*. Zoetermeer.
- Brady, D. (n.d.). *Glass campus*. Retrieved January 31, 2019, from <http://www.glasscampus.com/tutorials.htm>
- Bristogianni, T., Nijse, R., Oikonomopoulou, F., & Veer, F. A. (2016). *Design and production of a structural cast glass element for a transparent dome*. In A. Zingoni (Ed.), *Insights and Innovations in Structural Engineering, Mechanics and Computation* (pp. 1662–1667). CRC Press. <https://doi.org/10.1201/9781315641645-27>
- Bristogianni, T., Oikonomopoulou, F., Barou, L., Veer, F., Nijse, R., Jacobs, E., & Frigo, G. (2017a). *Re<sup>3</sup> glass*. Delft University of Technology, Delft.
- Bristogianni, T., Oikonomopoulou, F., Justino, C., Lima, D., Veer, F. A., & Nijse, R. (2018a). *Cast Glass Components out of Recycled Glass: Potential and Limitations of Upgrading Waste to Load - bearing Structures*. Delft: Challenging Glass 6.
- Bristogianni, T., Oikonomopoulou, F., De Lima, C. J., Veer, F. A., & Nijse, R. (2018b). *Structural cast glass components manufactured from waste glass: Diverting everyday discarded glass from the landfill to the building industry*. *Heron*, 63(1–2), 57–102.
- Bristogianni, T., Oikonomopoulou, F., Veer, F. A., Snijder, A., & Nijse, R. (2017b). *Production and Testing of Kiln-cast Glass Components for an Interlocking, Dry-assembled Transparent Bridge*. Delft: GPD Glass Performance Days 2017.
- Callister, W. D. (2007). *Materials science and engineering an introduction* (7th ed.). Utah: John Wiley & Sons.
- Casa da Musica / OMA. (2014, April 15). Retrieved February 26, 2019, from Arch Daily: <https://www.archdaily.com/619294/casa-da-musica-oma>
- CESEduPack. (2017a). *Alumino silicate – 1720*. Granta Design Limited. Retrieved June 2, 2018
- CESEduPack. (2017b). *Borosilicate – KG33*. Granta Design Limited. Retrieved June 2, 2018
- CESEduPack. (2017c). *Potash soda lead glass- 0138*. Granta Design Limited. Retrieved June 2, 2018
- CESEduPack. (2017d). *Soda lime – 0080*. Granta Design Limited. Retrieved June 2, 2018
- Corning. (2017). *Corning® Gorilla® Glass 5*. New York.
- Corning Museum of Glass. (2011a). *Chemistry of Glass*. Retrieved June 10, 2018, from Corning Museum of Glass: <https://www.cmog.org/article/chemistry-glass>
- Corning Museum of Glass. (2011b). *Finding the right recipe: borosilicate glass*. Retrieved June 10, 2018, from Corning Museum of Glass: <https://www.cmog.org/article/finding-right-recipe-borosilicate-glass>

- Corning Museum of Glass. (2011c). *The Origins of Glassmaking*. Retrieved June 10, 2018, from Corning Museum of Glass: <https://www.cmog.org/article/origins-glassmaking?page=1>
- Corning Museum of Glass. (2011d). *Types of Glass*. Retrieved June 10, 2018, from Corning Museum of Glass: <https://www.cmog.org/article/types-glass>
- Corning Museum of Glass. (2011e). What is Glass? Retrieved June 10, 2018, from Corning Museum of Glass: <https://www.cmog.org/article/what-is-glass>
- Corning Museum of Glass. (n.d.). *Core-forming*. Retrieved June 10, 2018, from Corning Museum of Glass: <https://www.cmog.org/video/core-forming>
- de Vries, E. (2018). *The Stackable Glass Column*. TU Delft: Architecture, Urbanism & Building Sciences, Delft.
- Dyskin, A. V., Pasternak, E., & Estrin, Y. (2012). Mortarless structures based on topological interlocking. *Frontiers of Structural and Civil Engineering*, 6(2), 188–197. <https://doi.org/10.1007/s11709-012-0156-8>
- Dlubal Software GmbH. (n.d.). Wind load. Retrieved February 20, 2019, from Dlubal - Structural Analysis Software and Design Modules: <https://www.dlubal.com/en/solutions/online-services/snow-wind-and-seismic-zoning-maps>
- Duurzaam glas. (2018). Glas is eindeloos. Retrieved June 10, 2018, from Duurzaam glas: <http://www.duurzaamglas.nl/glas-is-eindeloos>
- FEVE European Container Glass Federation. (2016). *Container glass collection for recycling rates in Europe*. Brussels.
- Frearson, A. (2013). *Optical Glass House by Hiroshi Nakamura & NAP*. Retrieved 07 3, 2018, from Dezeen: <https://www.dezeen.com/2013/01/27/optical-glass-house-by-hiroshi-nakamura-nap/>
- Friedrich, & Dimmock. (2014). Comparative Values of Borosilicate Glasses, (856), 1–5.
- Glass alliance Europe. (2017). *Glass Specific Guidelines for Conformity Testing as Food Contact Material* (Vol. 2017).
- Glass for Europe. (2013). *Recycling of end-of-life building glass. Brussels: Glass for Europe*. Retrieved from [http://www.glassforeurope.com/images/cont/38\\_83208\\_file.pdf](http://www.glassforeurope.com/images/cont/38_83208_file.pdf)
- GROUP NSG. (2011). CULLET USAGE WITHIN THE NSG GROUP.
- Haldimann, M., Luible, A., & Overend, M. (2008). *Structural use of Glass*. Zürich: International Association for Bridge and Structural Engineering.
- Hartley, A. (2004). *Recovered container glass : Development of test methods and inorganic contamination limits*. Oxon: The Waste & Resources Action Programme.
- Hudson, D. (2013). *hiroshi nakamura & NAP: optical glass house*. Retrieved from Designboom: <https://www.designboom.com/architecture/hiroshi-nakamura-nap-optical-glass-house/>
- Introductory Astronomy: Ellipses. (n.d.). Retrieved February 08, 2019, from <http://astro.wsu.edu/worthey/astro/html/lec-ellipse.html>
- Jacobs, E. A. M. (2017). Structural consolidation of historic monuments by interlocking cast glass components: A computational analysis of interlocking cast glass brickwork. TU Delft: Civil Engineering and Geosciences.
- Janssens, E. J. (2018). *The Glass Dome - design technology for a dry assembled and cast glass dome*. TU

Lauriks, L., Collette, Q., Wouters, I., & Belis, J. (2012). Technical improvements in 19 th century Belgian window glass production, (November 2012), 84220E. <https://doi.org/10.1117/12.974589>

Leeuwen, M. v. (n.d.). what-does-shore-hardness-mean. Retrieved April 02, 2019, from Tweha: <https://www.tweha.com/en/what-does-shore-hardness-mean/>

Lesko, J. (2008). *Industrial design; materials and manufacturing guide* (2nd ed.). New Jersey: John Wiley & Sons, Inc.

Lewis, D. (n.d.). The War Against Pyrex. Retrieved March 31, 2019, from Now i know: <http://nowiknow.com/the-war-against-pyrex/>

Marcu, A., Roth, S., & Stoefs, W. (2014). FOR A STUDY ON COMPOSITION AND DRIVERS OF ENERGY PRICES AND COSTS IN ENERGY INTENSIVE INDUSTRIES: THE CASE OF THE FLAT GLASS INDUSTRY. Brussels.

Mittal, J., Kaur, I., & Sharma, R. (1992). *Industrial engineering and materials* (Vols. Encyclopaedia of technical education-13). New Delhi: Mittal Publications.

Module 3 : Cables. (n.d.). Retrieved February 15, 2019, from Application of the General Cable Theorem for Distributed Loading: [https://nptel.ac.in/courses/105101085/Slides/Module-3/Lecture-3/3.3\\_2.html](https://nptel.ac.in/courses/105101085/Slides/Module-3/Lecture-3/3.3_2.html)

Nedvang. (n.d.). *De kringloop van glazen verpakking*. Retrieved June 13, 2018, from Duurzaamglas.nl: <http://www.duurzaamglas.nl/informatie-en-beeld/fotos/infographics/>

Nijssse, R. (2009). *Corrugated glass as improvement to the structural resistance of glass*. Research in Architectural Engineering Series, 9, 19–31. <https://doi.org/10.3233/978-1-60750-524-2-18>

octatube. (n.d.). Market Hall. Retrieved February 20, 2019, from octatube: [https://www.octatube.nl/en\\_GB/project-item/projectitem/6-market-hall.html](https://www.octatube.nl/en_GB/project-item/projectitem/6-market-hall.html)

Oikonomopoulou, F., Bristogianni, T., Barou, L., Jacobs, E., Frigo, G., & Veer, F. A. (2018a). A novel , demountable structural glass system out of dry- assembly , interlocking cast glass components ., (May). <https://doi.org/10.7480/cgc.6.2118>

Oikonomopoulou, F., Bristogianni, T., Veer, F., & Nijssse, R. (2017). *The construction of the Crystal Houses façade: challenges and innovations*. Glass Structures and Engineering, 1-22. DOI: 10.1007/s40940-017-0039-4

Oikonomopoulou, F., Bristogianni, T., Barou, L., Jacobs, E., Frigo, G., Veer, F. A., & Nijssse, R. (2018b). *Interlocking cast glass components, Exploring a demountable dry-assembly structural glass system*. Heron, 63(1–2), 103–137.

Oikonomopoulou, F., Veer, F., Nijssse, R., & Baardolf, K. (2015). *A completely transparent, adhesively bonded soda-lime glass block masonry system*. Journal of Facade Design and Engineering, 2(3–4), 201–221. <https://doi.org/10.3233/FDE-150021>

Oikonomopoulou, F., Bristogianni, T., Barou, L., Veer, F. A., & Nijssse, R. (2018c). *The potential of cast glass in structural applications. Lessons learned from large-scale castings and state-of-the art load-bearing cast glass in architecture*. Journal of Building Engineering(20 ), 213–234.

O'Regan, C., & Institution of Structural Engineers (Great Britain). (2014). *Structural use of glass in buildings* (Second edition. ed.). London: Institution of Structural Engineers.

Paech, C., & Goppert, K. (2008). *Innovative Glass Joints - The 11 March Memorial in Madrid*. Delft: Challenging Glass: Conference on Architectural and Structural Applications of Glass.

- Rich, J. (1988). *The Materials and Methods of Sculpture*. Courier Corporation
- Rodriguez Vieitez, E. R., Eder, P., Villanueva, A., & Saveyn, H. (2011). End-of-waste criteria for glass cullet: Technical proposals. JRC Scientific and Technical Reports. Seville: Publications Office of the European Union. <https://doi.org/10.2791/7150>
- Scalet, B. M., Garcia Muñoz, M., Sissa Aivi, Q., Roudier, S., & Luis, D. S. (2013). Best Available Techniques (BAT) Reference Document for the Manufacture of Glass. Joint Research Centre Reference Report. <https://doi.org/10.2791/69502>
- Schmitz, A., Kamiński, J., Maria Scalet, B., & Soria, A. (2011). Energy consumption and CO<sub>2</sub> emissions of the European glass industry. *Energy Policy*, 39(1), 142–155. <https://doi.org/10.1016/j.enpol.2010.09.022>
- Schott. (2004). TIE-27 : Stress in optical glass. Technical Information Advanced Optics, 1–13.
- Schott. (2010). *SCHOTT Technical Glasses Physical*. Mainz. Mainz. <https://doi.org/10.1016/B978-0-08-002597-1.50008-5>
- Shelby, J. E. (2005). *Introduction to Glass Science and Technology* (2nd ed.). Cambridge: The Royal Society of Chemistry.
- Stormont, R. (2010). Electric melting and boosting for glass quality improvement. *Glass Worldwide*, 1–4.
- Testa, M., Malandrino, O., Sessa, M. R., Supino, S., & Sica, D. (2017). Long-term sustainability from the perspective of cullet recycling in the container glass industry: Evidence from Italy. *Sustainability (Switzerland)*, 9(10). <https://doi.org/10.3390/su9101752>
- The Engineering Toolbox. (2012). Retrieved February 18, 2019, from Euler's Column Formula; Buckling of columns: [https://www.engineeringtoolbox.com/euler-column-formula-d\\_1813.html](https://www.engineeringtoolbox.com/euler-column-formula-d_1813.html)
- Vlakglas recycling Nederland. (2016). *Productie: van scherven naar glas*. Retrieved June 10, 2018, from Vlakglas recycling Nederland: <https://www.vlakglasrecycling.nl/index.php?page=wat-gebeurt-er-met-de-scherven-nl>
- Vlakglas recycling Nederland. (2018). *Productie van verpakkingsglas*. Retrieved June 10, 2018, from Vlakglas recycling Nederland: <https://www.vlakglasrecycling.nl/index.php?page=productie-van-verpakkingsglas-nl>
- Verening Nederlandse Glasfabrikanten. (2012). *Routekaart 2030 Nederlandse glasindustrie*. Hoogezaand: Libertas.
- Vieitez, E. R., Eder, P., Villanueva, A., & Saveyn, H. (2011). *End-of-waste criteria for glass cullet: Technical proposals. JRC Scientific and Technical Reports*. Seville: Publications Office of the European Union. <https://doi.org/10.2791/7150>
- Weisstein, E. W. (n.d.). Eccentricity. Retrieved February 08, 2019, from MathWorld--A Wolfram Web Resource: <http://mathworld.wolfram.com/Eccentricity.html>
- Weller, B., Unnewehr, S., Tasche, S., & Härth, K. (2009). *Glass in Building: Principles, Applications, Examples*. Munich: Walter de Gruyter.
- Wikivoyage-Iberia. (n.d.). Retrieved March 17, 2019, from <https://en.wikivoyage.org/wiki/Iberia>
- Worrell, E., & Reuter, M. A. (2014). Handbook of Recycling: State-of-the-art for Practitioners, Analysts, and Scientists. Handbook of Recycling: State-of-the-art for Practitioners, Analysts, and Scientists. Oxford: Elsevier. <https://doi.org/10.1016/C2011-0-07046-1>
- Wurm, J. (2007). *Glass Structures: Design and Construction of Self-supporting Skins*. Basel: Birkhäuser Verlag AG.





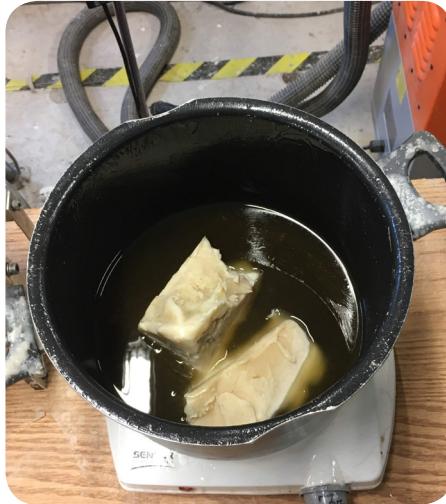
## 5.2 APPENDICES

### Creation of the glass beams

Appendices  
APPENDIX 5.3



Step 1: Silicon mould beam shape of 150\*40\*40 mm



Step 2: Melting wax



Step 3: Silicon mould



Step 4: Silicon mould with hot wax



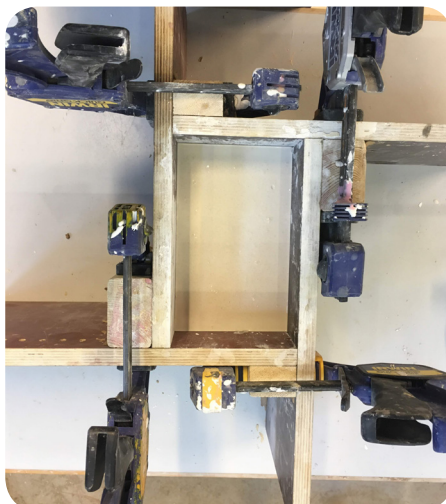
Step 5: Wax beam of 150\*40\*40 mm



Step 6: Wax beam fixed with clay on top of a wooden block



Step 7: Wax beam inside wooden planks for the creation of the Crystal Cast mould



Step 8: Creation of the Crystal Cast mould

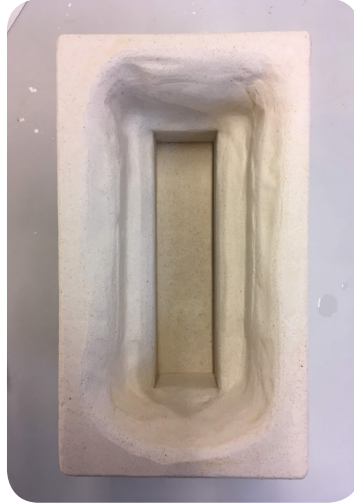


Step 9: Two Crystal Cast moulds with wax beam still inside





Step 10: Steaming the wax out of the Crystal Cast mould



Step 11: A Crystal Cast mould of a beam of 150\*40\*40 mm



Step 12: Borosilicate glass rods by Schott



Step 13: Smashing the rods



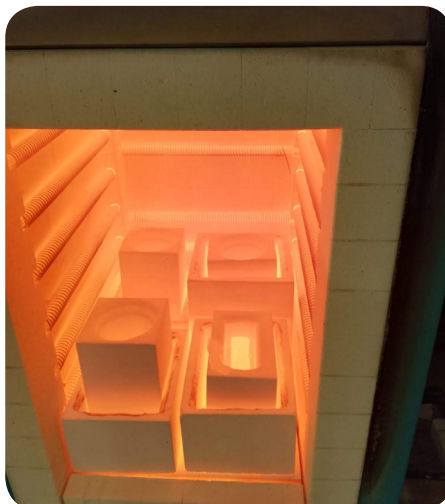
Step 14: Smashed rods



Step 15: Smashed rods inside the mould



Step 19: Four moulds with borosilicate glass before entering the kiln



Step 20: Four moulds with borosilicate glass inside the kiln



Step 21: Four moulds with borosilicate glass after firing in the kiln



Step 16: A borosilicate glass beam of 150\*40\*40 mm, but with too much glass on the top part

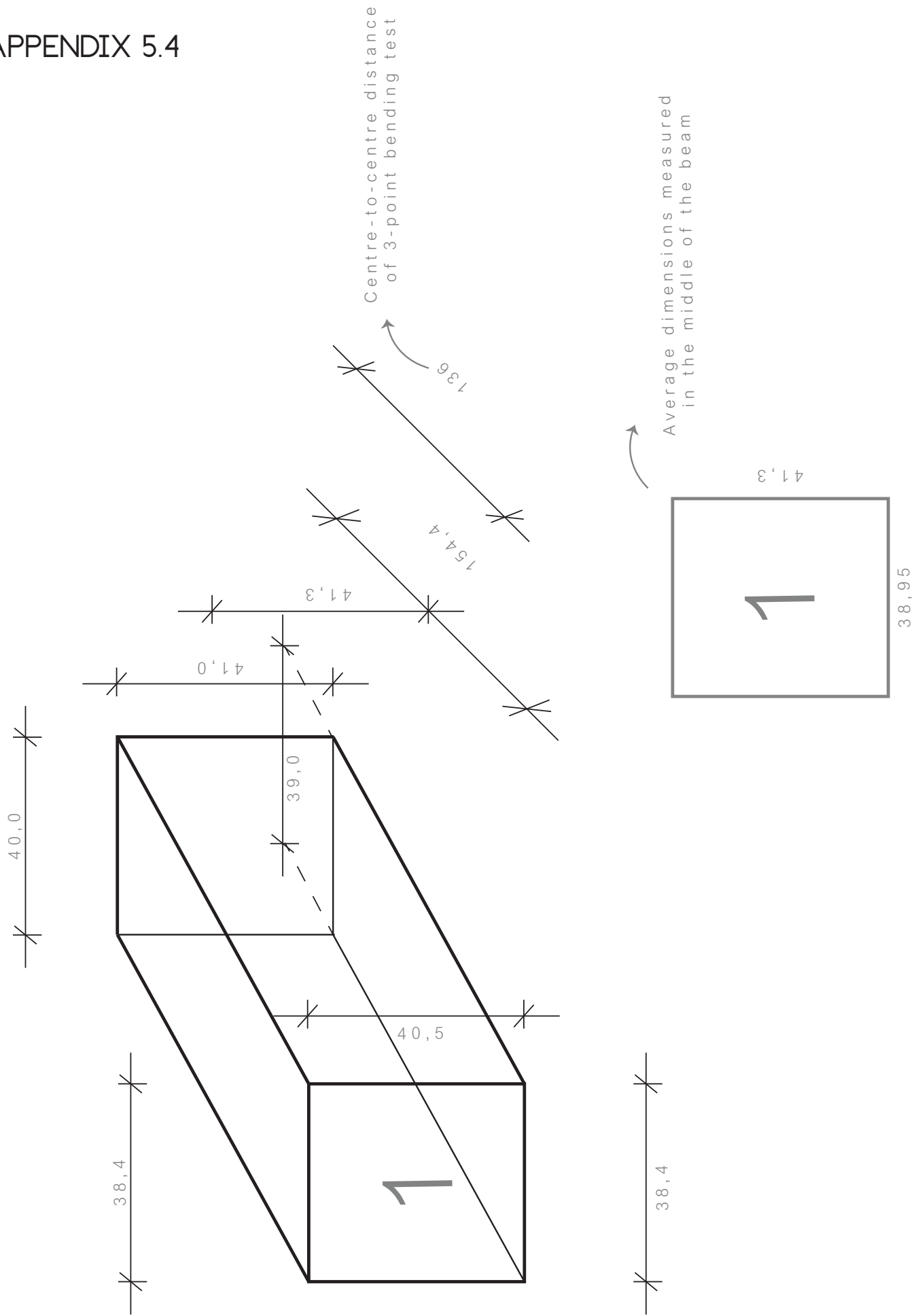


Step 17: Grinding the beam to the desired shape and for a smooth/transparent finish

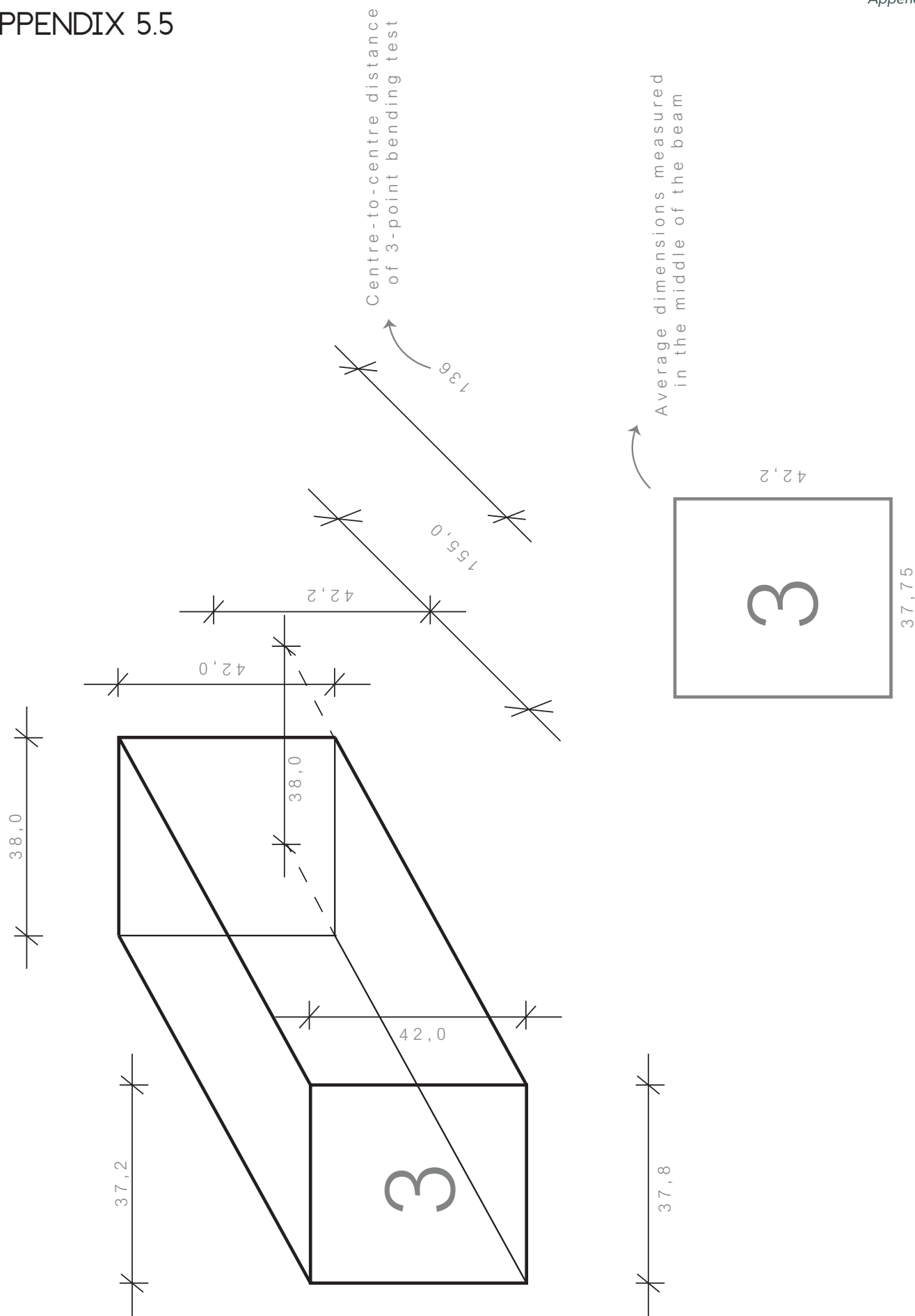


Step 18: Final cast glass beam

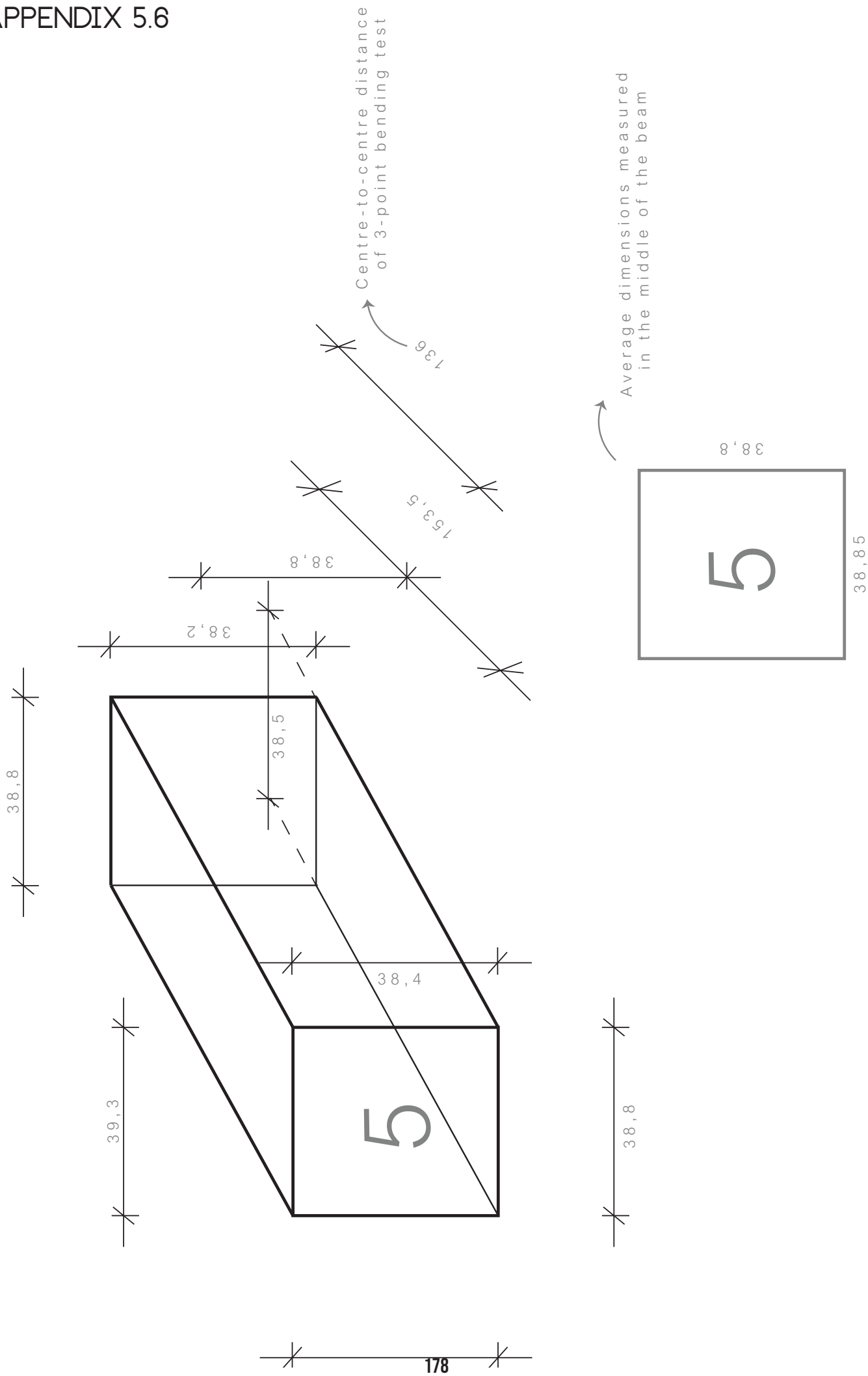
APPENDIX 5.4

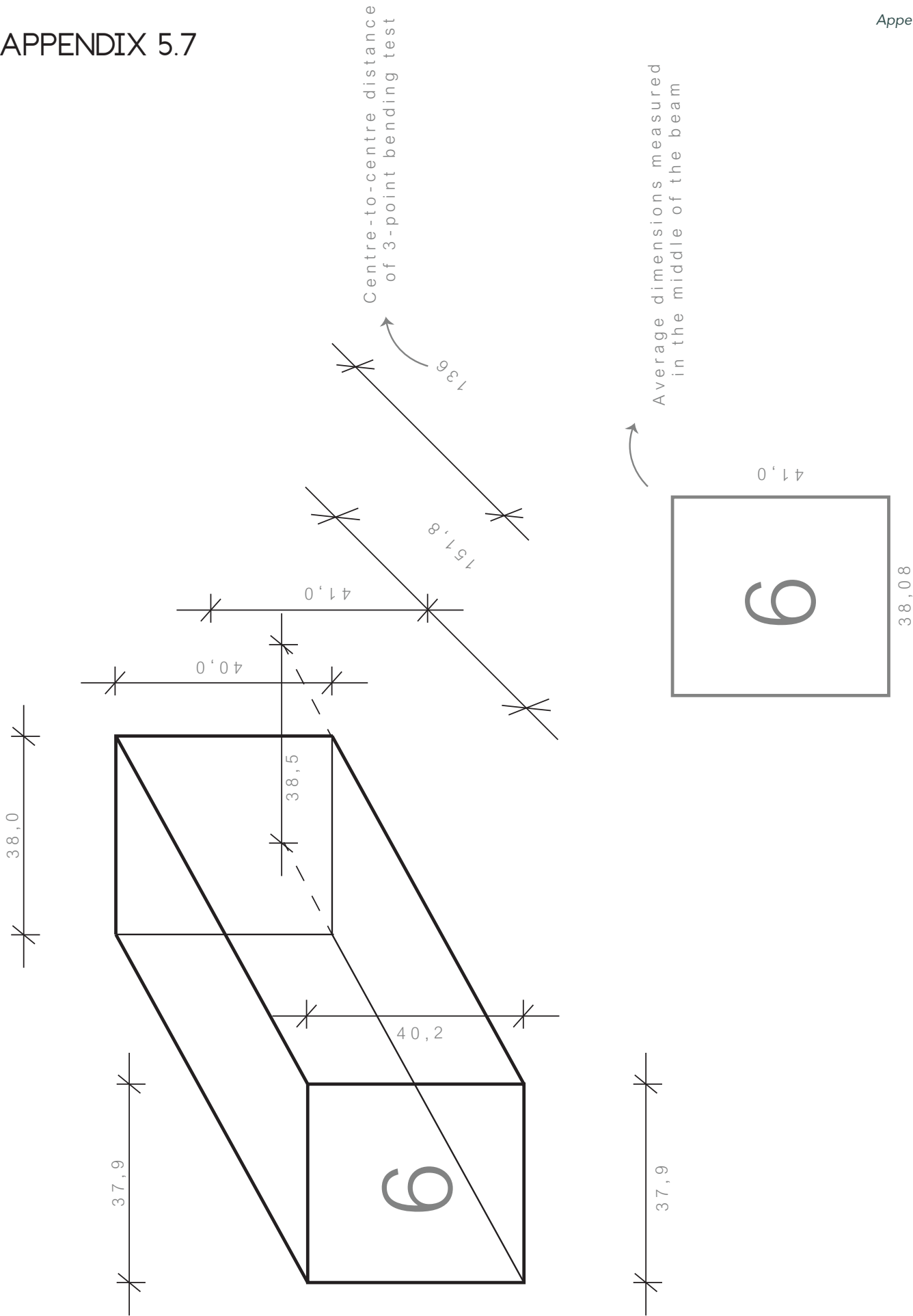




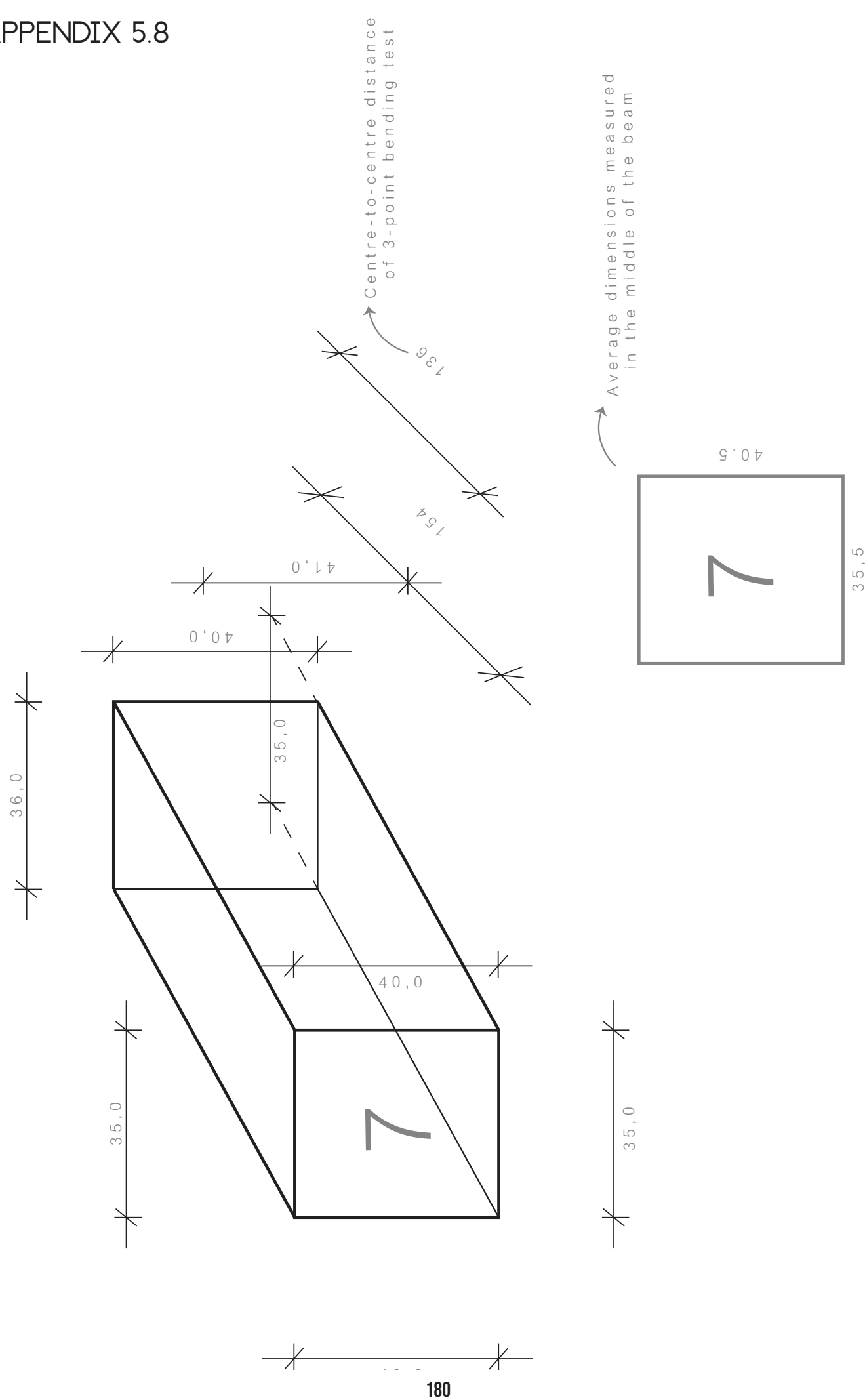


APPENDIX 5.6





APPENDIX 5.8

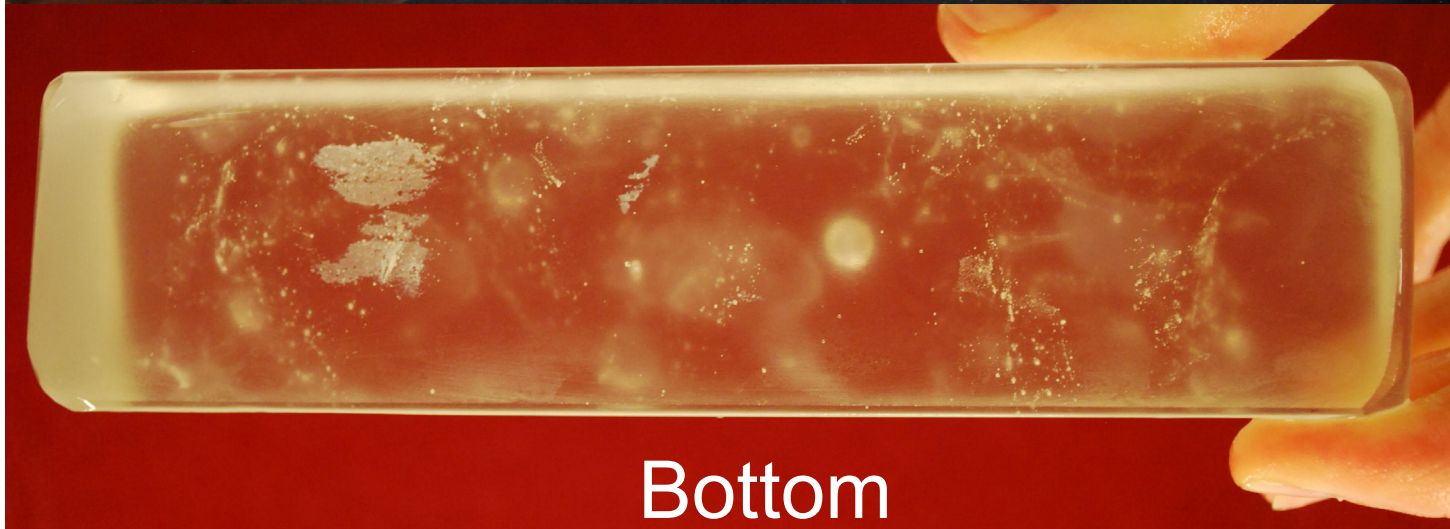
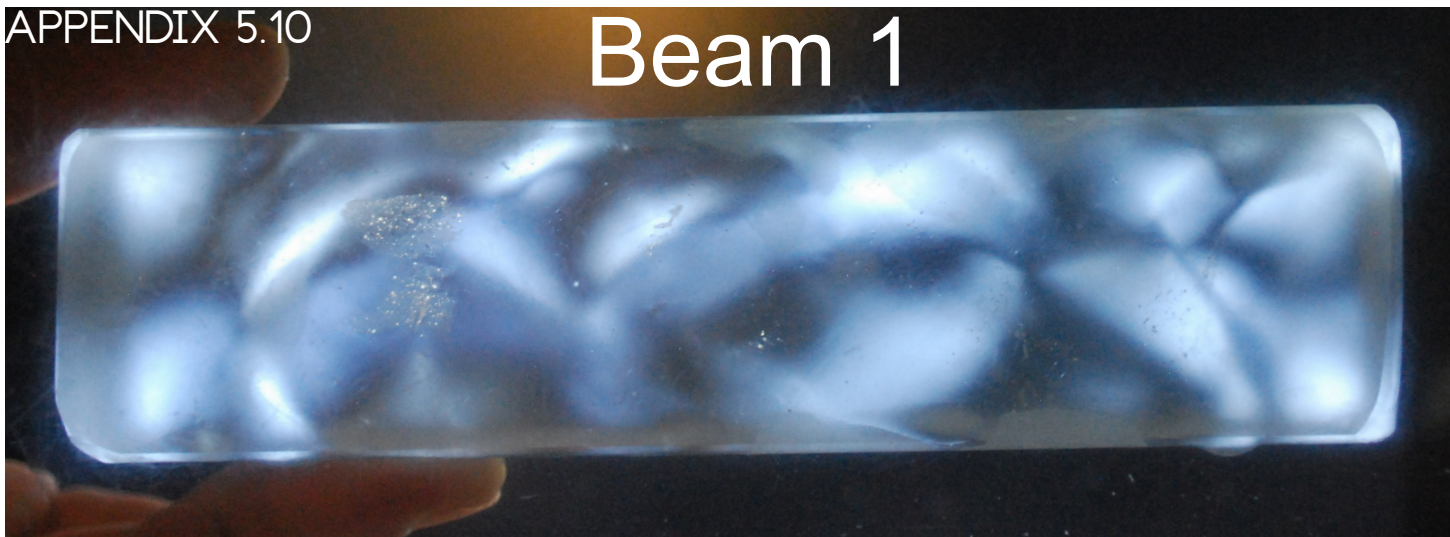


	BEAM 1	BEAM 3	BEAM 5	BEAM 6	BEAM 7
GLASS TYPE (Borosilicate)	Rods Laboratory ware	Rods	Rods	Tube* Lab. ware* PYREX oven tray rect. PYREX oven tray round	Tube* Lab. ware* PYREX oven tray rect. PYREX oven tray round
DESCRIPTION/FLAWS	Big air bubbles on top surface. Several flaws at tension surface. 3 big ones	A lot of small air bubbles inside. A few big ones on top surface. A few small flaws at bottom side.	Very rough bottom surface. Several small air bubbles on top. A lot of small air bubbles inside. (less than beam 3)	Contaminated with stone. Enormous amount of air bubbles in the total beam. Few big ones on top surface. Few small flaws at tension-zone.	Extreme amount of internal air bubbles. A lot present on top surface as well. Placement of shards is visible (as a 'waving pattern'). Several small flaws at bottom side of the beam.
ULTIMATE FAILURE FORCE (N)	16916	18596	15555	8804	7581
DEFORMATION AT ULTIMATE FORCE (mm)	0,94	0,66	0,57	0,41	0,69
FAILURE MODE	Most likely cracked due to a very small surface flaw at the tension-zone of the beam	Most likely cracked due to a very small surface flaw at the tension-zone of the beam	Most likely cracked due to a very small surface flaw at the tension-zone of the beam	Molecular structure of the beam changed due to the stone contamination --> weaker bonds	A lot of internal stresses --> weaker zones/connections
FLEXURAL STRENGTH (MPa)	52	56	54	28	27
YOUNG'S MODULUS	52	60 (Less accurate measurement tool)	52	50	53

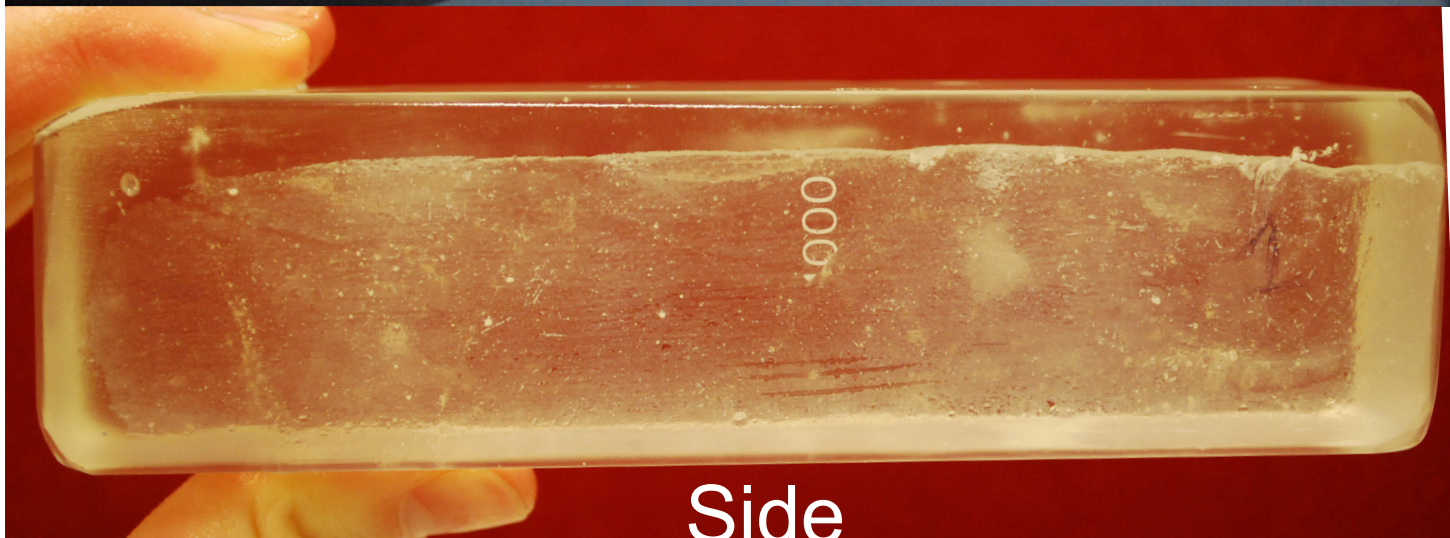
\*Beam 2 and 4 cracked upon firing. Cube not mechanically tested



# Beam 1

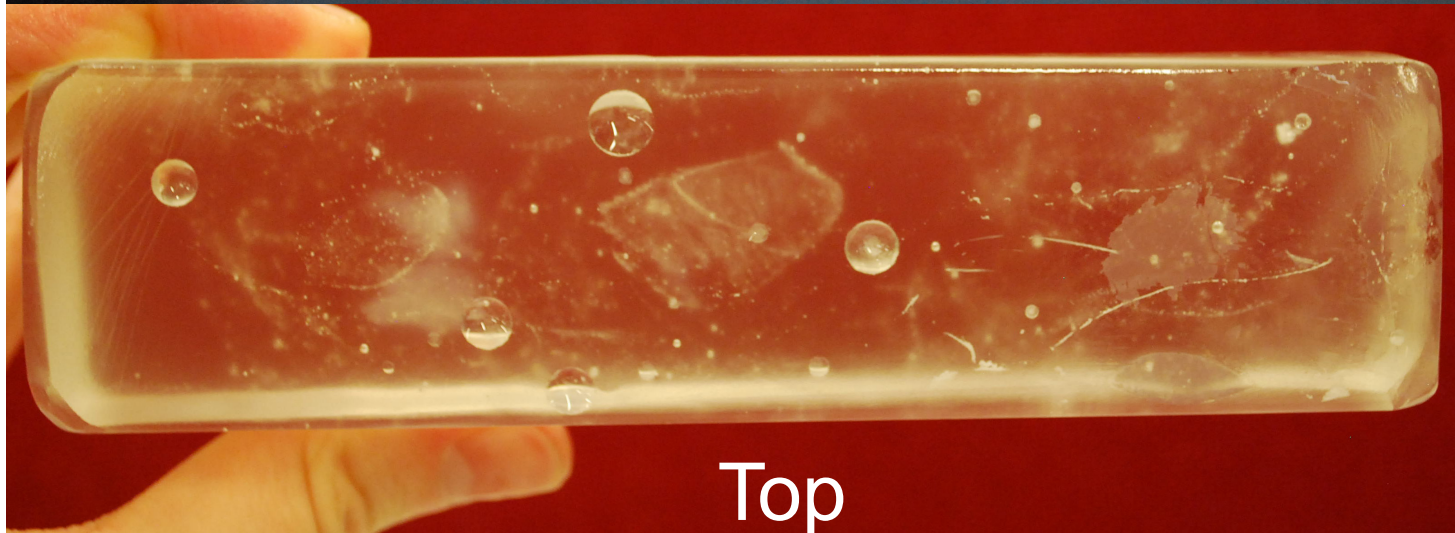
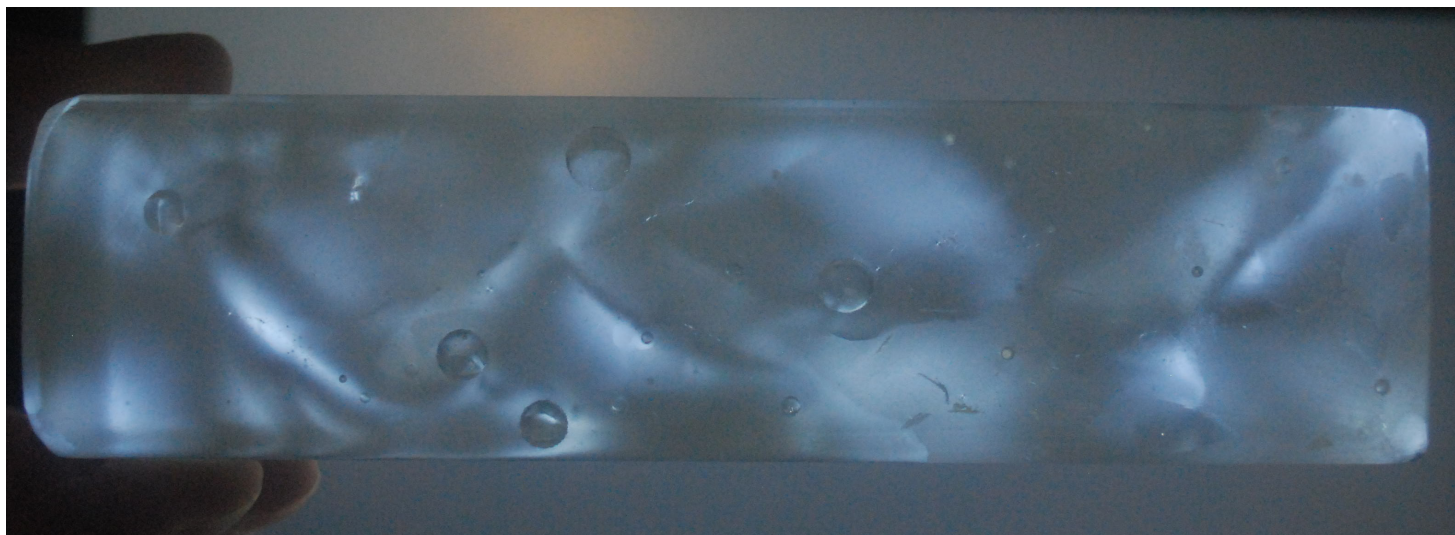


Bottom

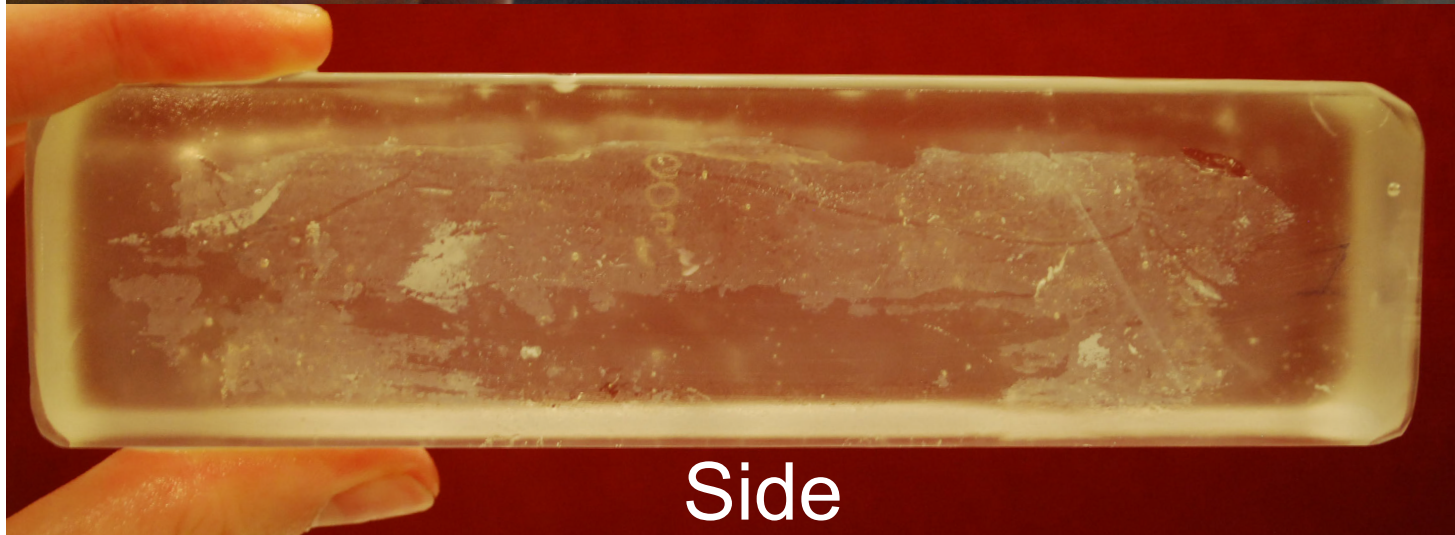


Side





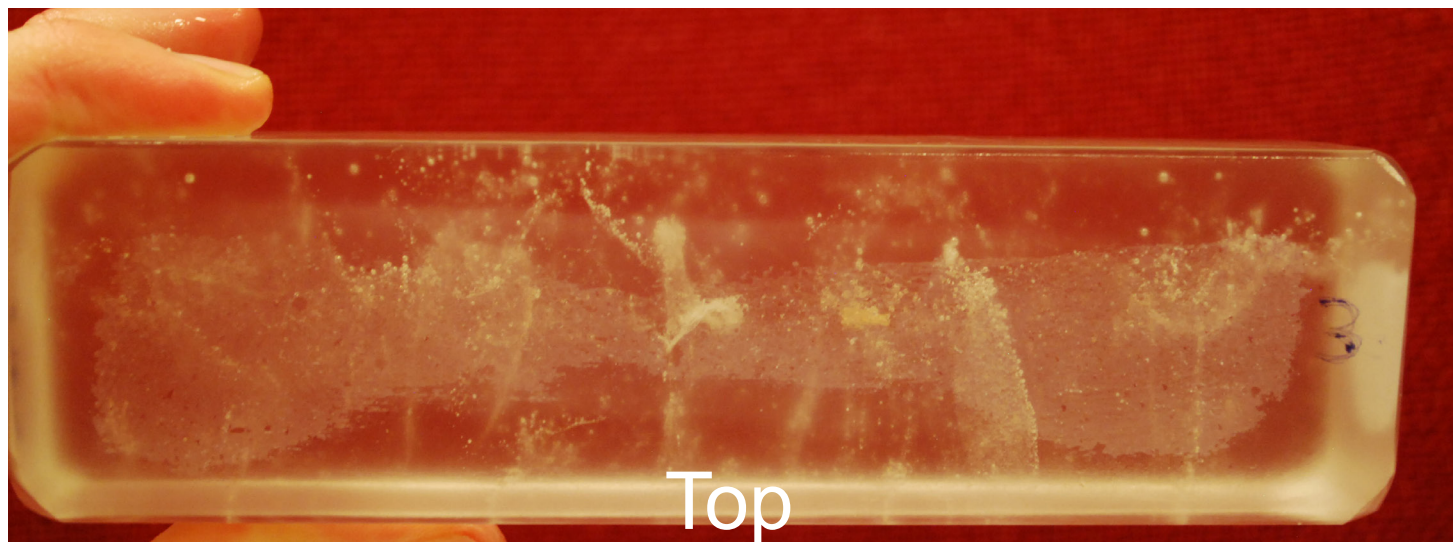
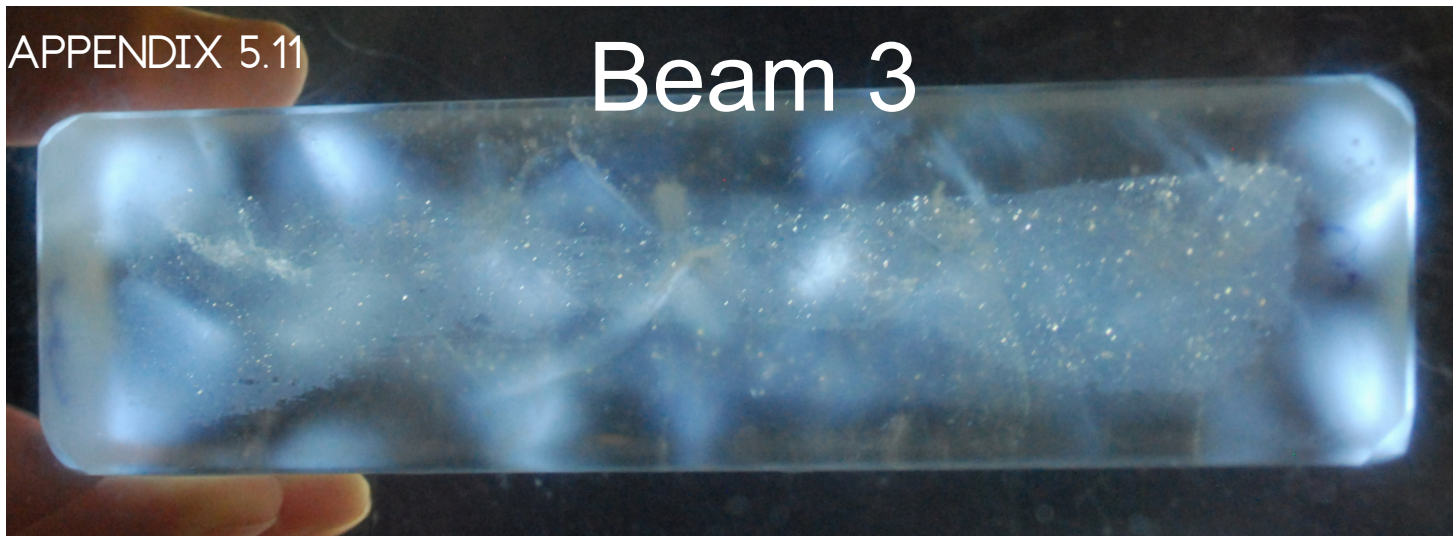
Top



Side



# Beam 3

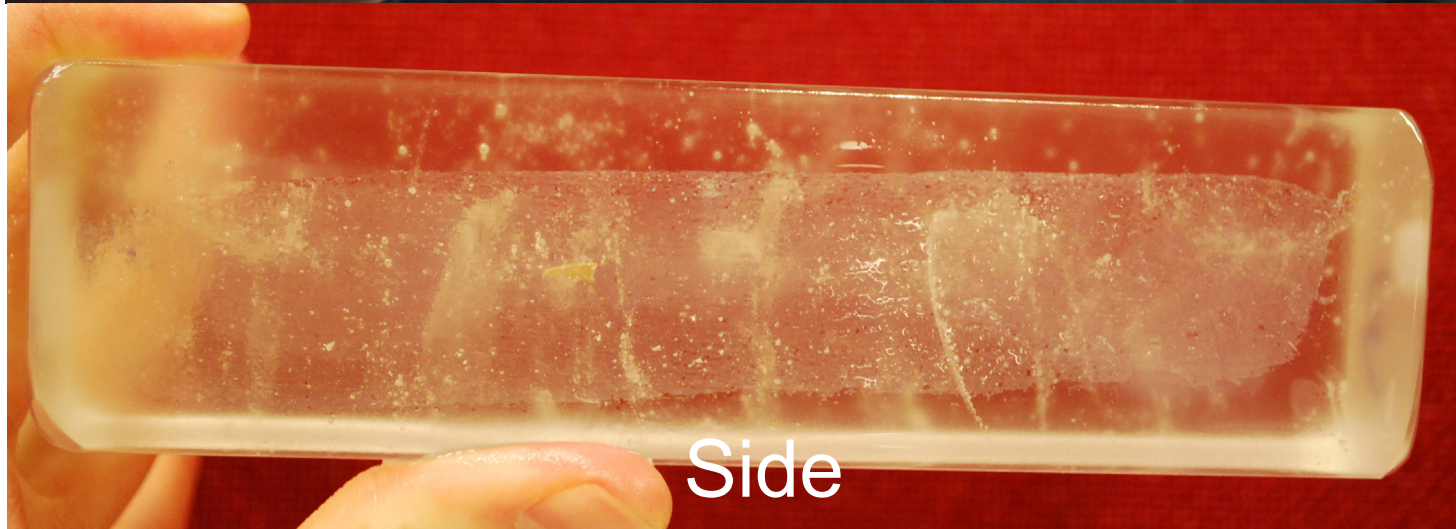
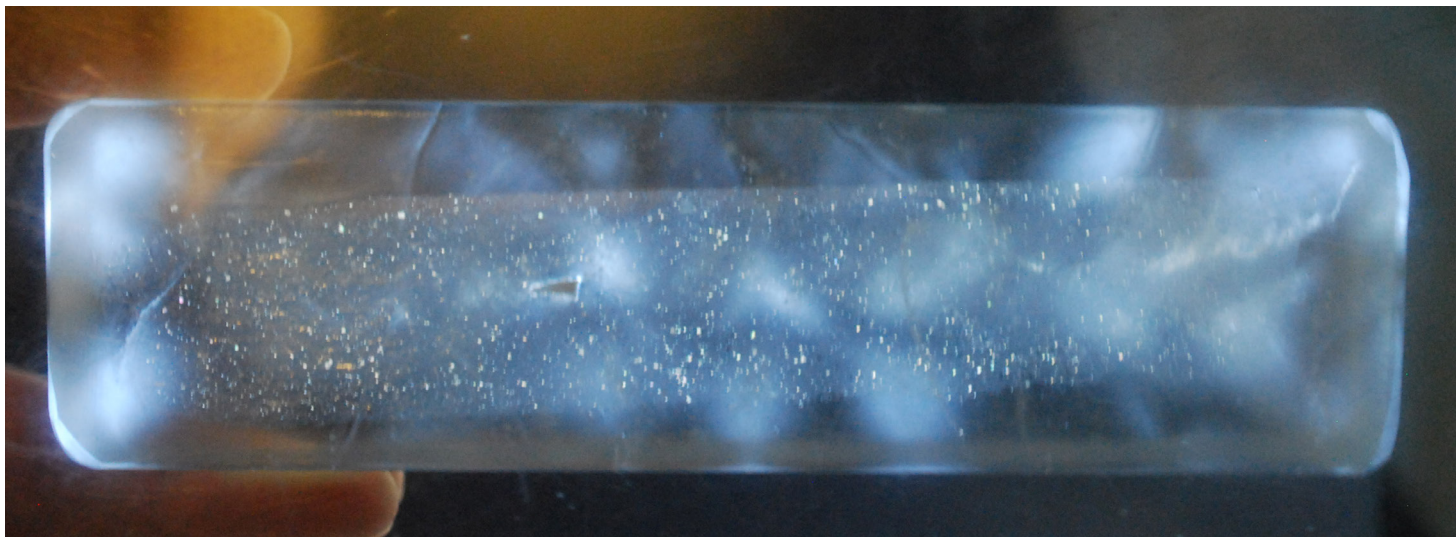
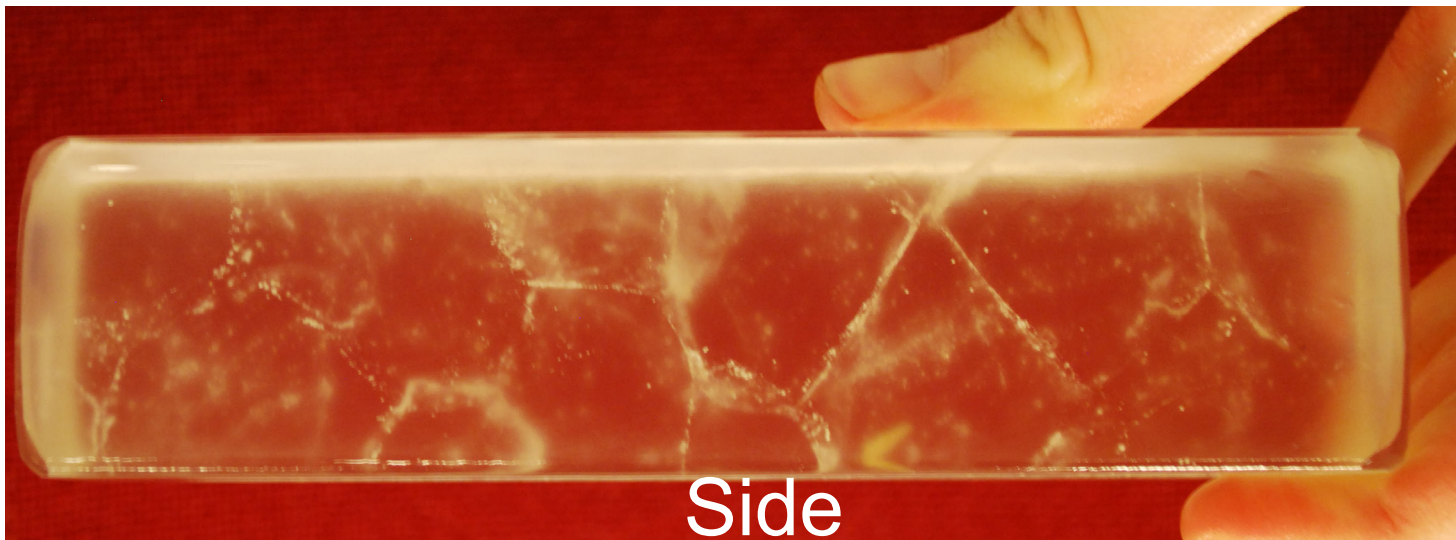
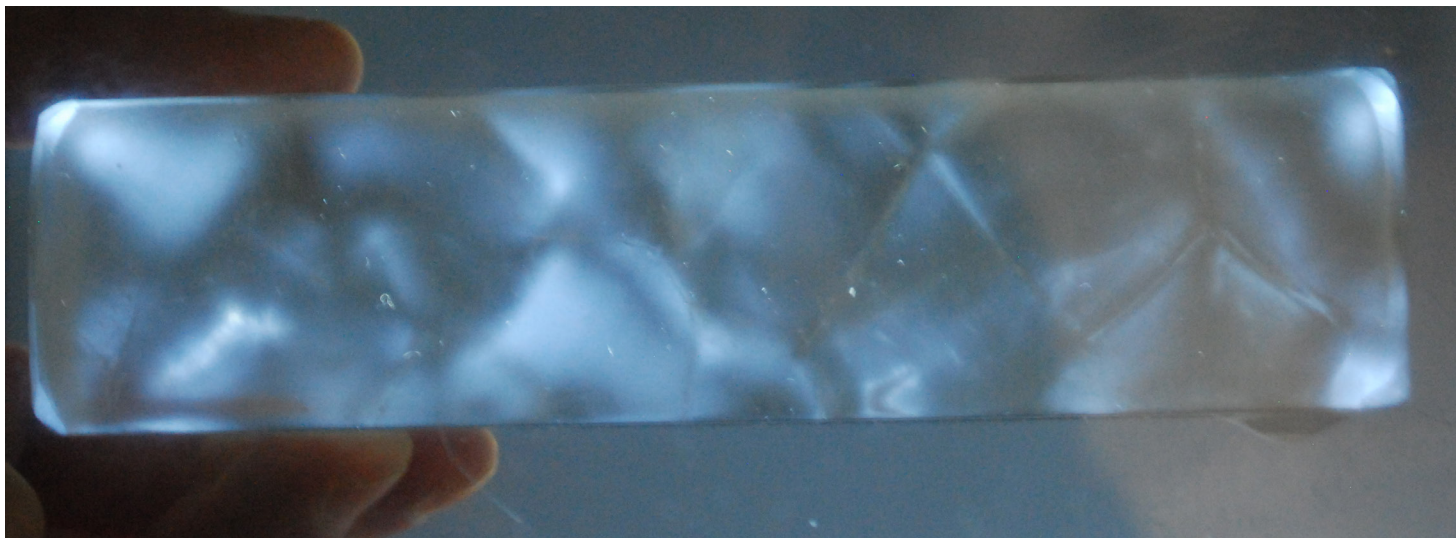


Top



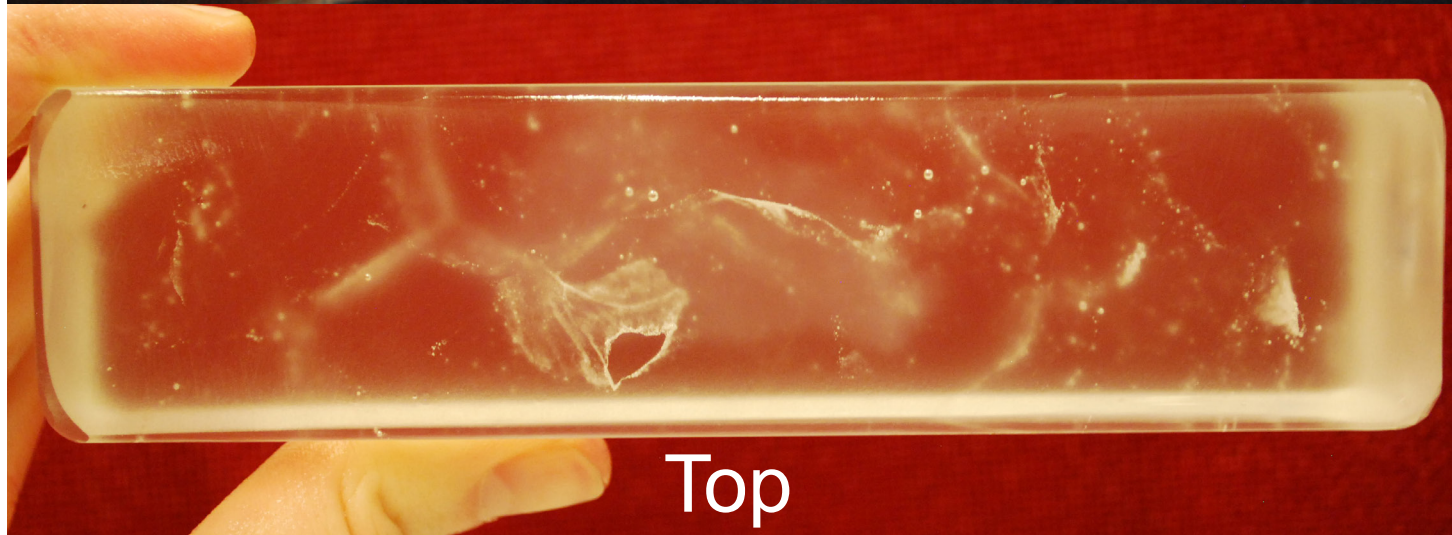
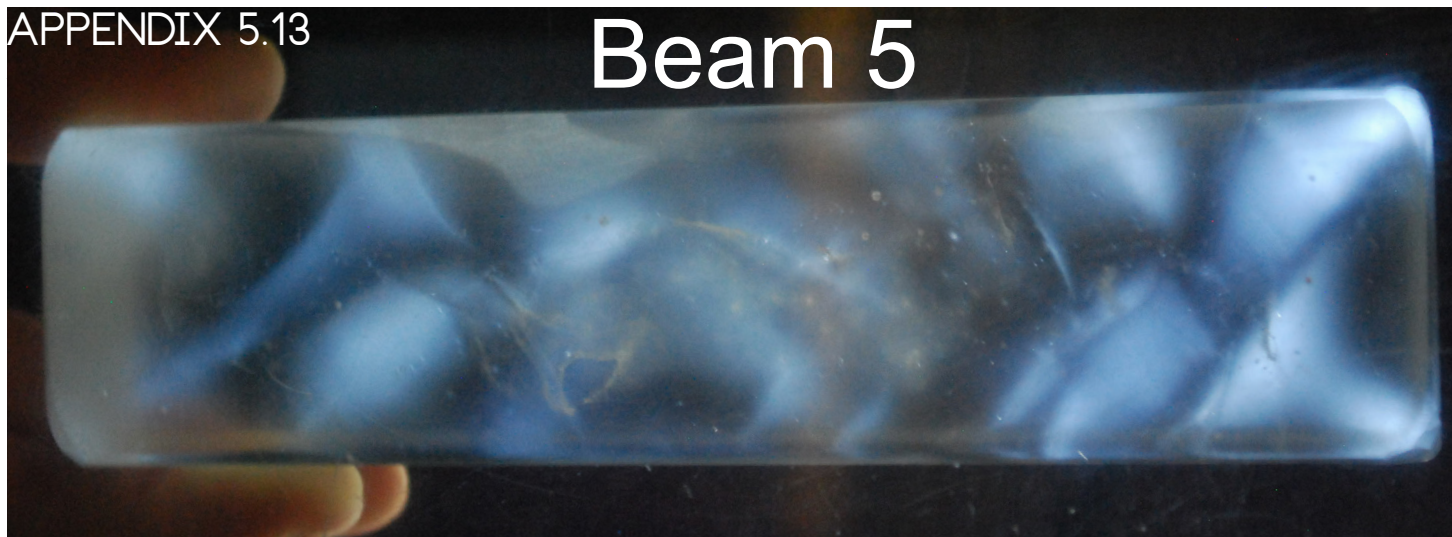
Bottom



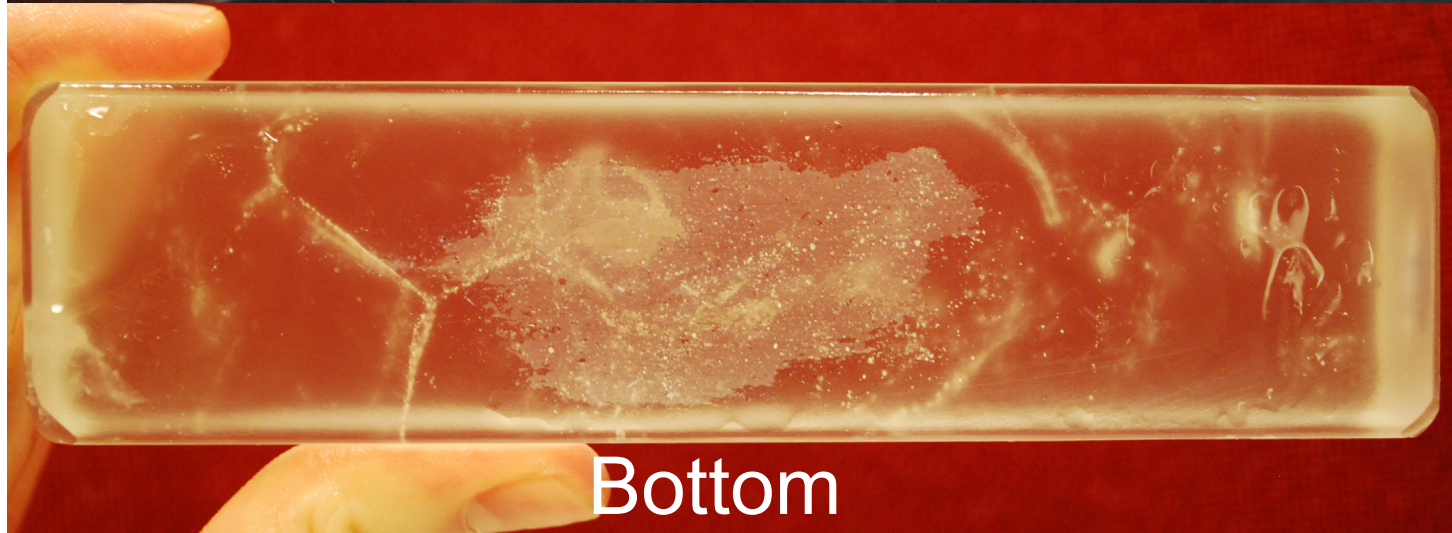




# Beam 5

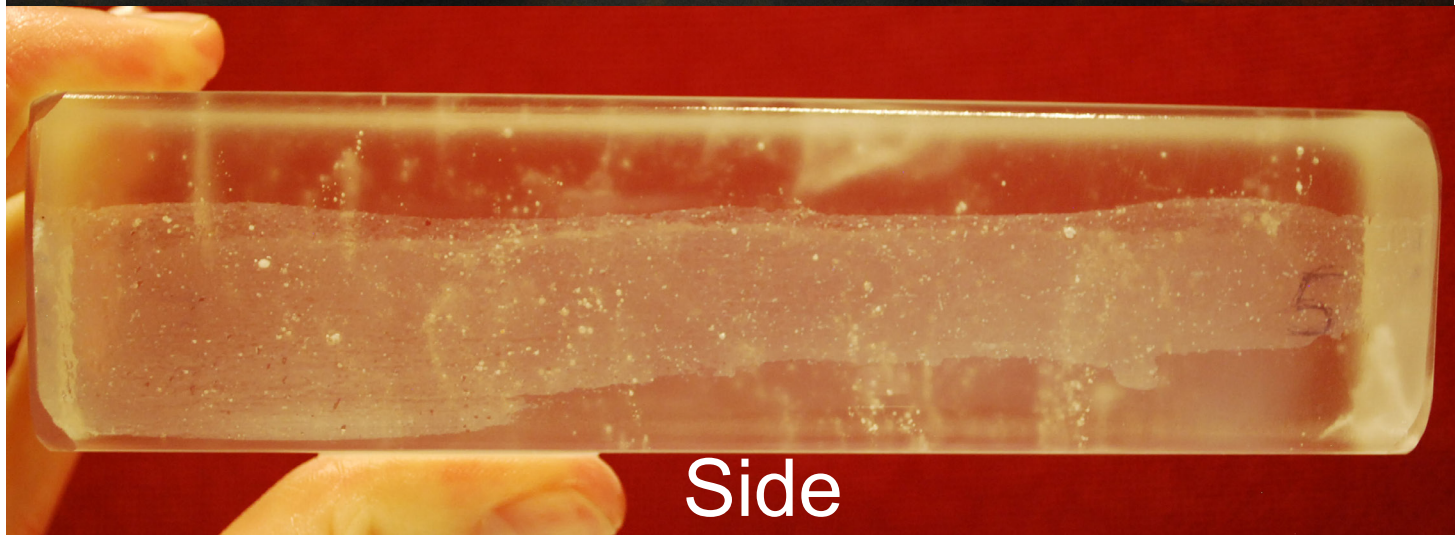
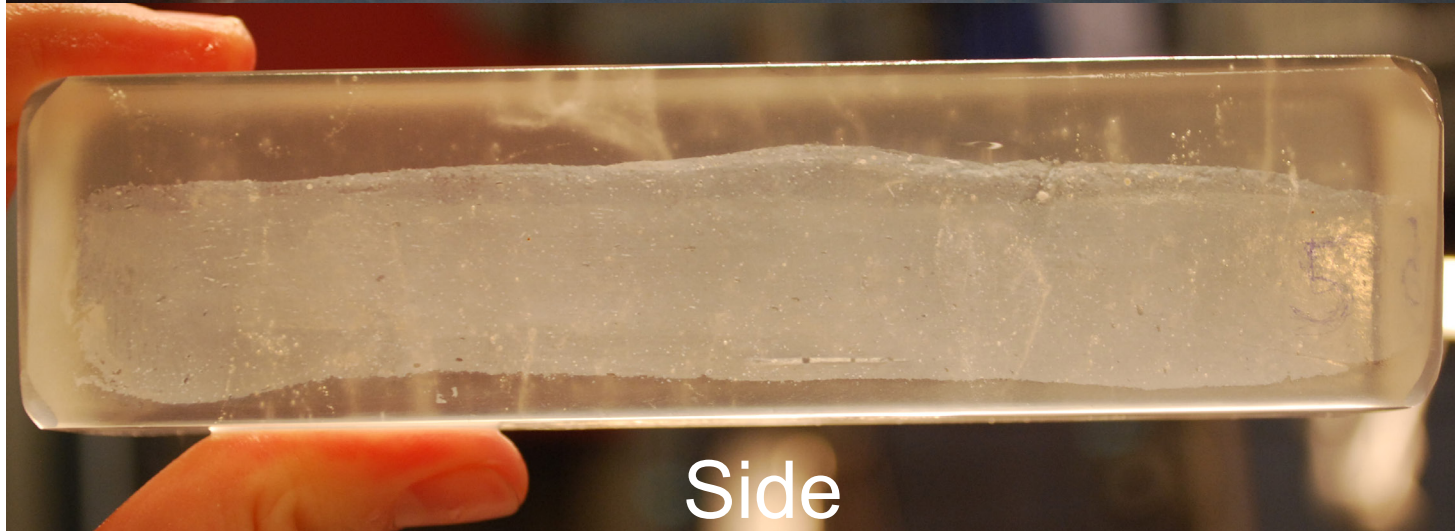
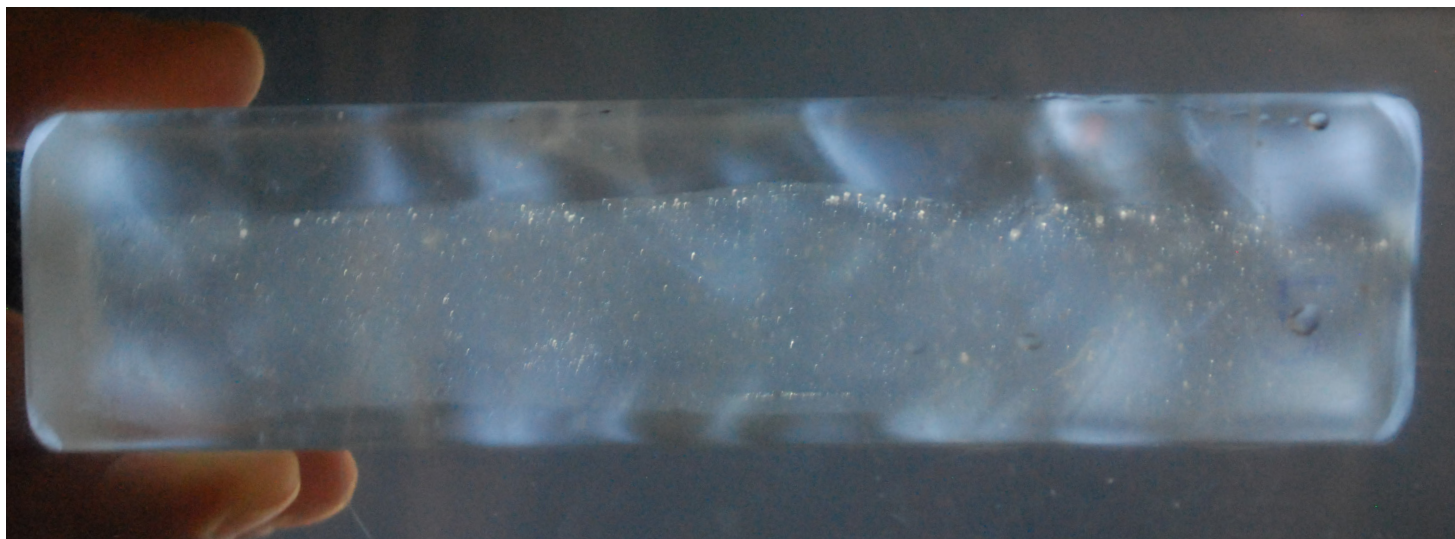


Top



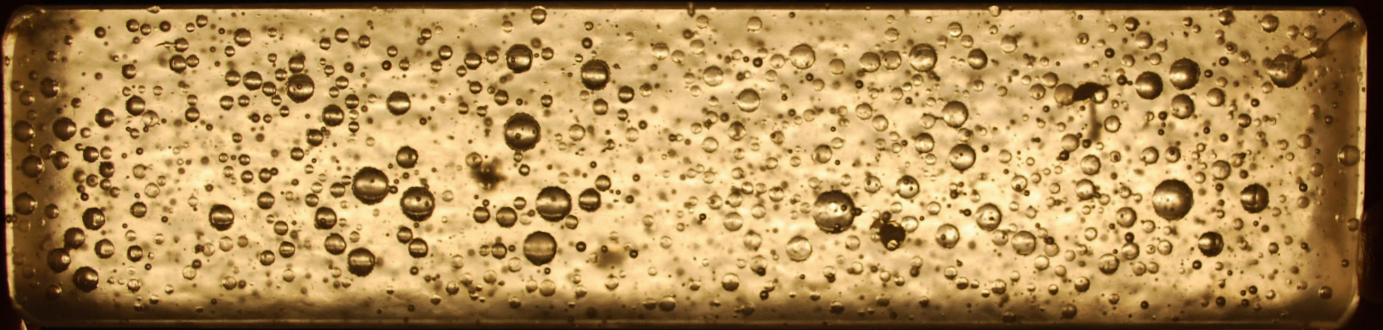
Bottom



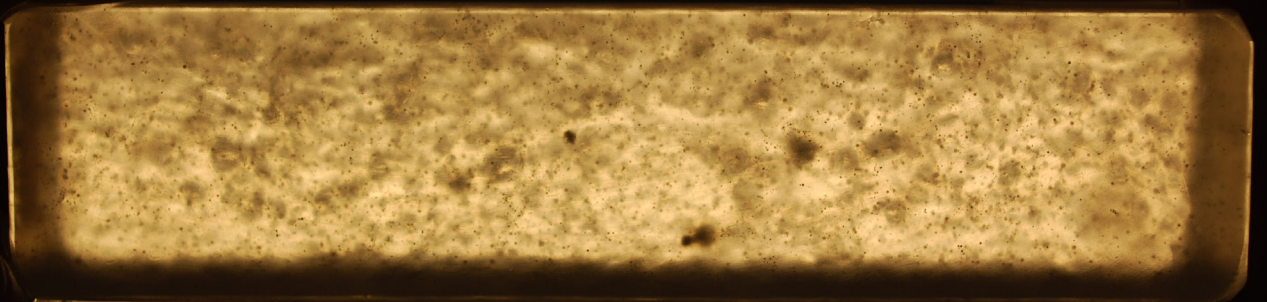
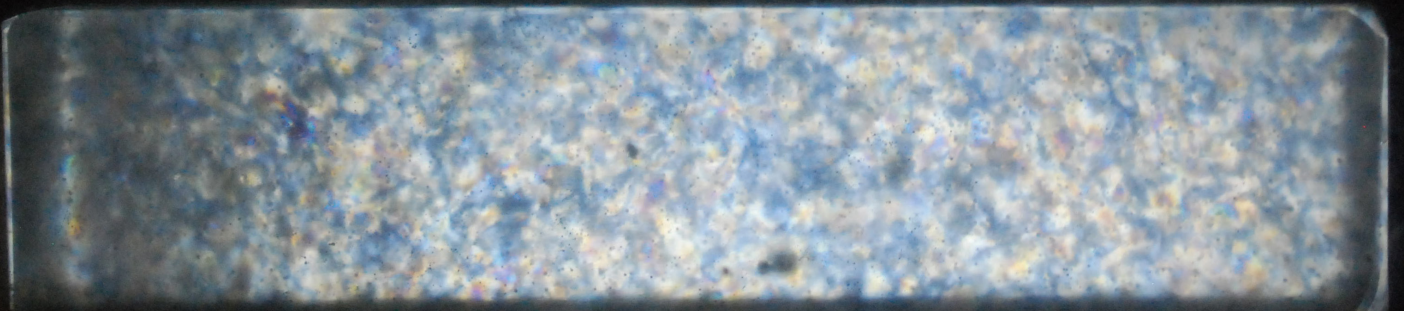




# Beam 7

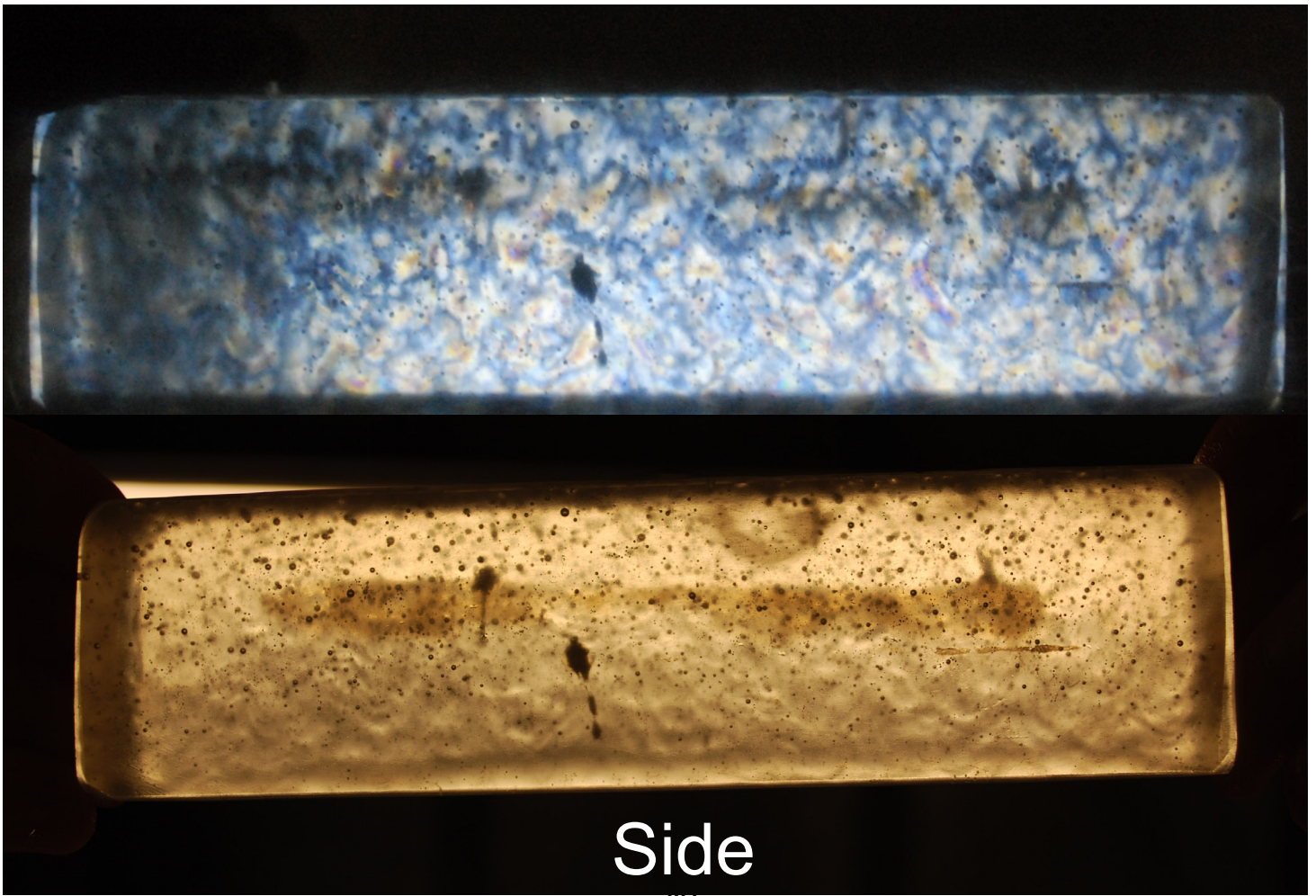
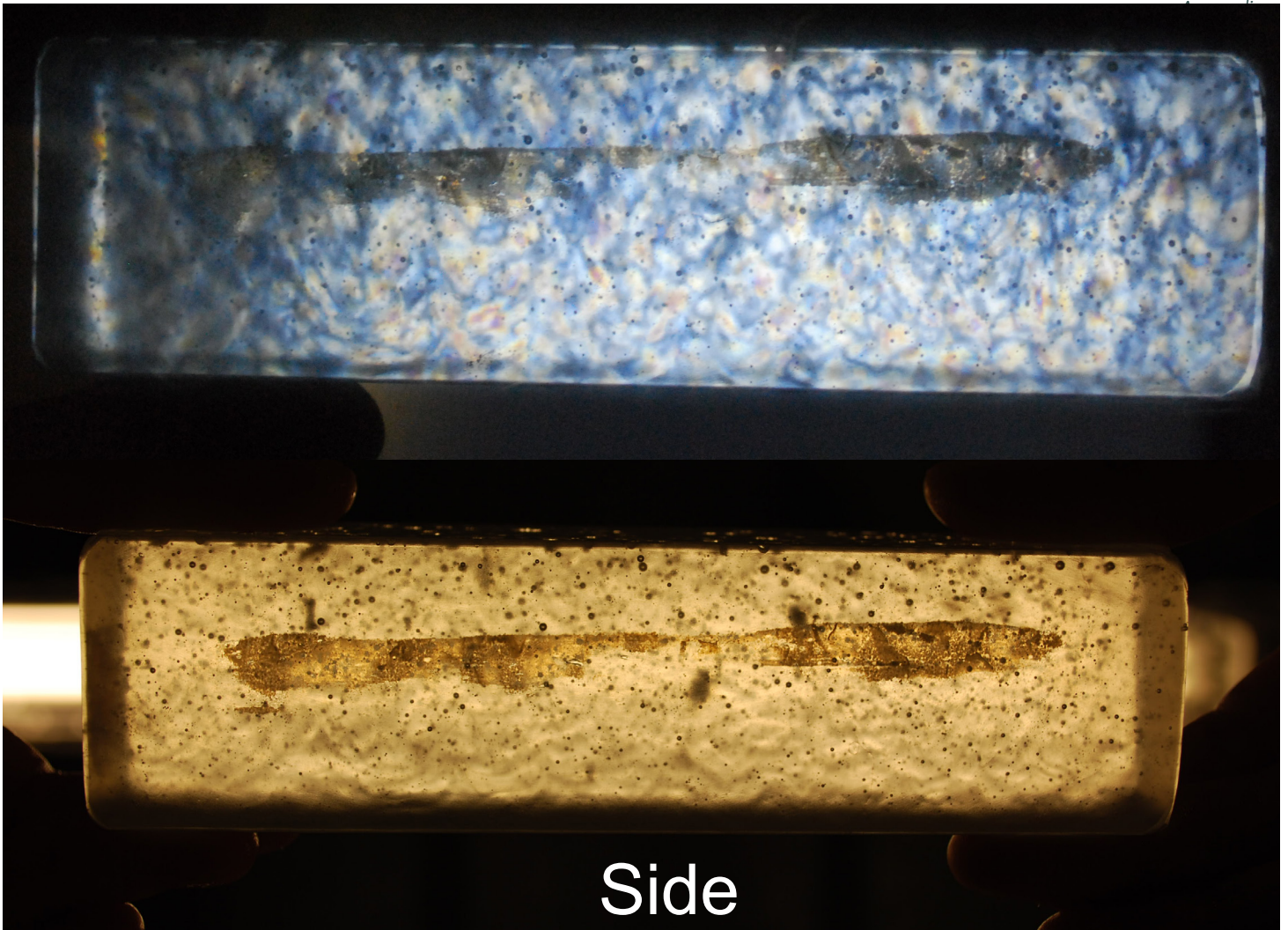


Top



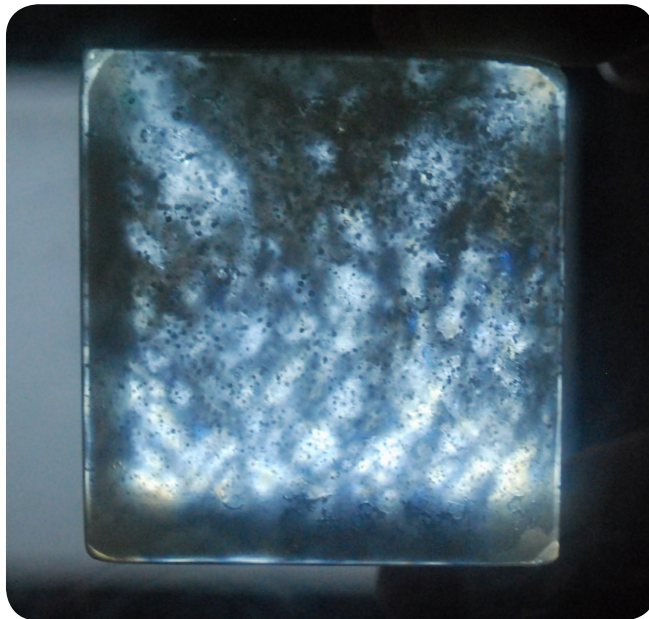
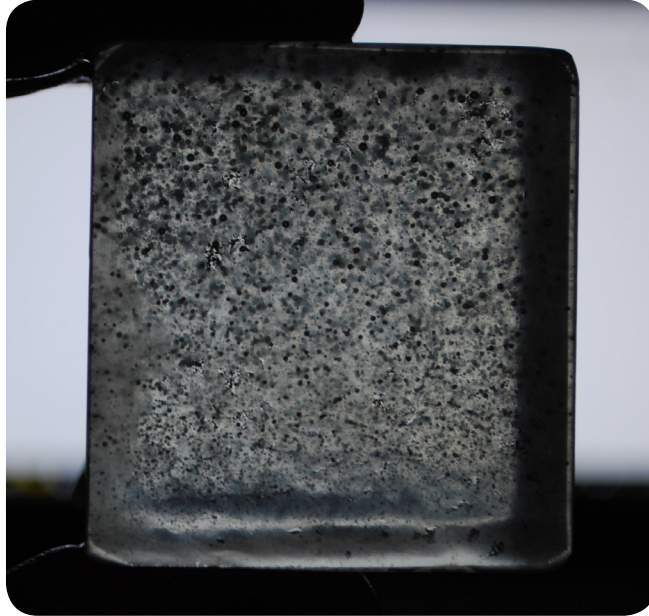
Bottom





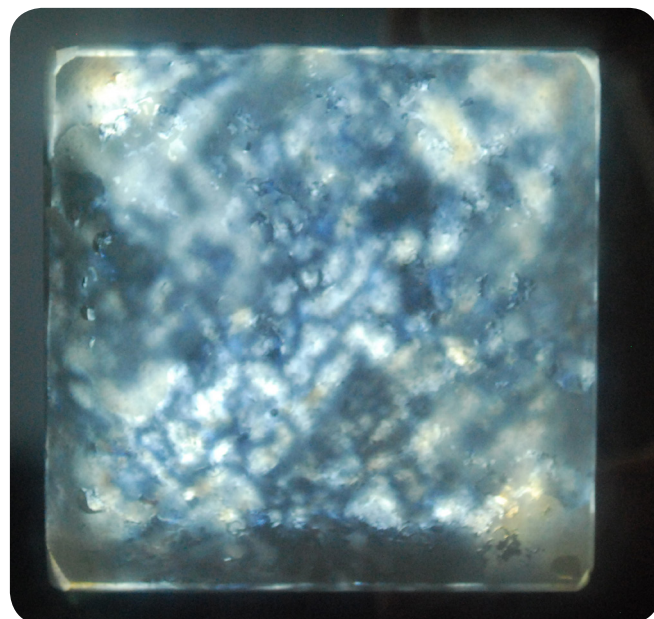
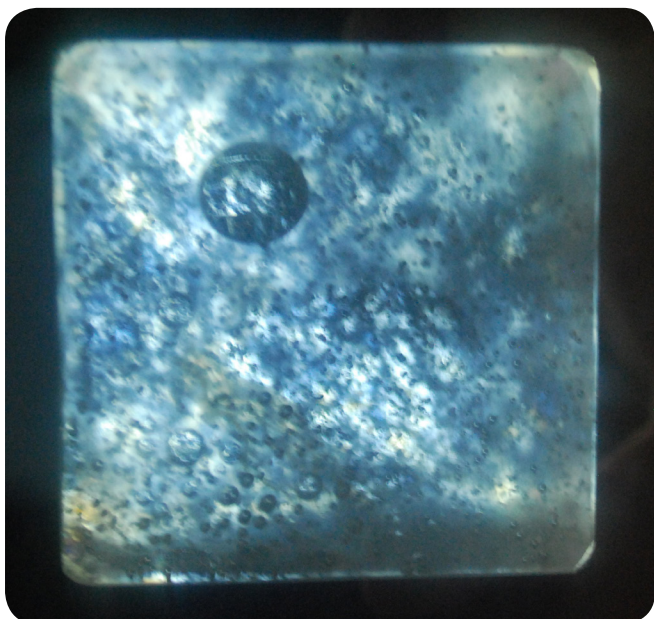
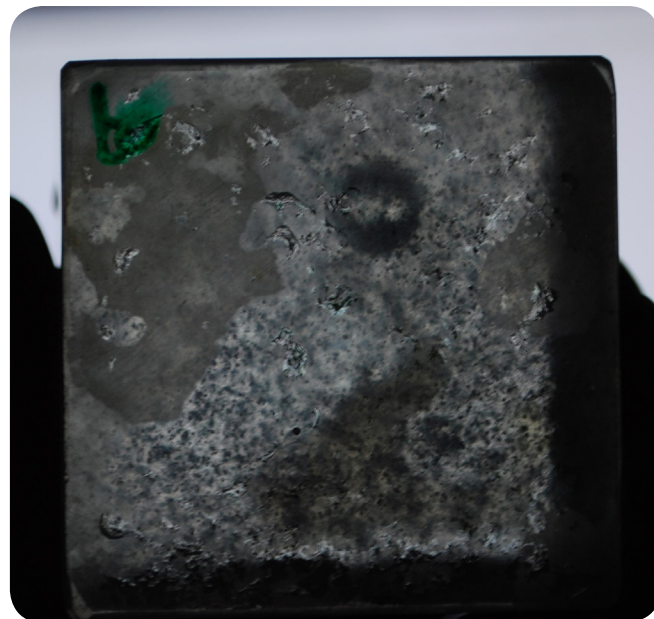
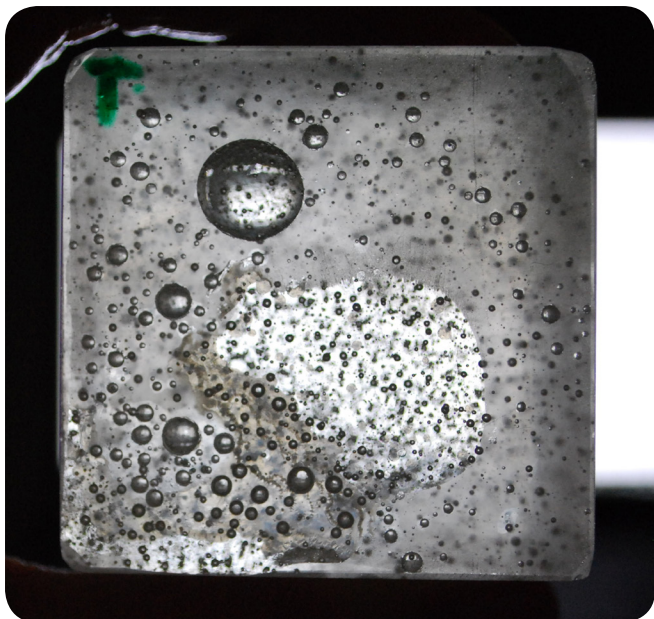


# Cube



# Side

Note: All four sides look similar, therefore only one side is shown.



Top

Bottom



## APPENDIX 5.16

### Monolithic glass wall buckling check – minimum thickness

Boundaries

$$M_{\text{glass}} = \rho_{\text{glass}} * V = 2230 \frac{\text{kg}}{\text{m}^3} * 126 \text{ t} = 280980 \text{ kg} * 9.81 \frac{\text{m}}{\text{s}^2} * \frac{1}{10^3} = 2756.41 \text{ t kN}$$

$$t = \text{thickness [m]}$$

$$\sigma_{\text{critical}} = \frac{F}{A} = \frac{2756.41 \text{ t kN}}{14 \text{ t m}^2} = 196.89 \text{ kN/m}^2$$

$$E = 63 \text{ GPa} = 63000 \frac{\text{N}}{\text{mm}^2} = 6.3 * 10^7 \frac{\text{kN}}{\text{m}^2}$$

Safety factor

$$\sigma_{\text{safe}} = 4 * \sigma_{\text{critical}} = 4 * 196.89 \frac{\text{kN}}{\text{m}^2} = 787.55 \frac{\text{kN}}{\text{m}^2}$$

Bryan's Formula

$$\sigma_{\text{critical}} = k * \frac{\pi^2 * E}{12(1-\nu^2) \left(\frac{b}{t}\right)^2} \left[ \frac{\text{kN}}{\text{m}^2} \right]$$

$k$  = Buckling coefficient

$E$  = Young's modulus

$\nu$  = Poisson's ratio

$b$  = width [m]

$t$  = thickness [m]

Calculating minimum thickness

$$787.55 \frac{\text{kN}}{\text{m}^2} = 4 * \frac{\pi^2 * 6.3 * 10^7}{12(1-0.2^2) \left(\frac{14}{t}\right)^2} = \frac{2.49 * 10^9}{\frac{2257.92}{t^2}}$$

$$1.8 * 10^6 = 2.49 * 10^9 t^2$$

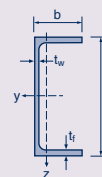
$$t = \sqrt{(7.14 * 10^{-4})} = 0.027 \text{ m} = 2.7 \text{ cm}$$

## APPENDIX 5.17

54

**balkstaal****profielbalken, UPE**

leveringsvoorwaarden: NEN-EN 10025-1 en -2  
 toleranties: NEN-EN 10279; DIN 1026/2  
 max. handelslengte: 18 m



55

profiel nr.	$G_8$ kg/m	$A$ mm <sup>2</sup>	$h$ mm	$b$ mm	$t_w$ mm	$t_f$ mm	$A_L$ m <sup>2</sup> /m	$I_y$ x10 <sup>4</sup> mm <sup>4</sup>	$W_{y,el}$ x10 <sup>3</sup> mm <sup>3</sup>	$I_z$ x10 <sup>4</sup> mm <sup>4</sup>	$W_{z,el}$ x10 <sup>3</sup> mm <sup>3</sup>	profiel nr.
80	9,05	1131	80	50	4,5	8	0,342	118	29,4	28,3	8,99	80
100	11,1	1393	100	55	5	8,5	0,401	227	45,3	42,3	11,9	100
120	13,5	1684	120	60	5,5	9	0,460	392	65,4	60,7	15,3	120
140	16,0	2004	140	65	6	9,5	0,519	630	90,0	84,3	19,3	140
160	19,0	2372	160	70	6,5	10	0,577	965	121	114	23,9	160
180	22,0	2750	180	75	7	10,5	0,636	1404	156	151	29,1	180
200	25,3	3157	200	80	7,5	11	0,695	1972	197	196	35,0	200
220	29,4	3670	220	85	8	12	0,754	2767	252	256	43,1	220
240	34,0	4256	240	90	8,5	13	0,810	3816	318	331	52,4	240
270	39,5	4935	270	95	9	14	0,889	5559	412	425	63,3	270
300	45,3	5662	300	100	9,5	15	0,968	7823	522	538	75,6	300
330	54,2	6777	330	105	11	16	1,04	11008	667	681	89,7	330
360	62,3	7791	360	110	12	17	1,12	14825	824	844	105	360
400	73,5	9193	400	115	13,5	18	1,22	20981	1049	1045	123	400

Source: *Bouwen met Staal*, & van Eldik, C. H. (2006)

Buckling check		Thickness (t) (m)				Fcritical (N)	Fcritical subcolumn without interlocking correction
Parameters		b-ellipse	a-ellipse				
Height (m)	9	0,01	0,001667	0,002334	8955,75214		143,9317308
Width (m)	14	0,015	0,0025	0,003501	30225,6635		485,7695916
width half component	0,225	0,02	0,003333	0,004668	71646,0171		1151,453847
		0,025	0,004167	0,005835	139933,627		2248,933295
Density borosilicate (kg/m3)	2230	0,03	0,005	0,007001	241805,308		3886,156733
E (N/m2)	63000000000	0,035	0,005833	0,008168	383977,873		6171,07296
		0,04	0,006667	0,009335	573168,137		9211,630774
		0,045	0,0075	0,010502	816092,914		13115,77897
Safety factor	4	0,05	0,008333	0,011669	1119469,02		17991,46636
c (support connections)	4	0,055	0,009167	0,012836	1490013,26		23946,64172
(clamped both sides)		0,06	0,01	0,014003	1934442,46		31089,25386
eccentricity ellipse	0,7	0,065	0,010833	0,01517	2459473,43		39527,25158
		0,07	0,011667	0,016337	3071822,98		49368,58368
		0,075	0,0125	0,017504	3778207,93		60721,19895
		0,08	0,013333	0,01867	4585345,1		73693,04619
		0,085	0,014167	0,019837	5499951,28		88392,07421
		0,09	0,015	0,021004	6528743,31		104926,2318
		0,095	0,015833	0,022171	7678437,99		123403,4677
		0,1	0,016667	0,023338	8955752,14		143931,7308
		0,105	0,0175	0,024505	10367402,6		166618,9699
		0,11	0,018333	0,025672	11920106,1		191573,1338

Fdead load (N)	Fdead load (N) subcolumn	Fdead load (N) subcolumn total d	total wall	Fdead load (N)		I rect. Of sub column half component	I ellipse of sub column	I total of sub column	Fcritical subcolumn	
				component	subcolumn				with elliptical interlocking	
27564,138	442,995075	885,99015	1,16667E-06	1,875E-08	8,48594E-12	1,87415E-08	143,8665898			
41346,207	664,4926125	1328,985225	3,9375E-06	6,32813E-08	4,29601E-11	6,32383E-08	485,4398148			
55128,276	885,99015	1771,9803	9,33333E-06	0,00000015	1,35775E-10	1,49864E-07	1150,411589			
68910,345	1107,487688	2214,975375	1,82292E-05	2,92969E-07	3,31482E-10	2,92637E-07	2246,38872			
82692,414	1328,985225	2657,97045	0,0000315	5,0625E-07	6,87361E-10	5,05563E-07	3880,880304			
96474,483	1550,482763	3100,965525	5,00208E-05	8,03906E-07	1,27342E-09	8,02633E-07	6161,297724			
110256,552	1771,9803	3543,9606	7,46667E-05	0,0000012	2,1724E-09	1,19783E-06	9194,954654			
124038,621	1993,477838	3986,955675	0,000106313	1,70859E-06	3,47976E-09	1,70511E-06	13089,06705			
137820,69	2214,975375	4429,95075	0,000145833	2,34375E-06	5,30371E-09	2,33845E-06	17950,75317			
151602,759	2436,472913	4872,945825	0,000194104	3,11953E-06	7,76516E-09	3,11177E-06	23887,03354			
165384,828	2657,97045	5315,9409	0,000252	0,00000405	1,09978E-08	4,039E-06	31004,831			
179166,897	2879,467988	5758,935975	0,000320396	5,14922E-06	1,51479E-08	5,13407E-06	39410,97066			
192948,966	3100,965525	6201,93105	0,000400167	6,43125E-06	2,03747E-08	6,41088E-06	49212,17991			
206731,035	3322,463063	6644,926125	0,000492188	7,91016E-06	2,685E-08	7,88331E-06	60515,08845			
220513,104	3543,9606	7087,9212	0,000597	0,000009	3,47584E-08	9,56524E-06	73426,22826			
234295,173	3765,458138	7530,916275	0,000716479	1,15148E-05	4,42971E-08	1,14705E-05	88052,03361			
248077,242	3986,955675	7973,91135								
261859,311	4208,453213	8416,906425								
275641,38	4429,95075	8859,9015								
289423,449	4651,448288	9302,896575								
303205,518	4872,945825	9745,89165								



## APPENDIX 5.19 Wind load on facade calculation data one beam

input		tangens angle of rotation	Ym	H (N)
		0,3125	1,40625	12960
Height ellipse (m)	0,05			
Width component (m)	0,08			
		0,302884868		
Height cable (m)	9	17,35402464 degrees		
wind load (N/m)	1800			

### Input

Tension force of one cable (N)	12960			
Width of facade (mm)	14000			-1330806857
Height of facade (mm)	9000			
Distance between cables (mm)	1800	3600	5400	-2481654857
E of steel (mpa)	210000			-3272585143
x (middle of the beam)	7000			
Max. Deflection (mm)	-20			-3528000000
Set heigth (mm)	600			
tw (mm)	18			
set tf (mm)	26			
b profile (mm)	132			
set width of profile (mm)	150			

i, 1800=	i, 2x 1800	i, 3x1800	I,mid	I totaal necessary	I totaal proposed upe profile
66540342,86					889767488
6654,034286					88976,7488
	124082742,9				
	12408,27429				
		163629257,1			
			176400000		
				884904685,7	
				88490,46857	

## APPENDIX 5.20 Wind load on facade calculation data three beams

input		tangens angle of rotation	Ym	H (N)
		0,15625	0,703125	25920
Height ellipse	0,05		0,257143	70875
Width component	0,08			
		0,154996742		
Height cable	9	8,880659151		
wind load (N/m)	1800			

### Input

Tension force of one cable (N)	25920			i, at 2332 mm
Width of facade (mm)	14000		-3395541205	169777060,3
Height of facade	9000			16977,70603
			-6571783868	
Distance between cables (mm)	2332	5444		
E of steel (mpa)	210000			
x (middle of the beam)	7000			
			-7056000000	
Set Max. Deflection (mm)	-20			
Set heigth (mm)	610			
tw (mm)	19			
set tf (mm)	27			
b profile (mm)	141			
set width of profile (mm)	160			

i, at 5444 mm	I,mid 7000	I total Required	I total proposed upe profile 1006827845 100682,7845
328589193,4 32858,91934	352800000 35280	996732507 99673,2507	



